IMPACT HAMMER TESTING OF MASONRY SEWERS

BY

ALAN SIBBALD

BSc, MSc, CEng, MICE

A thesis submitted for the Degree

of

Doctor of Philosophy

UNIVERSITY OF EDINBURGH

1988

EX BIBL. UNIV. EDINBURGEN.

VOLUME 2

FIGURES AND PLATES

CHAPTER 1

INTRODUCTION

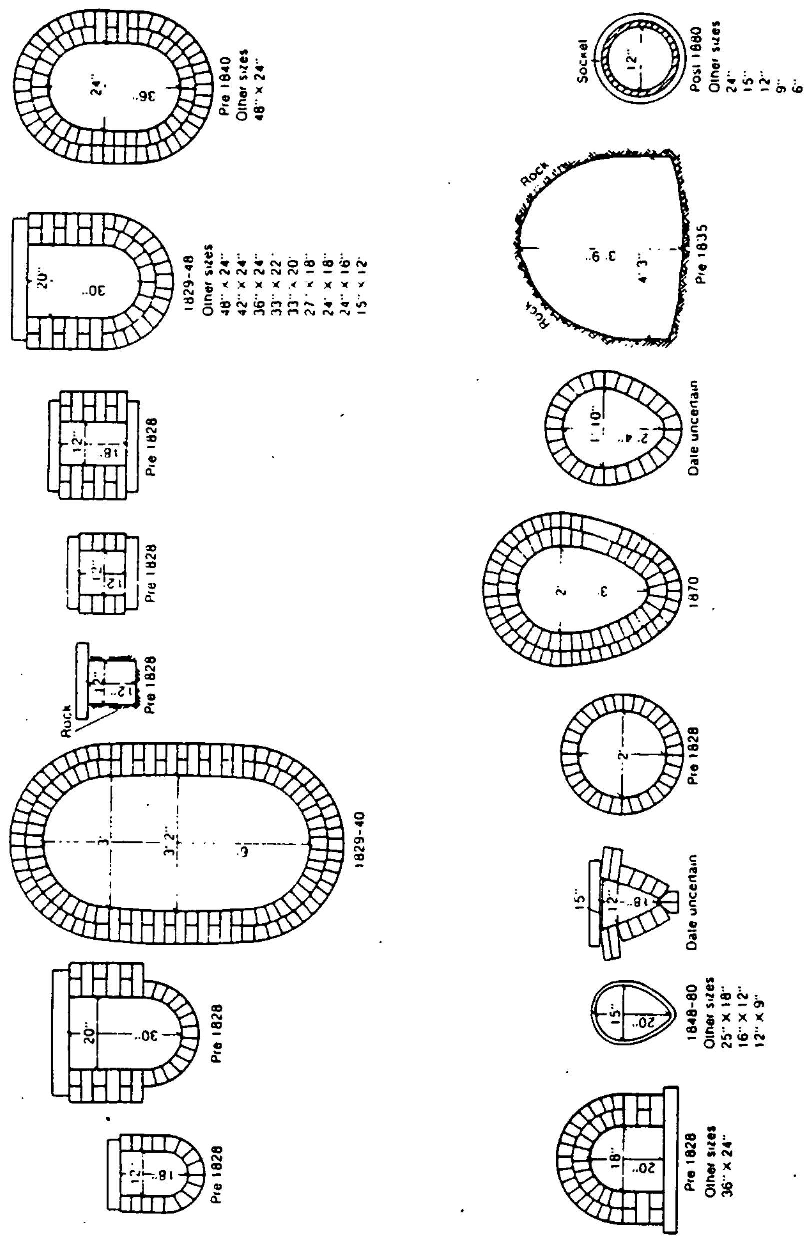

TYPICAL CROSS-SECTIONS OF EARLY SEWERS

FIGURE 1.1

(After Read, ref. 1)

STAGE 1
Mortar is eroded or attacked chemically.
Visible defect: mortar loss.

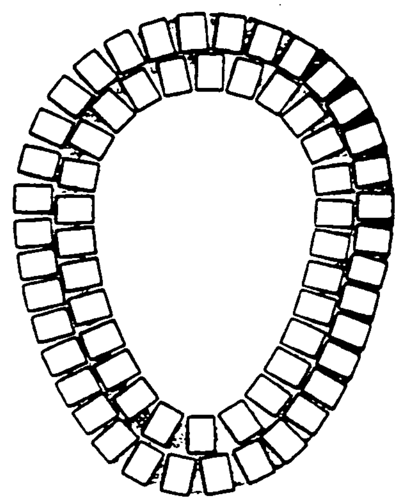

STAGE 2
Loss of mortar between bricks allows joints to close causing inner ring of crown to "squat" and separate from outer ring.
Visible defects: total mortar loss, deformation of crown, displaced bricks.

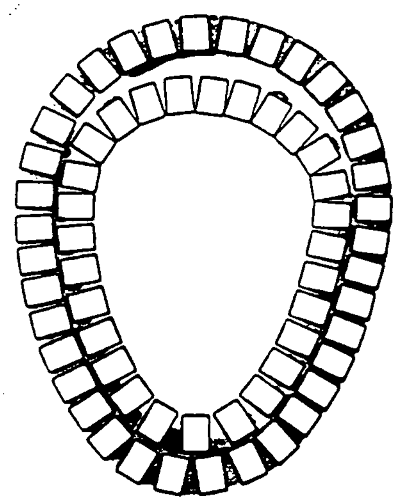

STAGE 3
Loss of compressive load on inner ring of bricks in crown allows bricks to be dislodged and fall causing progressive collapse of inner ring.
Visible defects: missing bricks, bricks in invert.

NB: this mechanism may occur in single ring sewers where the ground "arches" above the sewer, as well as in multi-ring sewers.

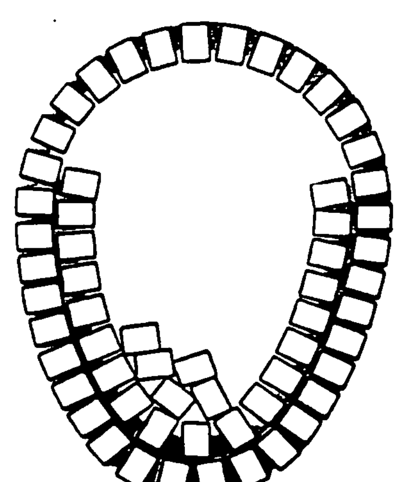

FAILURE DUE TO LOSS OF BRICKS IN CROWN

FIGURE 1.2

(After W.R.C., ref. 2)

STAGE 1
Deterioration of mortar allows infiltration.
Visible defects: mortar loss. Infiltration is rarely visible in the invert.

STAGE 2
Infiltration rate rises and brings in fine soil particles causing voids to form around sewer invert.
Visible defects: mortar loss, sand in sewer, longitudinal crack may be visible near water level.

STAGE 3
Deterioration of mortar and loss of support beneath sewer allows invert section to drop into void. Sewer loses structural integrity and side walls may drop or may be held by mortar or friction.
Visible defects: as above plus fracture around water line, dropped invert, displaced bricks in walls, deformation, loss of level.

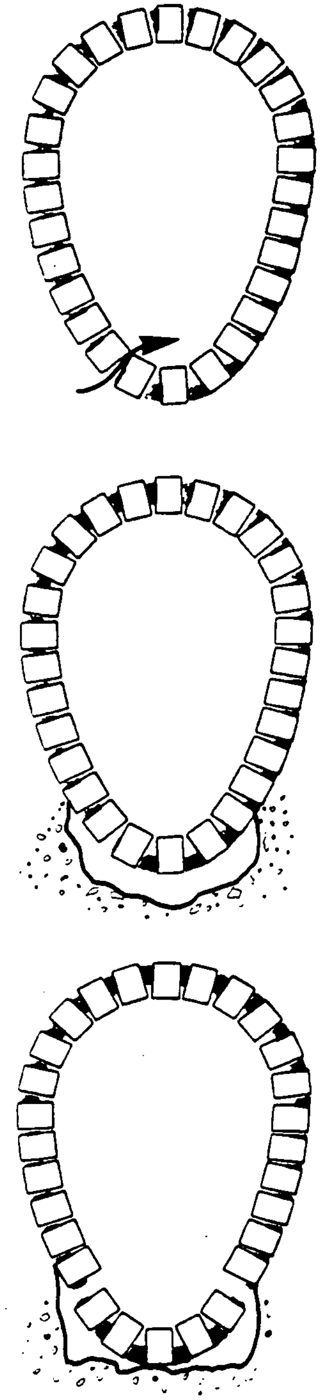

DROPPED INVERT MODE OF FAILURE

FIGURE 1.3

(After W.R.C., ref. 2)

STAGE 1
Mortar loss allows infiltration which begins to wash in fine soil.
Visible defects: mortar loss, infiltration.

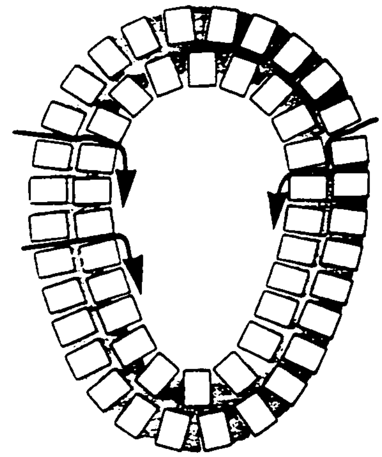

STAGE 2
Voids or zones of low compaction form outside sewer walls allowing the sewer to "spread" at springing level, causing crown to crack and drop.
Visible defects: deformation, crack at crown.

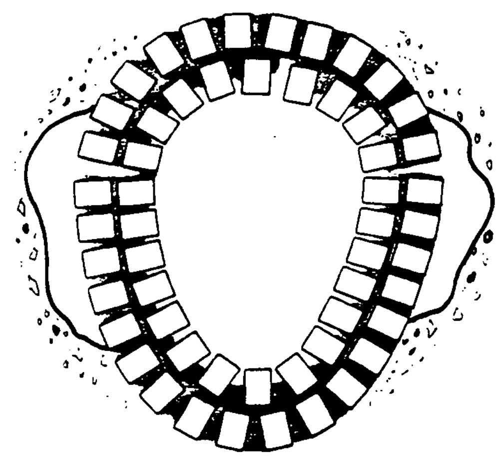

STAGE 3
Mechanism proceeds and fracture forms at crown as the springings continue to spread. Sewer develops "heart" shape and crown eventually collapses.
Visible defects: deformation, hearting, fracture at crown.

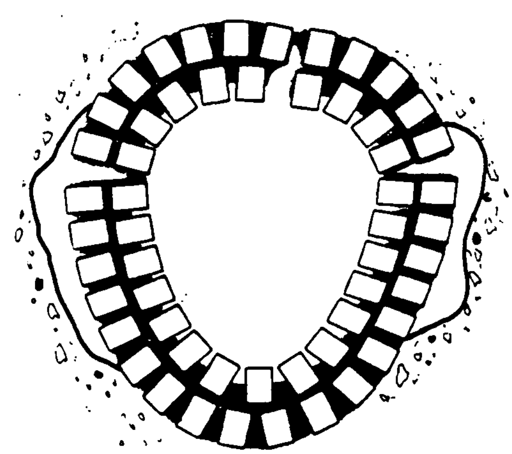

FAILURE DUE TO LOSS OF SIDE SUPPORT

FIGURE 1.4

(After W.R.C., ref. 2)

CHAPTER 2

NON-DESTRUCTIVE METHODS OF ASSESSING MASONRY STRUCTURES

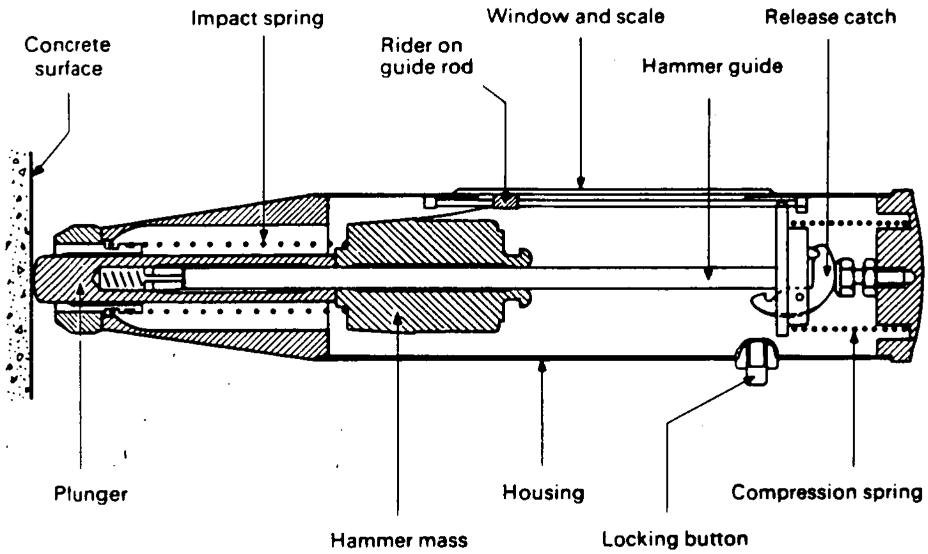

SCHMIDT REBOUND HAMMER

FIGURE 2.1

(After Bungey, ref. 6)

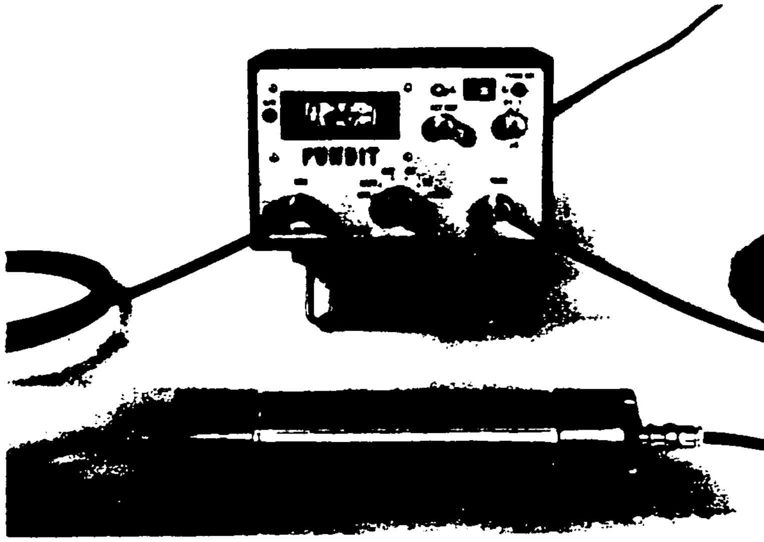

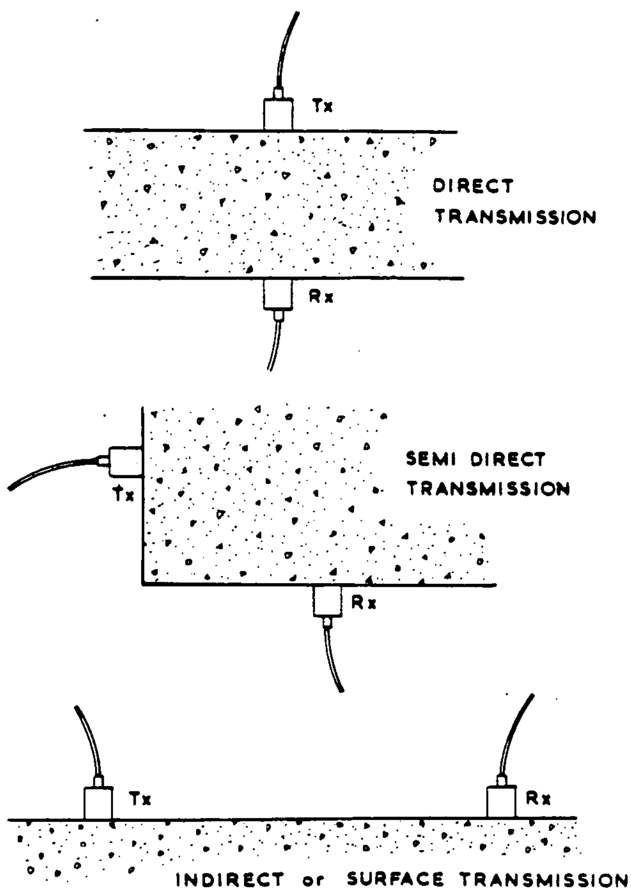

Methods of propogating ultrasonic pulses

ULTRASONIC PULSE VELOCITY MEASUREMENT USING PUNDIT

FIGURE 2.2

(After C.N.S., ref. 89)

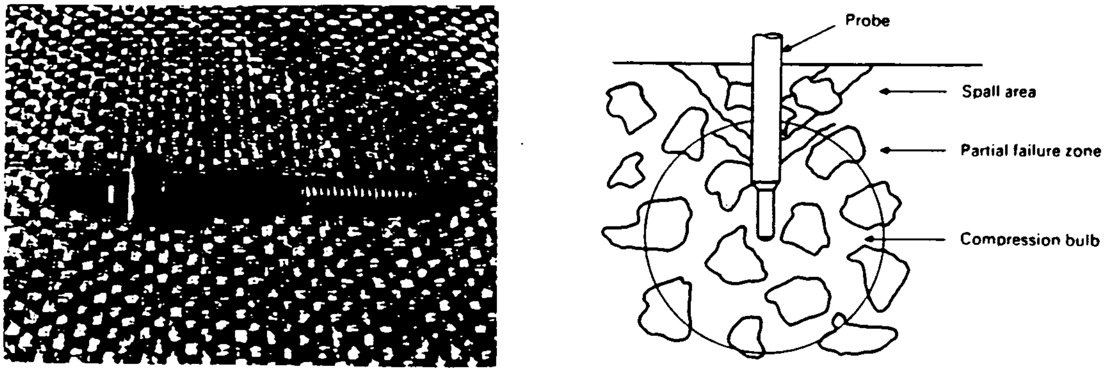

WINDSOR PROBE TEST

FIGURE 2.3

(After Bungey, ref. 6)

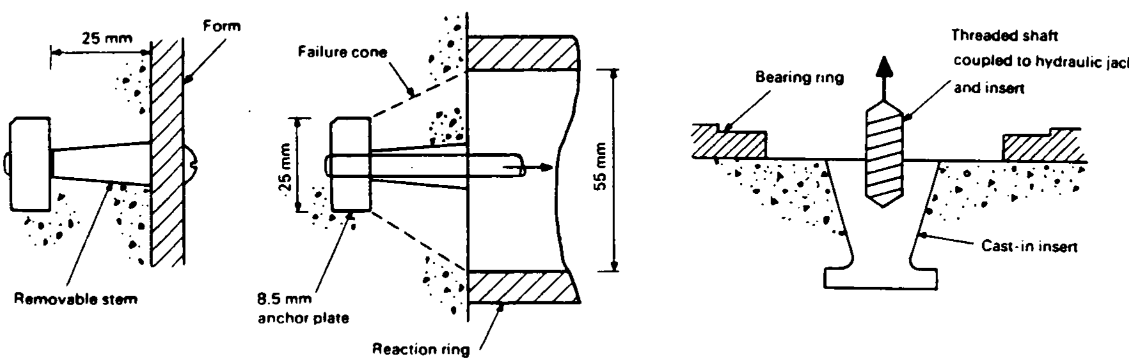

LOK-TEST INSERT AND "AMERICAN" INSERT

FIGURE 2.4

(After Bungey, ref. 6)

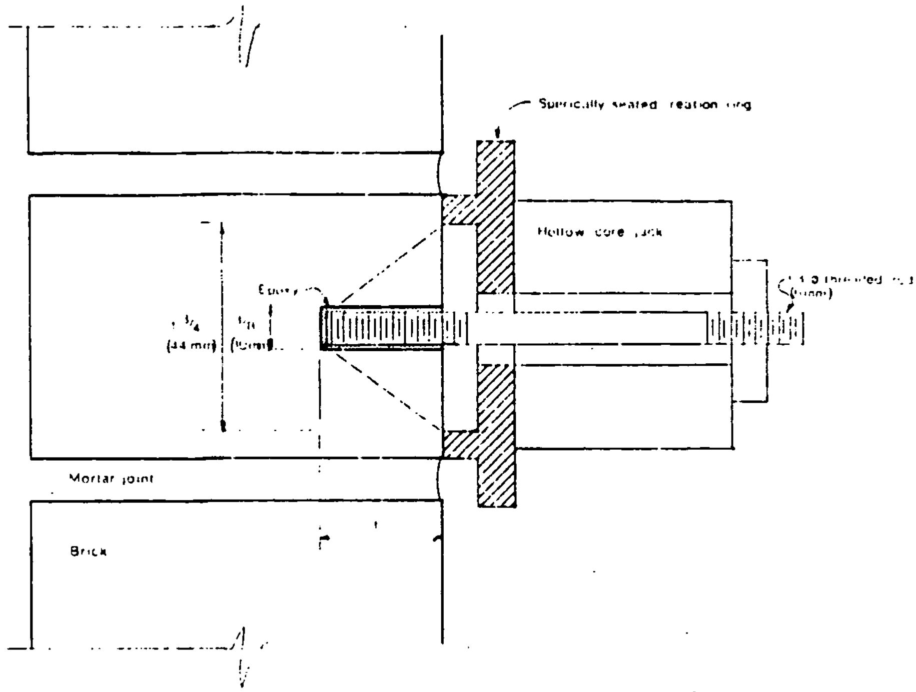

PULL-OUT TEST (MASONRY)

FIGURE 2.5

(After Noland et al, ref. 8)

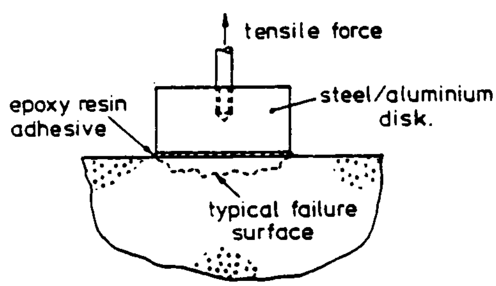

(a) Arrangement for testing uncored specimens

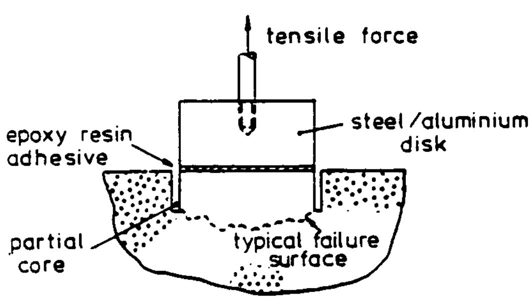

(b) Arrangement for testing partially cored specimens

PULL-OFF TEST

FIGURE 2.6

(After Long, ref. 19)

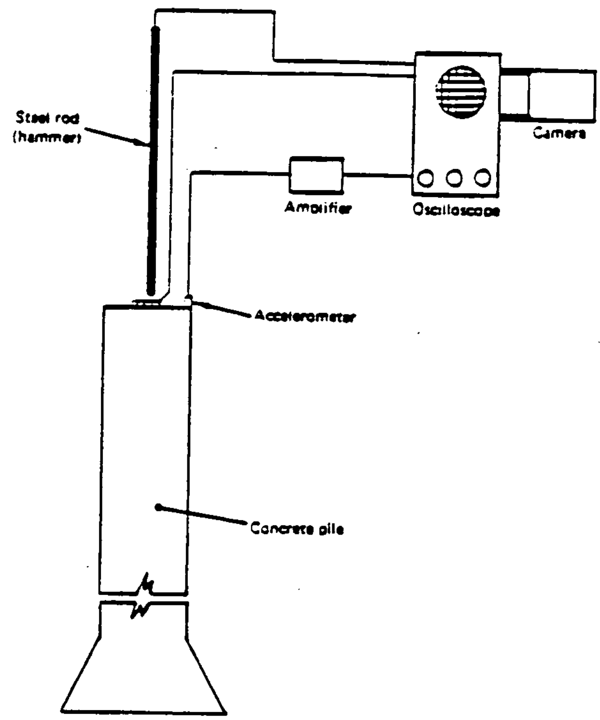

PULSE-ECHO METHOD

FIGURE 2.7

(After Steinbach & Vey, ref. 22)

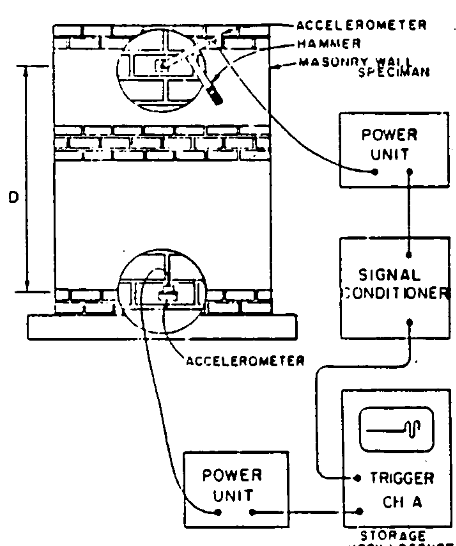

MECHANICAL PULSE SYSTEM

FIGURE 2.8

(After Noland et al, ref. 8)

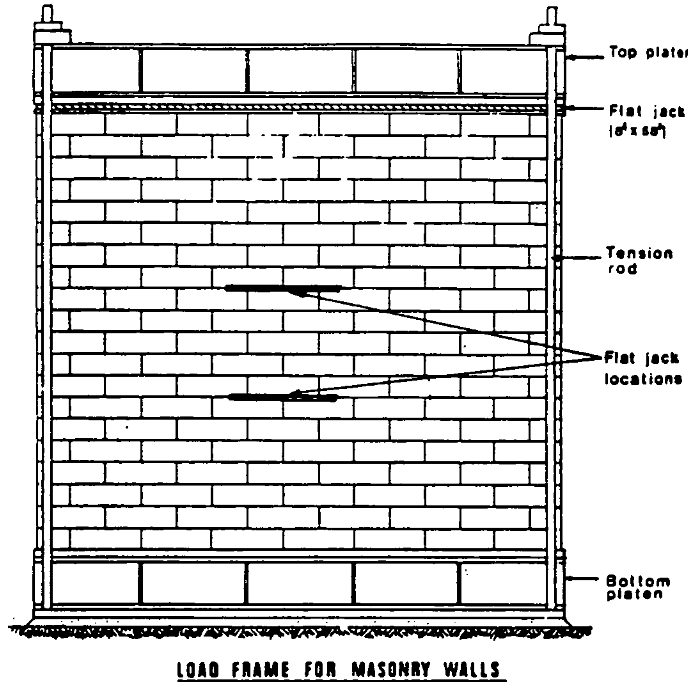

FLATJACK TEST

FIGURE 2.9

(After Rossi, ref. 26)

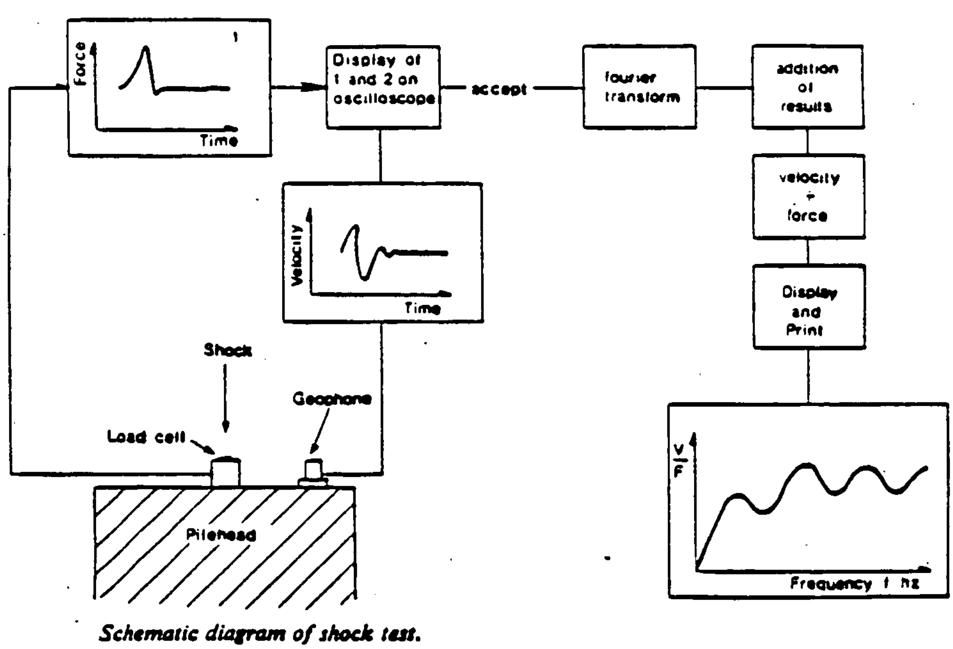

Schematic diagram of shock test.

IMPULSE SHOCK TEST

FIGURE 2.10

(After Higgs & Robertson, ref. 37)

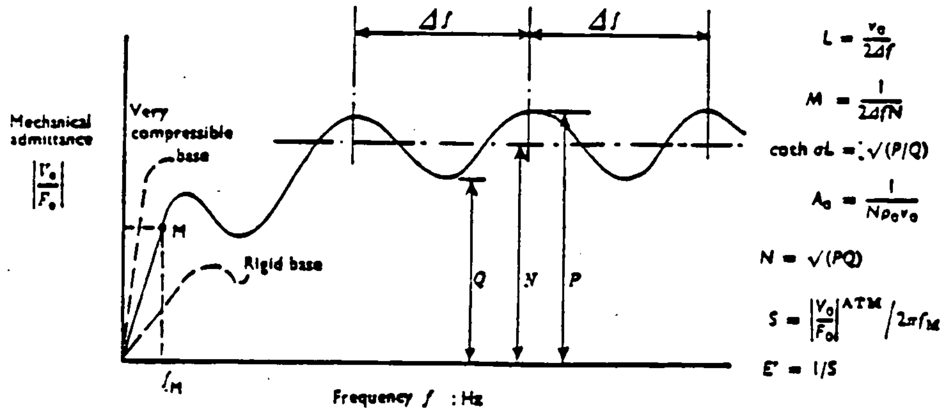

MECHANICAL ADMITTANCE RESPONSE CURVE
FOR A CYLINDRICAL PILE

FIGURE 2.11

(After Davis & Dunn, ref. 23)

(a) rigid base

(b) intermediate elastic base

(c) infinitely compressible base

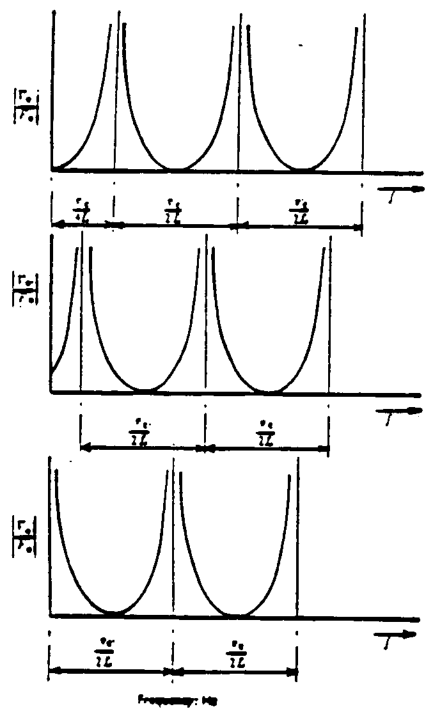

EFFECT OF BASE COMPRESSIBILITY ON RESONANCE FREQUENCY

FIGURE 2.12

(After Davis & Dunn, ref. 23)

CHAPTER 3

WAVE PROPAGATION

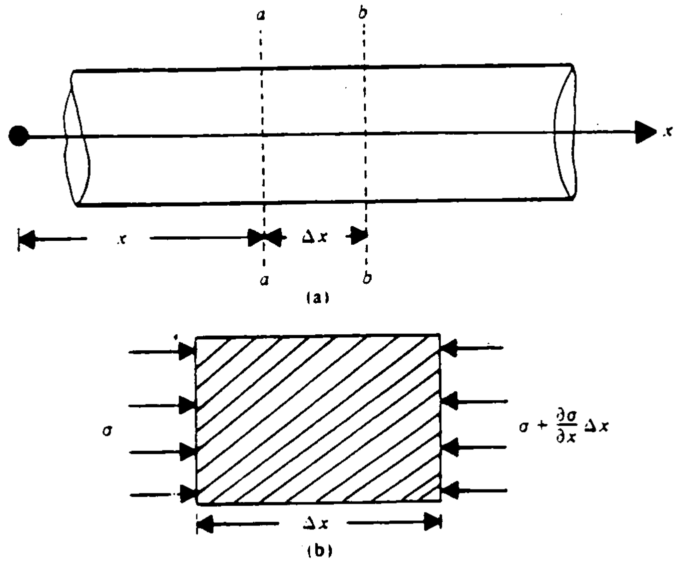

LONGITUDINAL ELASTIC WAVES IN A ROD

FIGURE 3.1

(after Das, ref. 59)

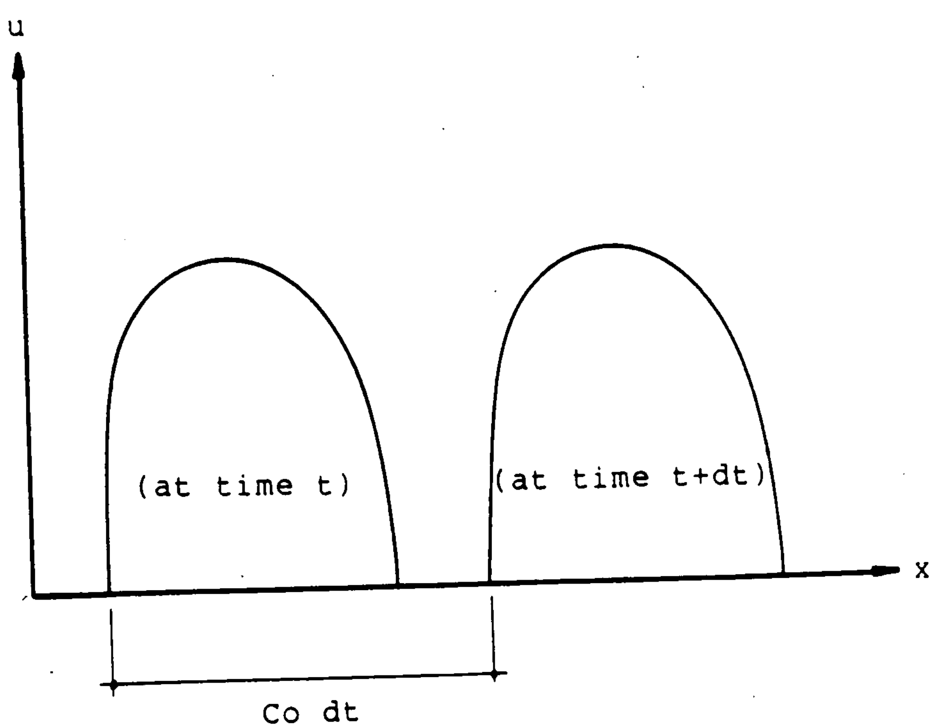

PROPAGATION OF A NON-DISPERSIVE STRESS WAVE

FIGURE 3.2

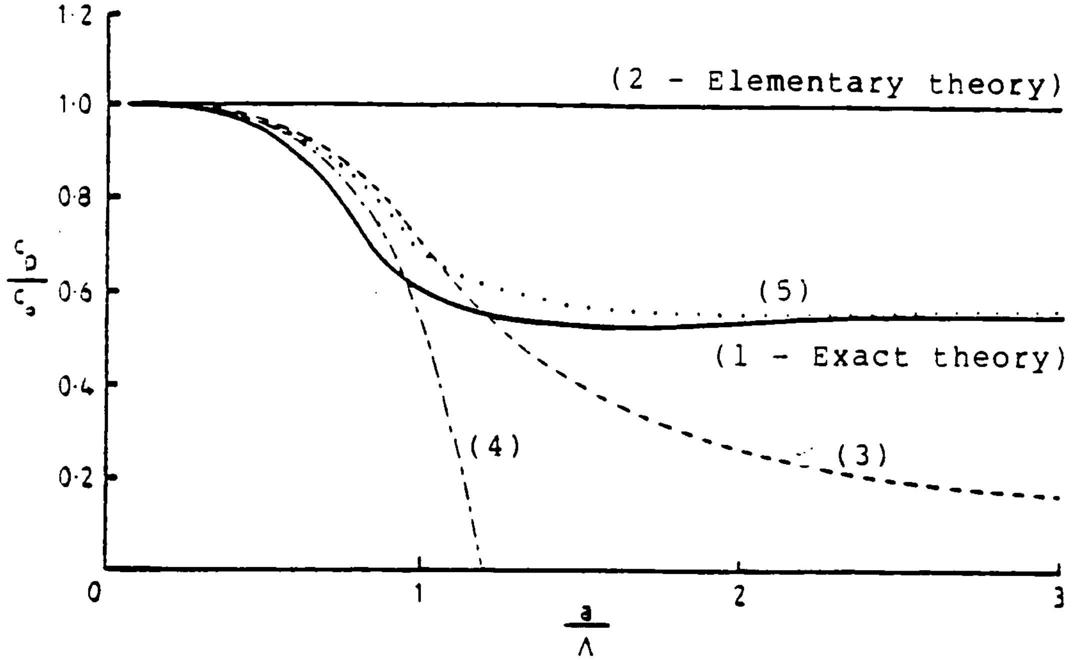

APPROXIMATE THEORIES OF
LONGITUDINAL ELASTIC WAVES IN A CYLINDER

FIGURE 3.3

(after Redwood, ref. 40)

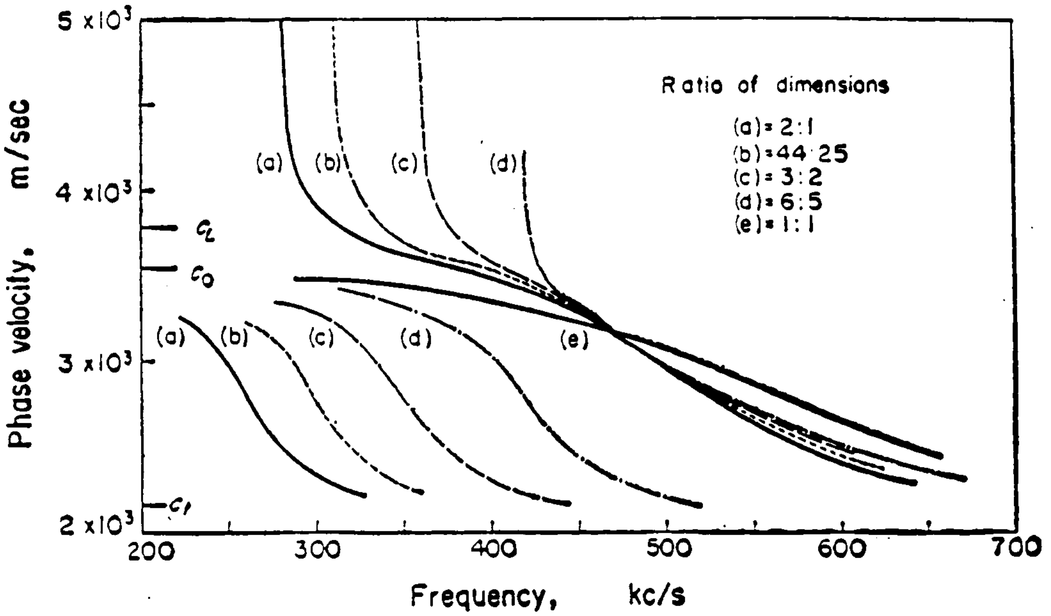

WAVE PROPAGATION IN RECTANGULAR RODS

FIGURE 3.4

(after Morse, ref. 49)

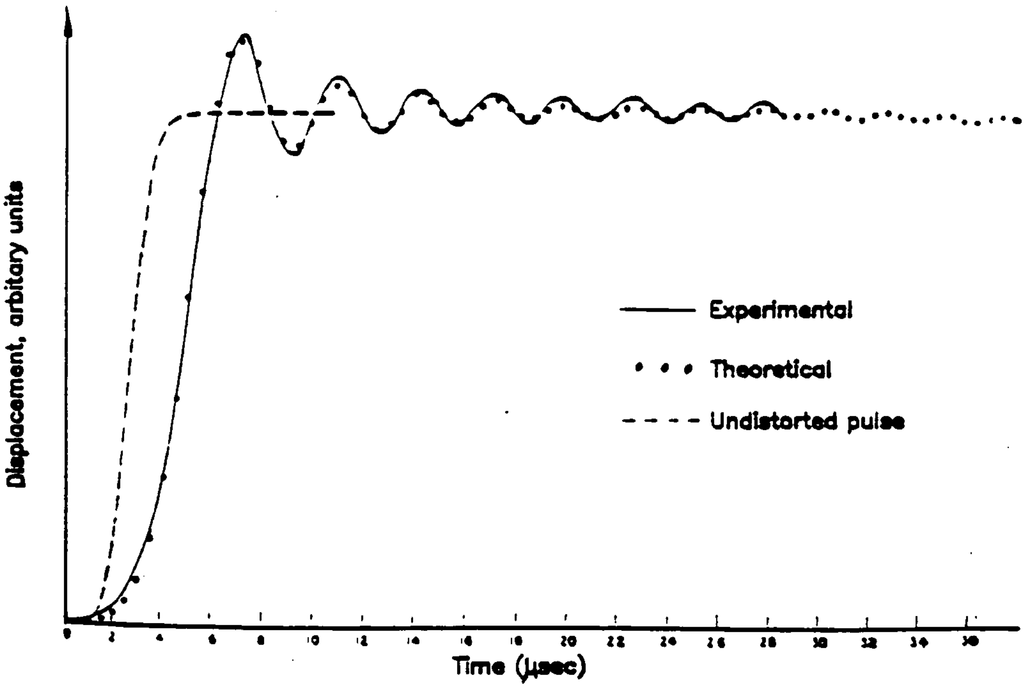

PULSE DISTORTION IN A CYLINDRICAL ROD

FIGURE 3.5

(after Hsieh and Kolsky, ref. 50)

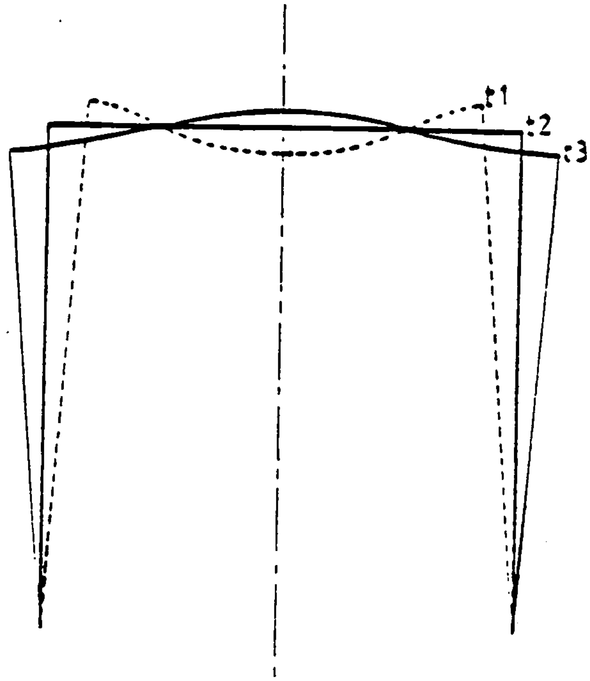

END RESONANCES IN A CYLINDRICAL ROD

FIGURE 3.6

(after Oliver, ref. 52)

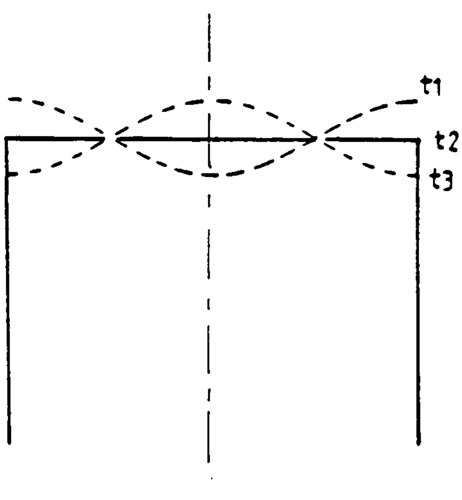

END RESONANCE MODE SHAPES IN A CYLINDRICAL ROD

FIGURE 3.7

(after Chan, ref. 30)

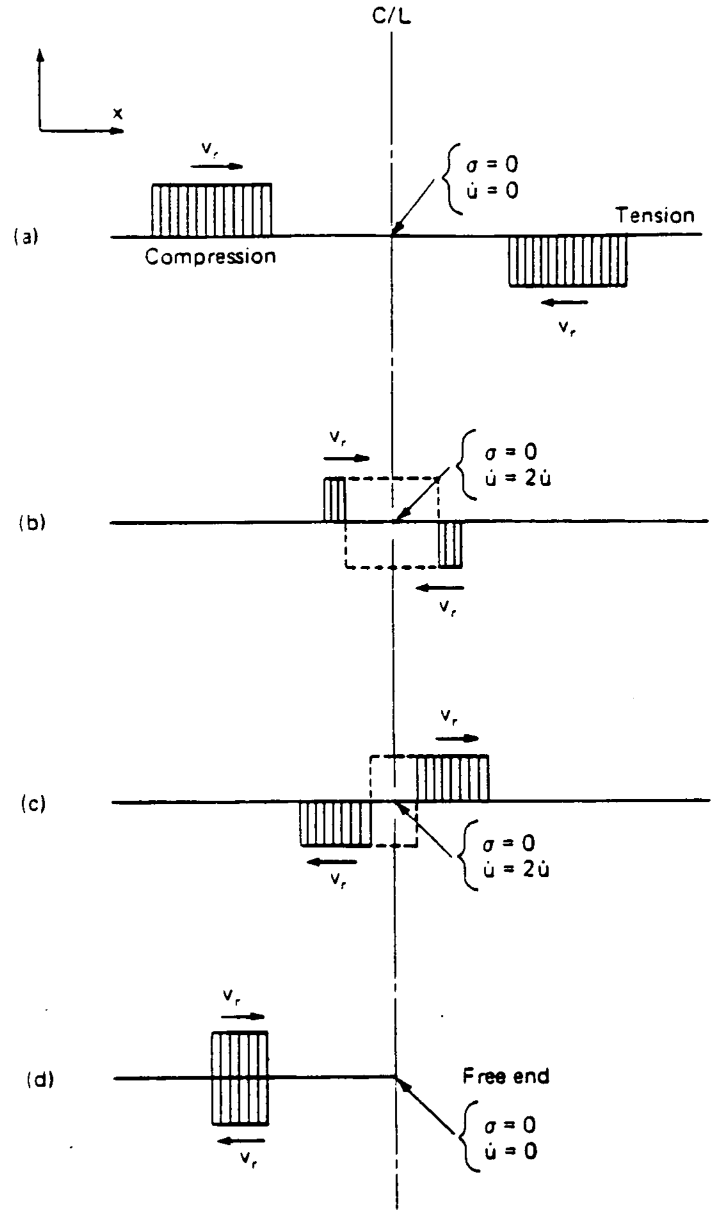

ELASTIC WAVE PROPAGATION IN A BAR WITH FREE ENDS

FIGURE 3.8

(after Prakash, ref. 58)

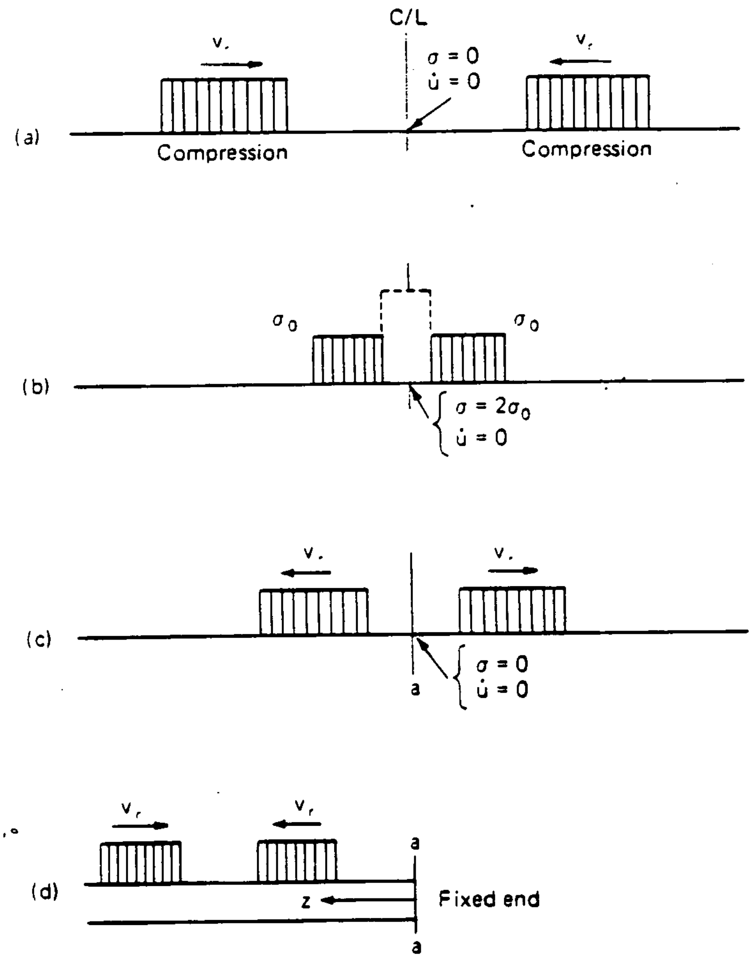

ELASTIC WAVE PROPAGATION IN A BAR WITH FIXED ENDS

FIGURE 3.9

(after Prakash, ref. 58)

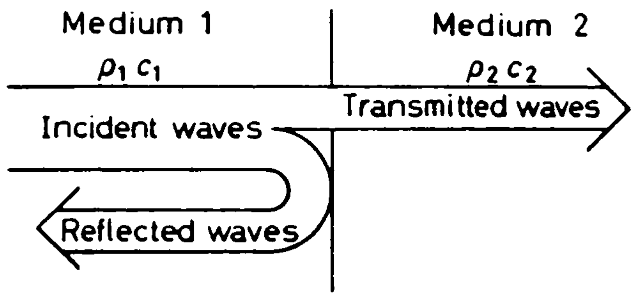

REFLECTION AND TRANSMISSION AT A MEDIUM BOUNDARY

FIGURE 3.10

(after Filipczynski, ref. 53)

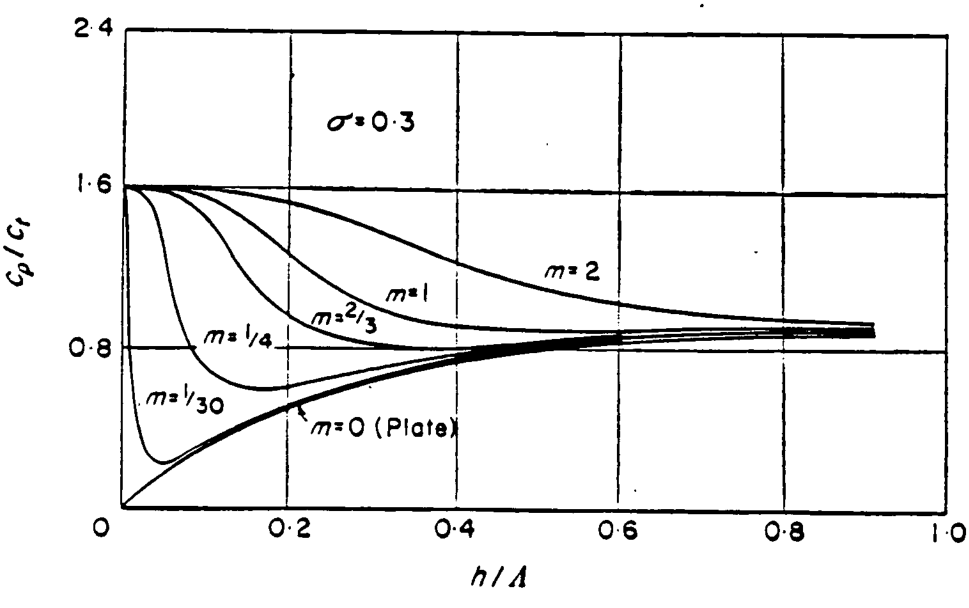

PHASE VELOCITY IN A CYLINDRICAL SHELL

FIGURE 3.11

(after Mirsky and Herrmann, ref. 55)

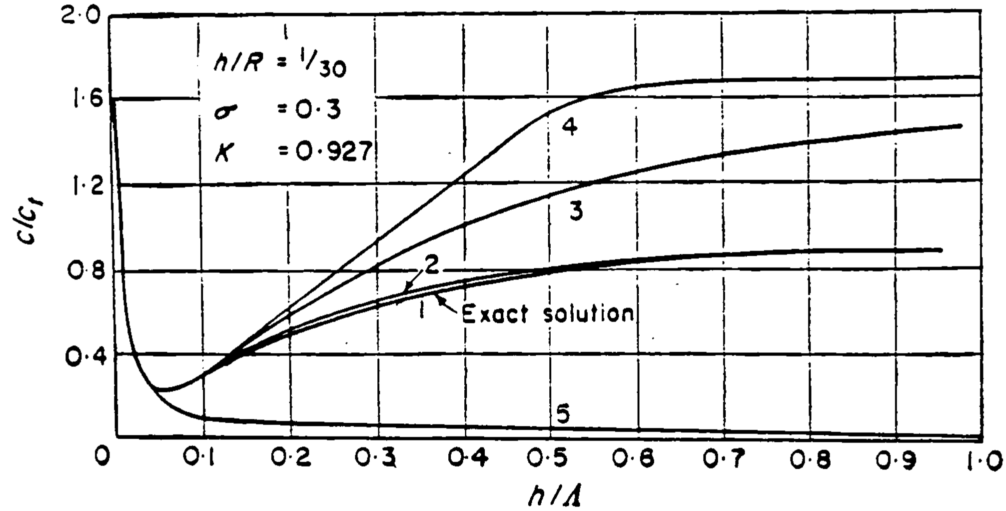

APPROXIMATE THEORY OF LONGITUDINAL WAVES IN A SHELL

FIGURE 3.12

(after Herrmann and Mirsky, ref. 56)

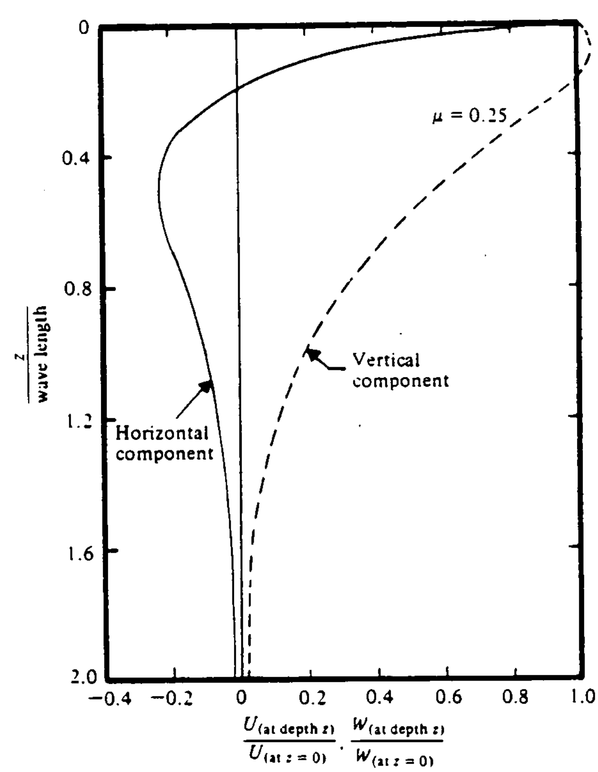

VARIATION OF THE AMPLITUDE OF VIBRATION OF THE HORIZONTAL AND VERTICAL COMPONENTS OF RAYLEIGH WAVES WITH DEPTH

FIGURE 3.13

(after Das, ref. 59)

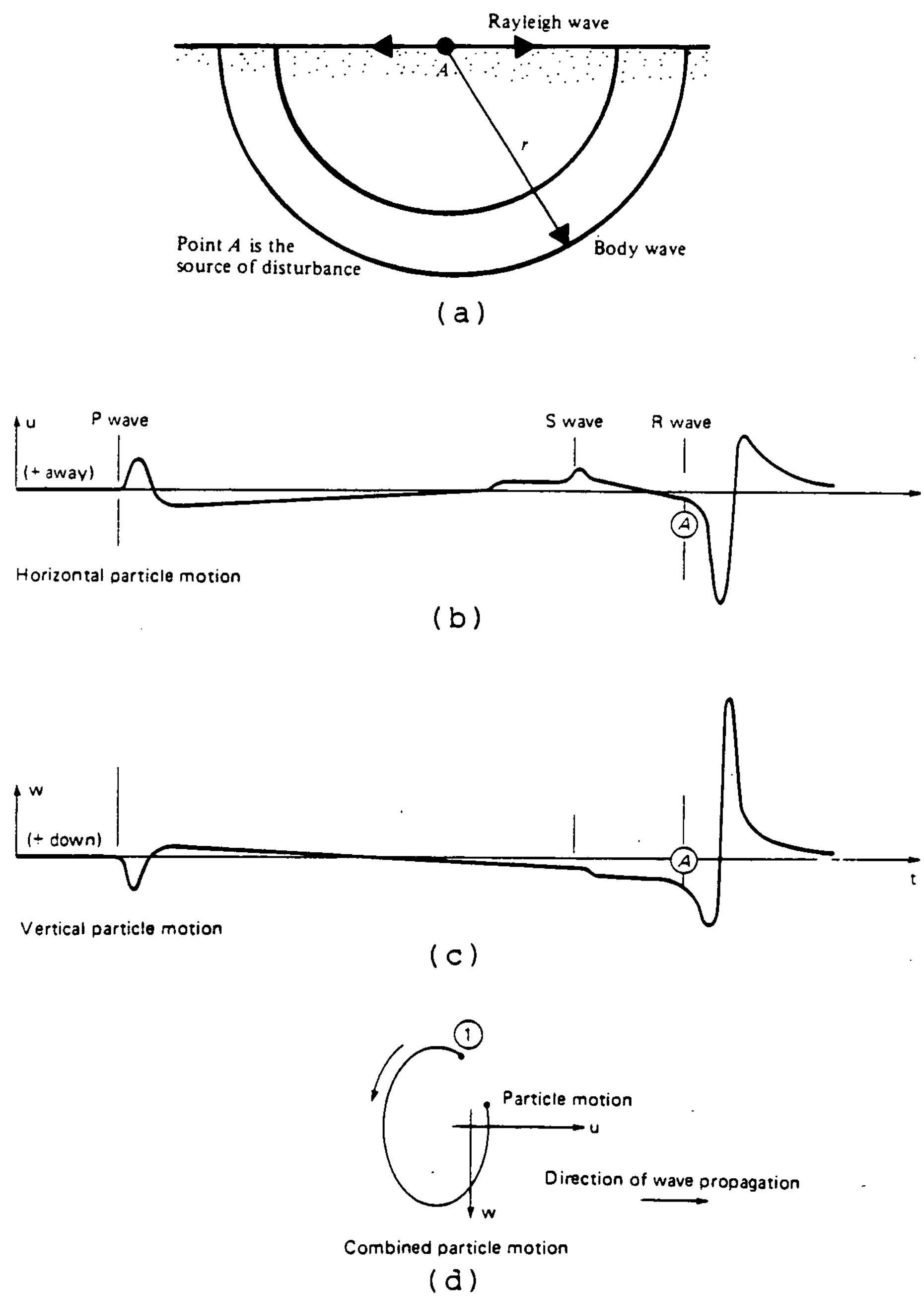

WAVE SYSTEM FROM SURFACE POINT SOURCE IN IDEAL MEDIUM

FIGURE 3.14

(after Woods, ref. 61)

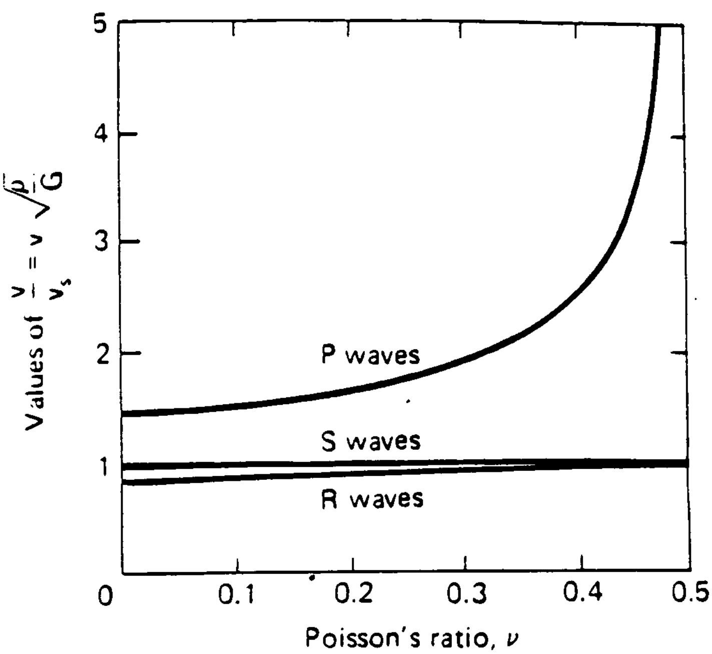

RELATIONSHIP BETWEEN POISSON'S RATIO AND VELOCITIES OF PROPAGATION OF COMPRESSION, SHEAR AND RAYLEIGH WAVES IN A SEMI-INFINITE ELASTIC MEDIUM

FIGURE 3.15

(after Richart, ref. 62)

CHAPTER 4

ANALYSIS AND PROCESSING OF SIGNALS IN TIME AND FREQUENCY DOMAINS

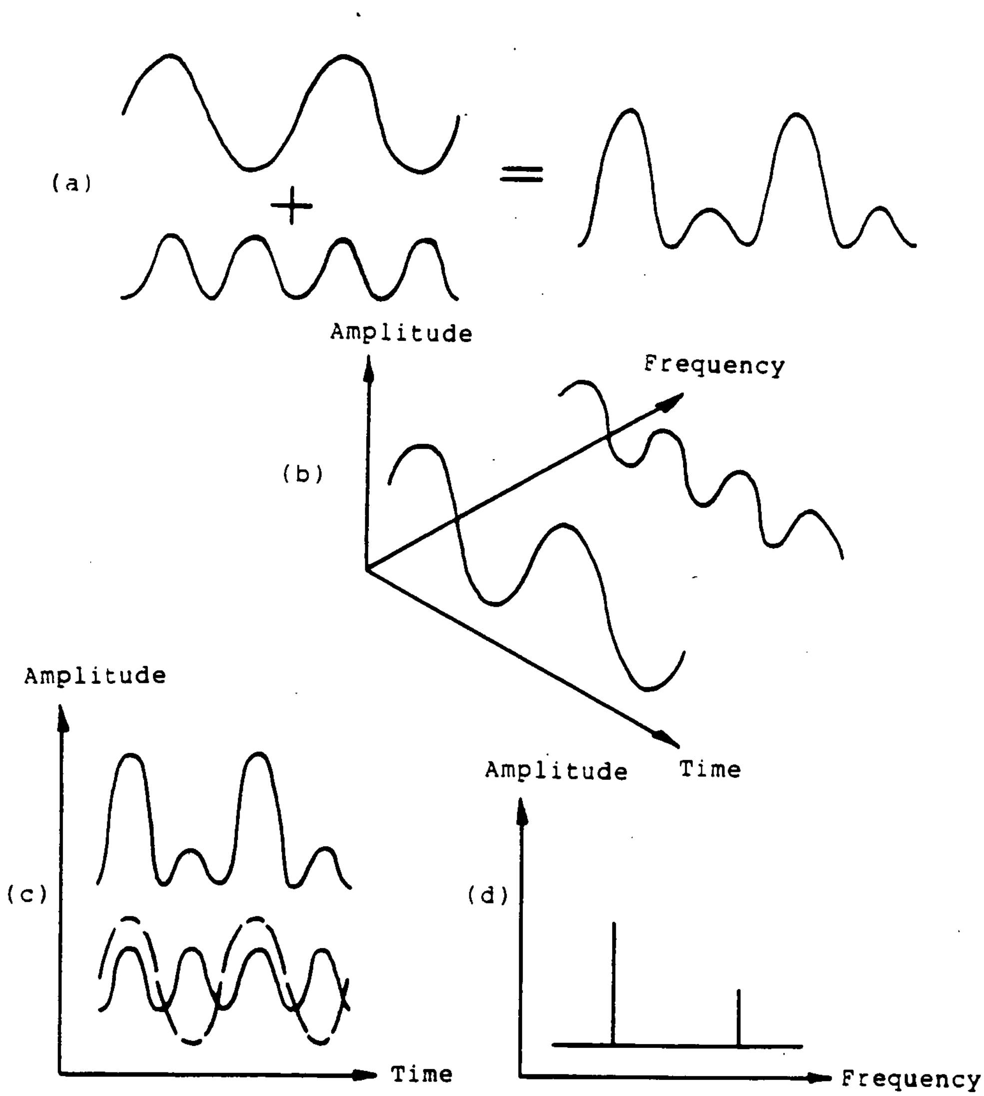

(a) Waveform combination
(b) Three dimensional coordinates showing time, frequency and amplitude
(c) Time domain view
(d) Frequency domain view

THE RELATIONSHIP BETWEEN THE TIME AND FREQUENCY DOMAINS

FIGURE 4.1

$$G(f) = \int_{-\infty}^{\infty} g(t) e^{-i\,2\pi f t}\, dt$$

$$g(t) = \int_{-\infty}^{\infty} G(f) e^{i 2\pi f t}\, df$$

Infinite and continuous in
time and frequency domains

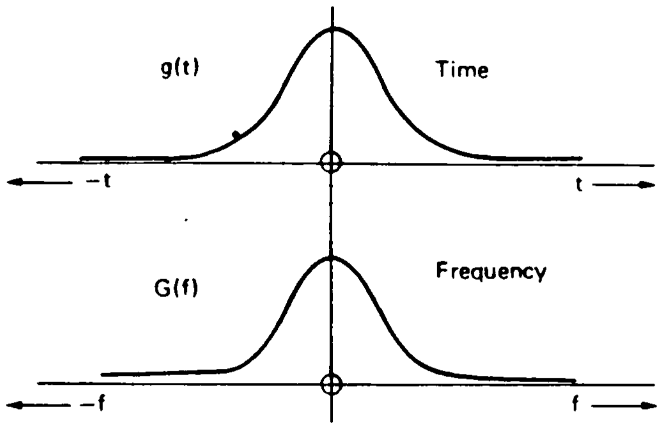

THE INTEGRAL TRANSFORM

FIGURE 4.2

(after Thrane, ref. 64)

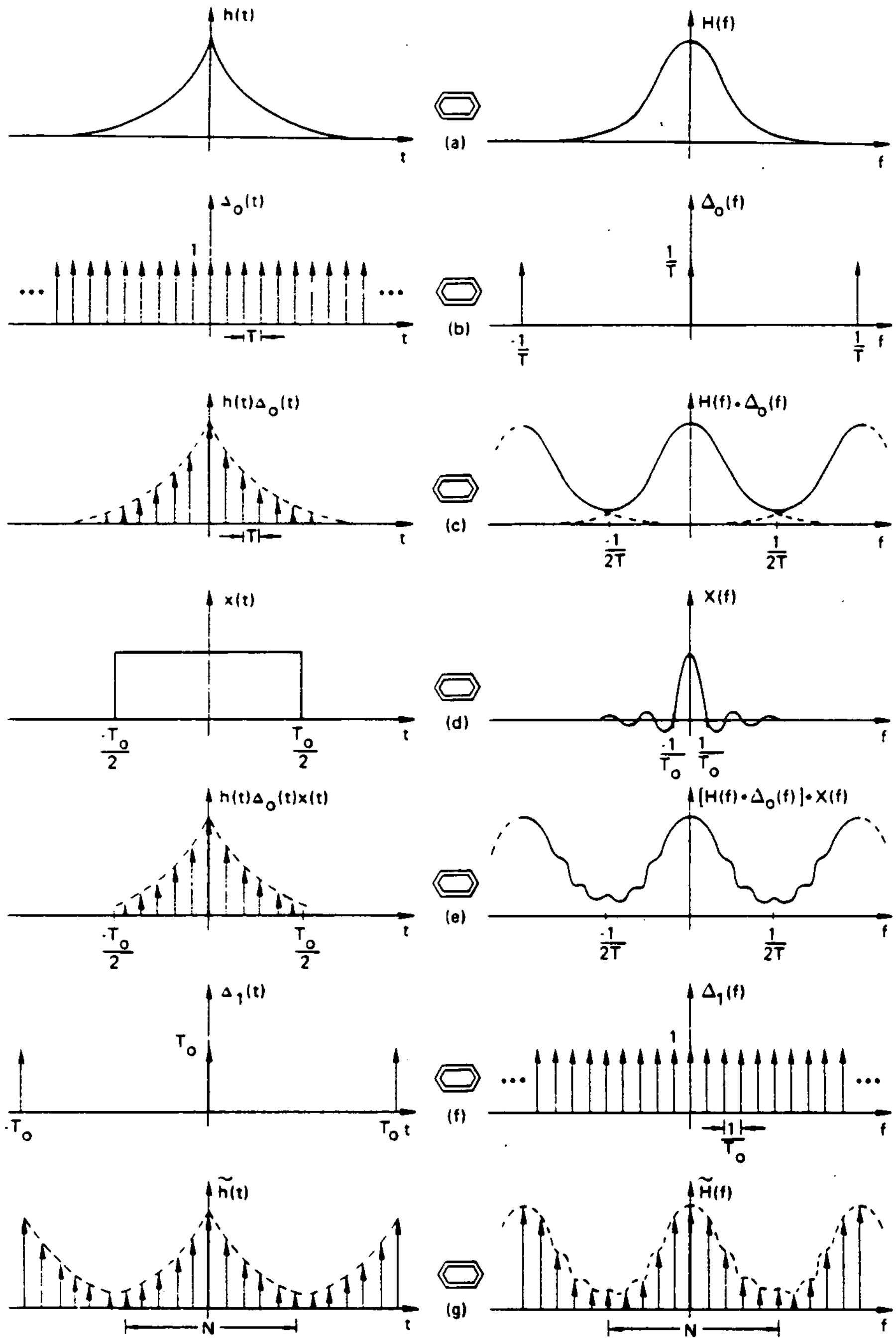

GRAPHICAL DEVELOPMENT OF THE DISCRETE FOURIER TRANSFORM

FIGURE 4.3

(after Brigham, ref. 63)

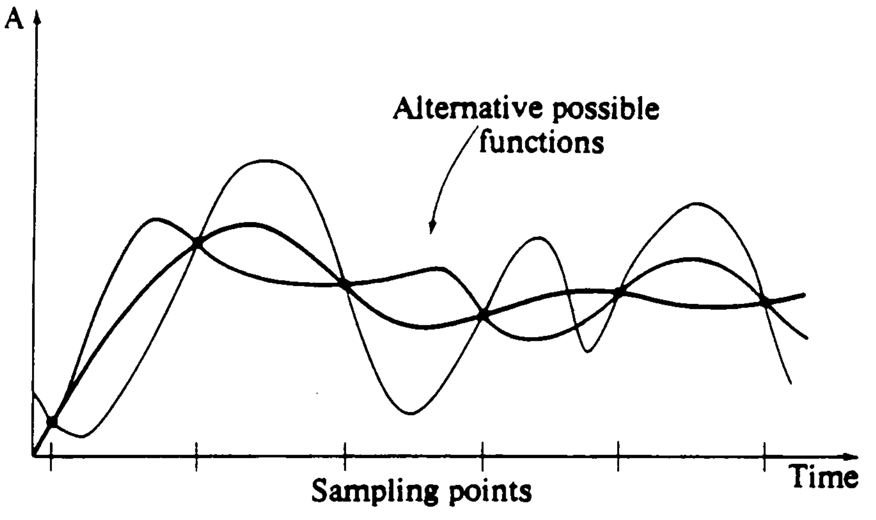

ALIASING

FIGURE 4.4

(after Beauchamp, ref. 65)

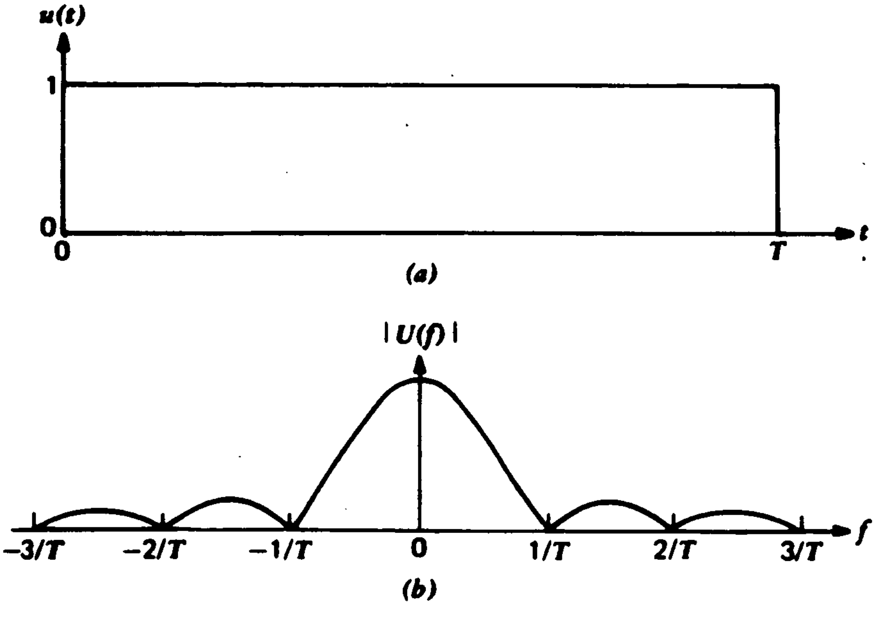

RECTANGULAR WEIGHTING FUNCTION

FIGURE 4.5

(after Bendat, ref. 74)

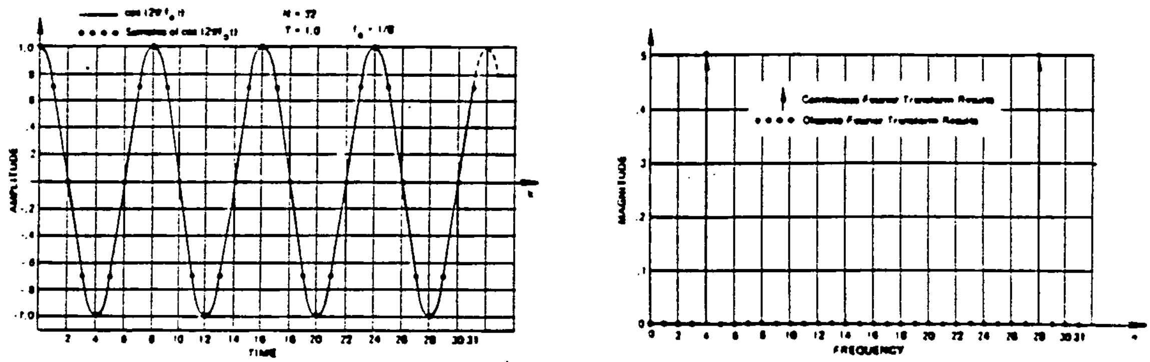

(a) Fourier transform of a cosine waveform: truncation interval equal to a multitude of the period.

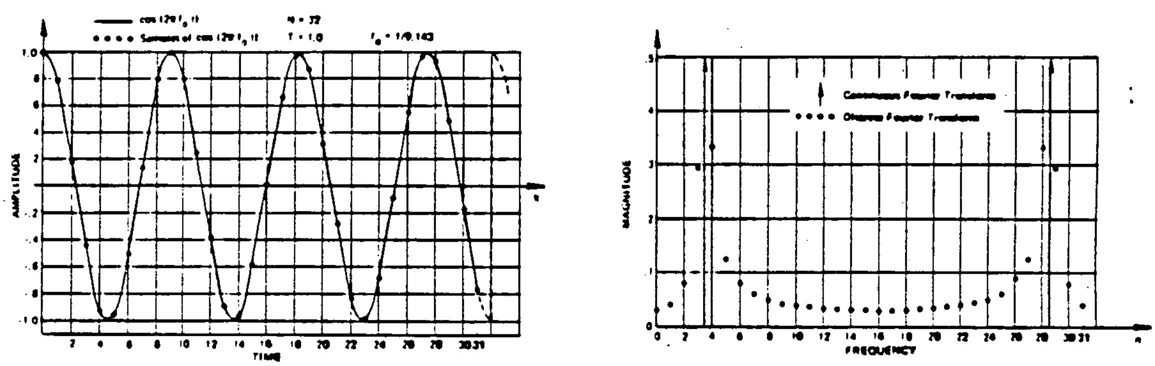

(b) Fourier transform of a cosine waveform: truncation interval not equal to a multiple of the period.

LEAKAGE EFFECTS WITH THE RECTANGULAR WINDOW

FIGURE 4.6

(after Brigham, ref. 63)

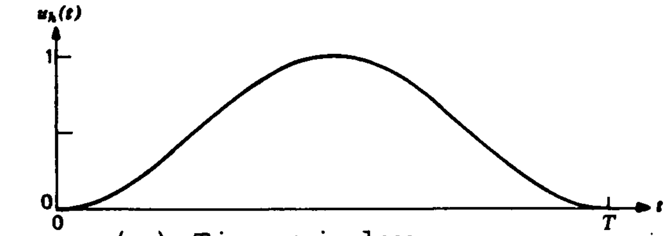

(a) Time window

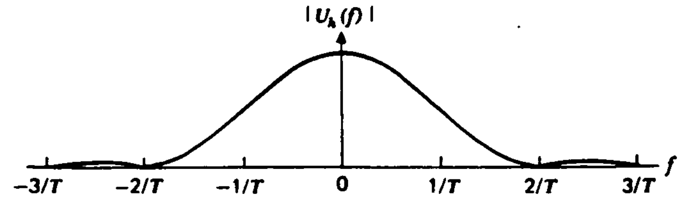

(b) Spectral window

HANNING ANALYSIS WINDOW

FIGURE 4.7

(after Bendat, ref. 74)

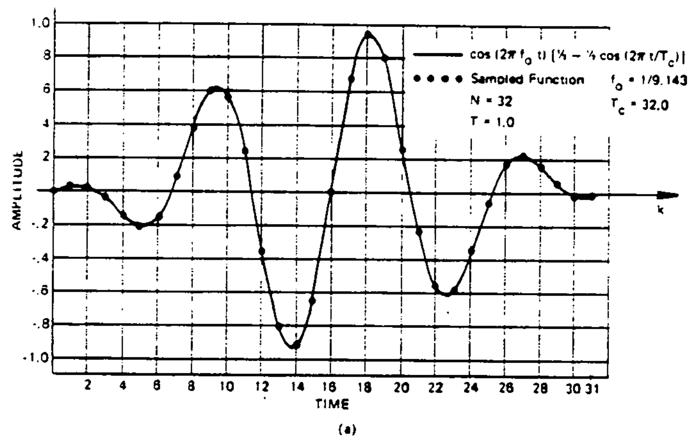

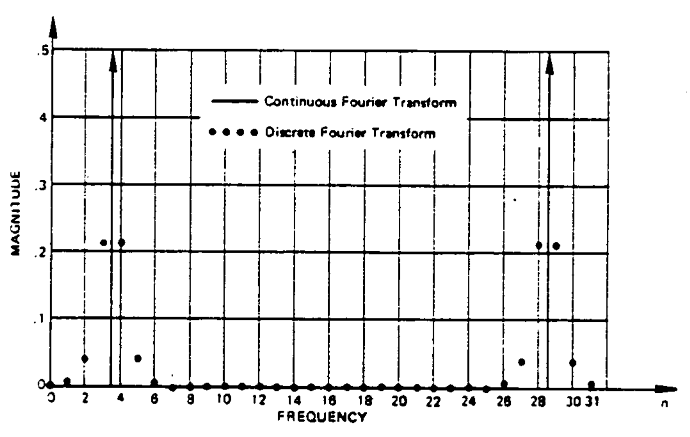

USE OF THE HANNING FUNCTION TO REDUCE LEAKAGE

FIGURE 4.8

(after Brigham, ref. 63)

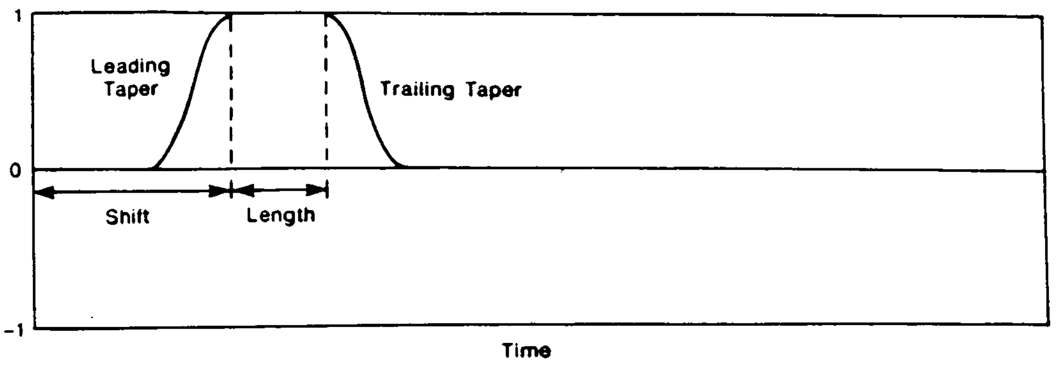

FORCE WINDOW

FIGURE 4.9

(after Sohaney, ref. 68)

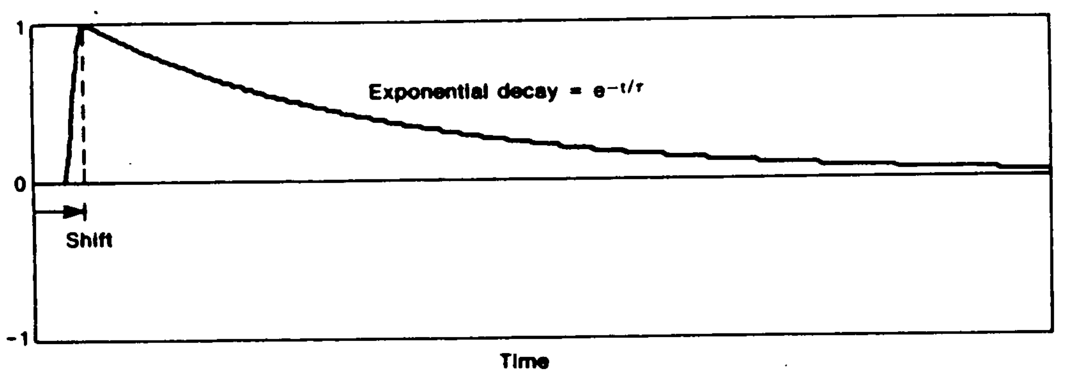

EXPONENTIAL WINDOW

FIGURE 4.10

(after Sohaney, ref. 68)

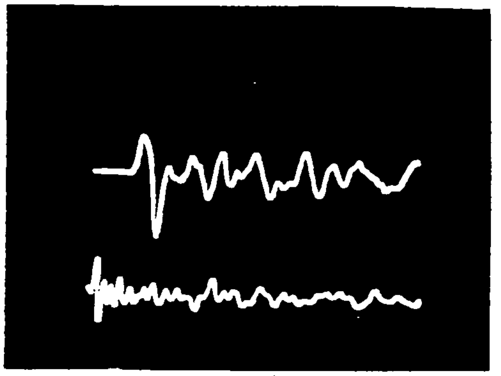

(a) Polaroid records from analogue oscilloscope

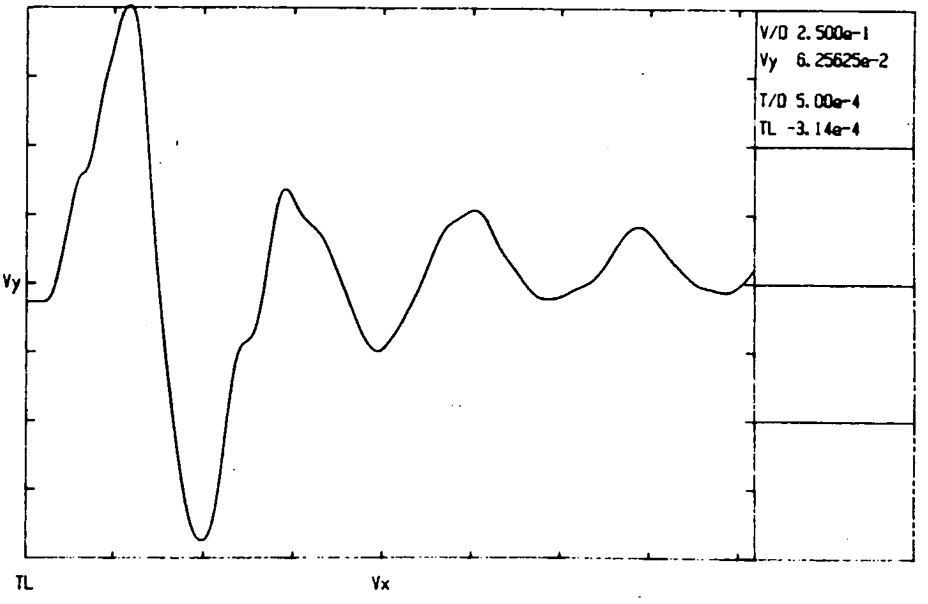

(b) Plot from a digital oscilloscope

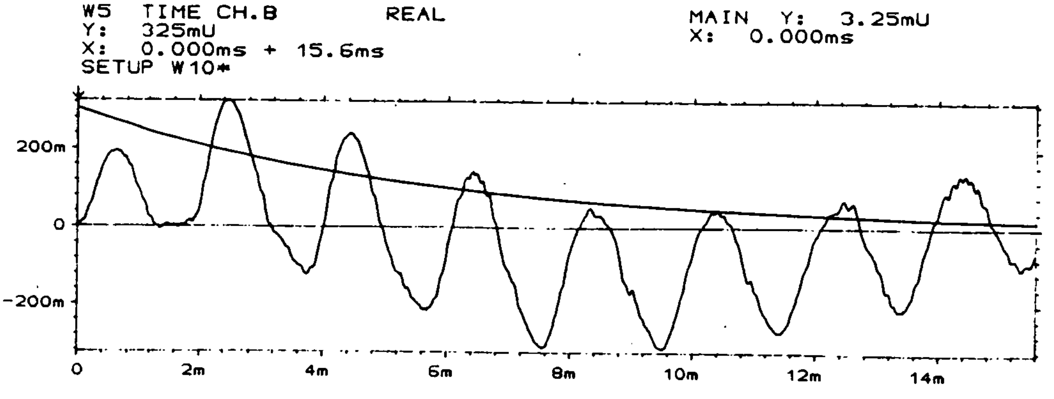

(c) Plots from a signal analyser

TYPICAL TIME HISTORY RECORDS

FIGURE 4.11

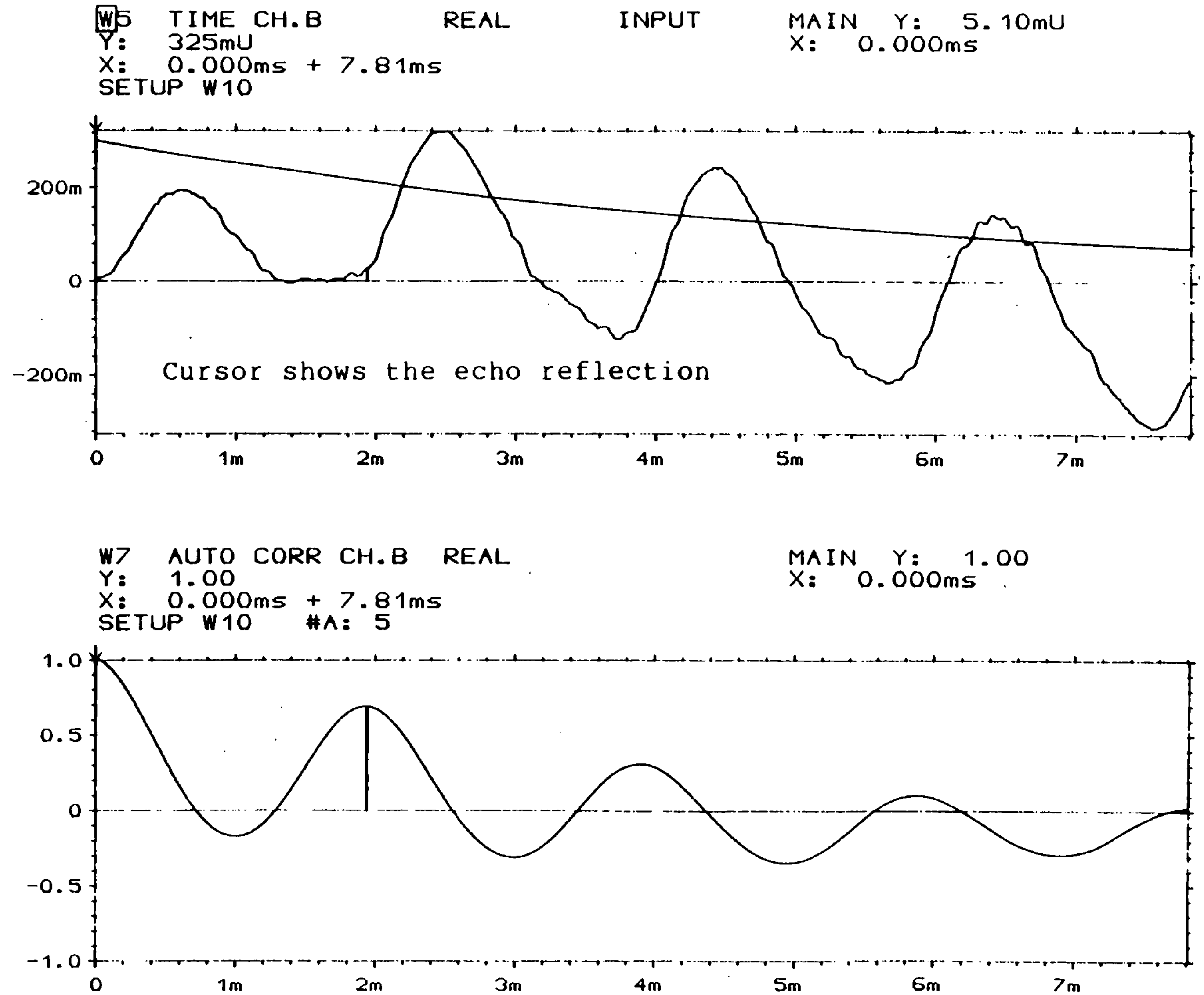

EXPERIMENTAL USE OF AUTO-CORRELATION TO DETECT AN ECHO

FIGURE 4.12

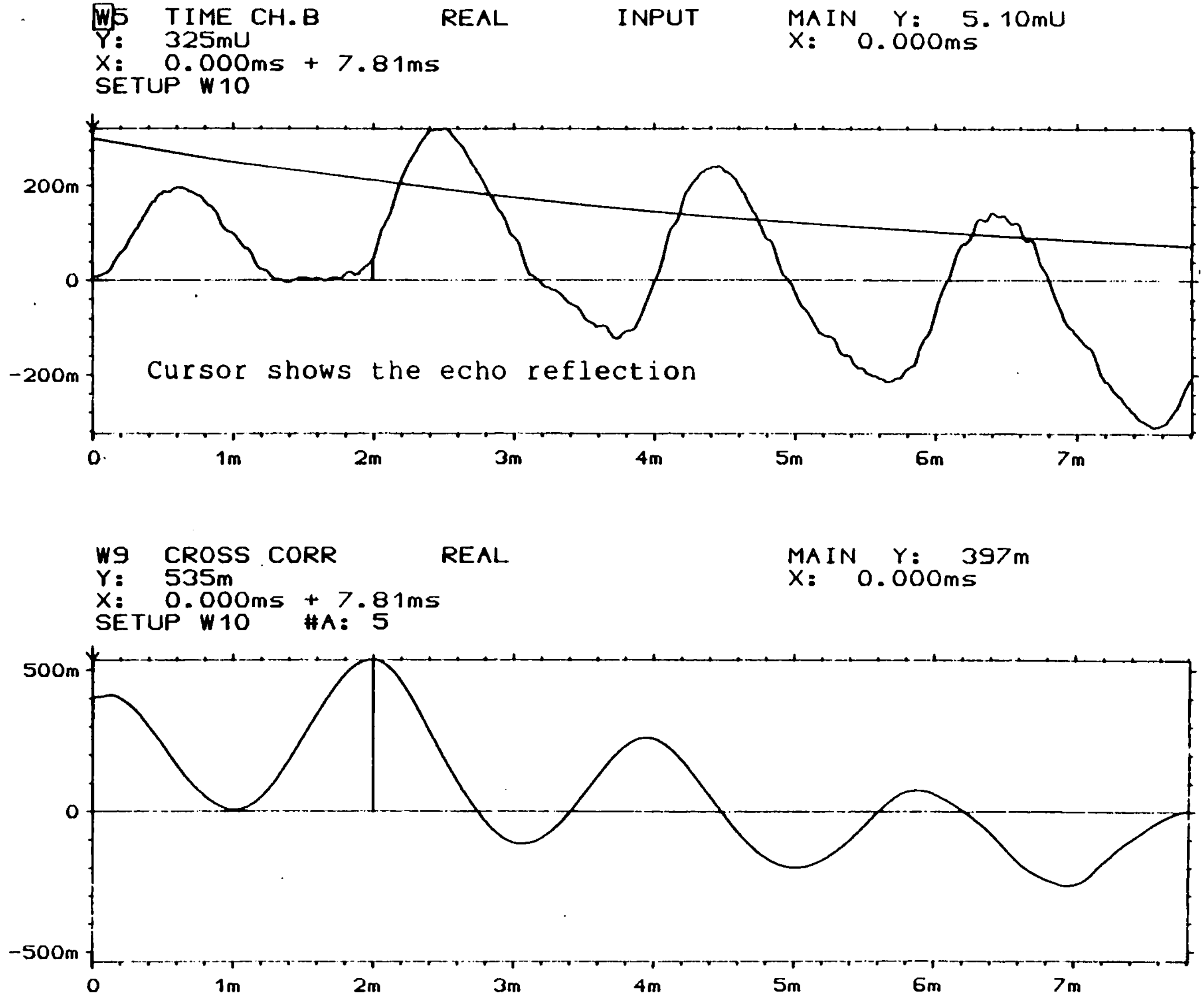

EXPERIMENTAL USE OF CROSS-CORRELATION TO DETECT AN ECHO

FIGURE 4.13

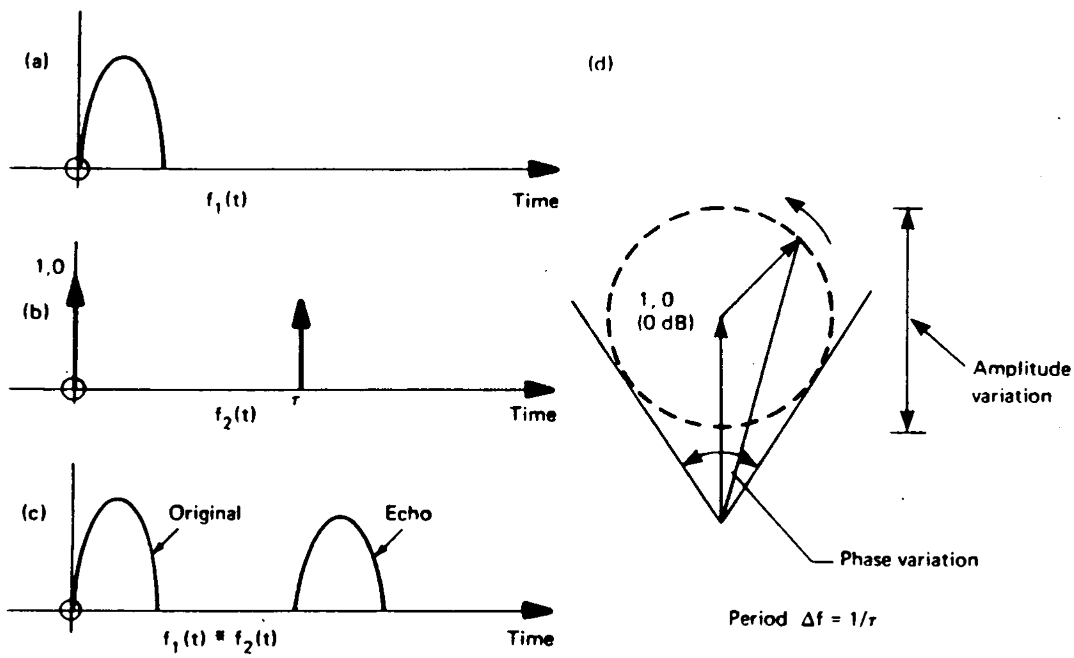

MODEL OF THE USE OF CEPSTRUM TO DETECT AN ECHO

FIGURE 4.14

(after Randall & Hee, ref. 72)

FIGURE 4.15

EXPERIMENTAL USE OF CEPSTRUM TO DETECT AN ECHO

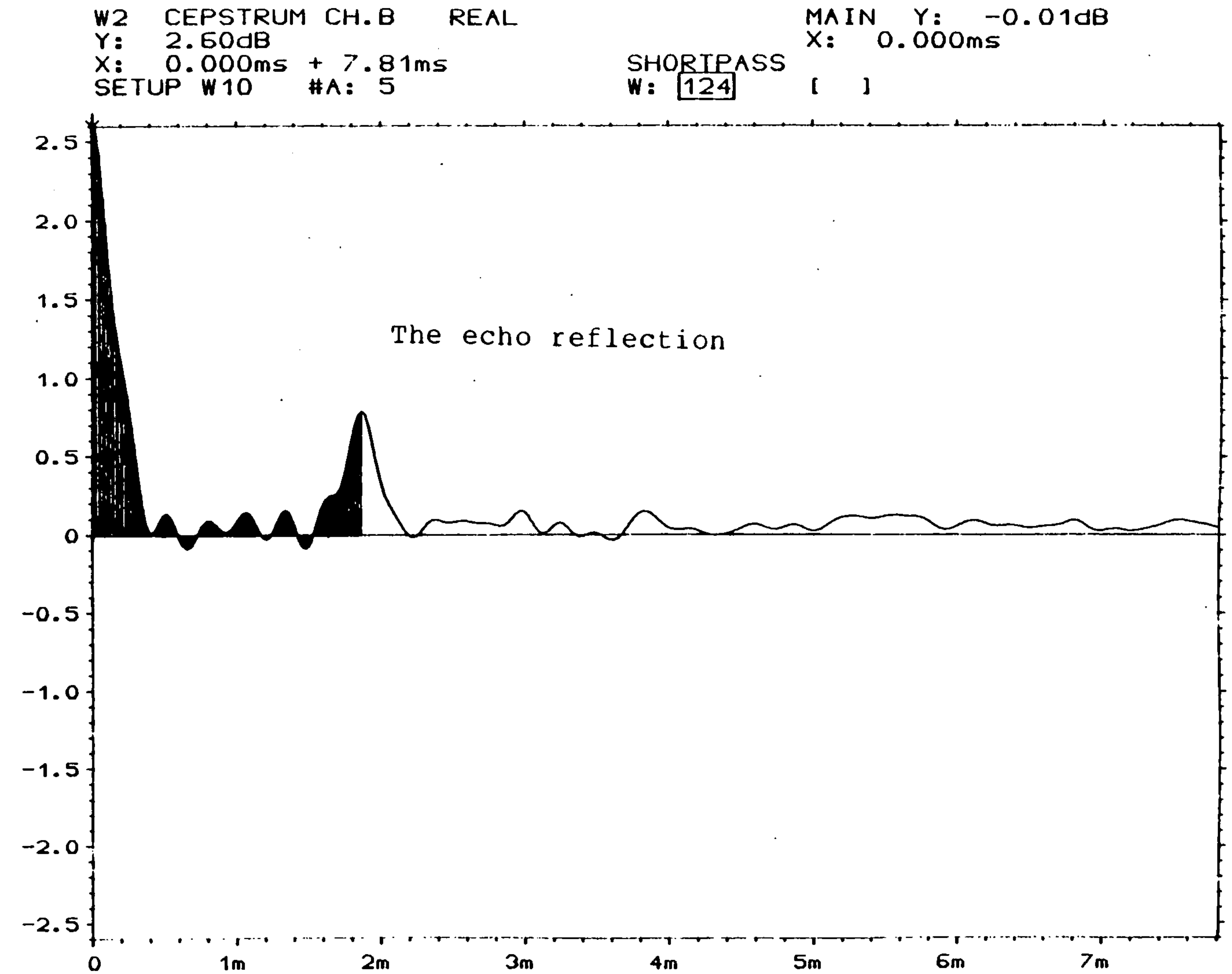

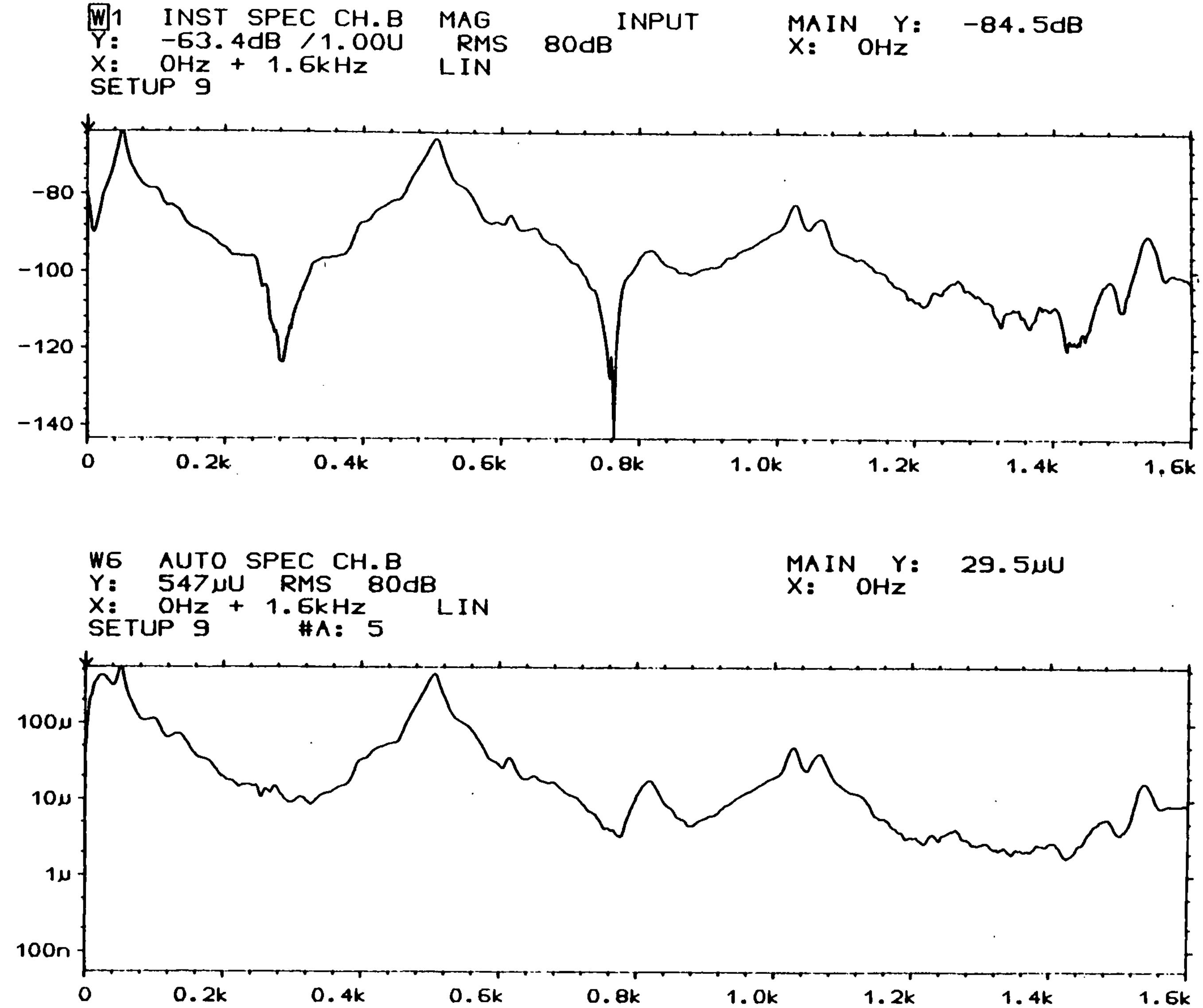

TYPICAL EXPERIMENTAL SPECTRA RECORDS

FIGURE 4.16

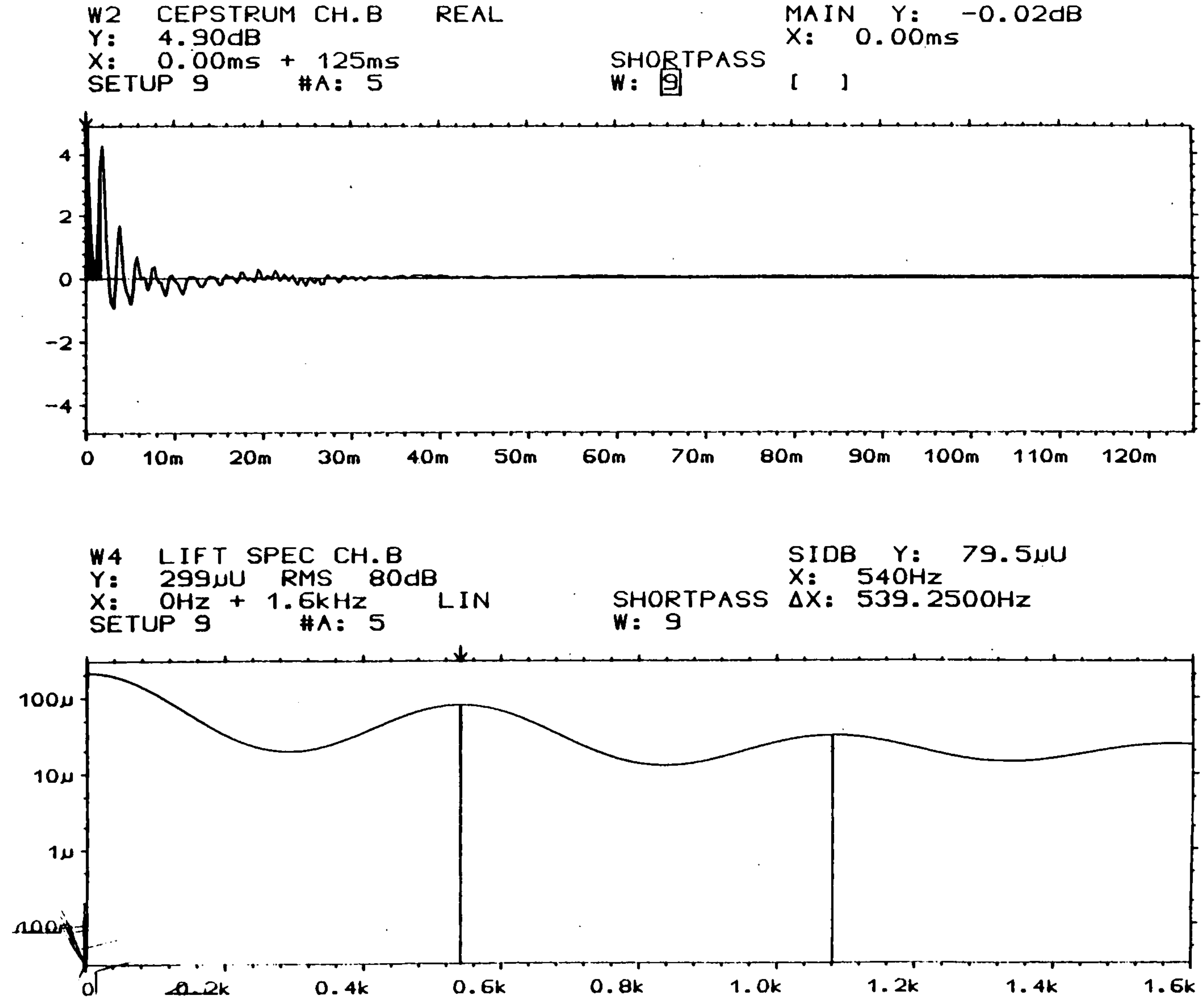

TYPICAL EXPERIMENTAL LIFTERED SPECTRUM RECORD

FIGURE 4.17

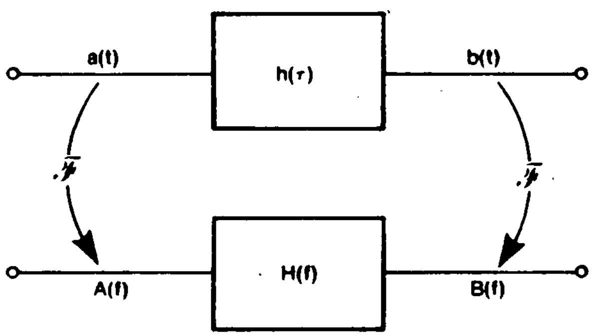

System with input signal a(t) and output signal b(t). The Fourier Transform of a(t) and b(t) are A(f) and B(f) respectively

FIGURE 4.18

(after Herlufsen, ref. 75)

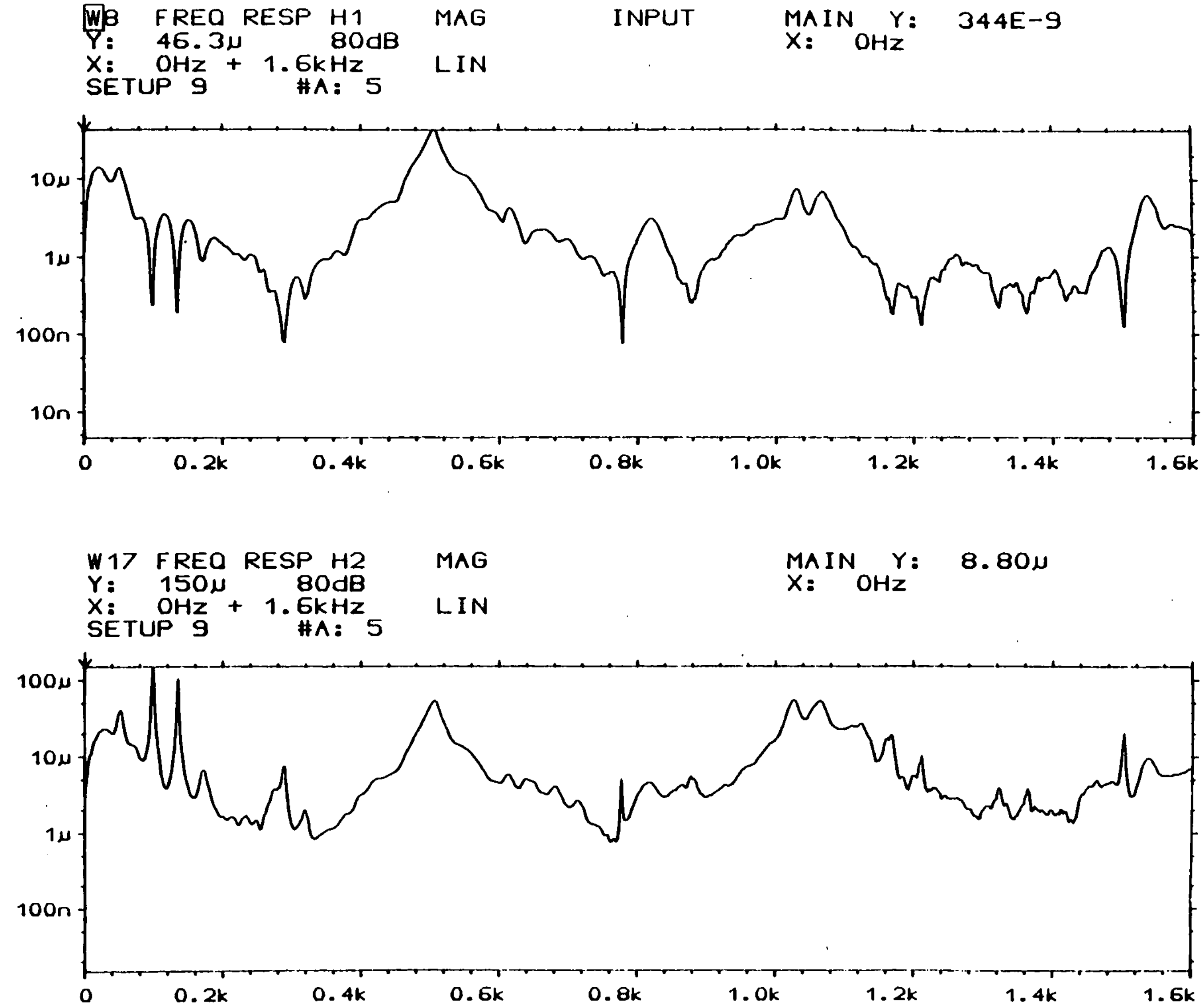

TYPICAL EXPERIMENTAL FREQUENCY RESPONSE FUNCTIONS

FIGURE 4.19

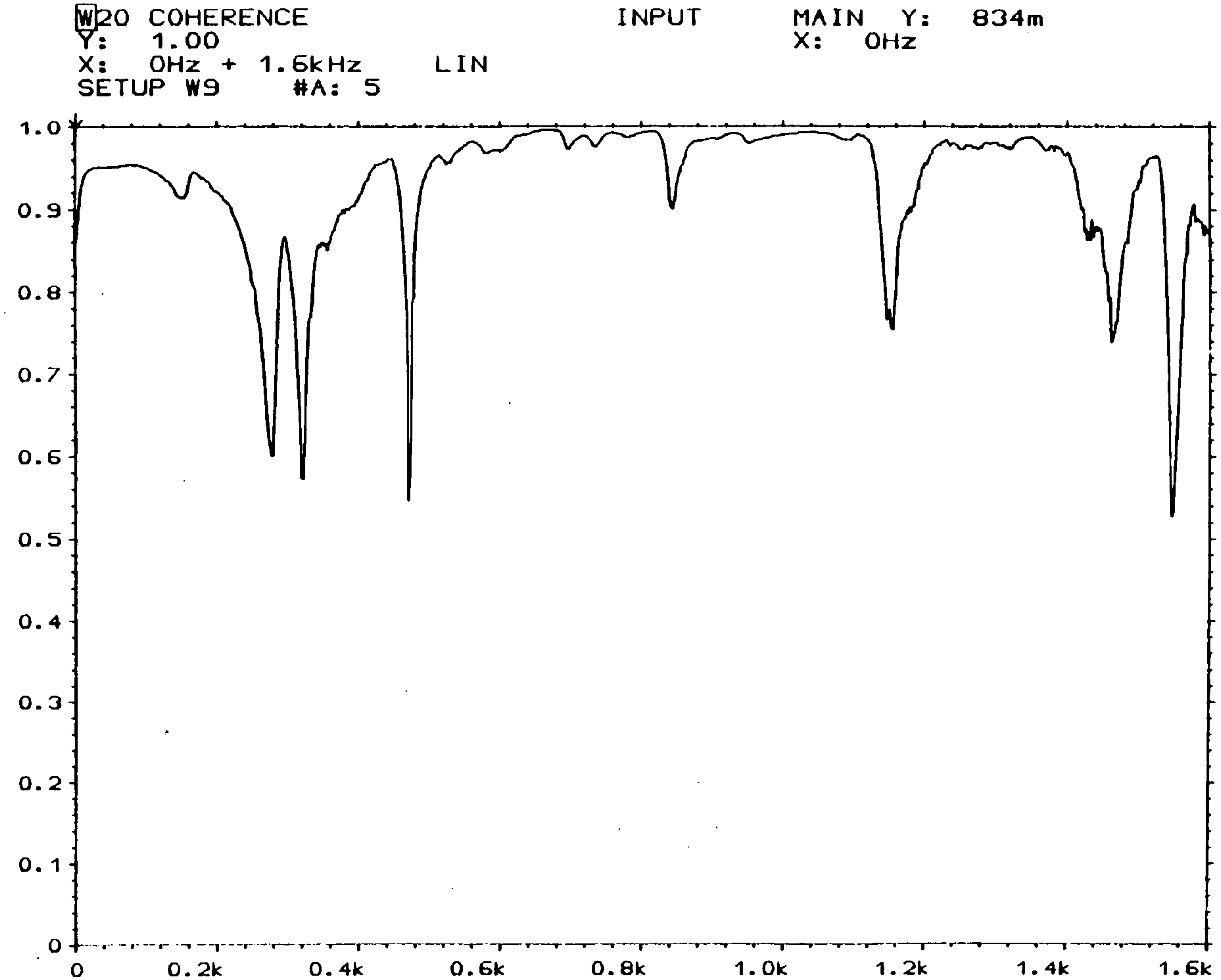

FIGURE 4.20

TYPICAL EXPERIMENTAL COHERENCE FUNCTION

CHAPTER 5

EXPERIMENTAL PROGRAMME

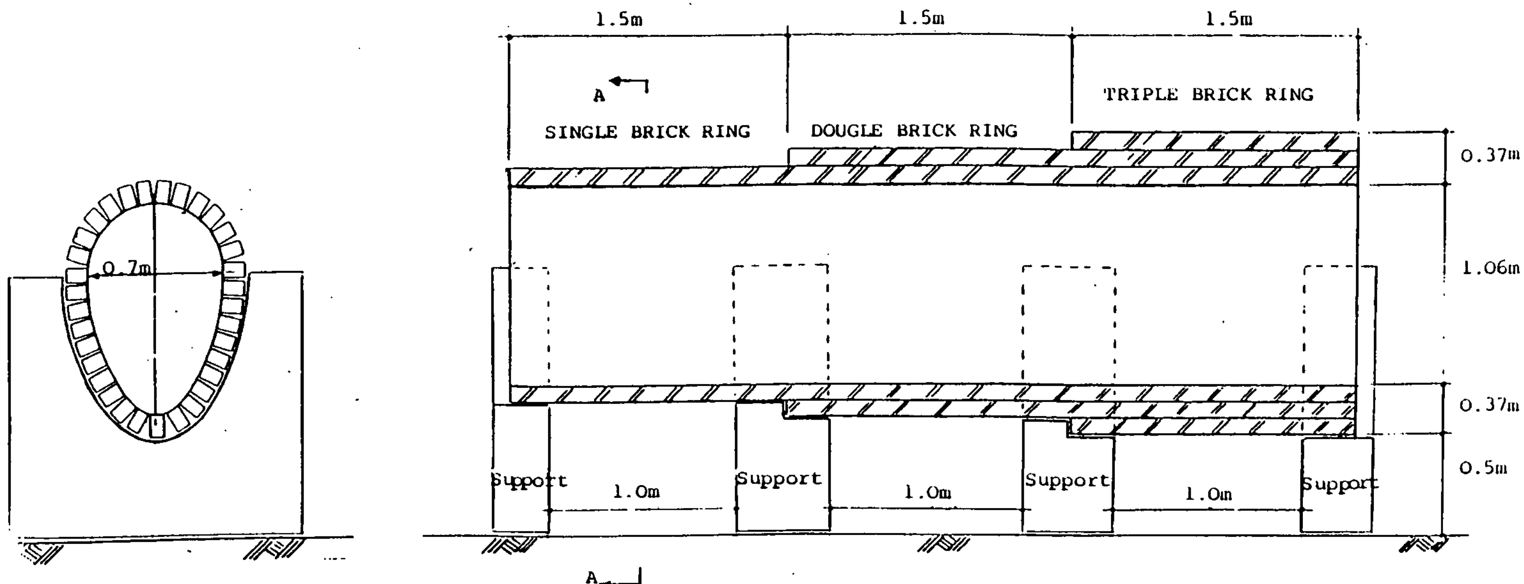

SECTION A-A

SECTIONAL ELEVATION

LABORATORY SEWER

FIGURE 5.1

WROUGHTON SEWER

FIGURE 5.2

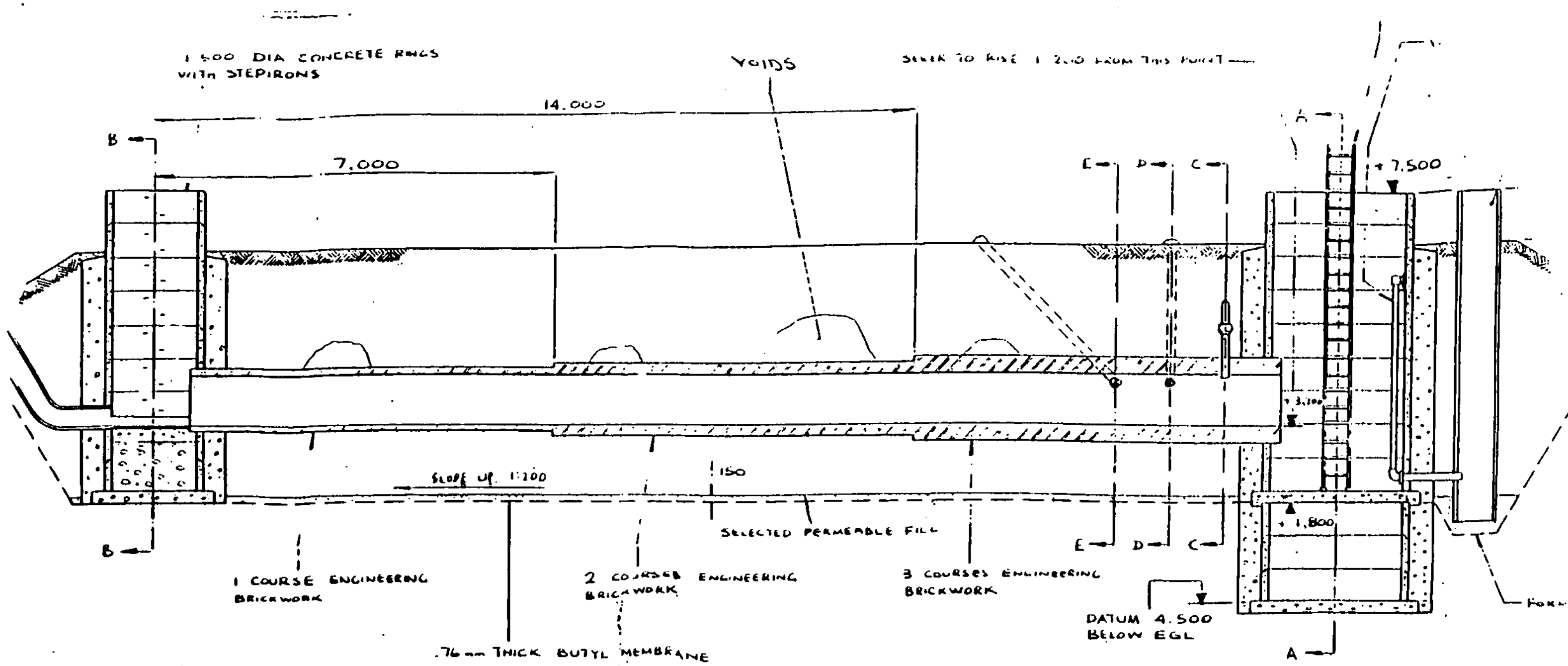

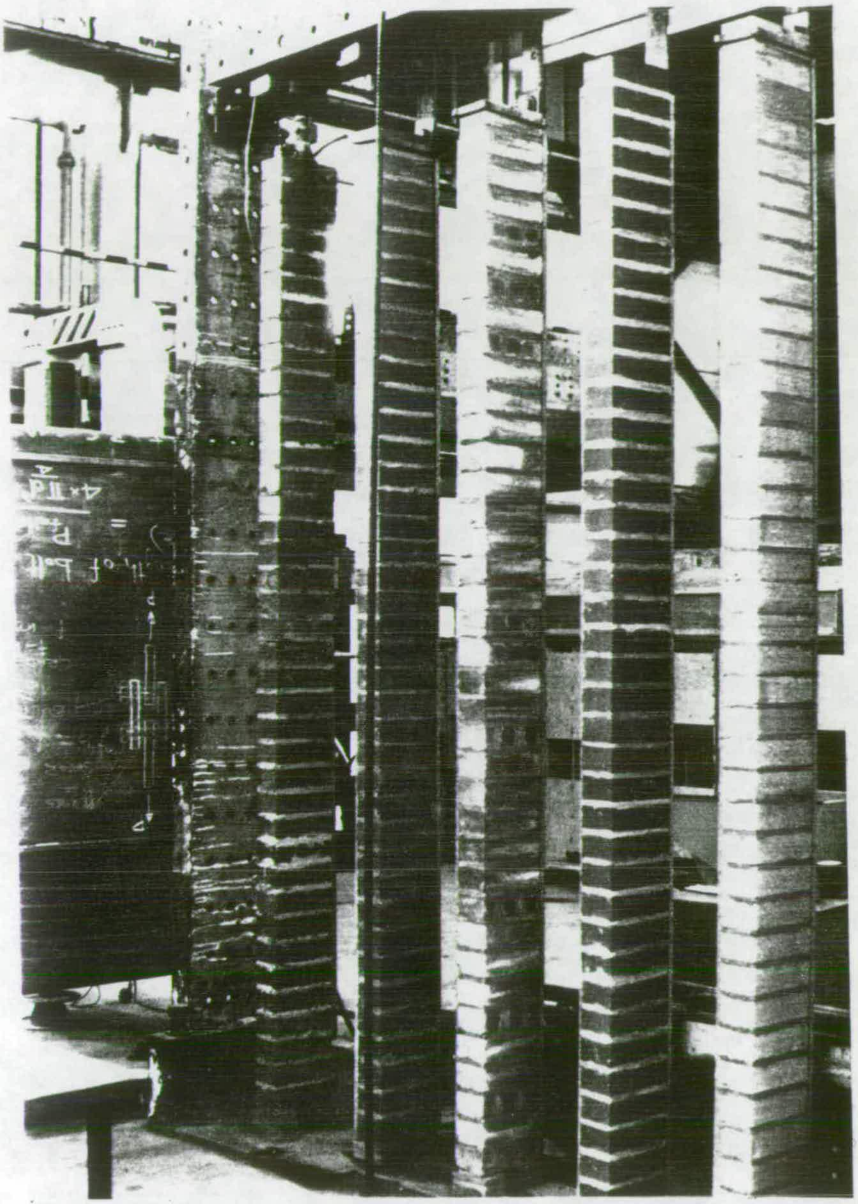

COLUMNS (GROUP 1)

PLATE 5.1

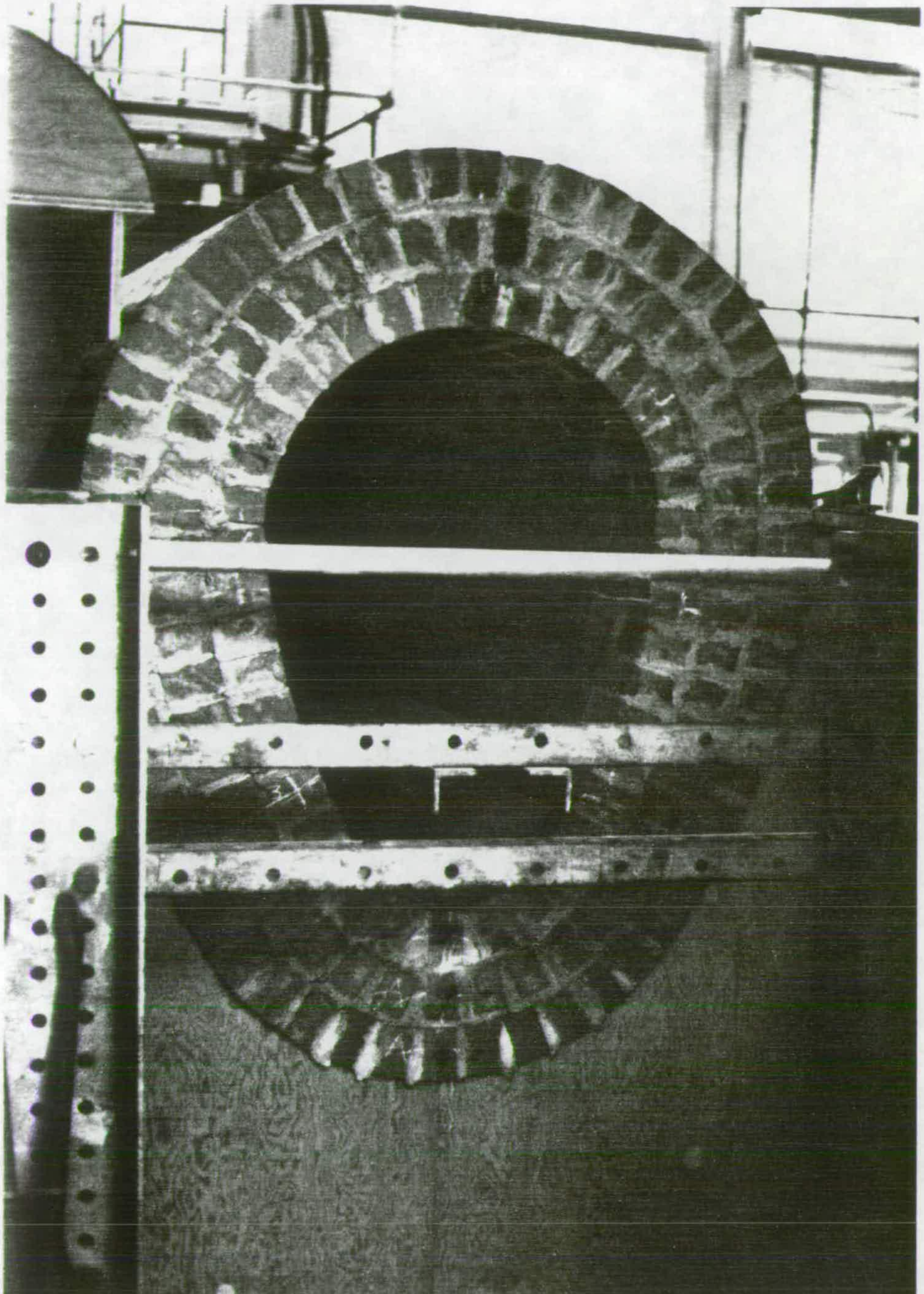

LABORATORY SEWER

PLATE 5.2

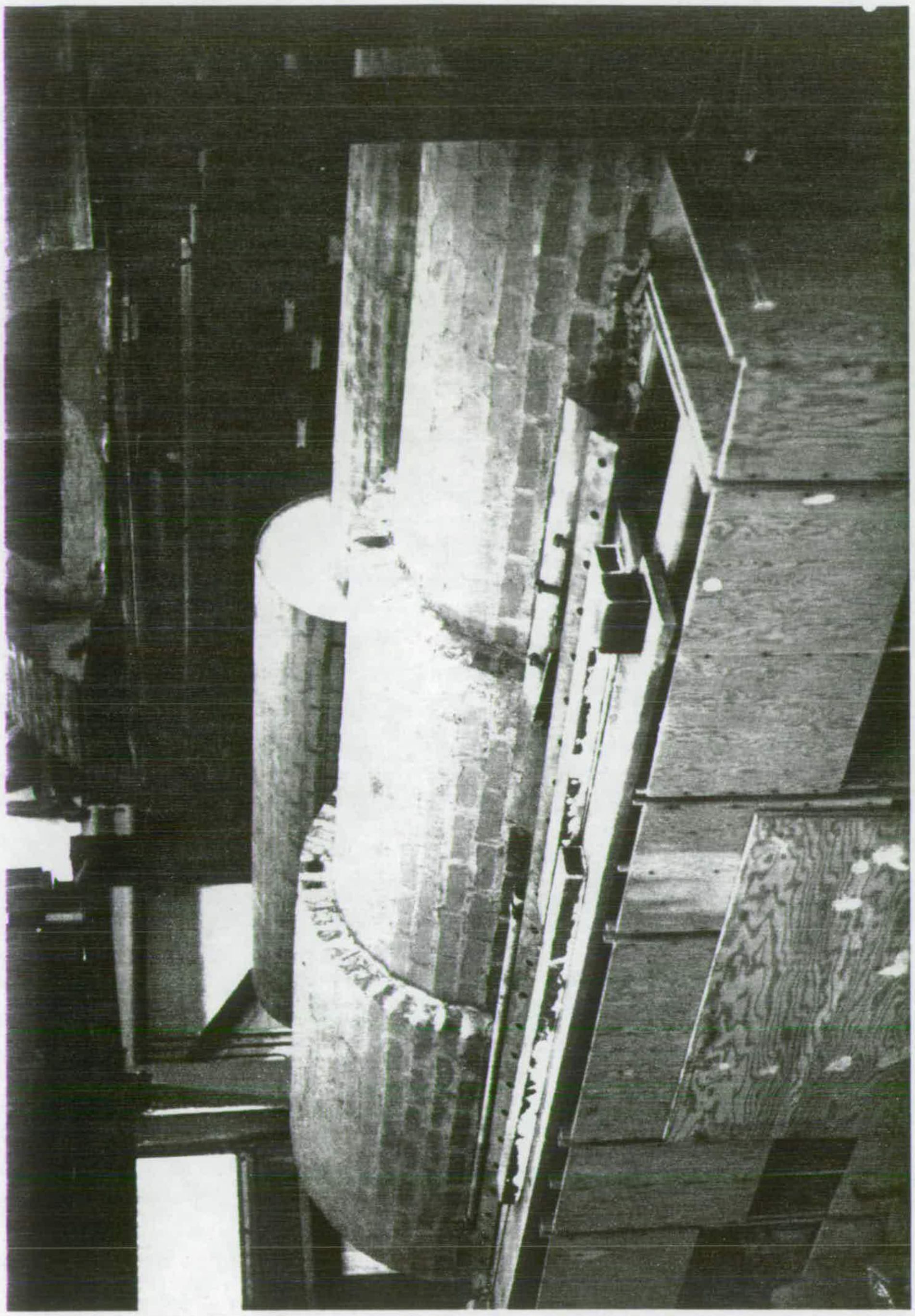

LABORATORY SEWER

PLATE 5.3

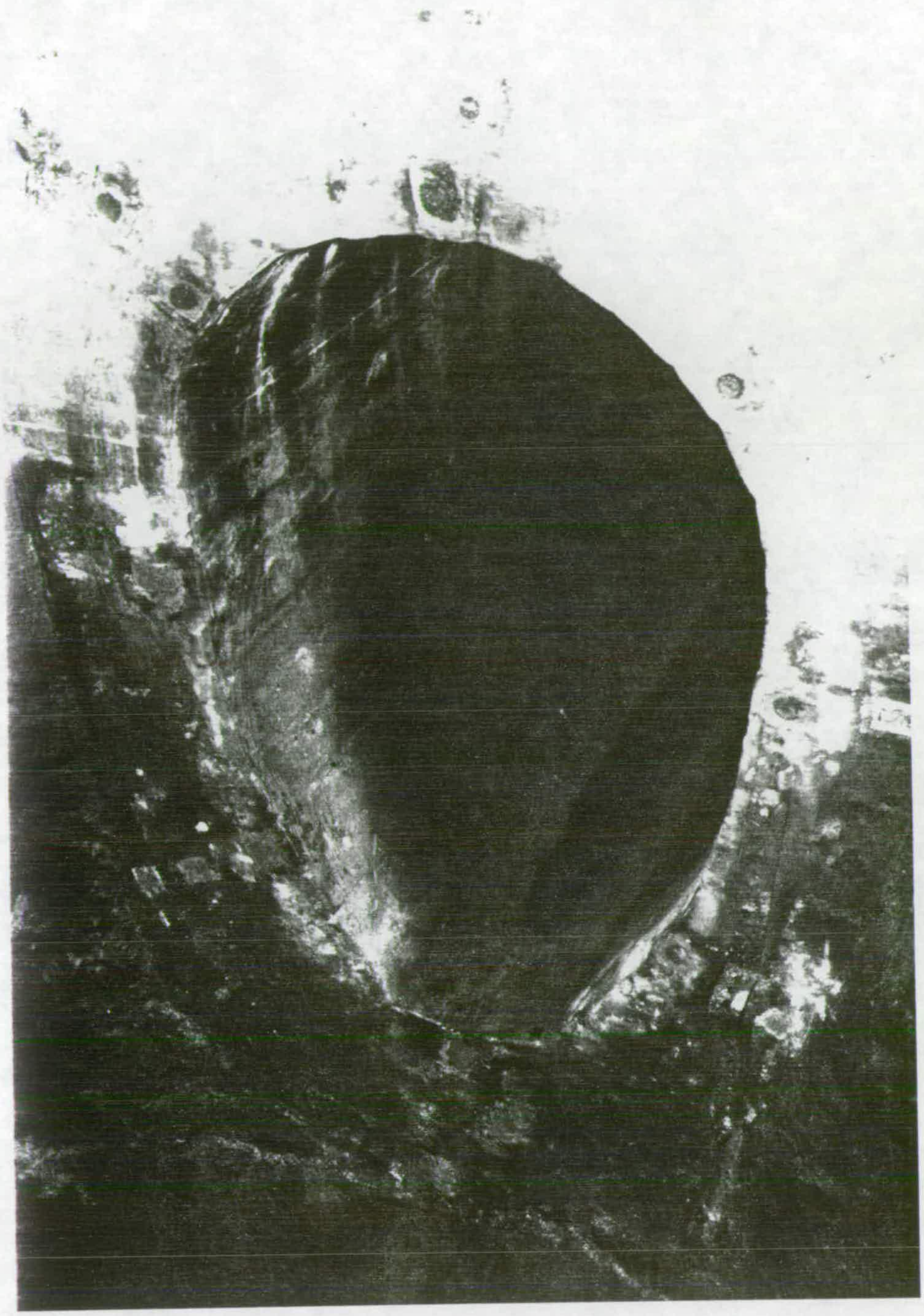

WROUGHTON SEWER

PLATE 5.4

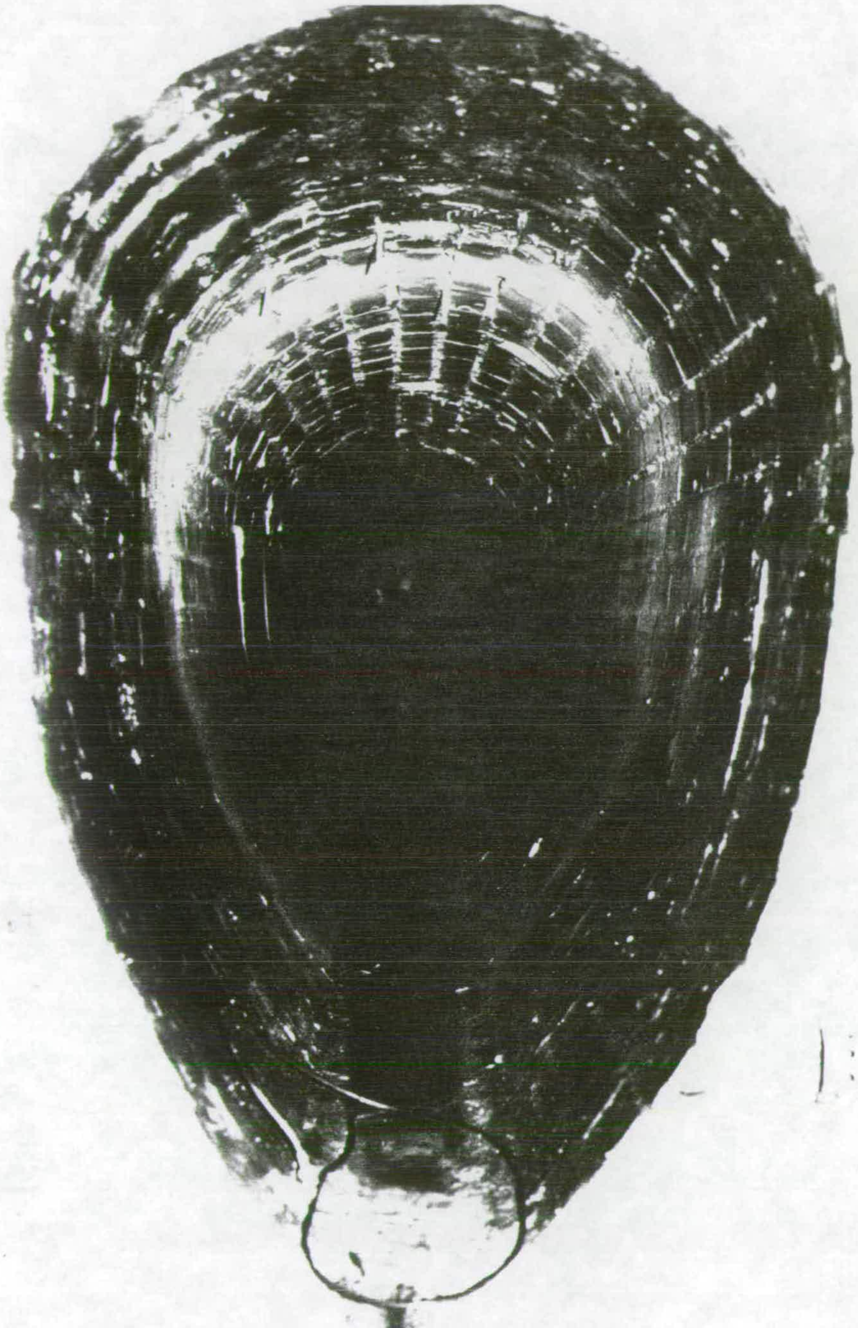

WROUGHTON SEWER

PLATE 5.5

CHAPTER 6

PRELIMINARY EXPERIMENTS
AND
INVESTIGATION OF EQUIPMENT

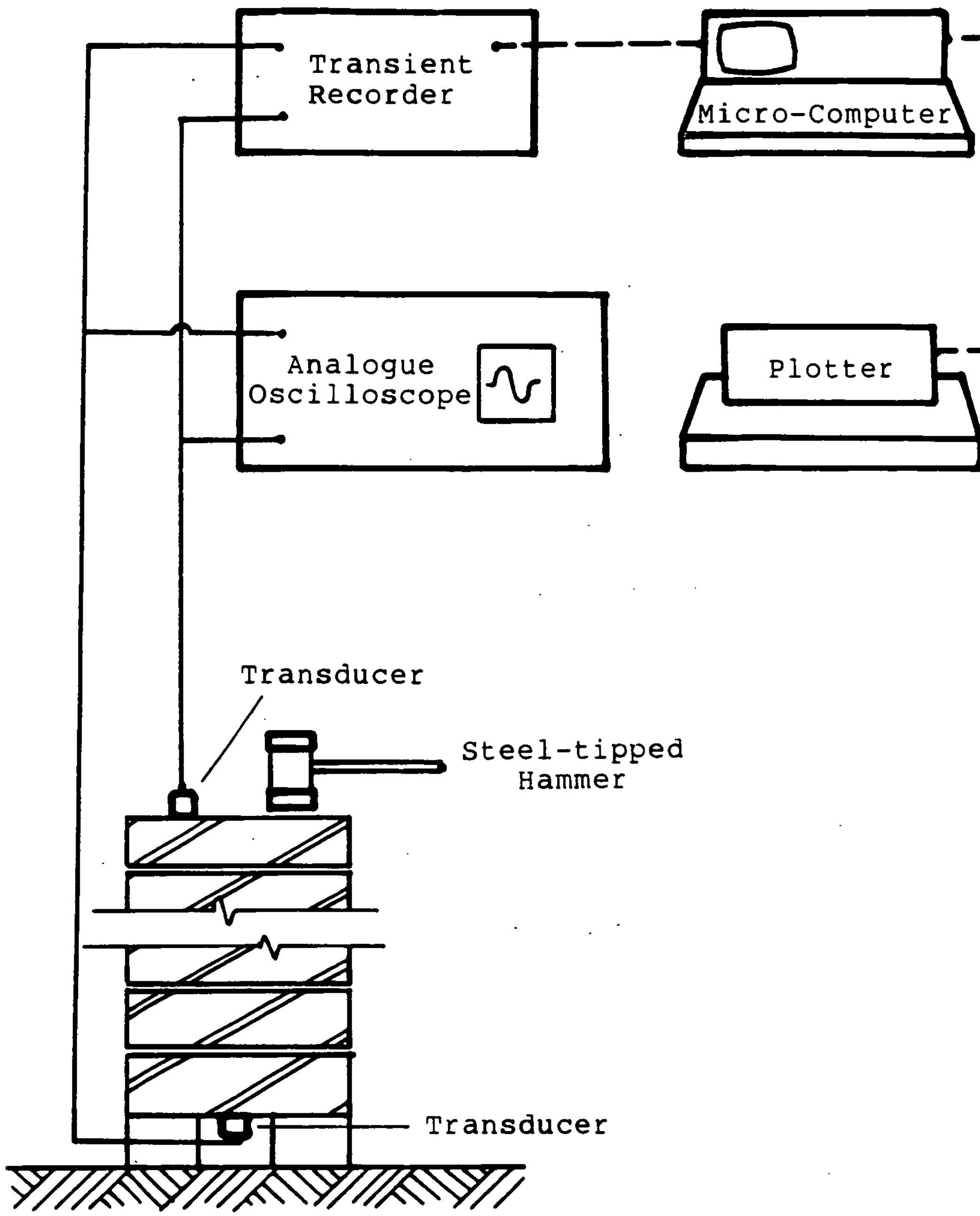

EQUIPMENT - PHASE A

FIGURE 6.1

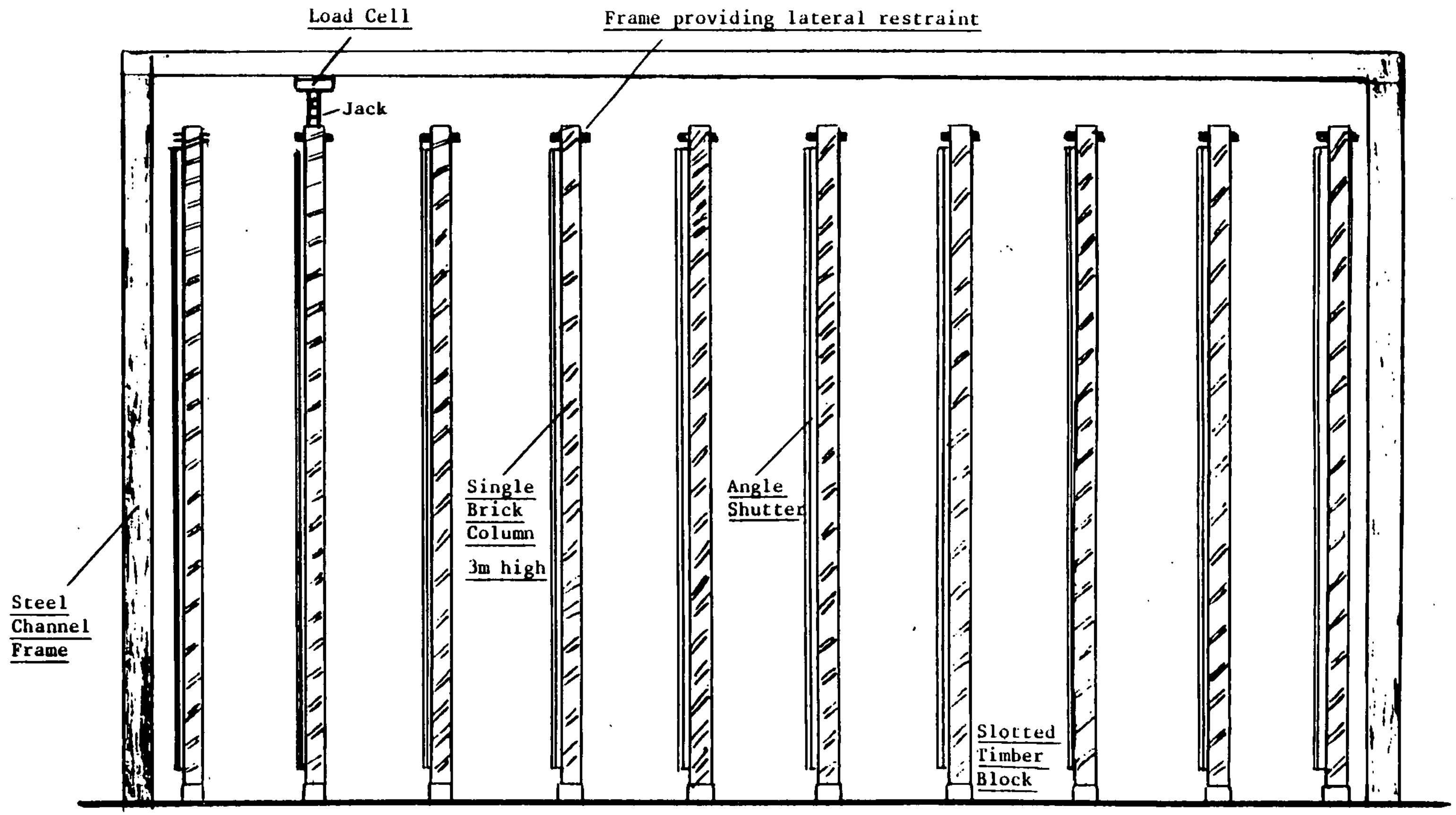

Schematic Details of Column Test Rig

FIGURE 6.2

COLUMN TEST FRAME

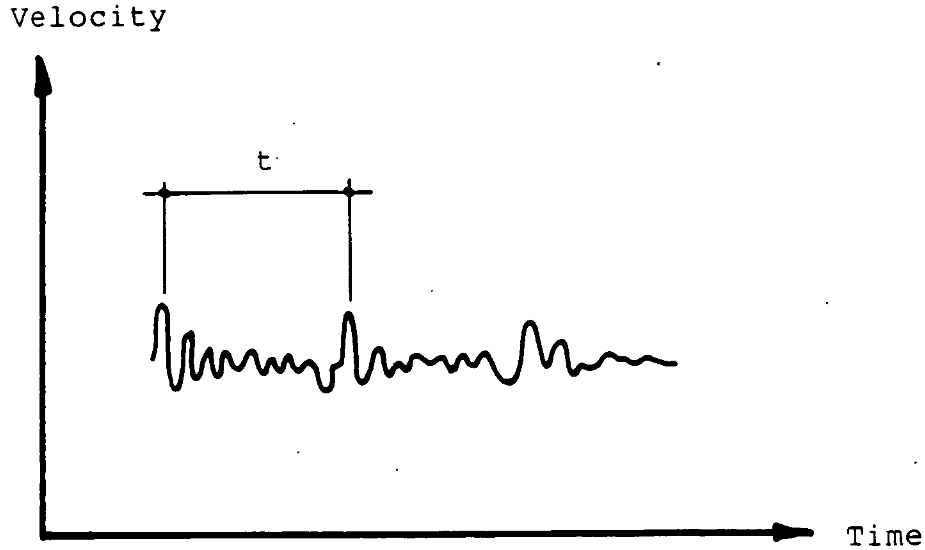

(a) Echo Method

Propagation time = t

Transmission velocity = path length / t

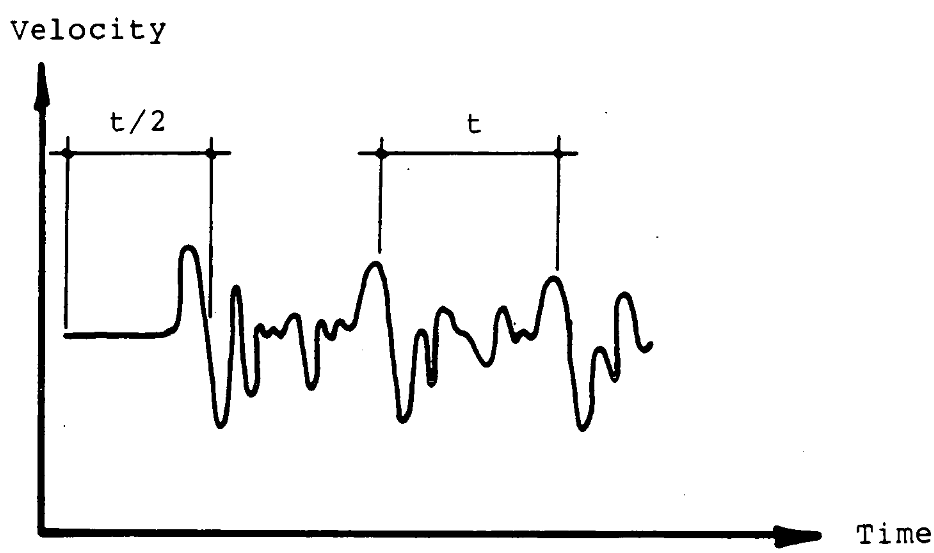

(b) Delay Echo Method

DETERMINATION OF PROPAGATION TIME USING PULSE METHODS

FIGURE 6.3

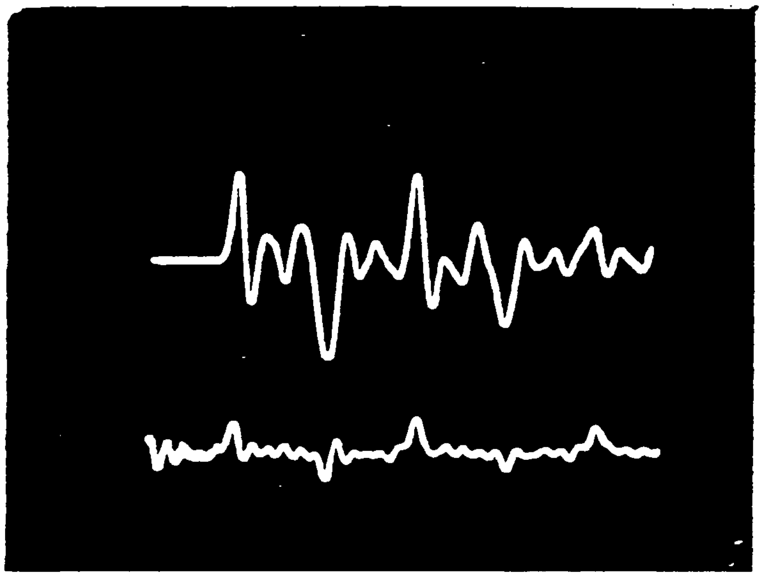

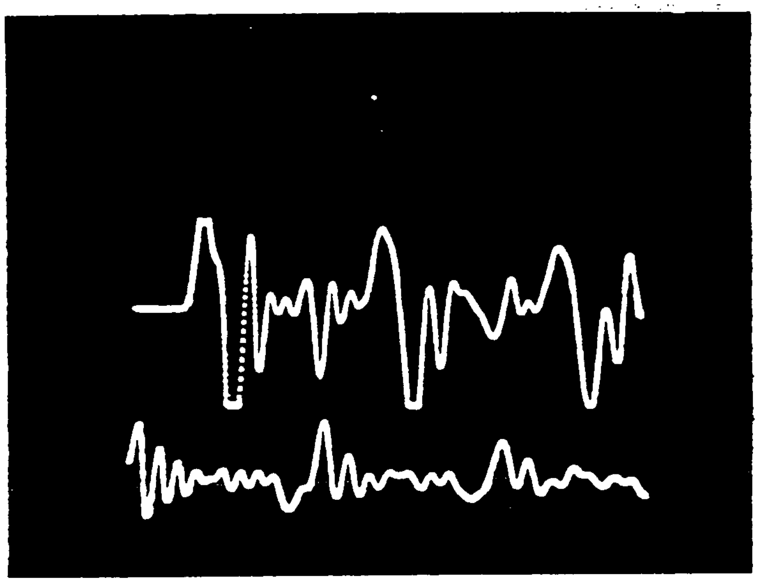

EQUIPMENT - PHASE A: TYPICAL TEST RESULTS

FIGURE 6.4

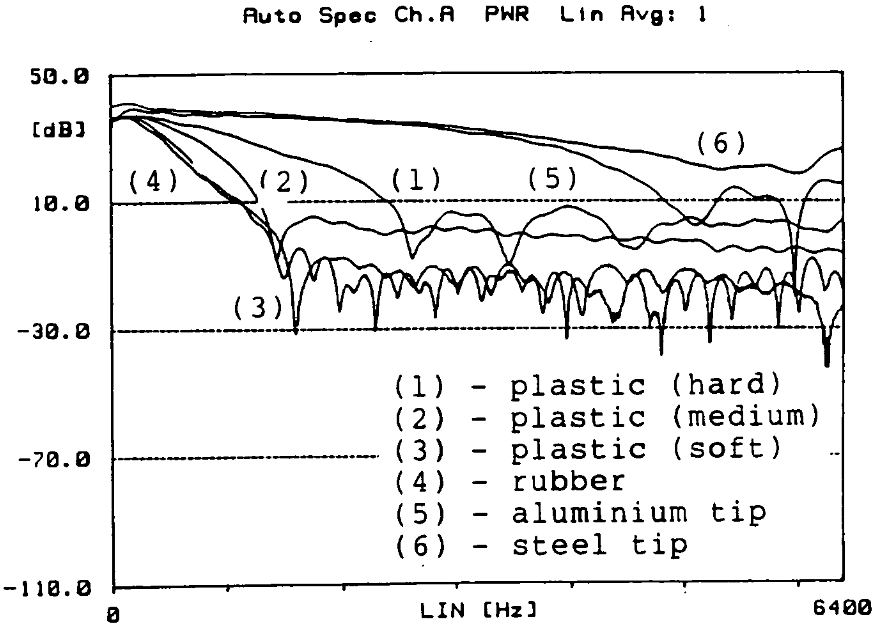

(a) 3 lb Hammer

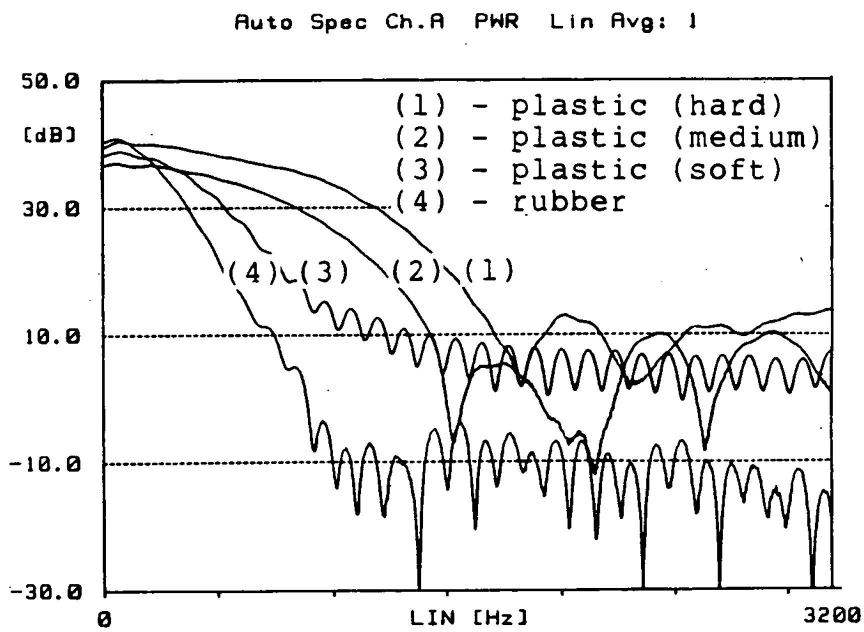

(b) 12 lb Hammer

HAMMER FORCE AUTO SPECTRA

FIGURE 6.5

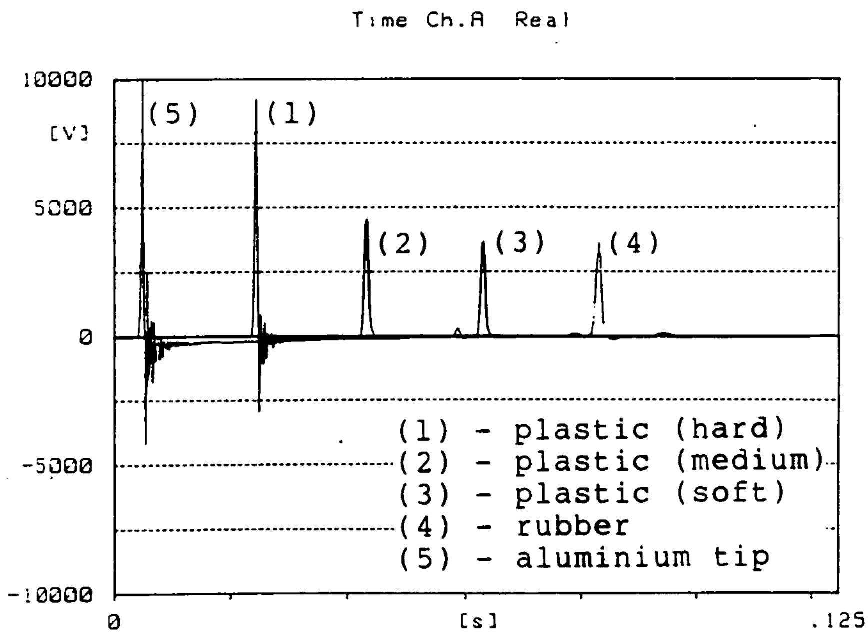

FORCE RECORDS - 3 LB HAMMER WITH DIFFERENT TIPS

FIGURE 6.6

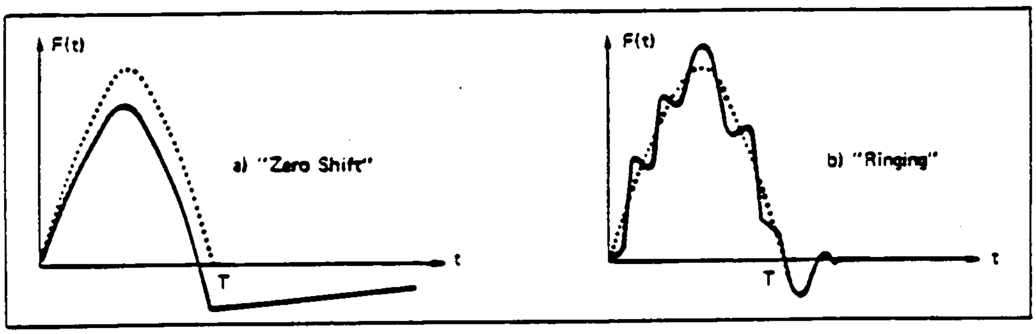

Vibration measurement system response to half sine wave pulse of length T.
a) "Zero Shift" limits the low-frequency response of the system.
b) "Ringing" limits the high frequency response of the system

ZERO SHIFT AND RINGING

FIGURE 6.7

(after Broch, ref. 81)

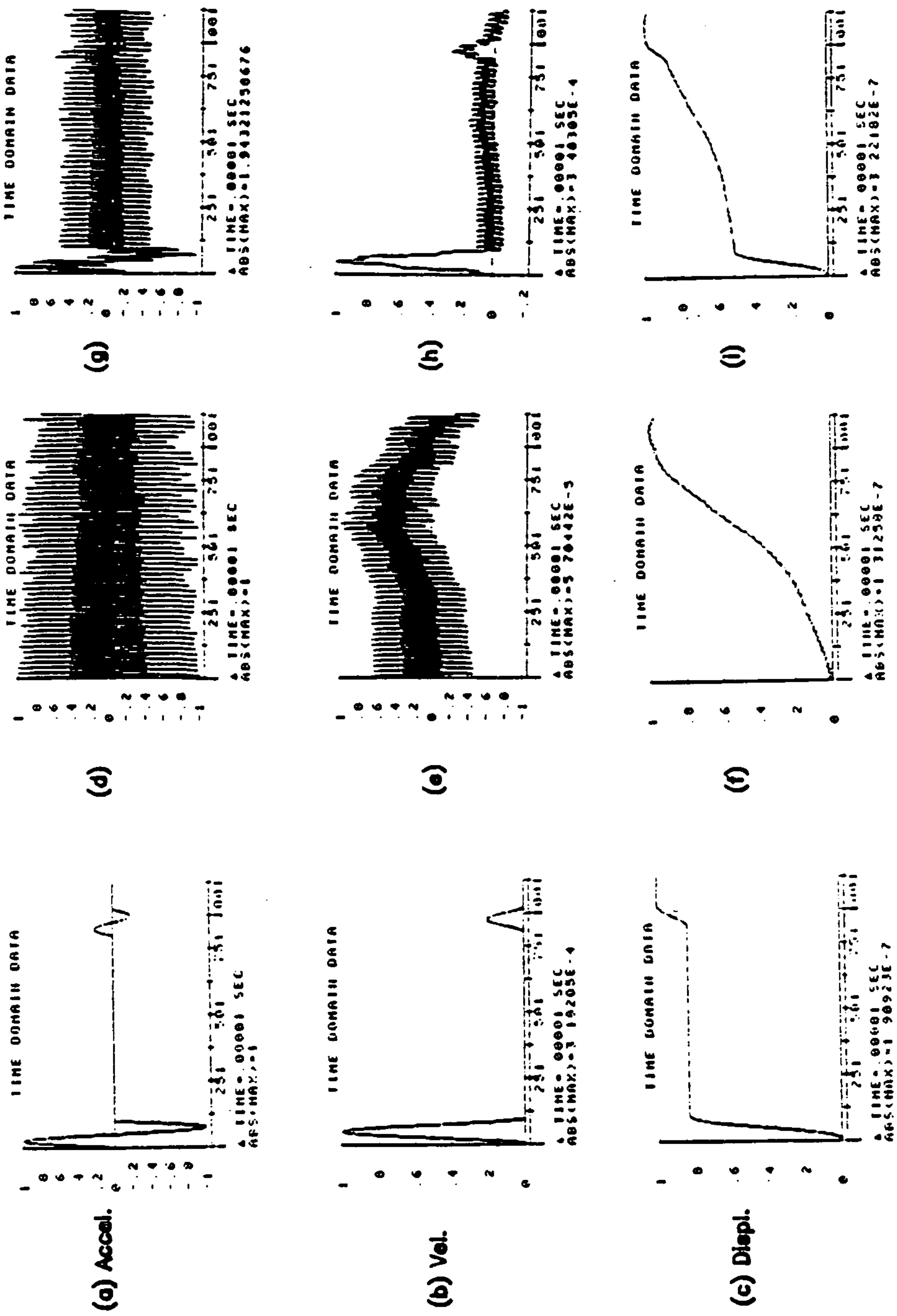

USE OF INTEGRATION TO FILTER SURFACE WAVES

FIGURE 6.8

(after Chan, ref. 30)

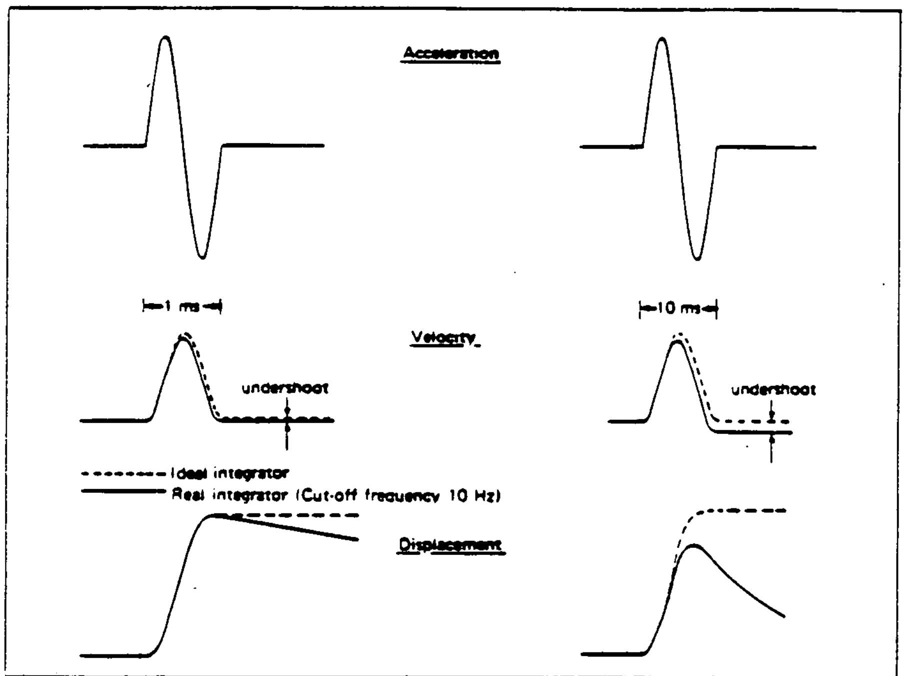

Practical integration of 2 different length acceleration pulses to velocity and displacement using the same integration cutoff frequency

Signal Distortion due to Integration - DC Shift

FIGURE 6.9

(after Broch, ref. 81)

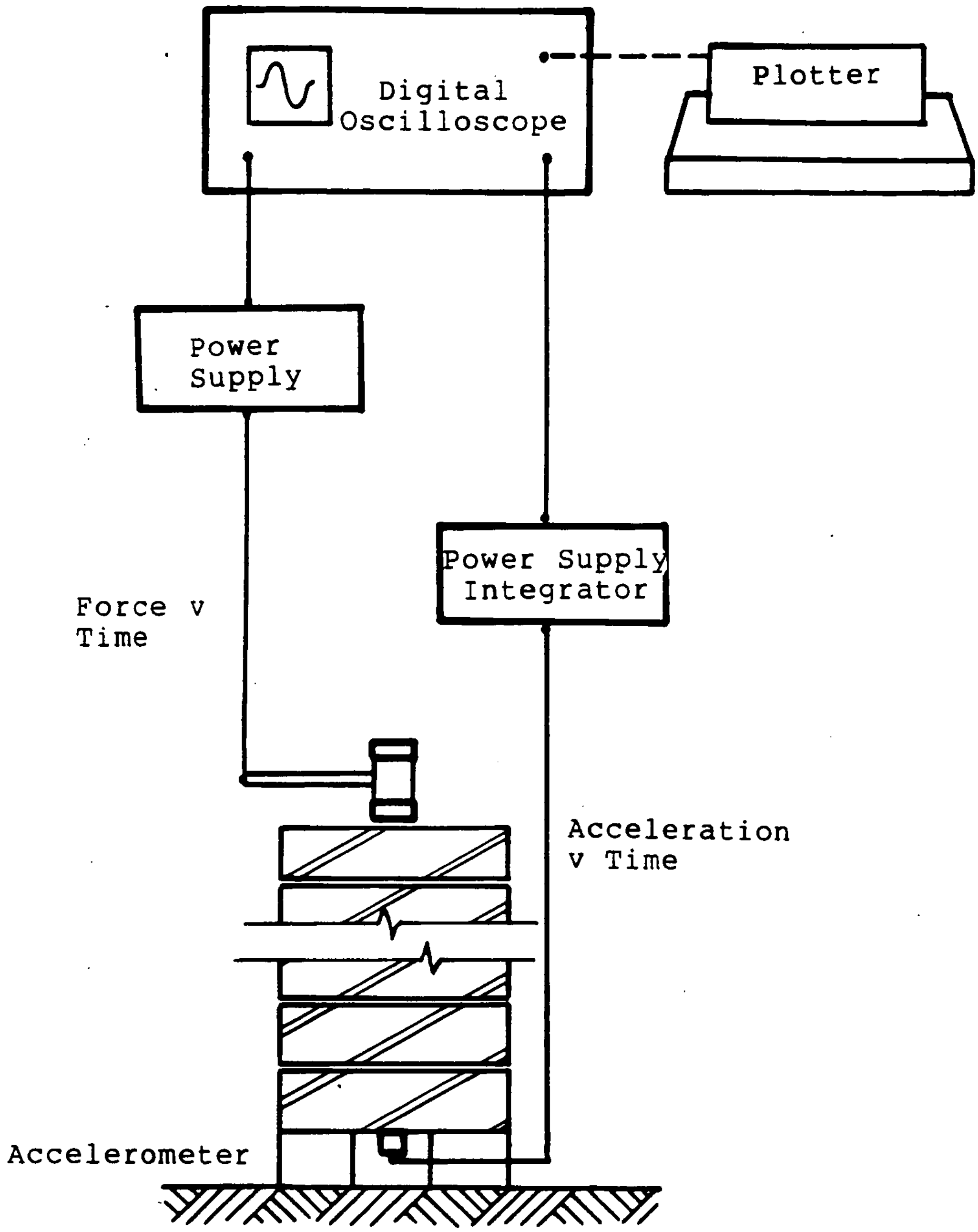

EQUIPMENT - PHASE B

FIGURE 6.10

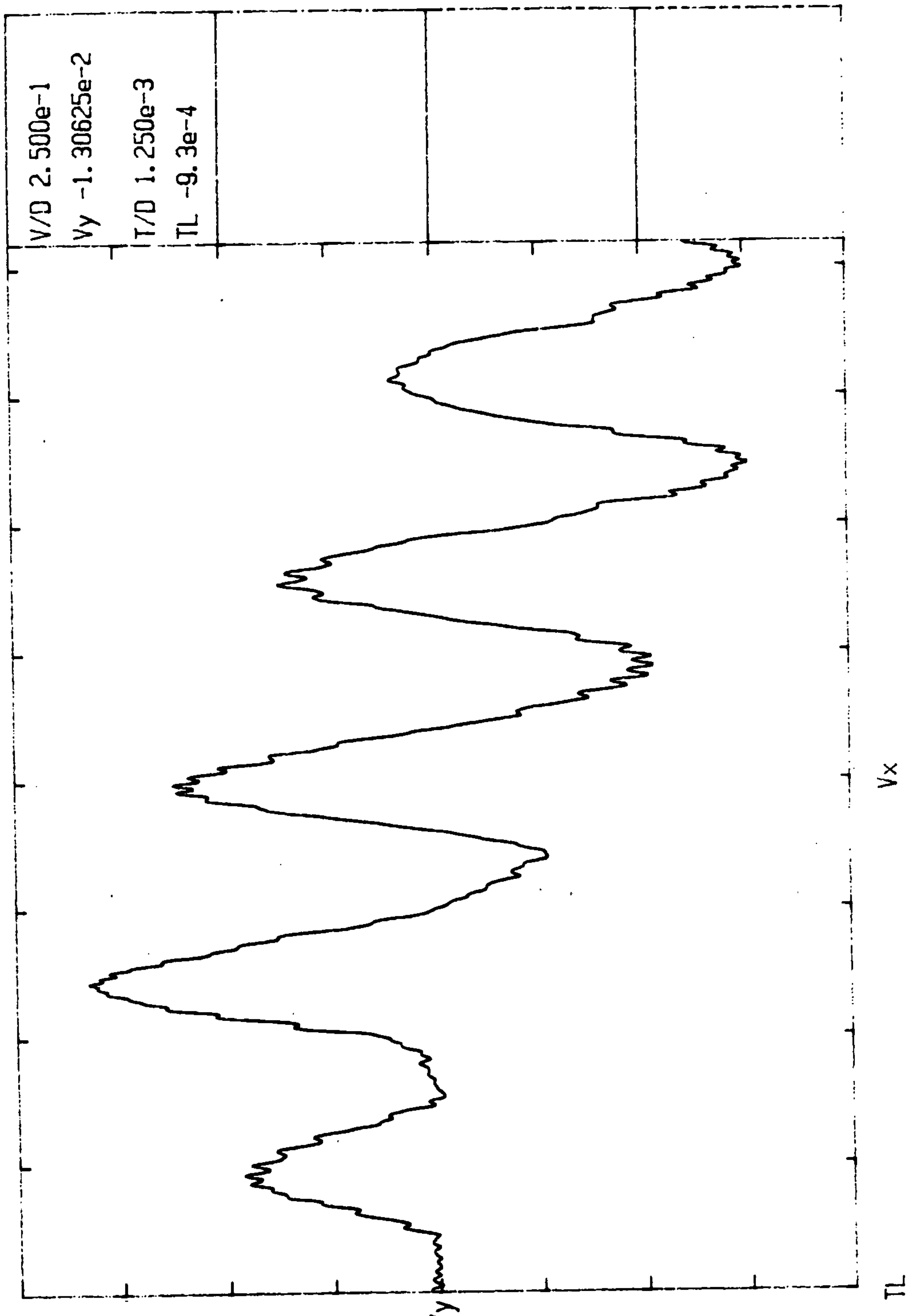

EQUIPMENT - PHASE B: TYPICAL ECHO METHOD RESULTS

FIGURE 6.11

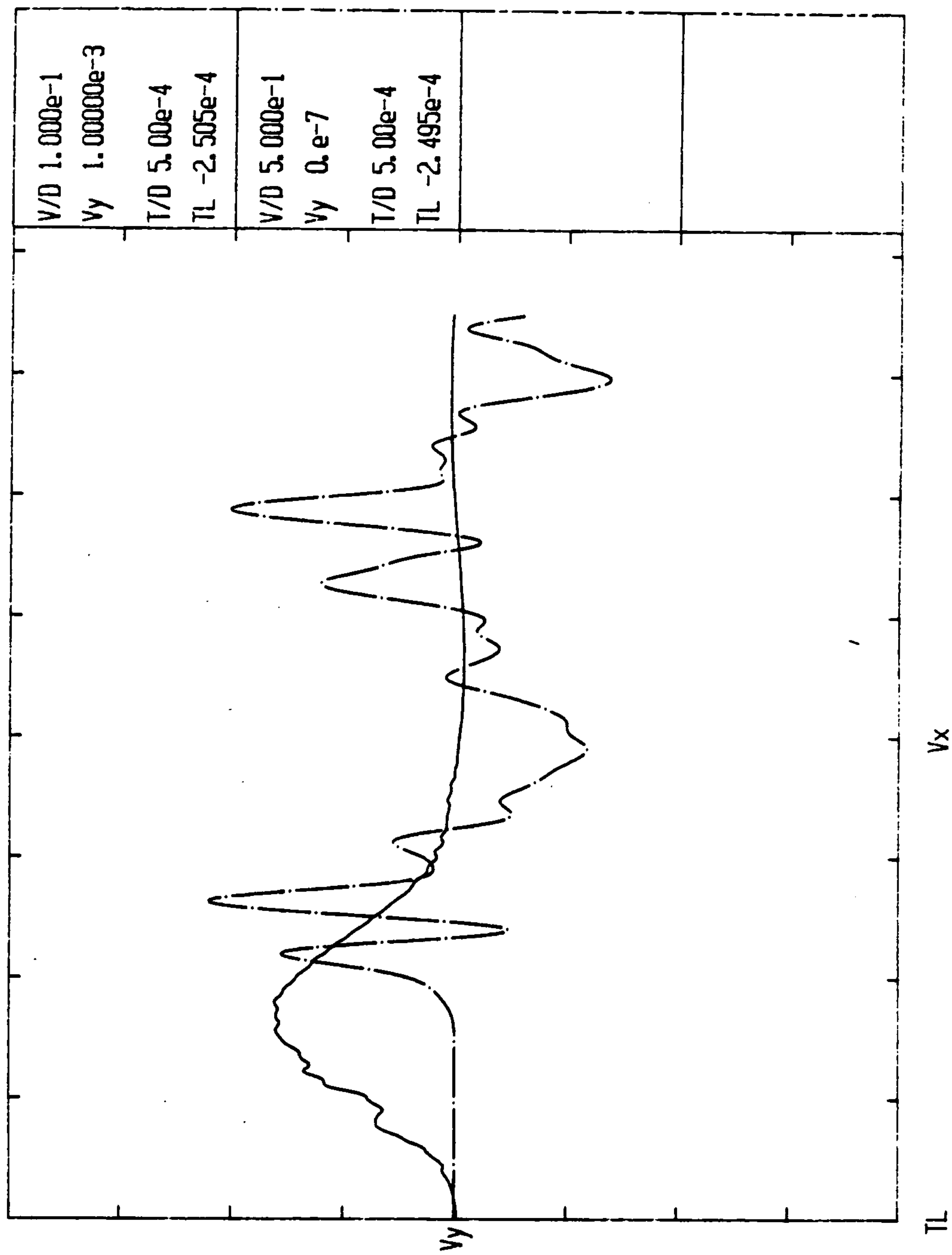

EQUIPMENT - PHASE B: TYPICAL DELAY METHOD RESULTS

FIGURE 6.12

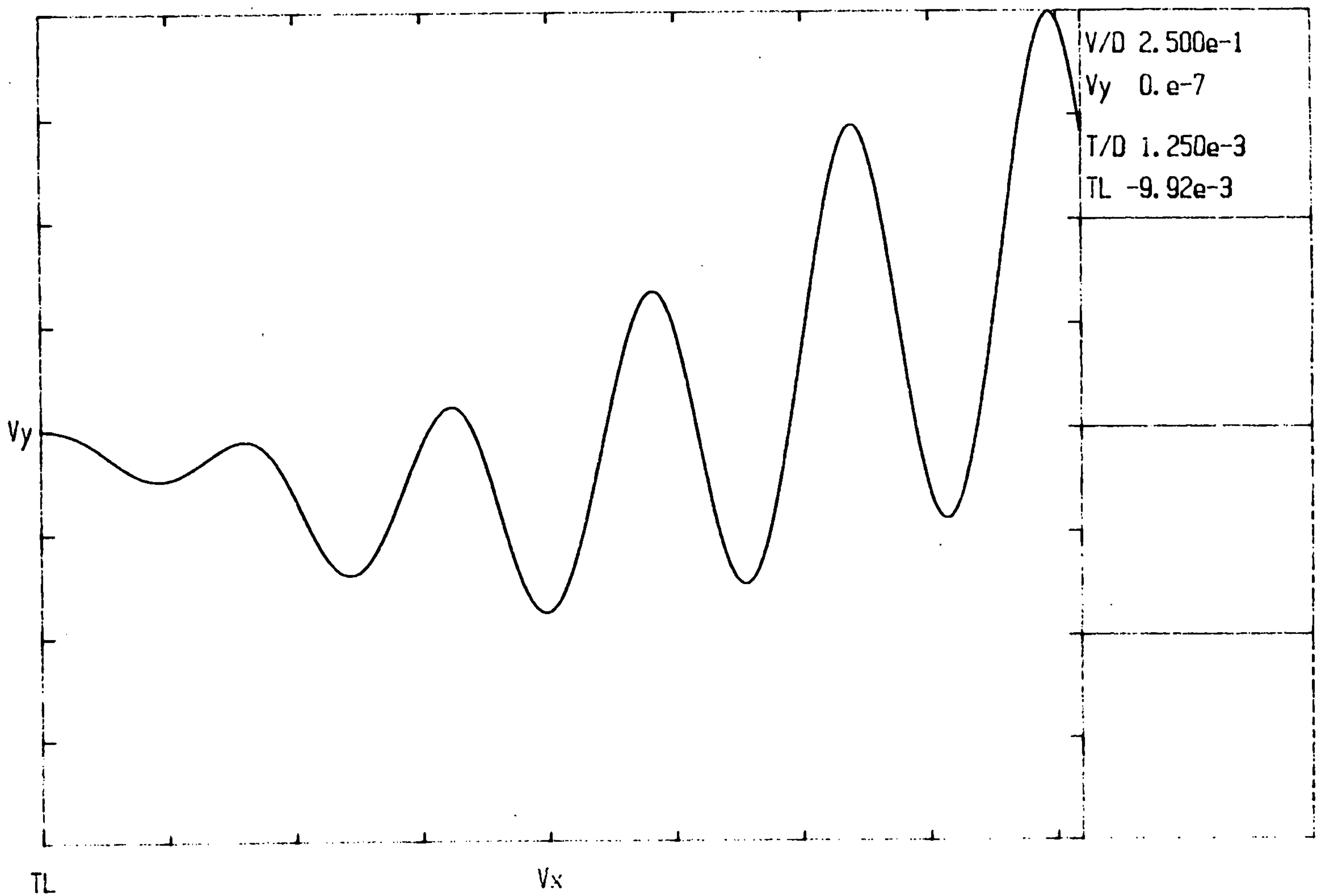

EQUIPMENT - PHASE B
AUTO-CORRELATION FOR AN ECHO TEST

FIGURE 6.13

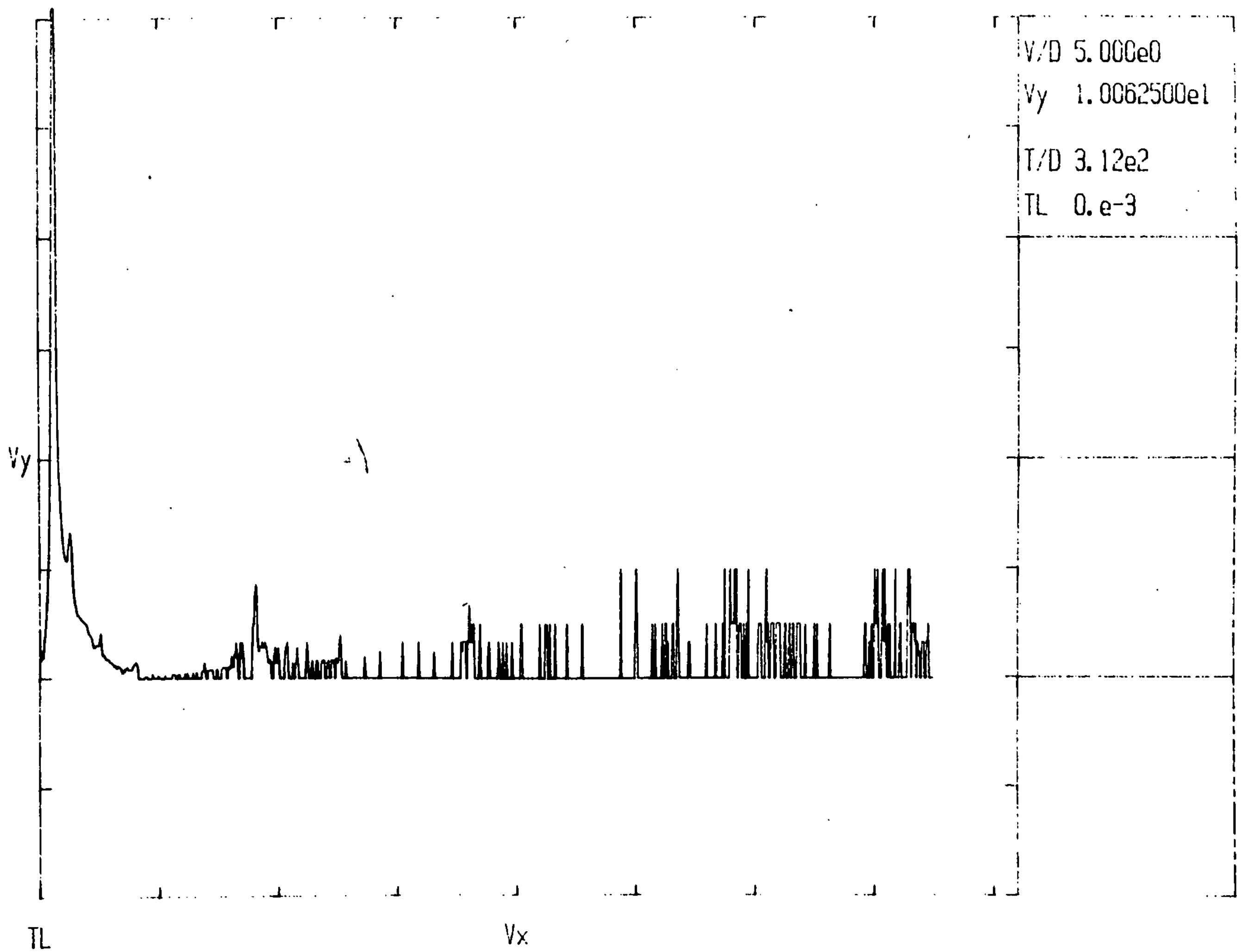

FIGURE 6.14

FREQUENCY RESPONSE FUNCTION FOR AN ECHO TEST

EQUIPMENT - PHASE B

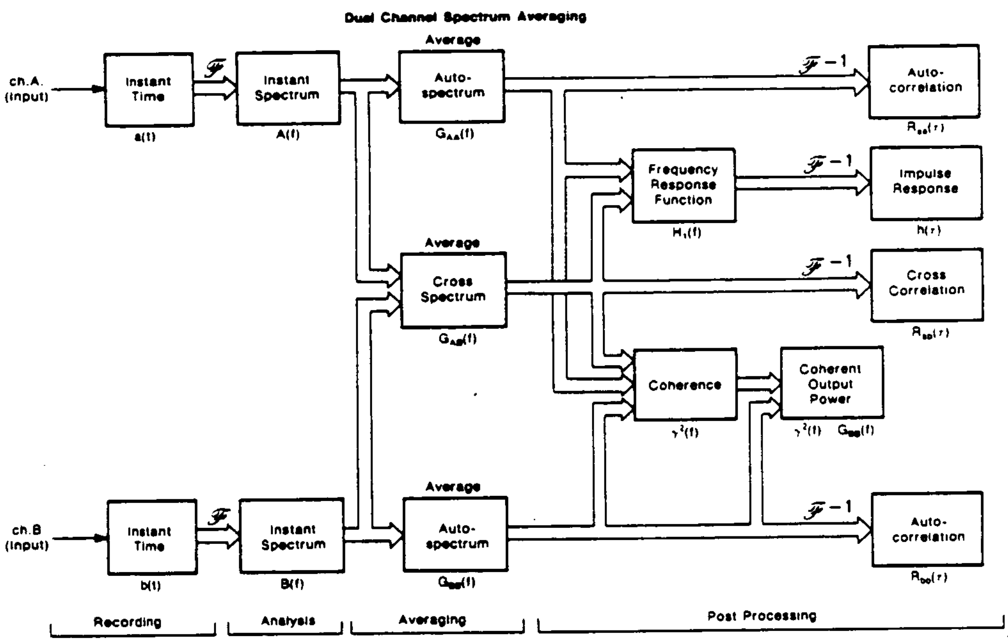

Simplified block diagram of the analyzer in the dual channel spectrum averaging mode

FIGURE 6.15

(after Herlufsen, ref. 75)

W3 TIME CH.A REAL INPUT MAIN Y: 111U
Y: 13.5kU X: 0.000ms
X: 0.000ms + 7.81ms

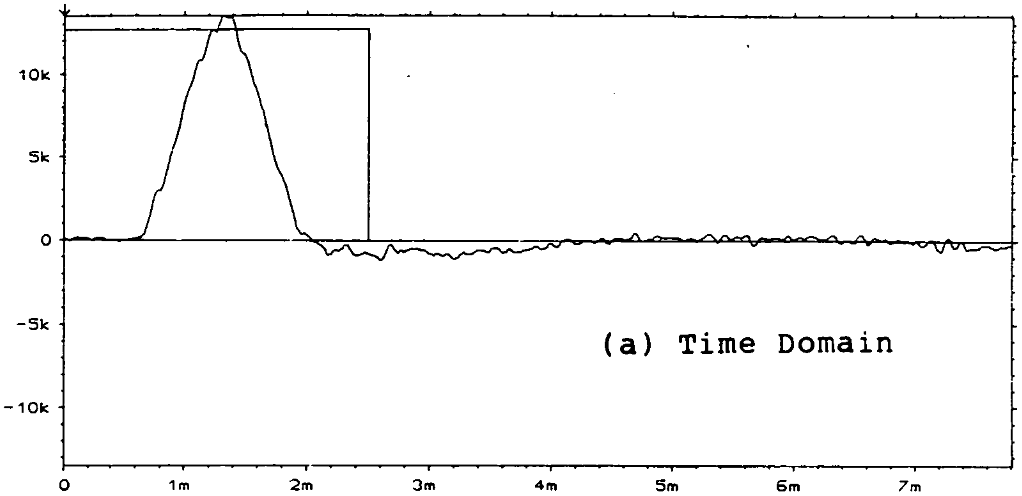

SETUP W10

MEASUREMENT:	DUAL SPECTRUM AVERAGING				
TRIGGER:	CH.A	+SLOPE	LEVEL: +0.10 MAX INPUT		
DELAY:	TRIG→A: -1.007ms		CH.A→B: 0.000ms		
AVERAGING:	LIN 5				
FREQ SPAN:	25.6kHz	ΔF:32Hz	T:31.3ms	ΔT:15.3µs	
CENTER FREQ:	BASEBAND				
WEIGHT CH.A:	TRANSIENT	SHIFT:0.000ms		LENGTH:2.502ms	
WEIGHT CH.B:	EXPONENTIAL	SHIFT:0.000ms		LENGTH:20.004ms	
CH.A:	6V +	3Hz DIR	FILT:BOTH	92.0µV/N	
CH.B:	6V +	3Hz DIR	FILT:BOTH	31.6V/m/s	
GENERATOR:	DISABLED				

W3 TIME CH.A REAL INPUT MAIN Y: 9.95U
Y: 8.94kU X: 0.00ms
X: 0.00ms + 125ms

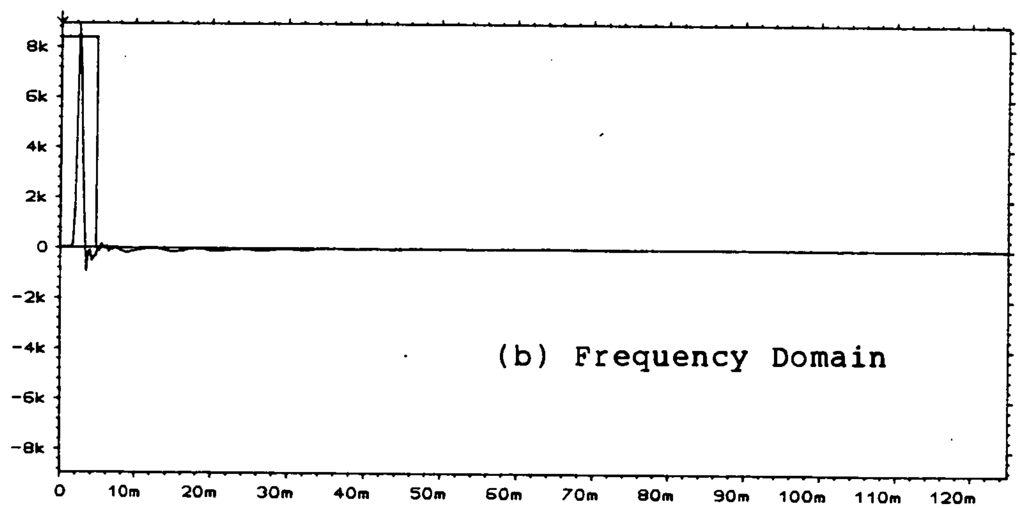

SETUP W9

MEASUREMENT:	DUAL SPECTRUM AVERAGING				
TRIGGER:	CH.A	+SLOPE	LEVEL: +0.10 MAX INPUT		
DELAY:	TRIG→A: -0.97ms		CH.A→B: 0.00ms		
AVERAGING:	LIN 5				
FREQ SPAN:	1.6kHz	ΔF:2Hz	T:500ms	ΔT:244µs	
CENTER FREQ:	BASEBAND				
WEIGHT CH.A:	TRANSIENT	SHIFT:0.00ms		LENGTH:4.63ms	
WEIGHT CH.B:	EXPONENTIAL	SHIFT:0.00ms		LENGTH:50.04ms	
CH.A:	6V +	3Hz DIR	FILT:BOTH	184µV/N	
CH.B:	6V +	3Hz DIR	FILT:BOTH	31.6V/m/s	
GENERATOR:	DISABLED				

EQUIPMENT - PHASE D
TIME AND FREQUENCY MEASUREMENT SET-UPS

FIGURE 6.16

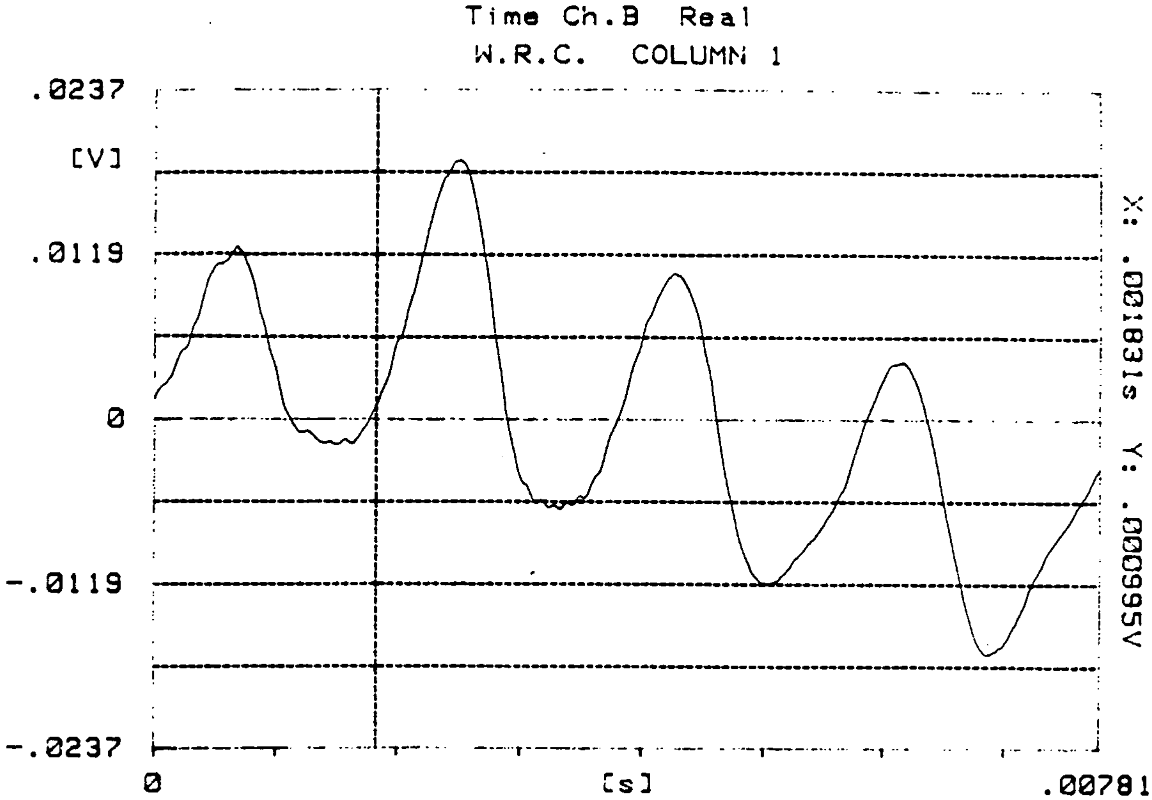

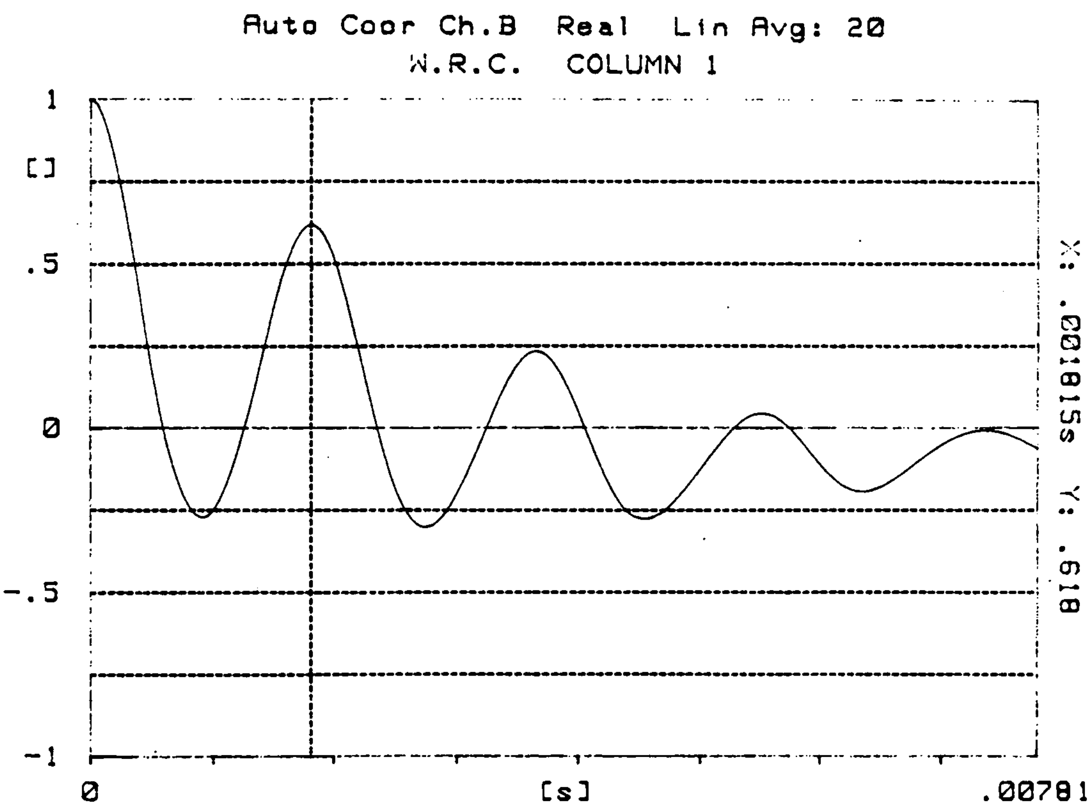

EQUIPMENT - PHASE D
VELOCITY TIME RECORD AND AUTO-CORRELATION FUNCTION

FIGURE 6.17

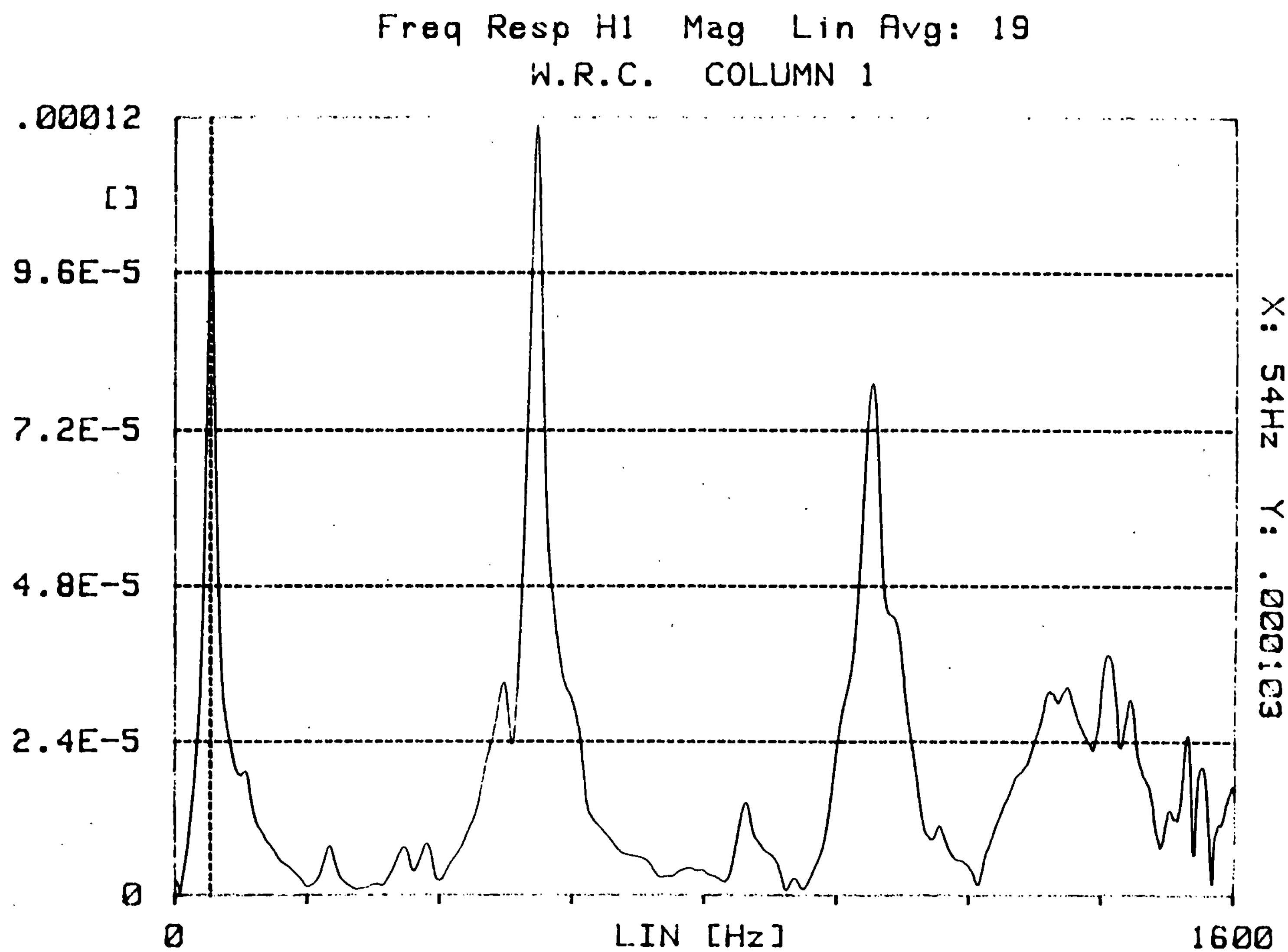

EQUIPMENT - PHASE D
TYPICAL FREQUENCY RESPONSE FUNCTION

FIGURE 6.18

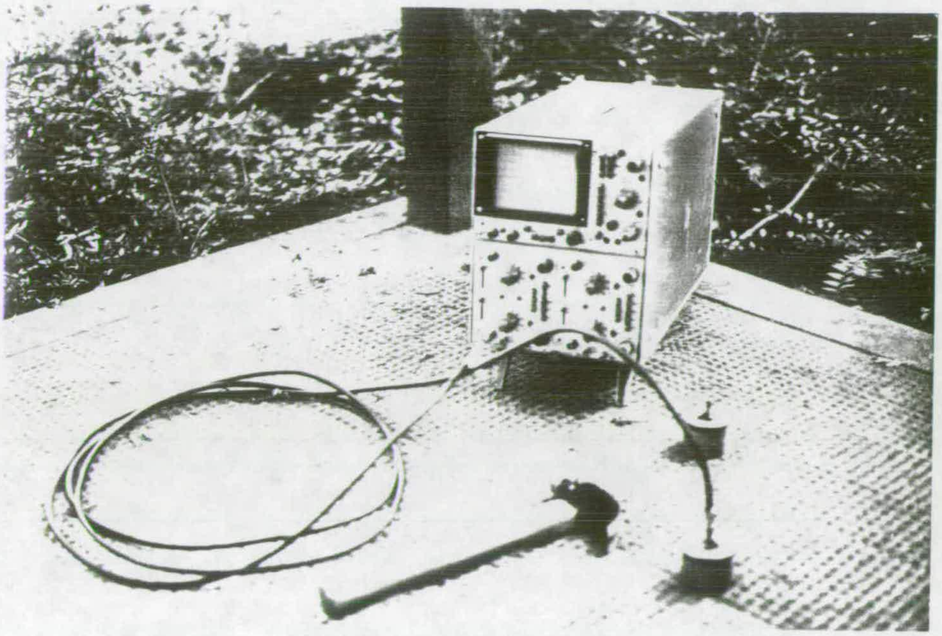

EQUIPMENT USED BY FEGEN

PLATE 6.1

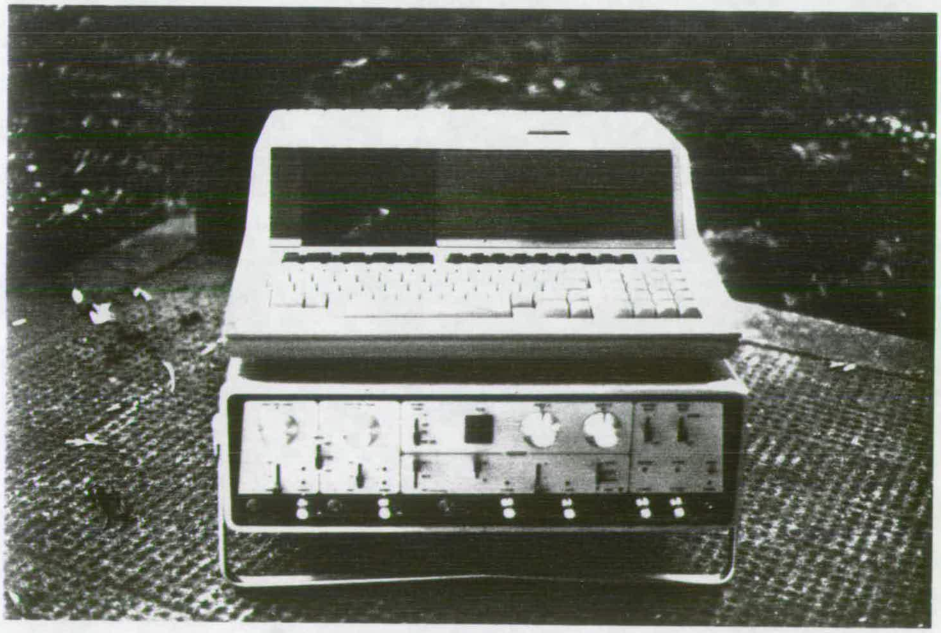

EQUIPMENT - PHASE A DEVELOPMENT

PLATE 6.2

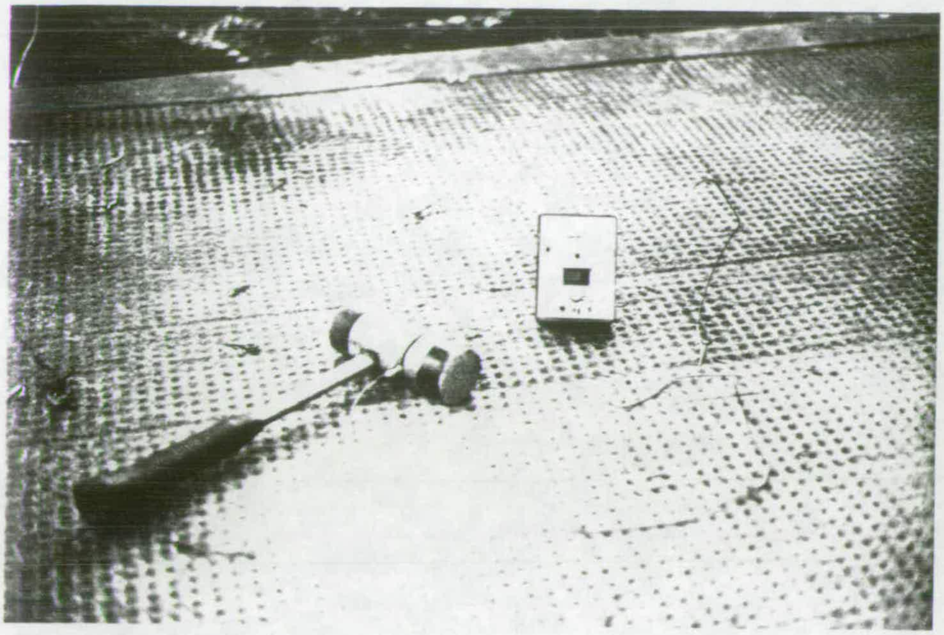

3 lb INSTRUMENTED HAMMER

PLATE 6.3

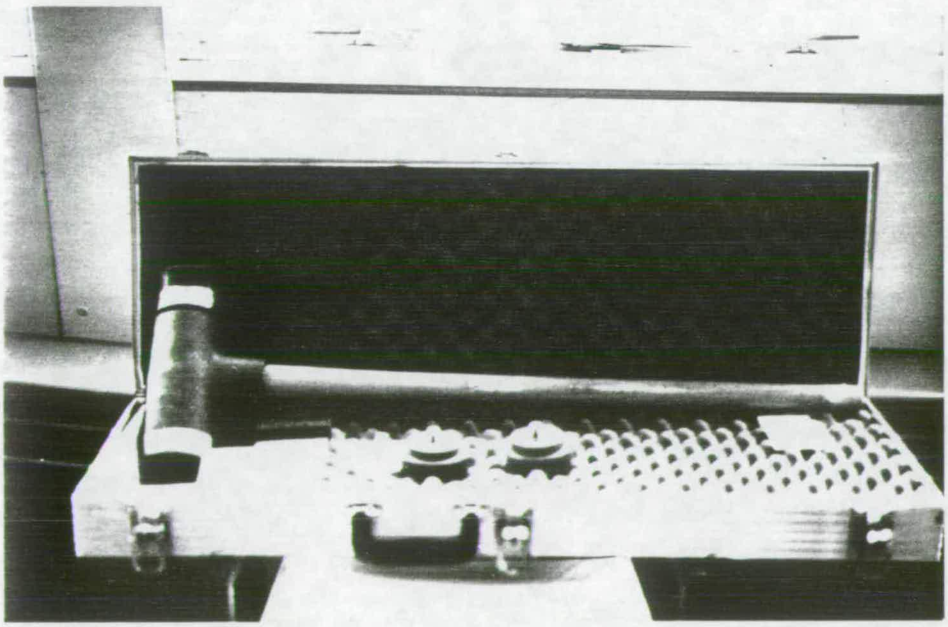

12 lb INSTRUMENTED HAMMER

PLATE 6.4

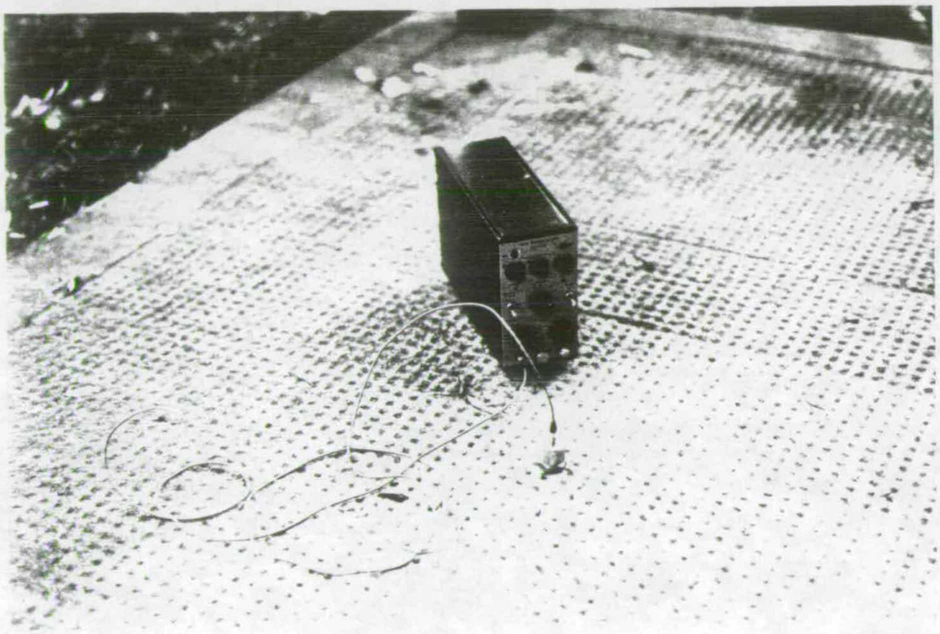

ACCELEROMETER AND CONDITIONING UNIT

PLATE 6.5

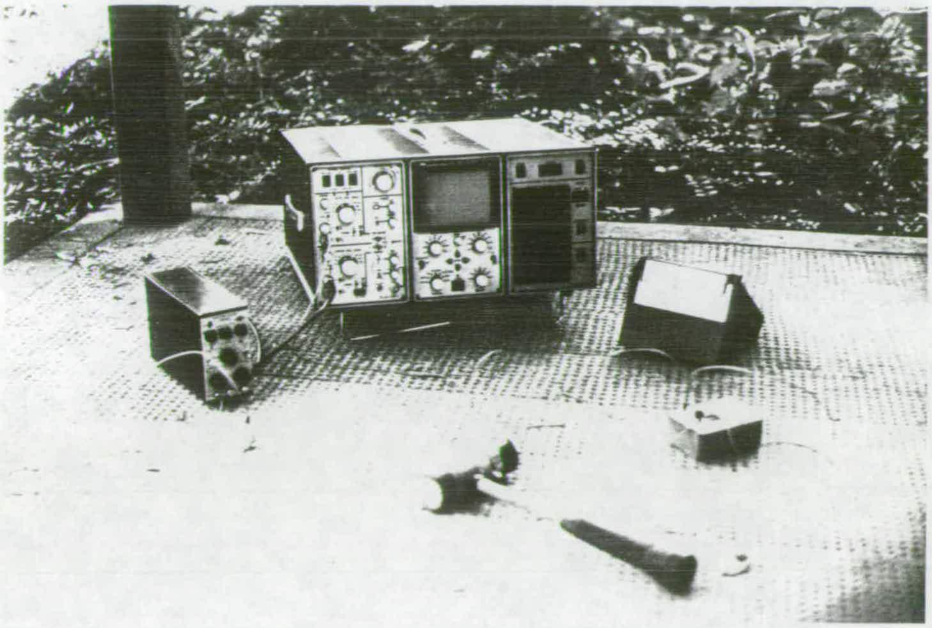

EQUIPMENT USED IN PHASE B EXPERIMENTS

PLATE 6.6

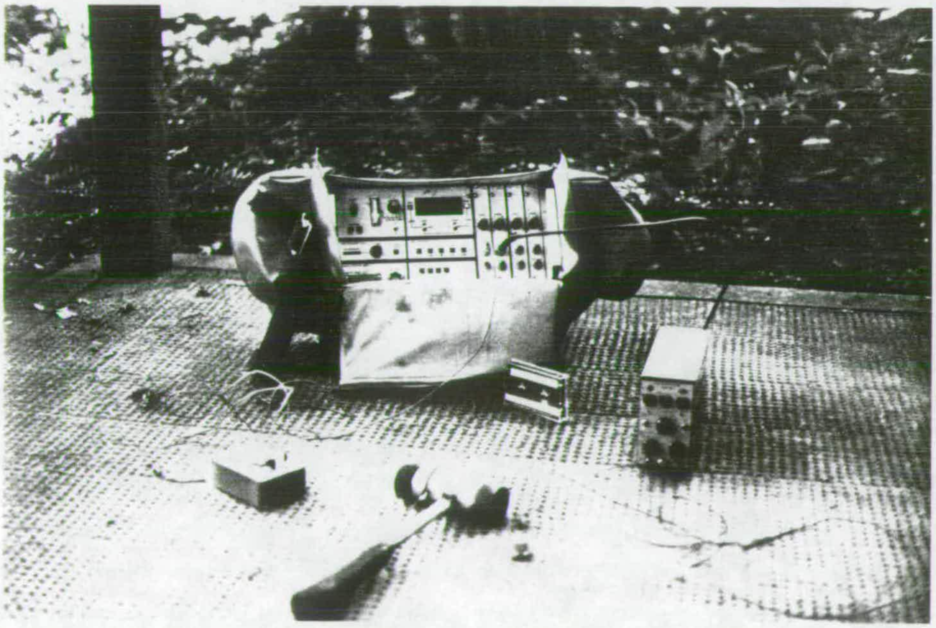

MEASUREMENT EQUIPMENT IN PHASE D EXPERIMENTS

PLATE 6.7

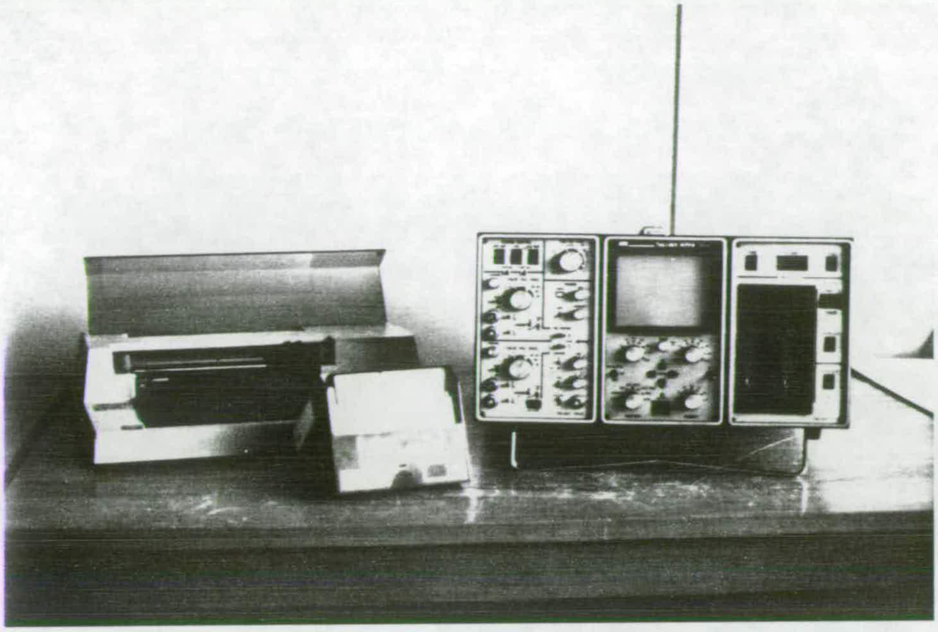

ANALYSIS INSTRUMENTATION USED IN PHASE D

PLATE 6.8

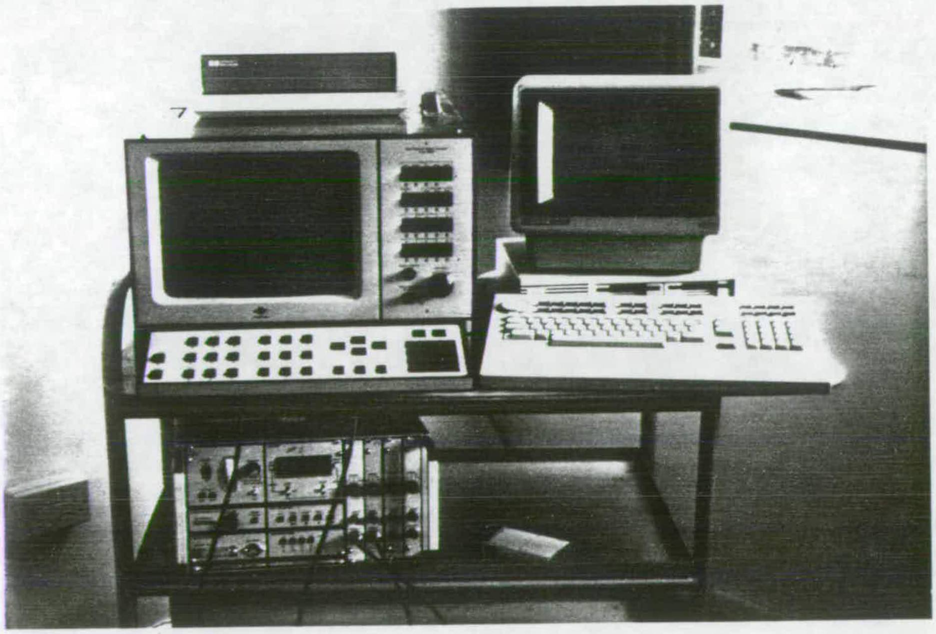

ANALYSIS INSTRUMENTATION USED IN PHASE D

PLATE 6.9

CHAPTER 7

COLUMNS

(ENHANCED SIGNAL PROCESSING AND ANALYSIS)

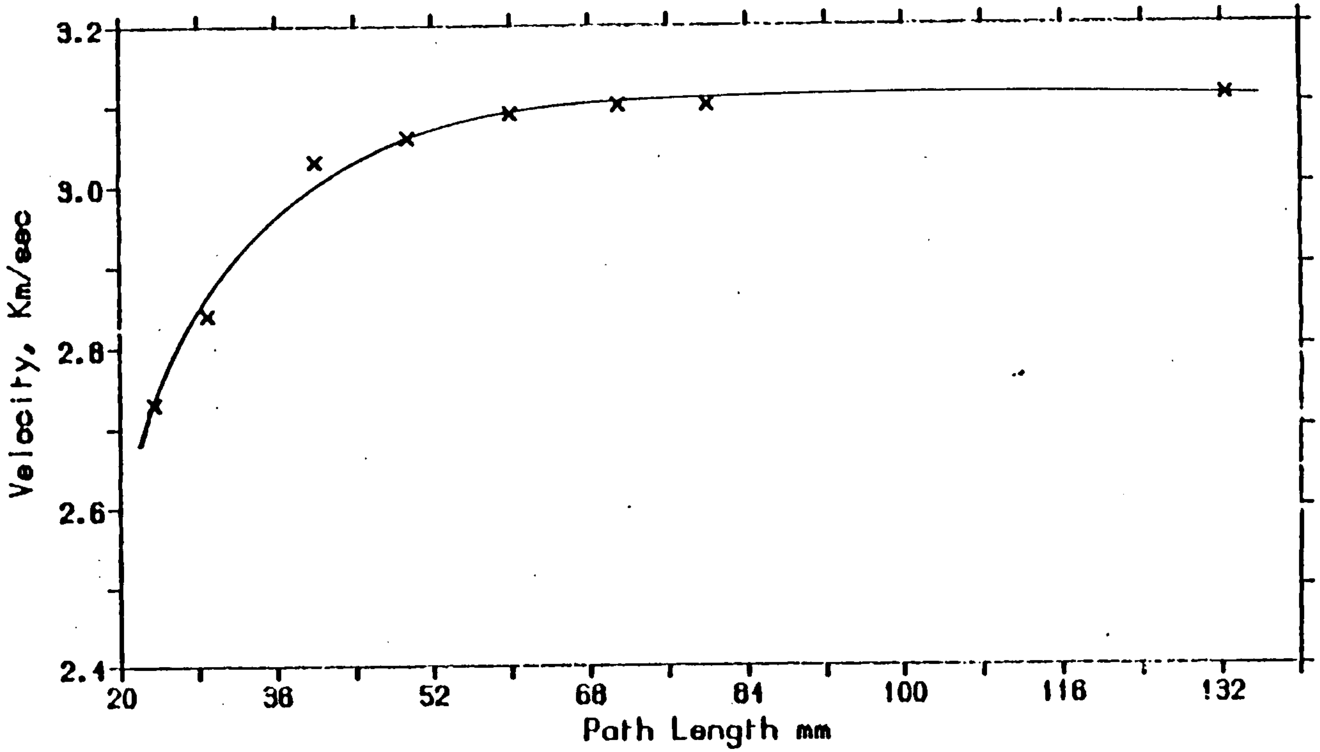

VARIATION OF UPV WITH MORTAR PATH LENGTH

FIGURE 7.1

(after Komeyli-Birjandi, ref. 4)

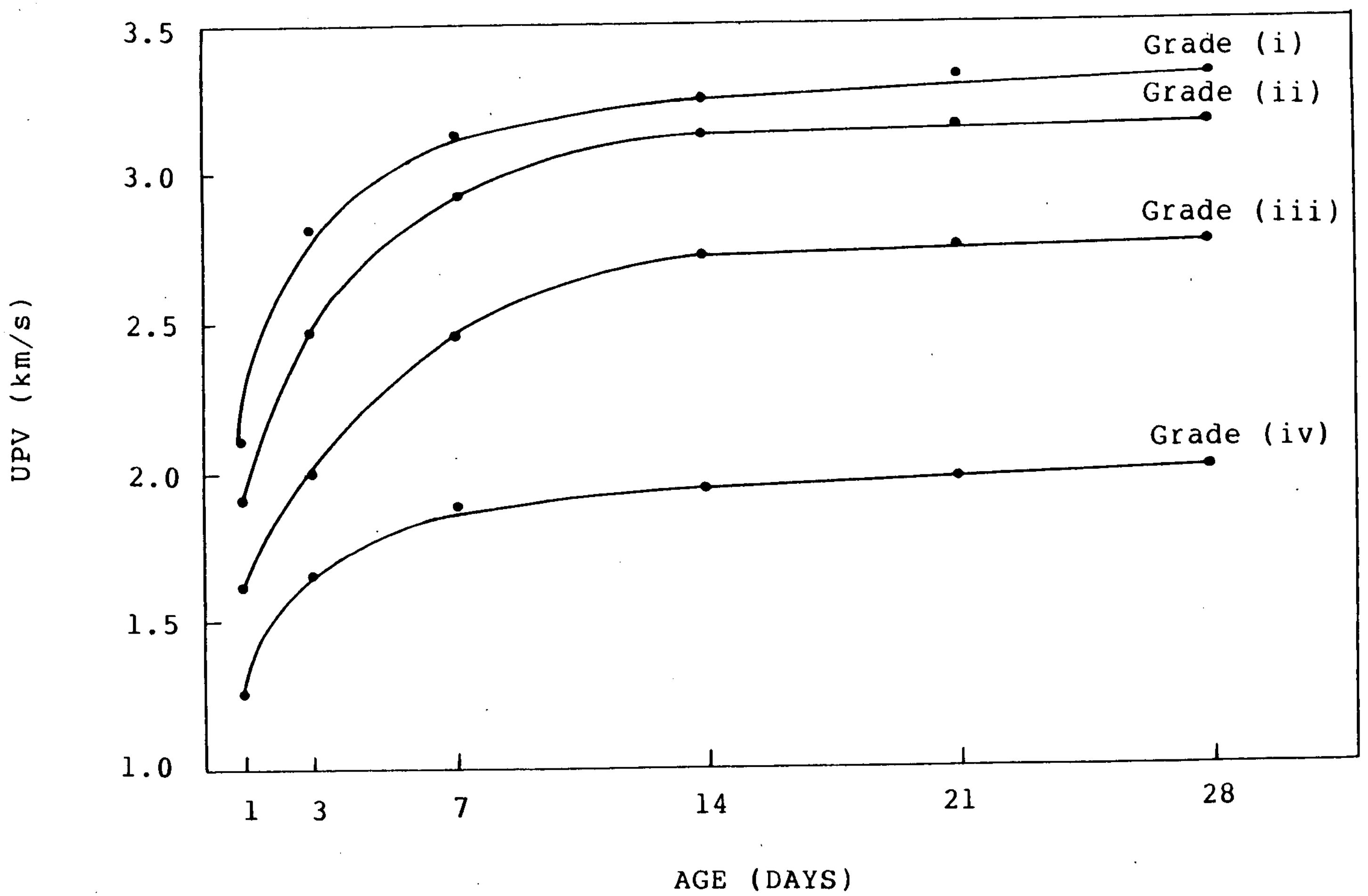

VARIATION OF UPV THROUGH MORTAR CUBES WITH AGE

FIGURE 7.2

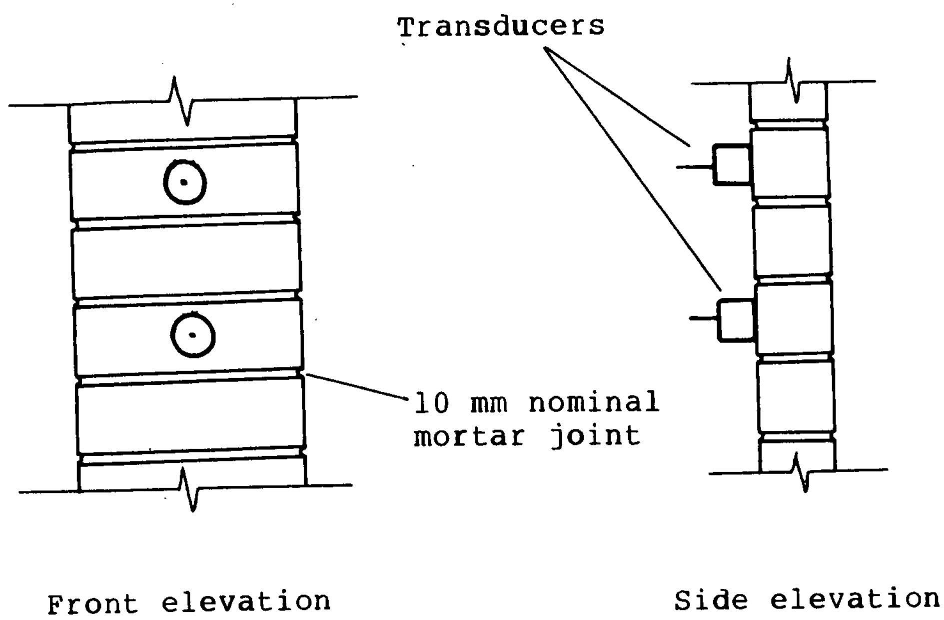

FIGURE 7.3

ARRANGEMENT FOR UPV TESTS ON COLUMNS

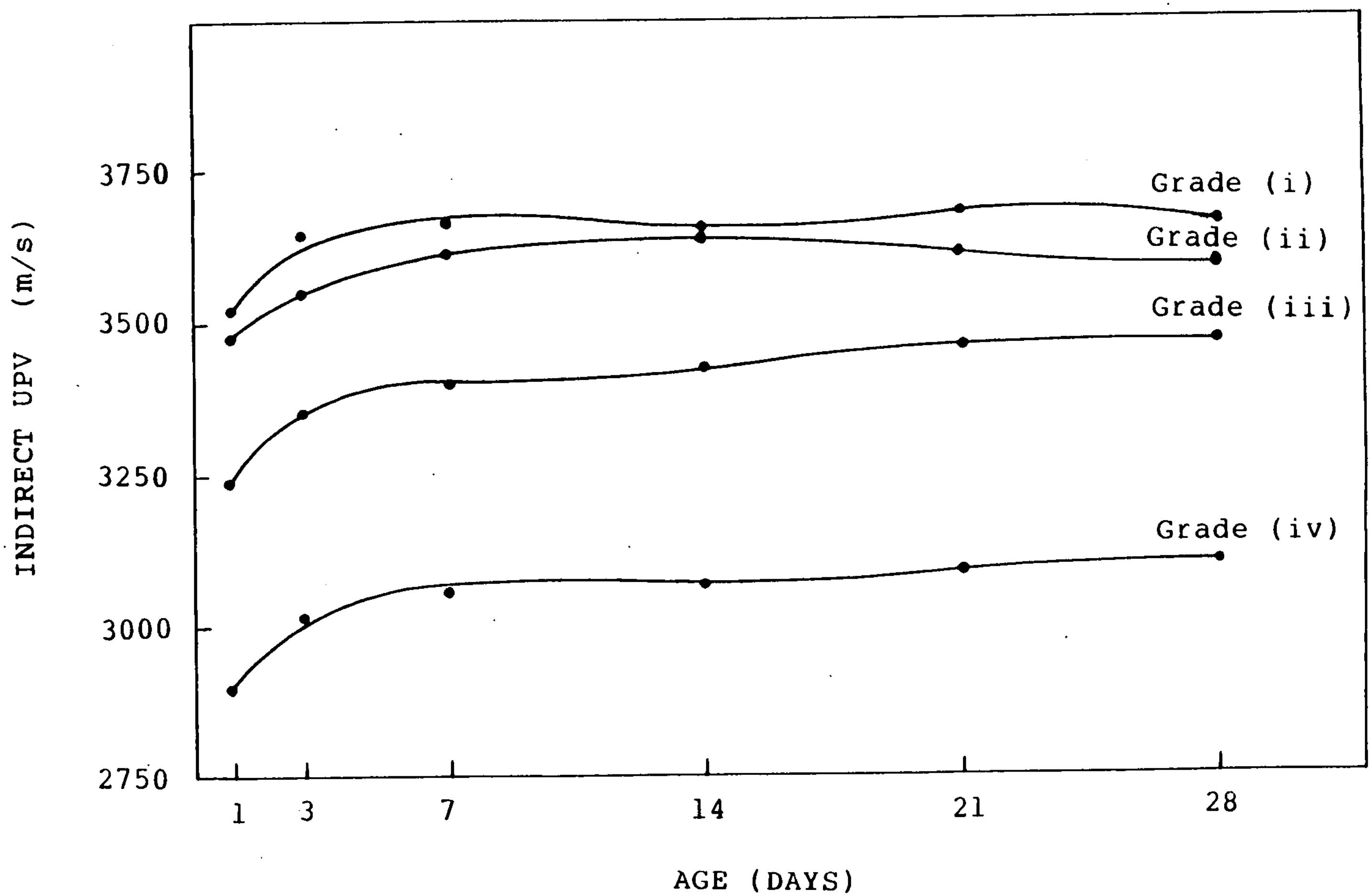

FIGURE 7.4

TYPICAL UPV TEST RESULT ON COLUMN MORTAR JOINTS
EFFECT OF MORTAR STRENGTH

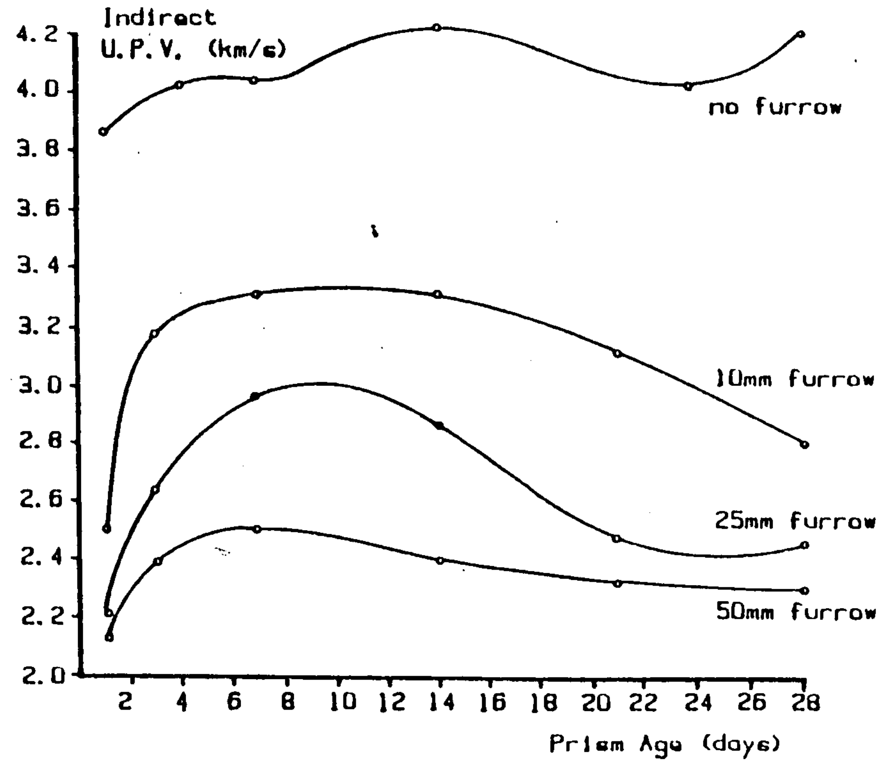

INFLUENCE OF FURROWED BED JOINTS

FIGURE 7.5

(after Hobbs, ref. 10)

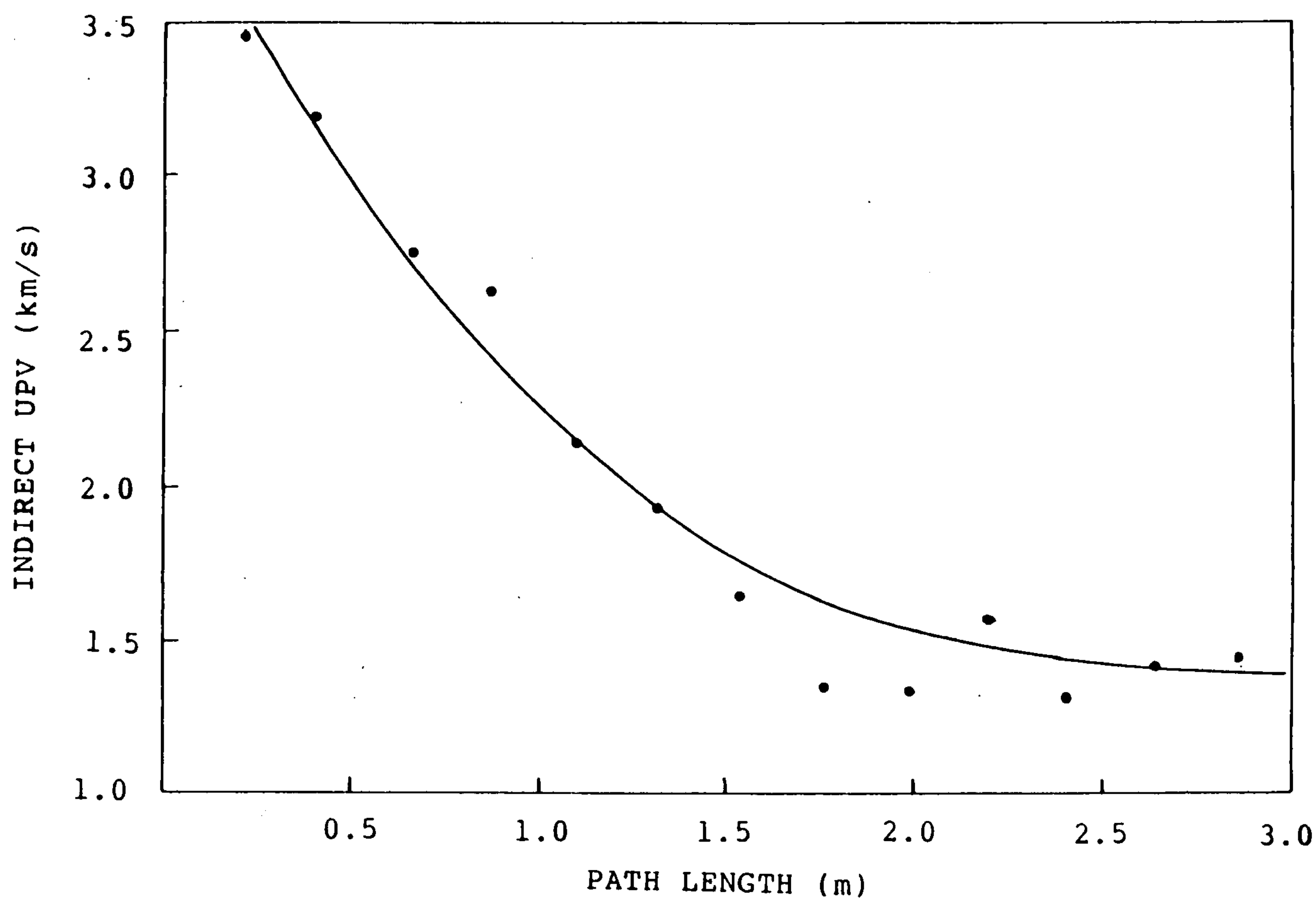

FIGURE 7.6

VARIATION IN INDIRECT UPV WITH MASONRY PATH LENGTH

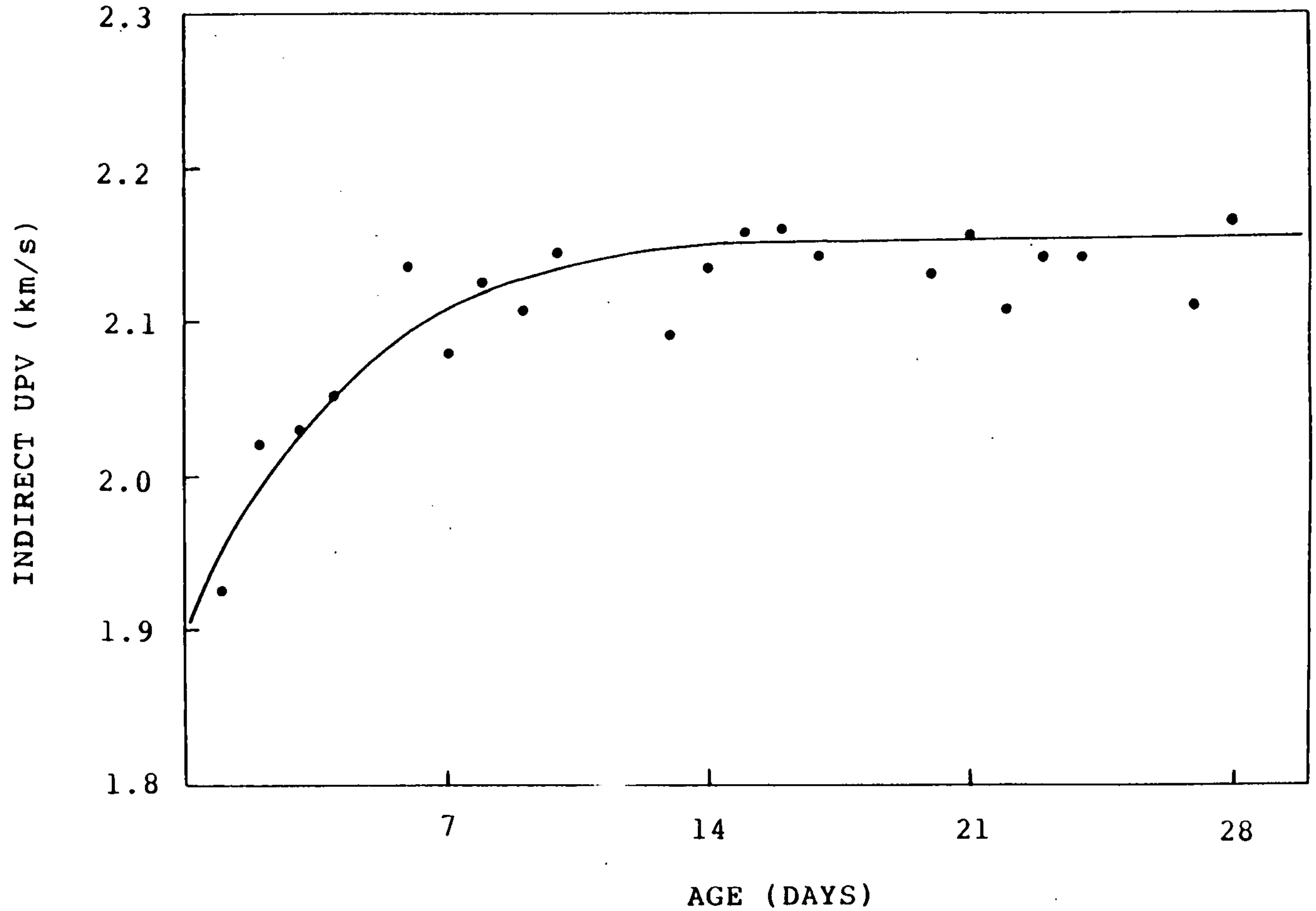

FIGURE 7.7

VARIATION OF INDIRECT UPV THROUGH MASONRY WITH AGE
(1 m PATH LENGTH)

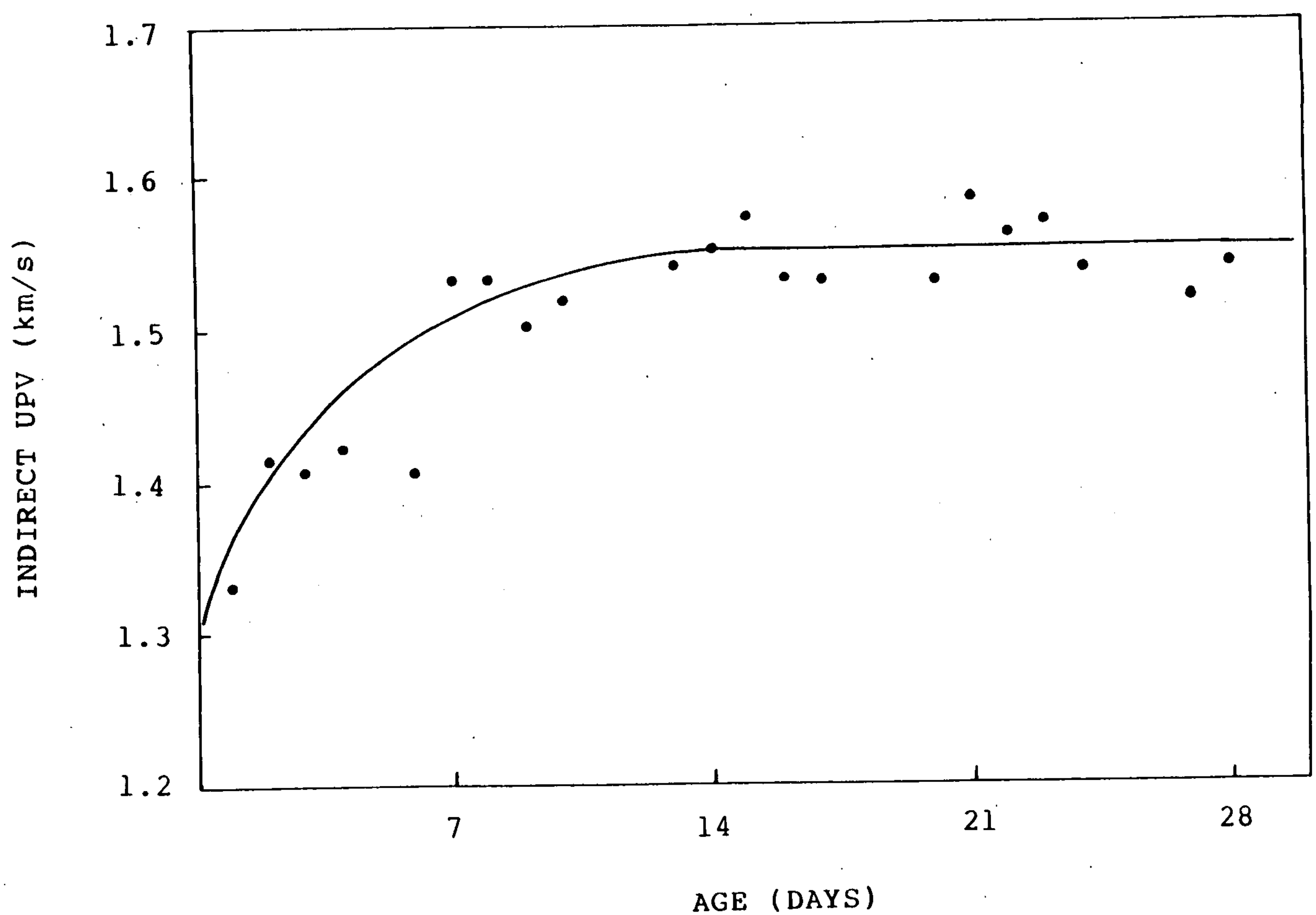

FIGURE 7.8

VARIATION OF INDIRECT UPV THROUGH MASONRY WITH AGE (2 m PATH LENGTH)

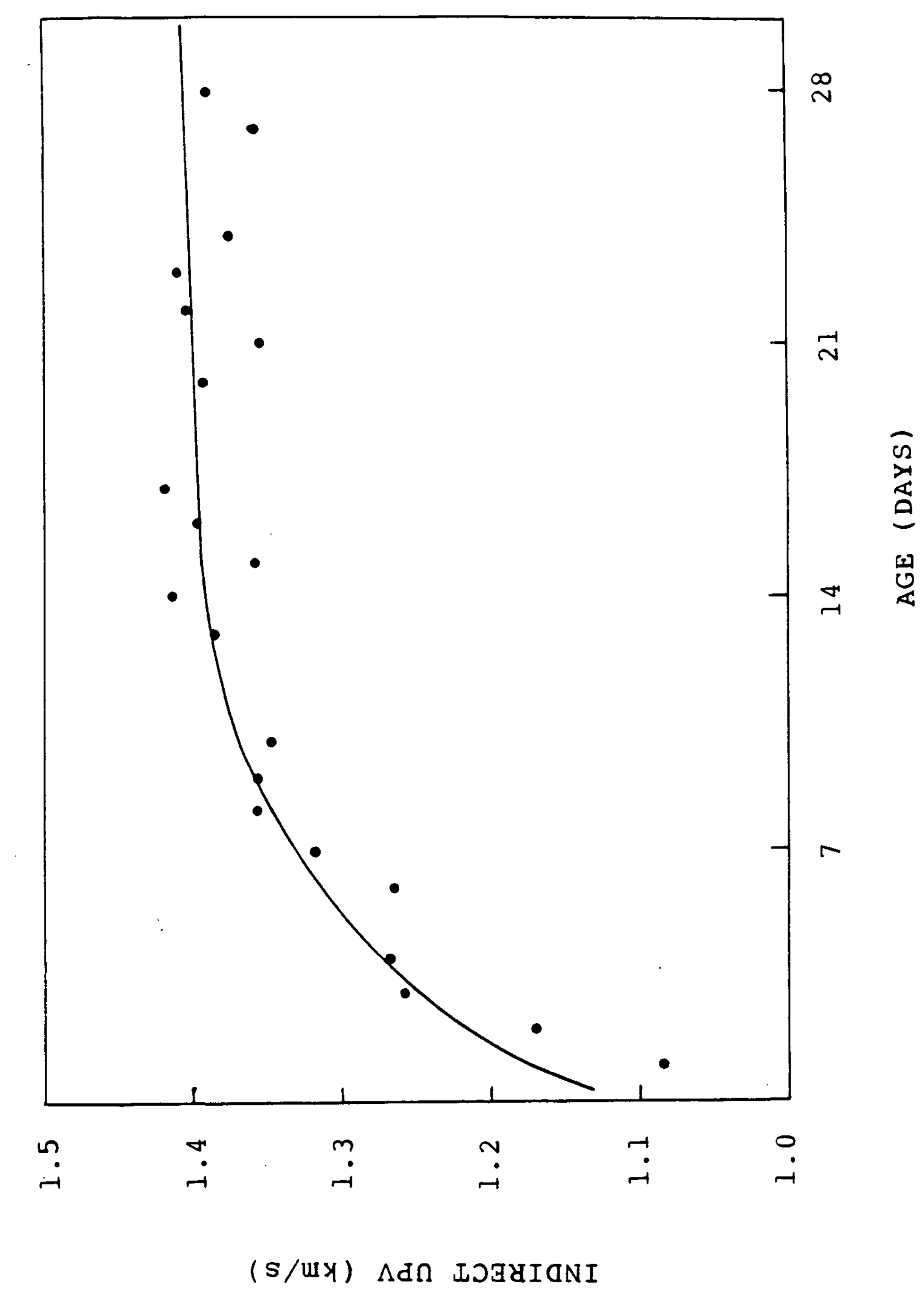

VARIATION OF INDIRECT UPV THROUGH MASONRY WITH AGE
(3 M PATH LENGTH)

FIGURE 7.9

W3 TIME CH.A REAL INPUT MAIN Y: 111U
Y: 13.5kU X: 0.000ms
X: 0.000ms + 7.81ms

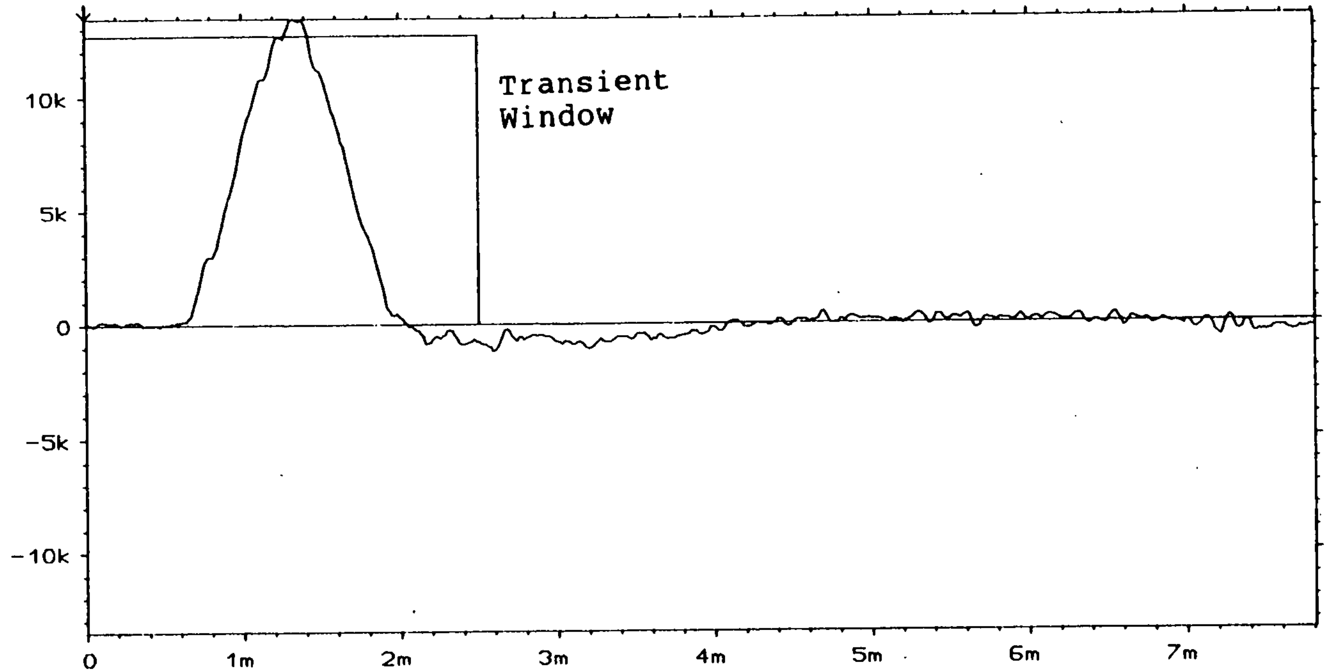

SETUP W10

MEASUREMENT:	DUAL SPECTRUM AVERAGING
TRIGGER:	CH.A +SLOPE LEVEL: +0.10 MAX INPUT
DELAY:	TRIG→A: -1.007ms CH.A→B: 0.000ms
AVERAGING:	LIN 5
FREQ SPAN:	25.6kHz ΔF:32Hz T:31.3ms ΔT:15.3µs
CENTER FREQ:	BASEBAND
WEIGHT CH.A:	TRANSIENT SHIFT:0.000ms LENGTH:2.502ms
WEIGHT CH.B:	EXPONENTIAL SHIFT:0.000ms LENGTH:20.004ms
CH.A:	6V + 3Hz DIR FILT:BOTH 92.0µV/N
CH.B:	6V + 3Hz DIR FILT:BOTH 31.6V/m/s
GENERATOR:	DISABLED

COLUMNS: TIME DOMAIN MEASUREMENT SET-UP
SHOWING HAMMER INPUT SIGNAL

FIGURE 7.10

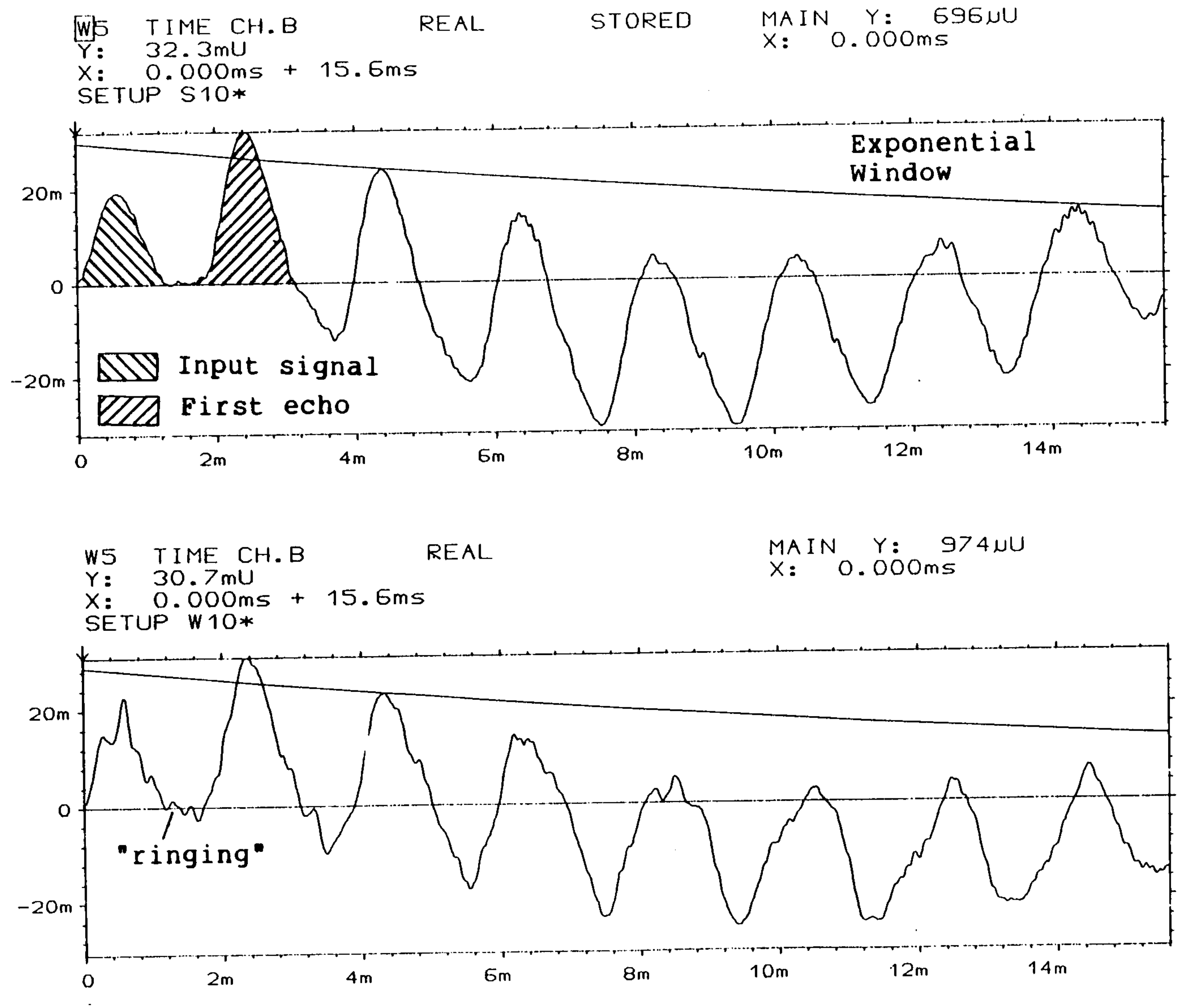

(a) Column 1

(b) Column 2

FIGURE 7.11

VELOCITY TIME RECORDS
COLUMNS: NO DEFECTS

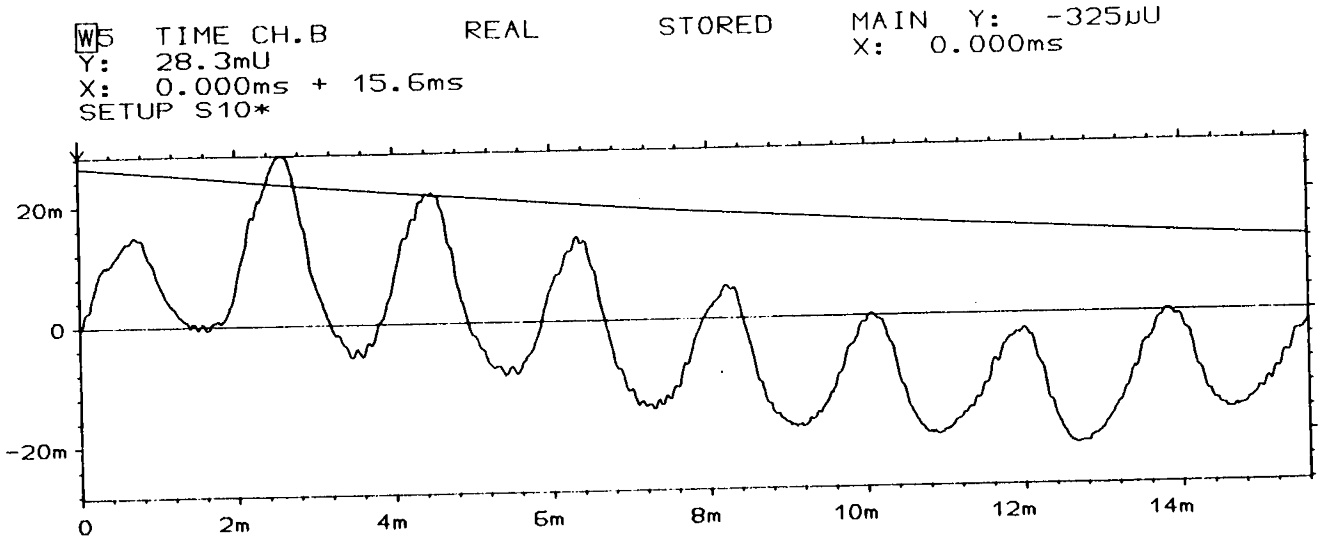

(a)
Column 3

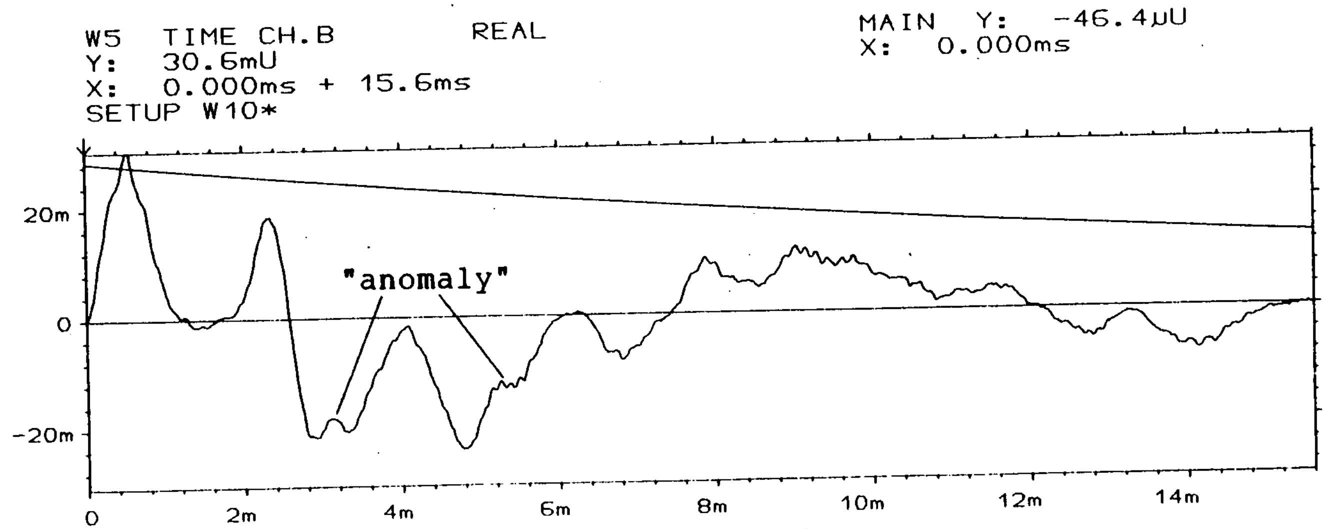

(b)
Column 4

FIGURE 7.12
VELOCITY TIME RECORDS
COLUMNS: NO DEFECTS

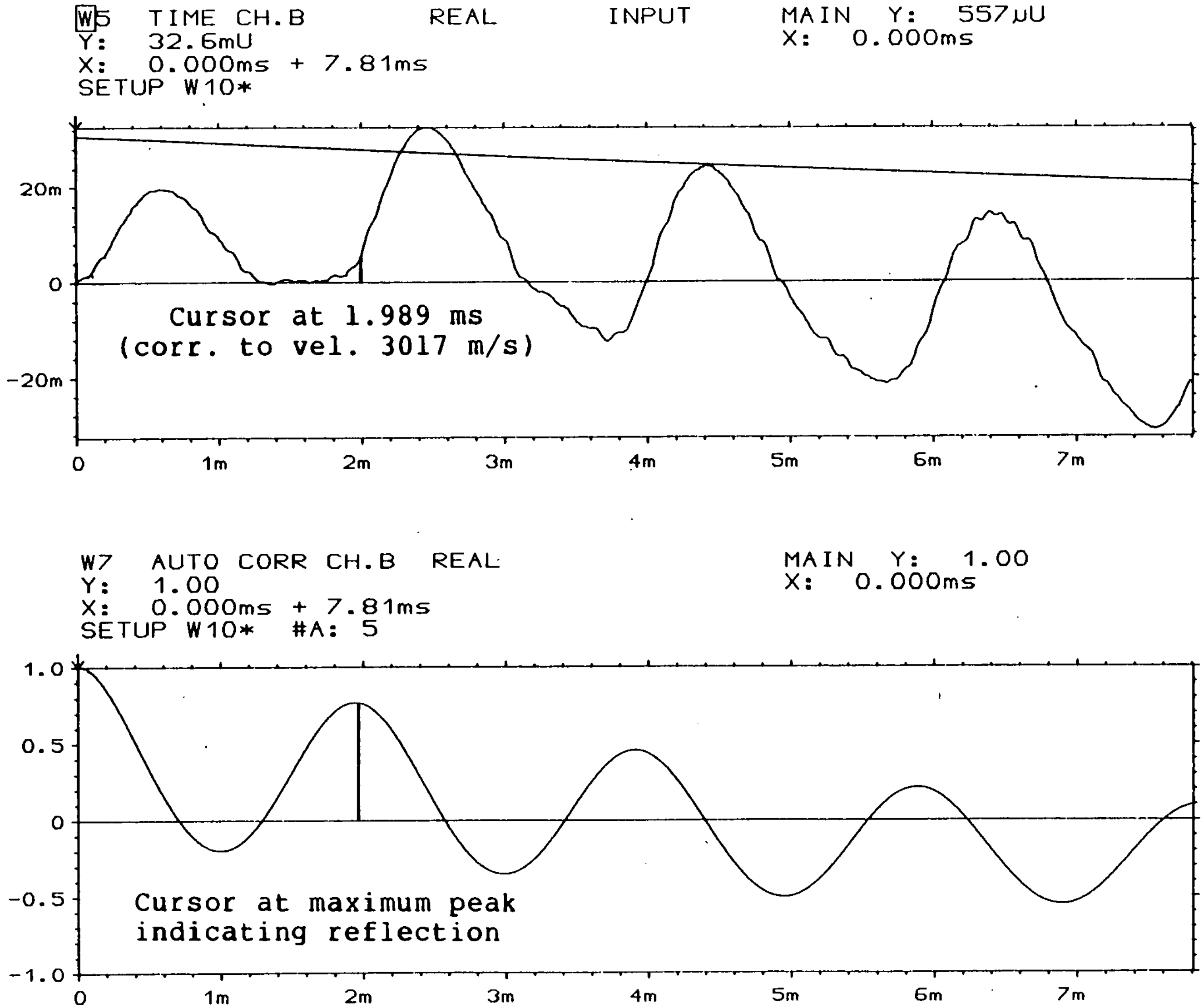

AUTO-CORRELATION FUNCTION
COLUMN 1: NO DEFECT
FIGURE 7.13

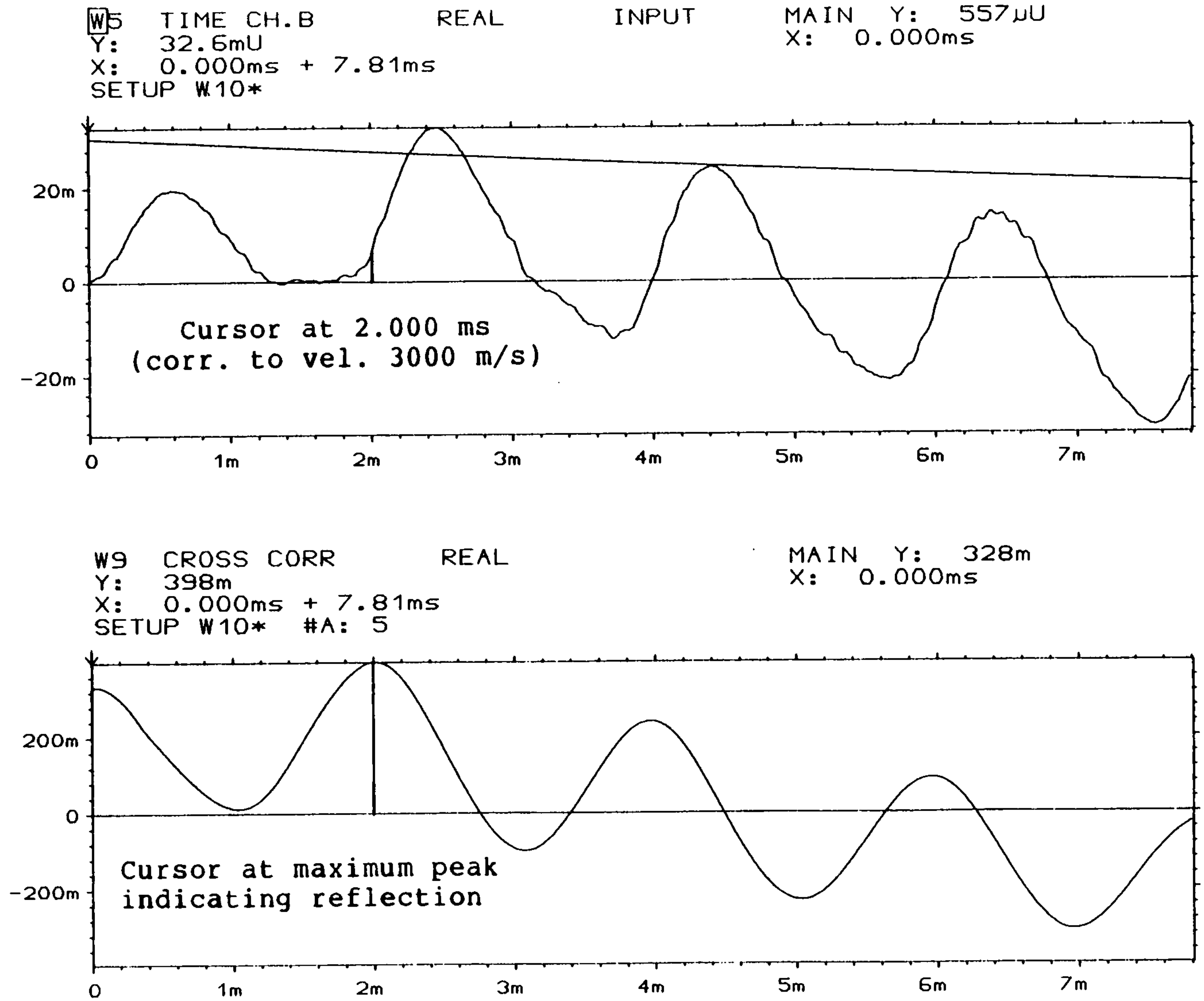

CROSS-CORRELATION (REAL) FUNCTION
COLUMN 1: NO DEFECT

FIGURE 7.14

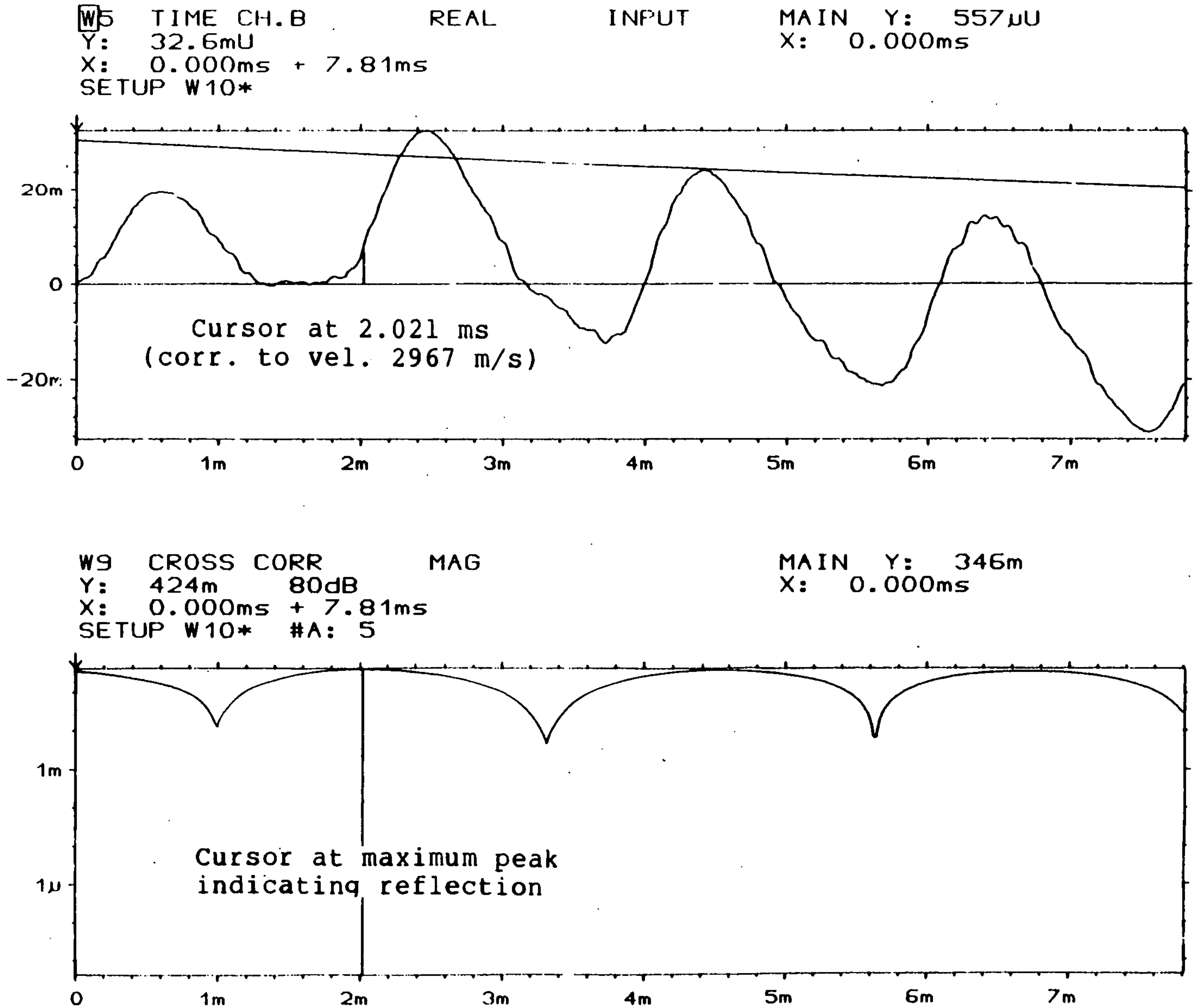

FIGURE 7.15

CROSS-CORRELATION (MAG.) FUNCTION
COLUMN 1: NO DEFECT

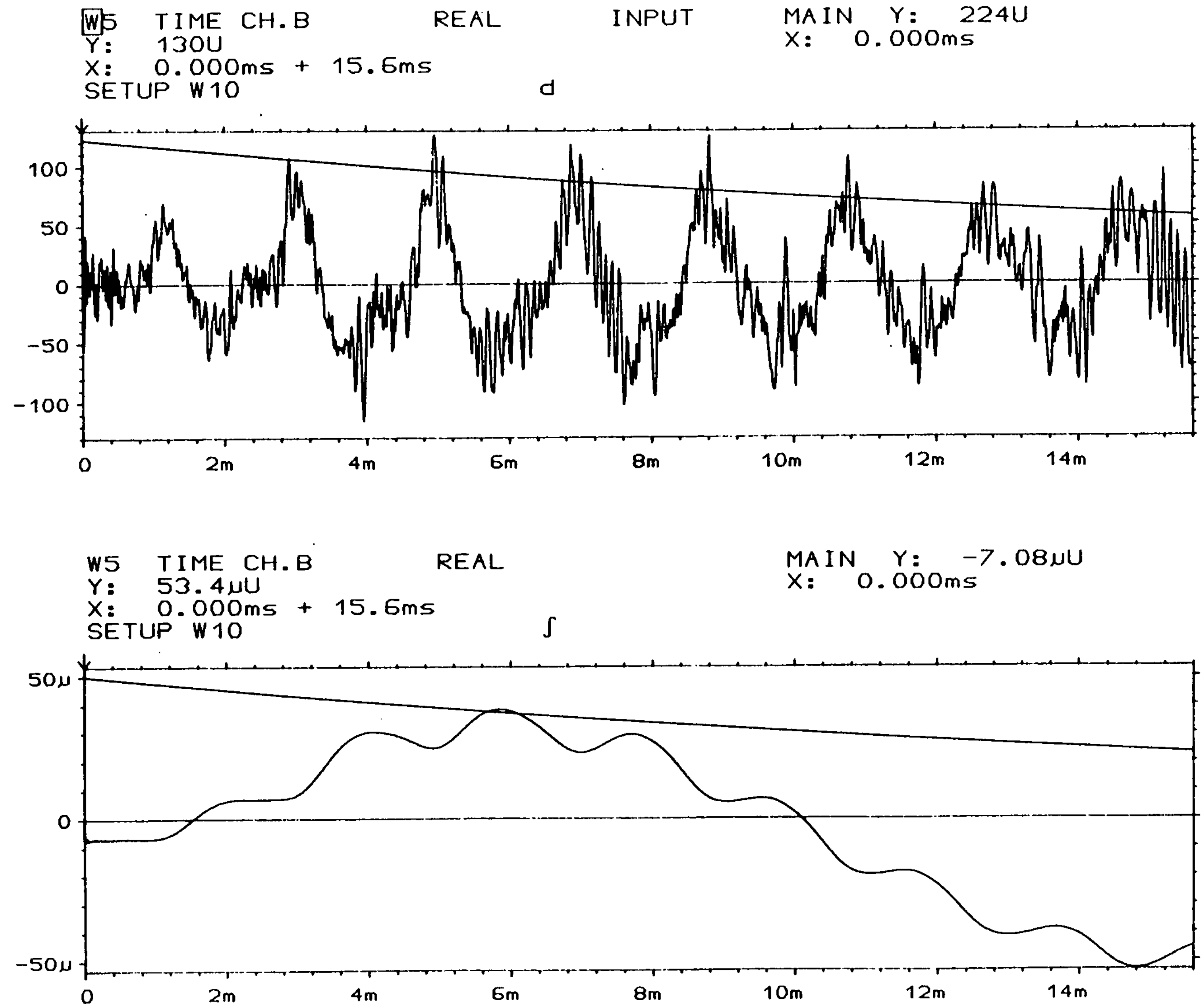

(a) Acceleration

(b) Displacement

FIGURE 7.16

TYPICAL ACCELERATION AND DISPLACEMENT TIME RECORDS

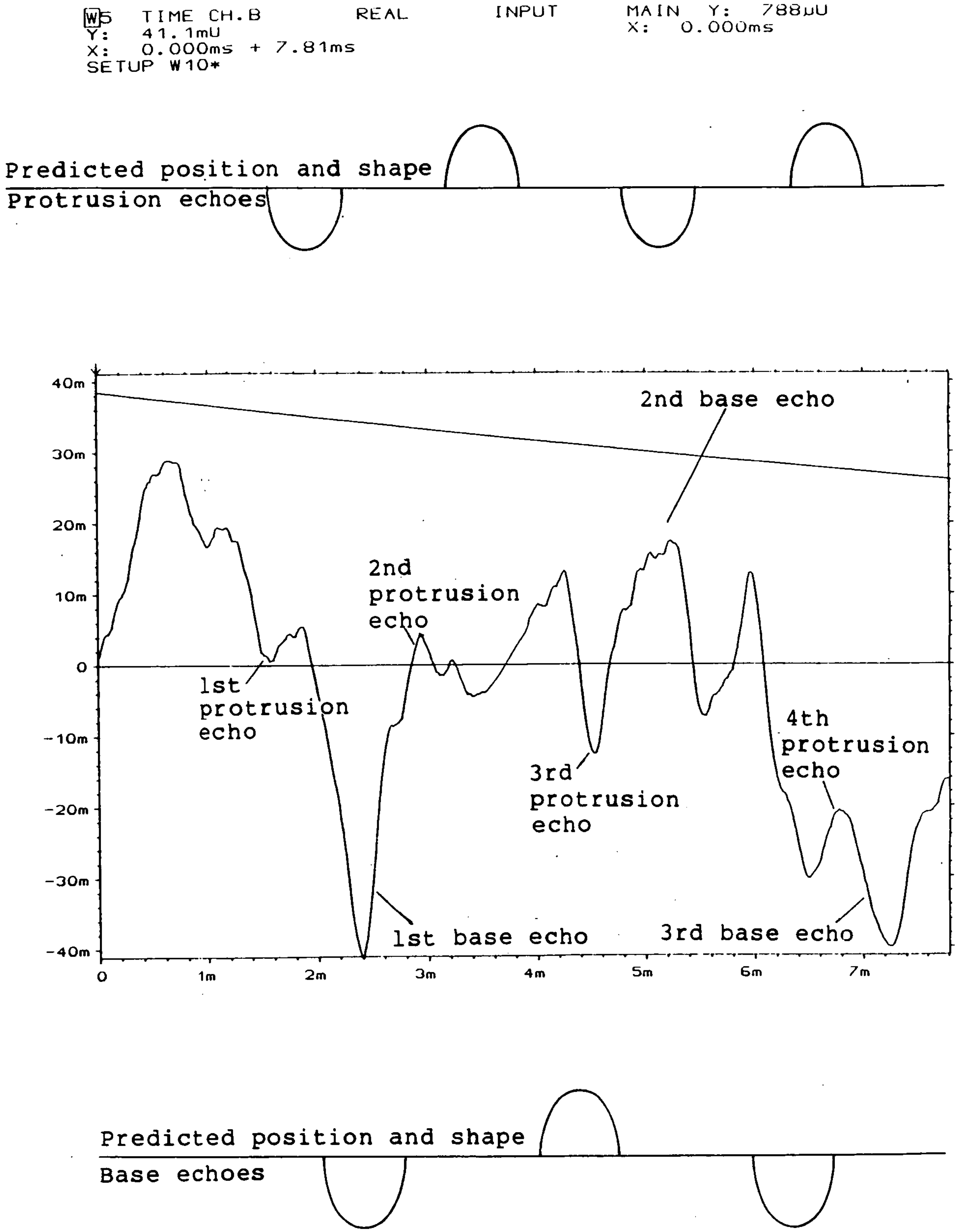

VELOCITY TIME RECORD
COLUMN 1: FIXED BASE

FIGURE 7.17

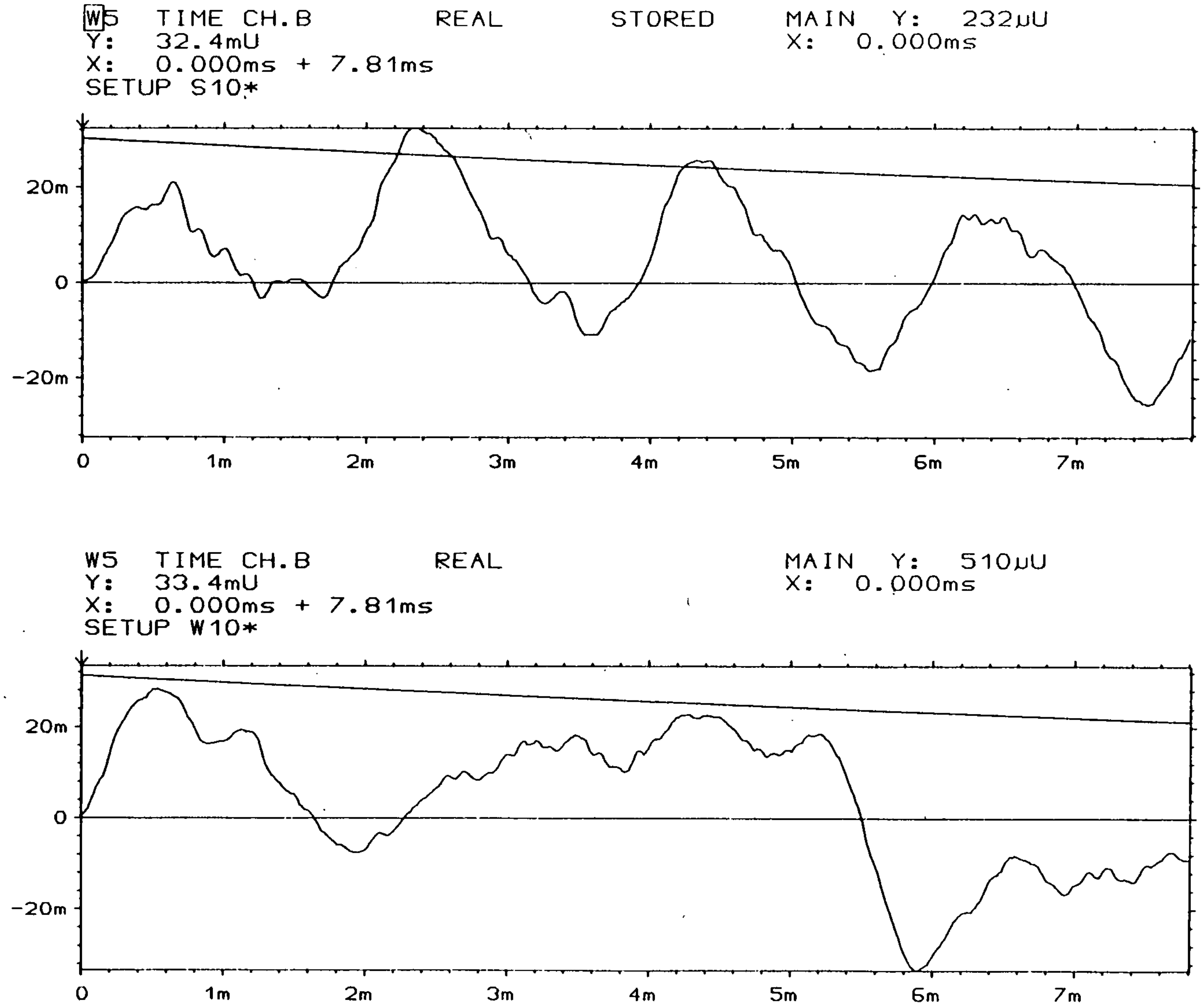

(a) 10 % cut

(b) 20 % cut

FIGURE 7.18

COLUMN 2: MORTAR DEFECT

VELOCITY TIME RECORD

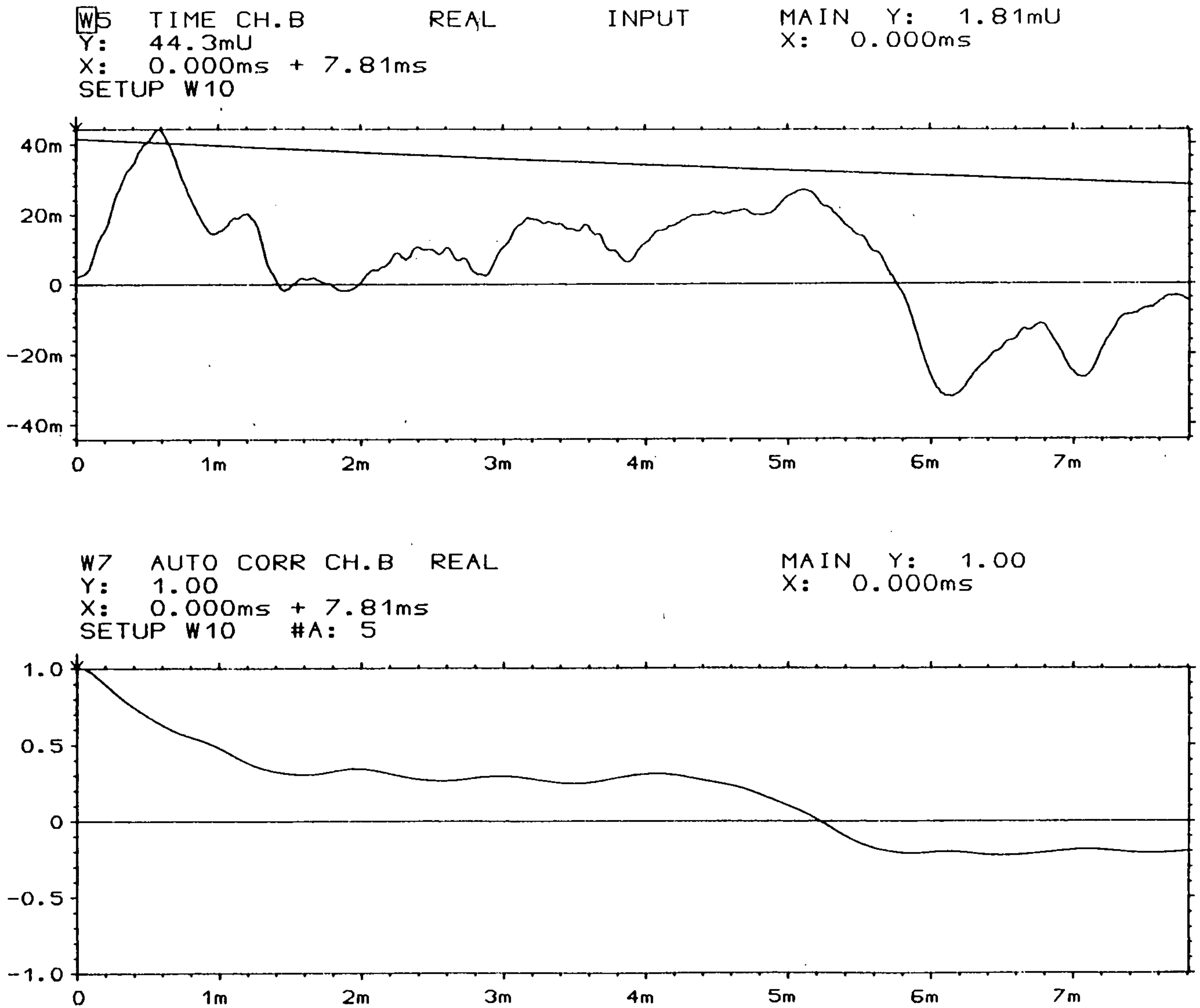

AUTO-CORRELATION AND VELOCITY TIME RECORD
COLUMN 2: 50 % MORTAR DEFECT

FIGURE 7.19

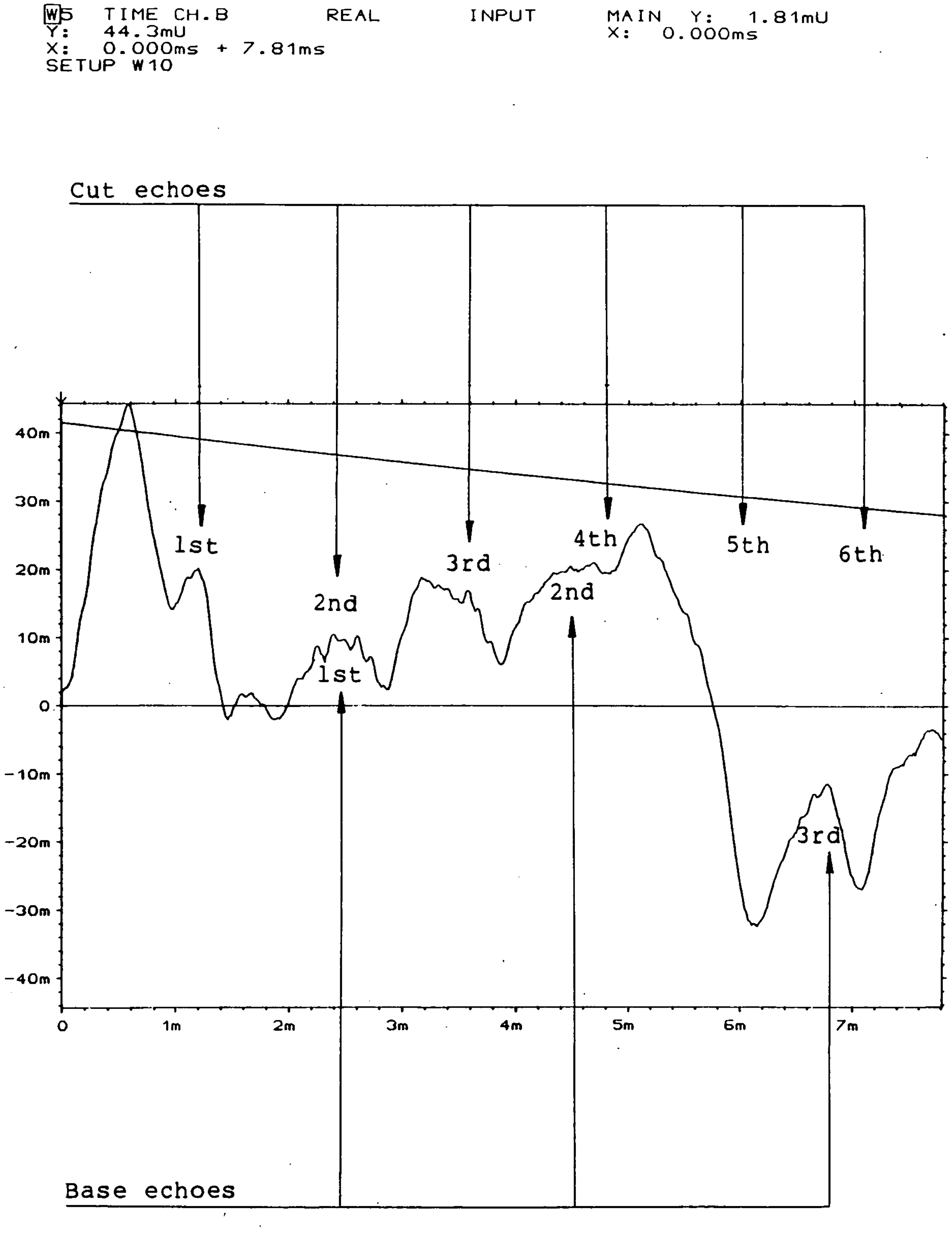

VELOCITY TIME RECORD
COLUMN 2: 50 % MORTAR DEFECT

FIGURE 7.20

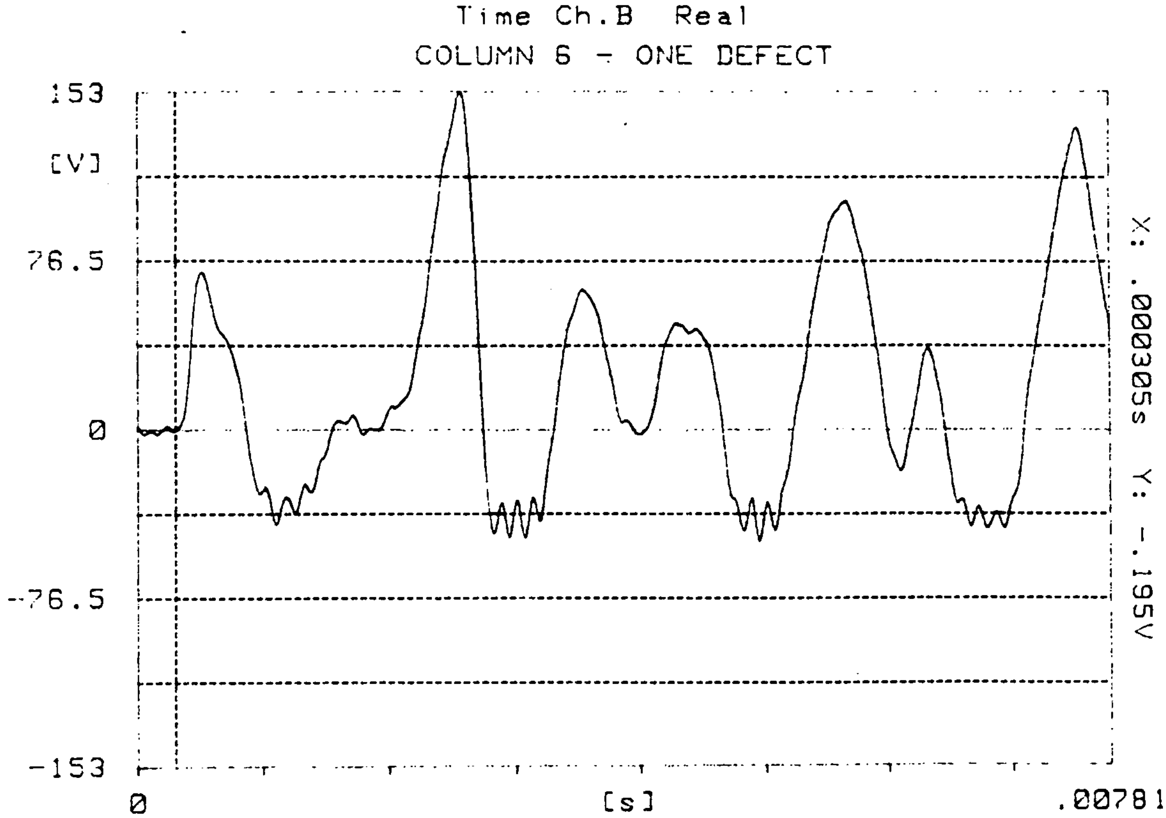

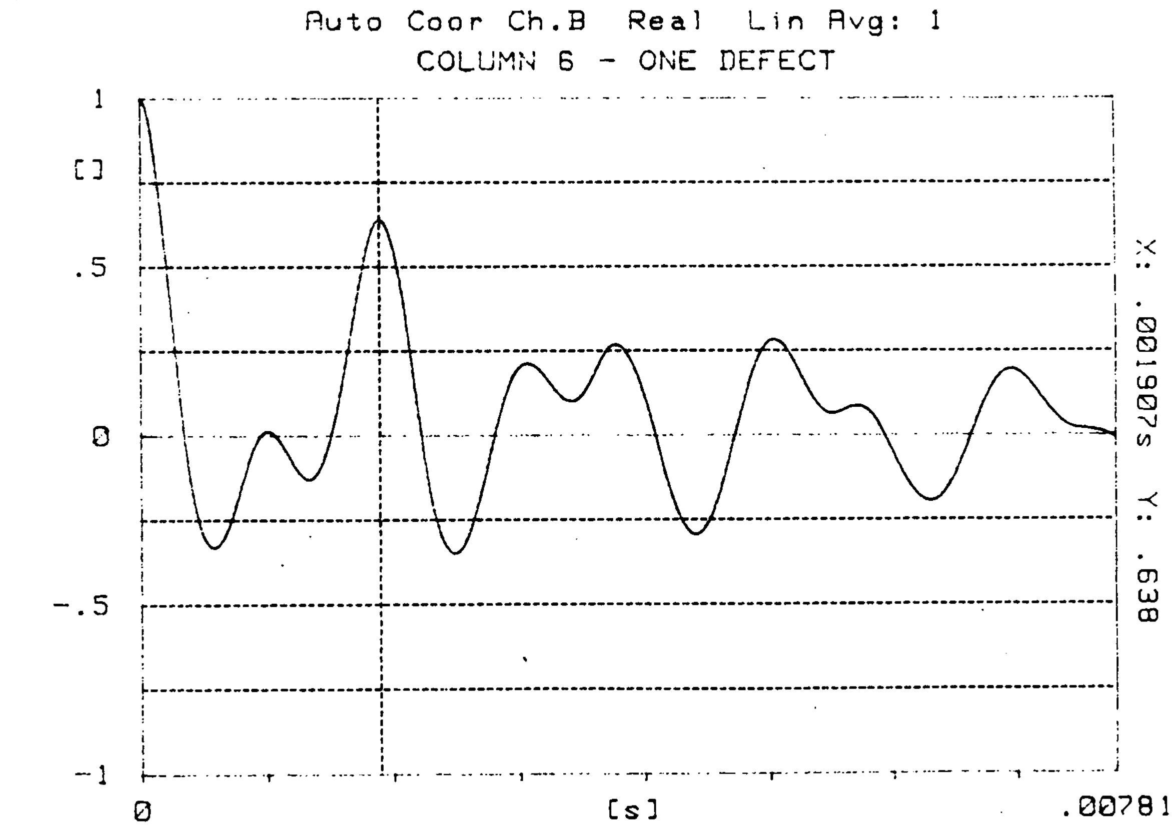

AUTO-CORRELATION AND VELOCITY TIME RECORD
COLUMN: 15 % MORTAR DEFECT

FIGURE 7.21

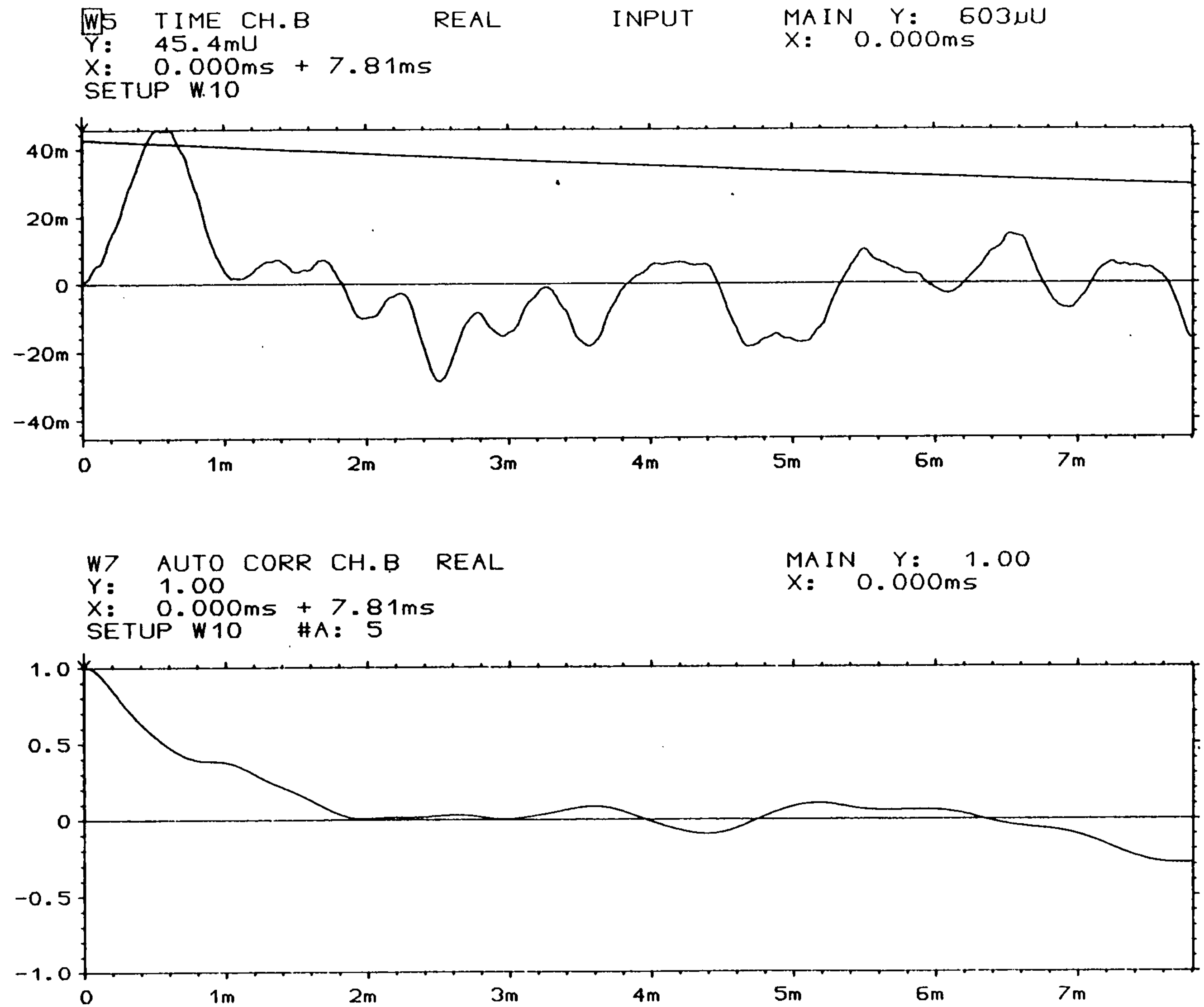

AUTO-CORRELATION AND VELOCITY TIME RECORD
COLUMN 1: 50 % MORTAR DEFECT

FIGURE 7.22

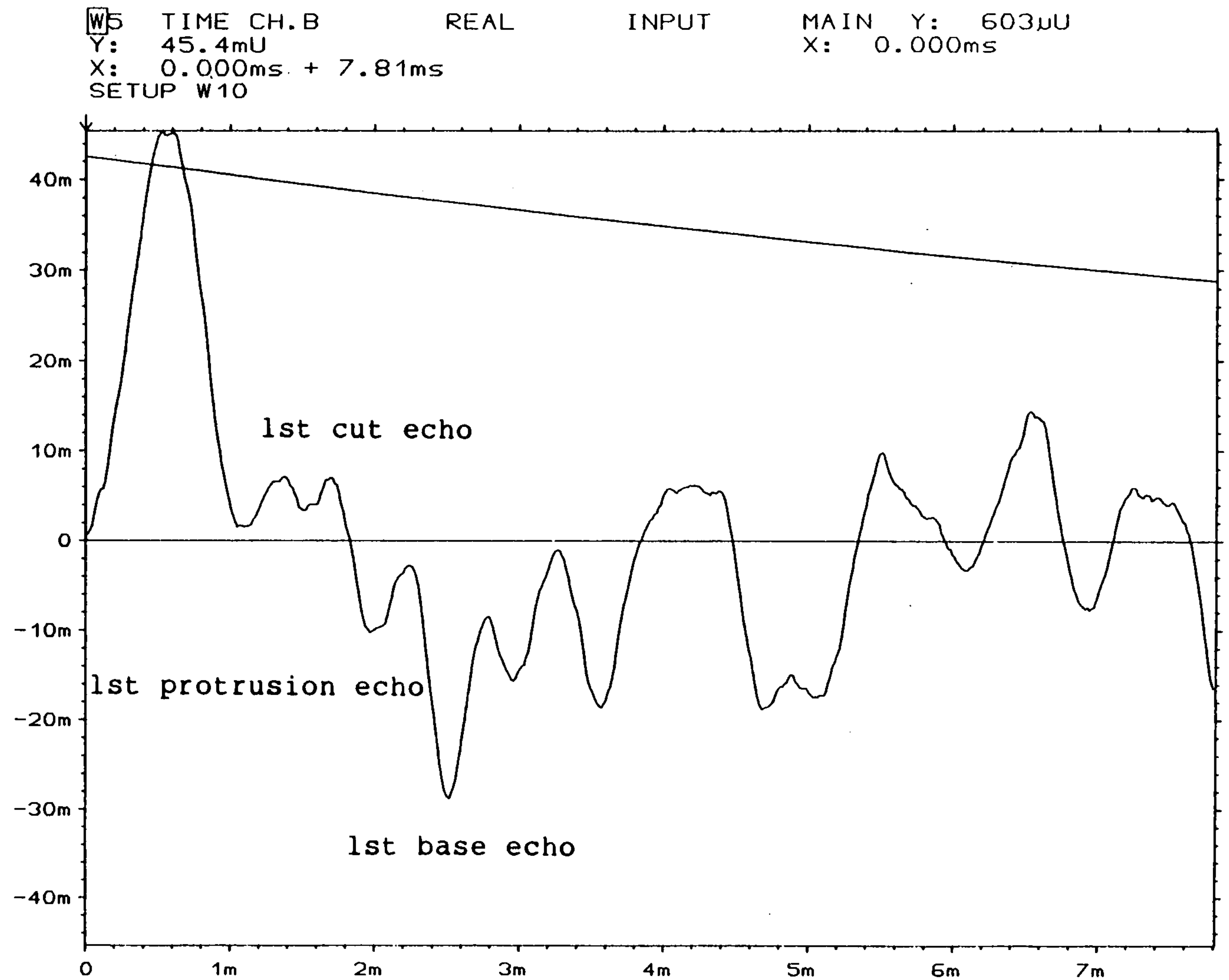

VELOCITY TIME RECORD
COLUMN 1: 50 % MORTAR DEFECT
FIGURE 7.23

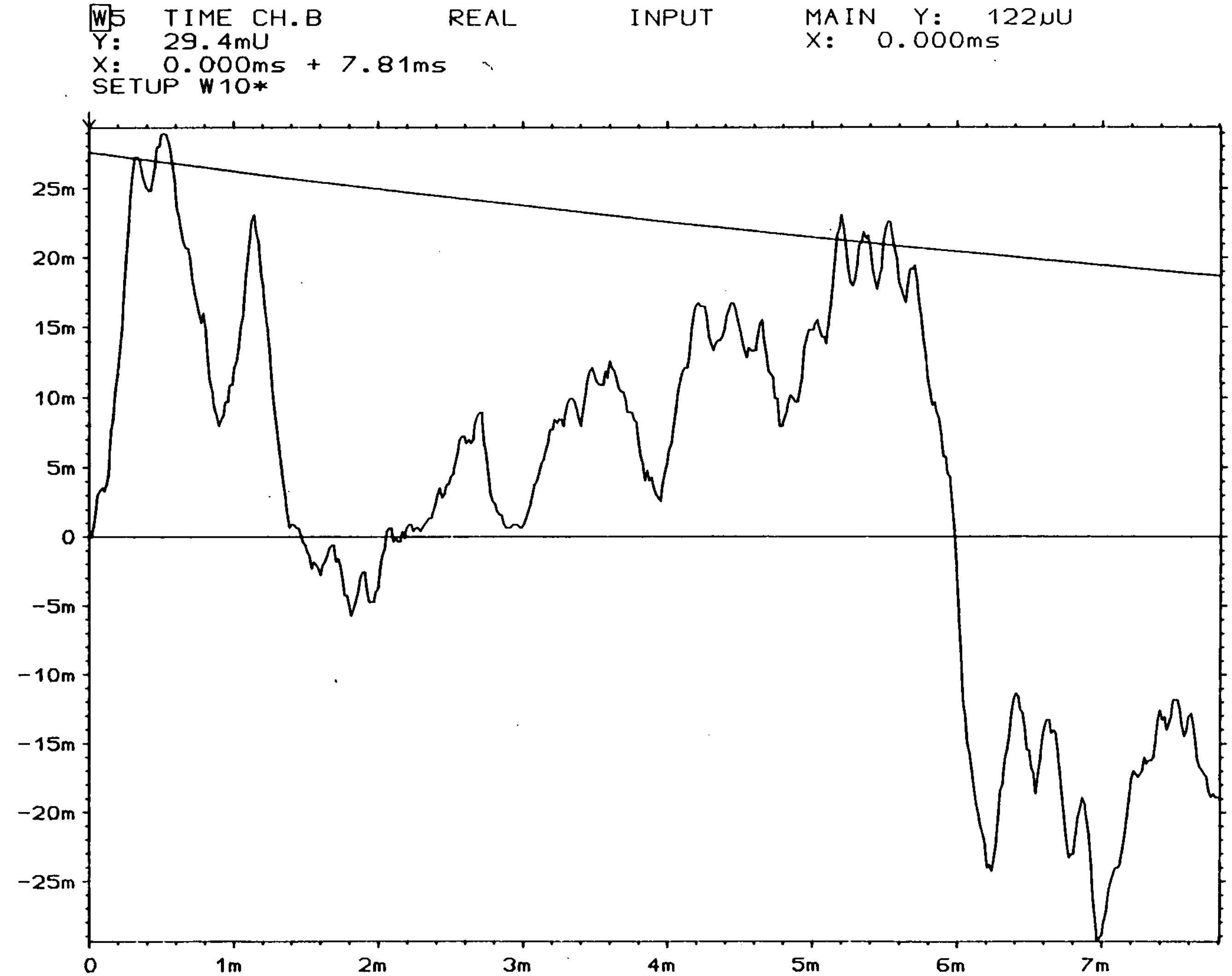

FIGURE 7.24

VELOCITY TIME RECORD
COLUMN 2: 1st REPAIR

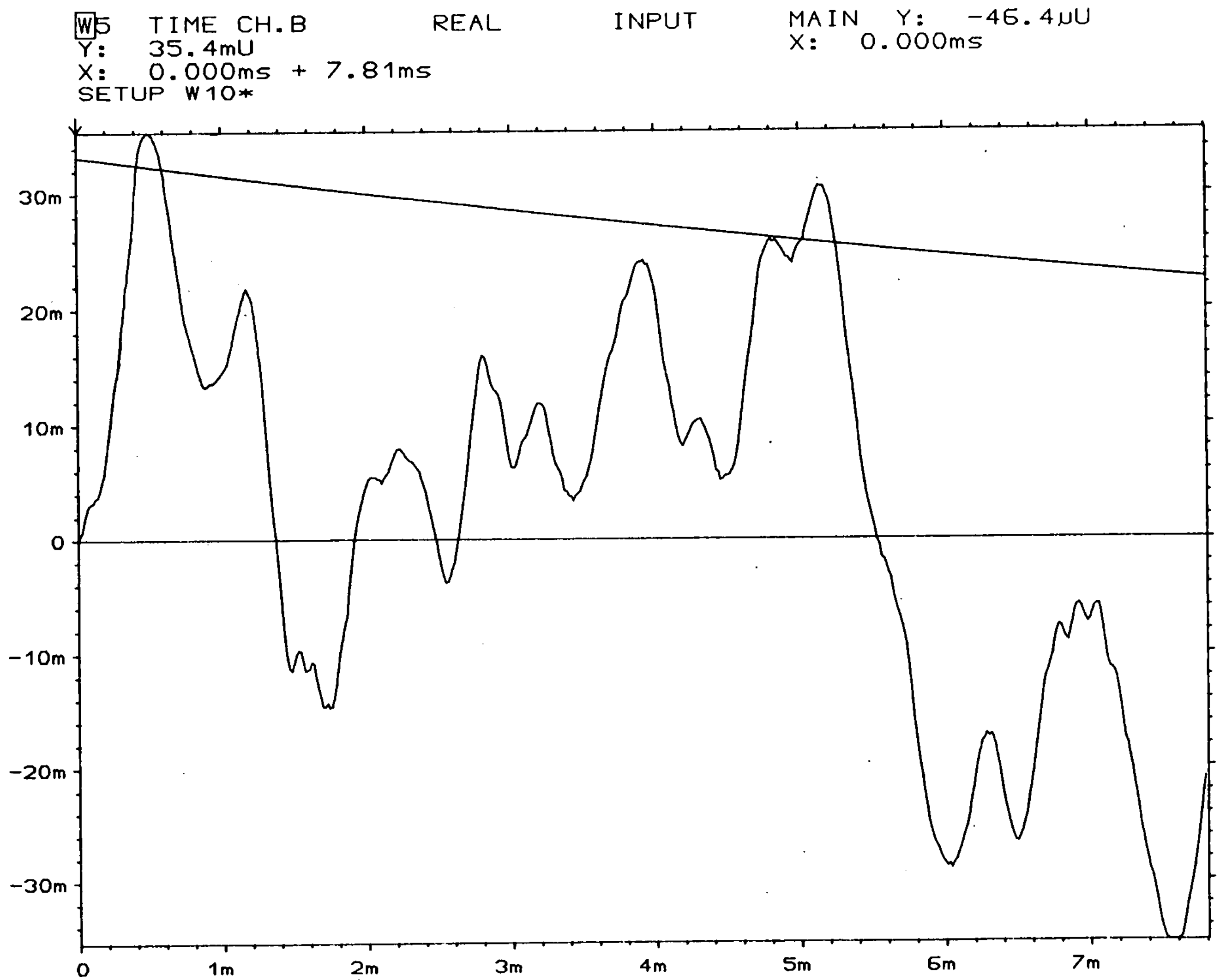

VELOCITY TIME RECORD
COLUMN 2: 2nd REPAIR

FIGURE 7.25

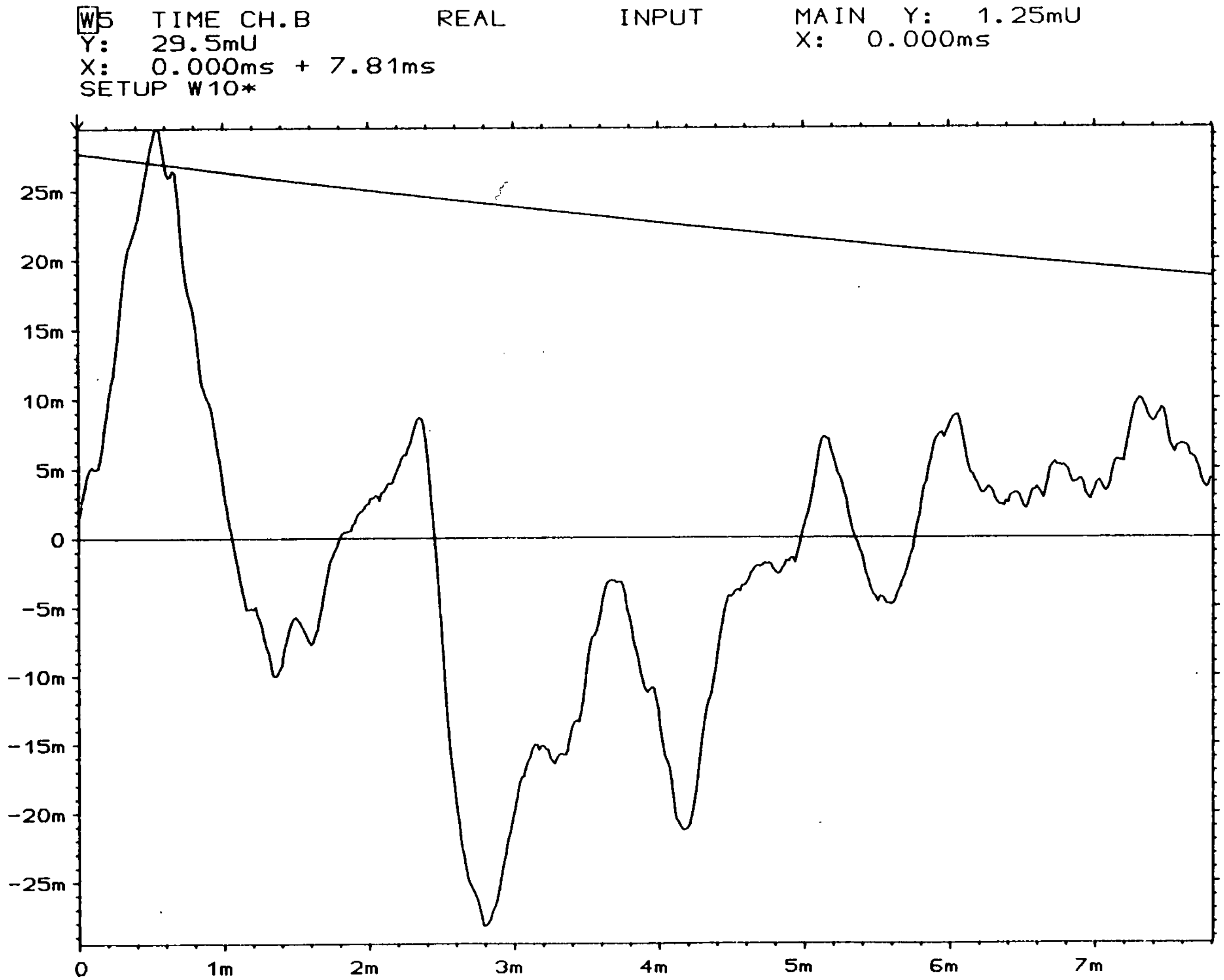

VELOCITY TIME RECORD
COLUMN 1: REPAIR

FIGURE 7.26

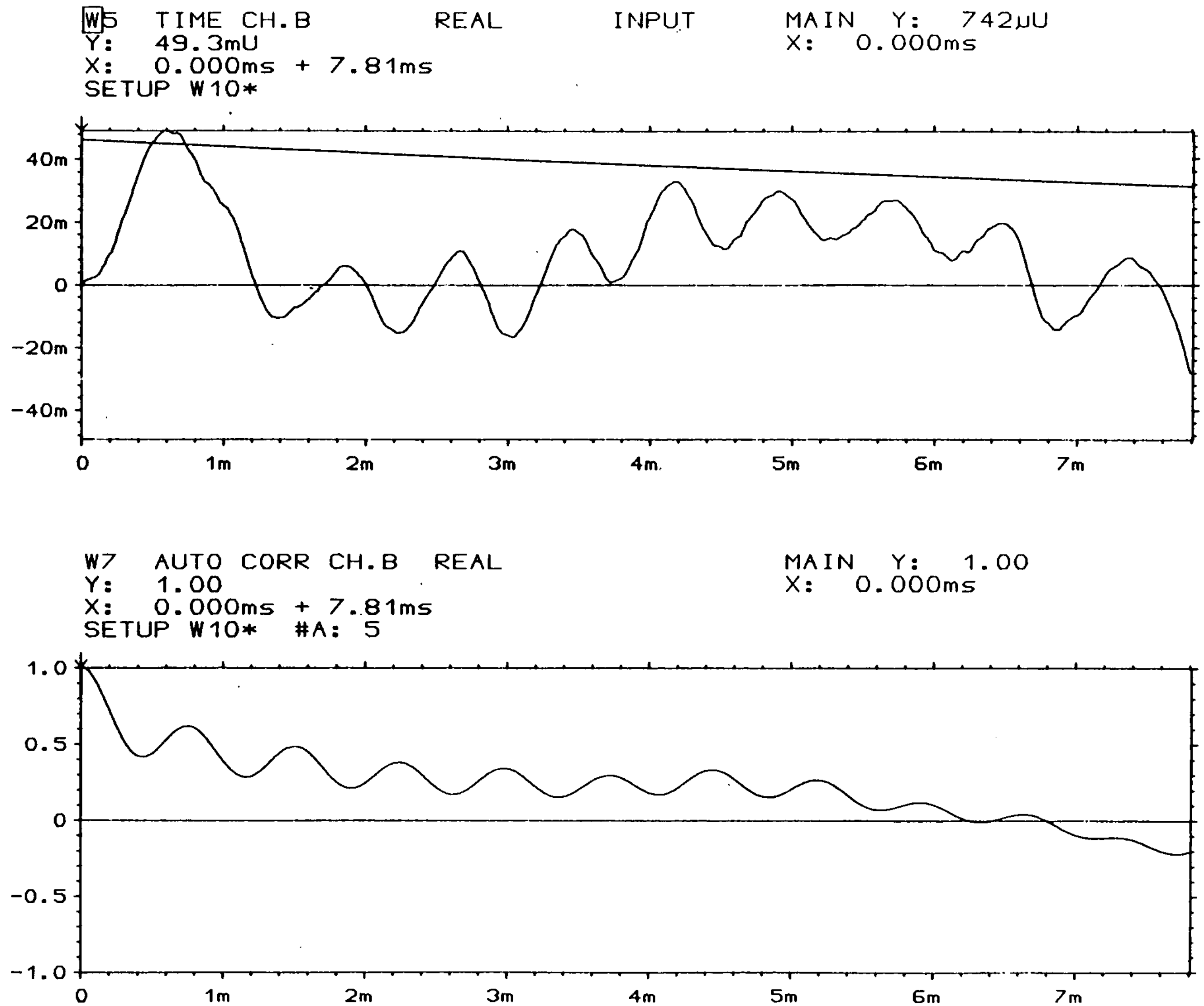

AUTO-CORRELATION AND VELOCITY TIME RECORD
COLUMN 3: ONE BRICK DEFECT

FIGURE 7.27

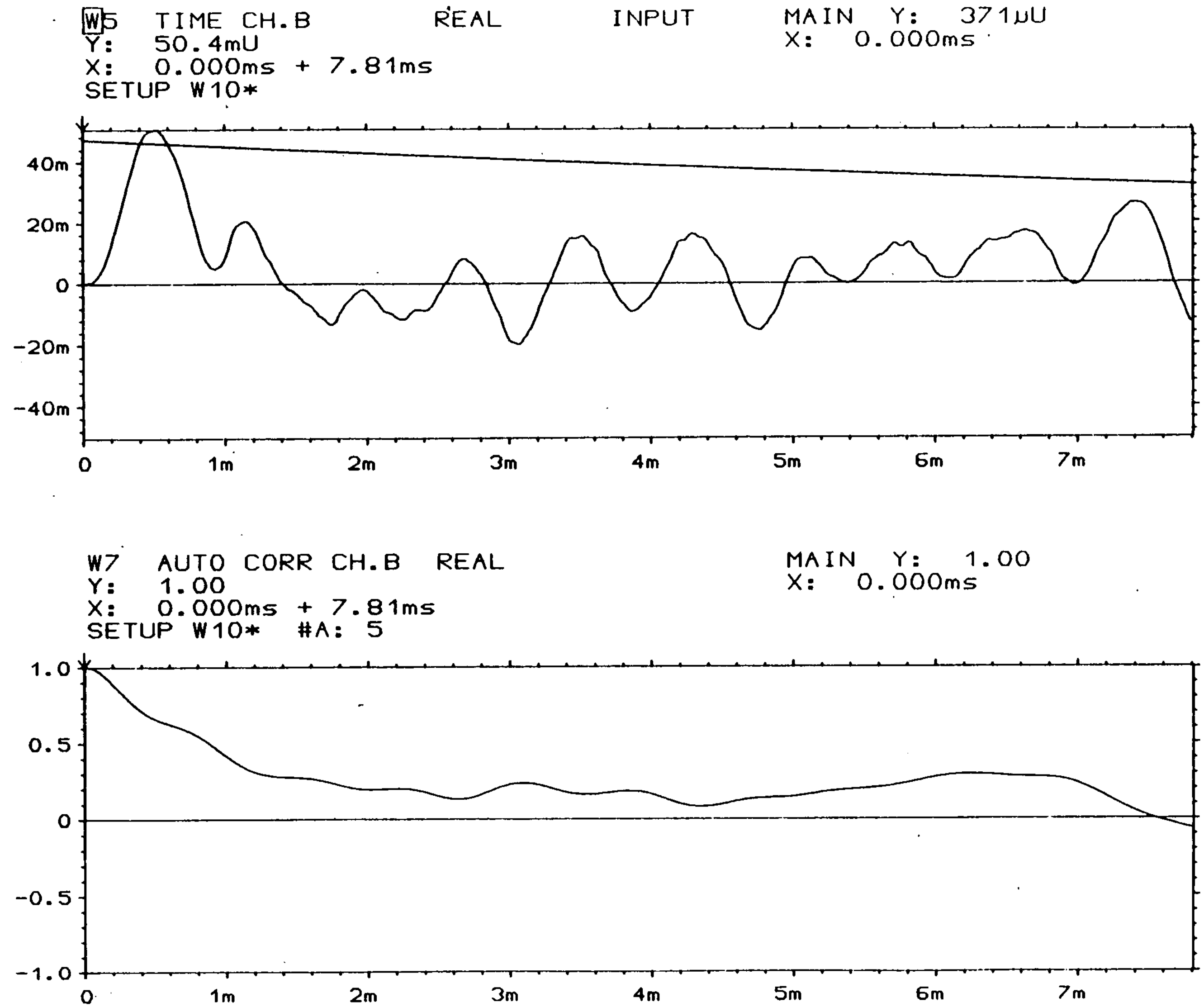

AUTO-CORRELATION AND VELOCITY TIME RECORD
COLUMN 3: TWO BRICK DEFECTS

FIGURE 7.28

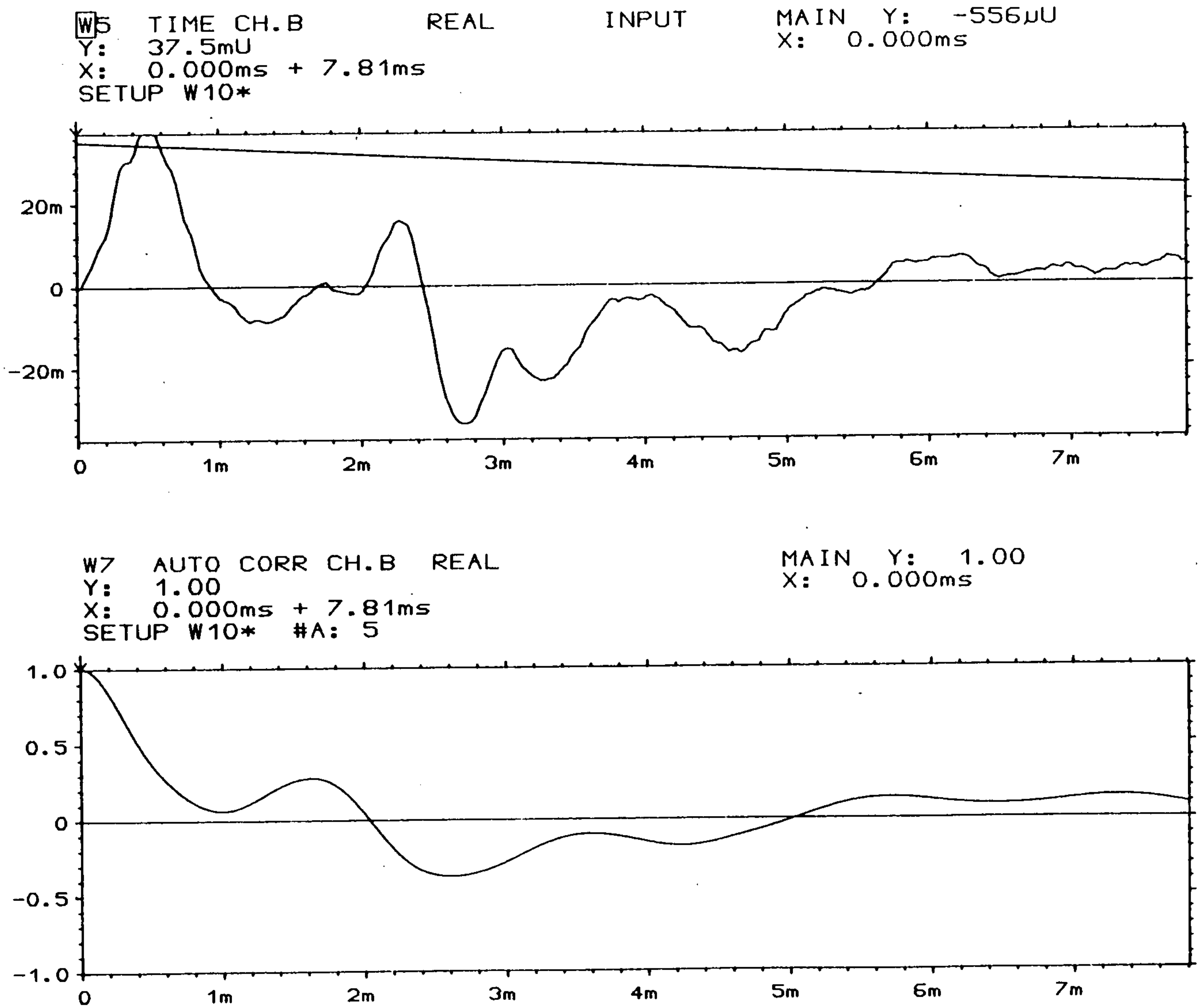

FIGURE 7.29

AUTO-CORRELATION AND VELOCITY TIME RECORD
COLUMN 4: DAMPED

W3 TIME CH.A REAL INPUT MAIN Y: 9.95U
Y: 8.94kU X: 0.00ms
X: 0.00ms + 125ms

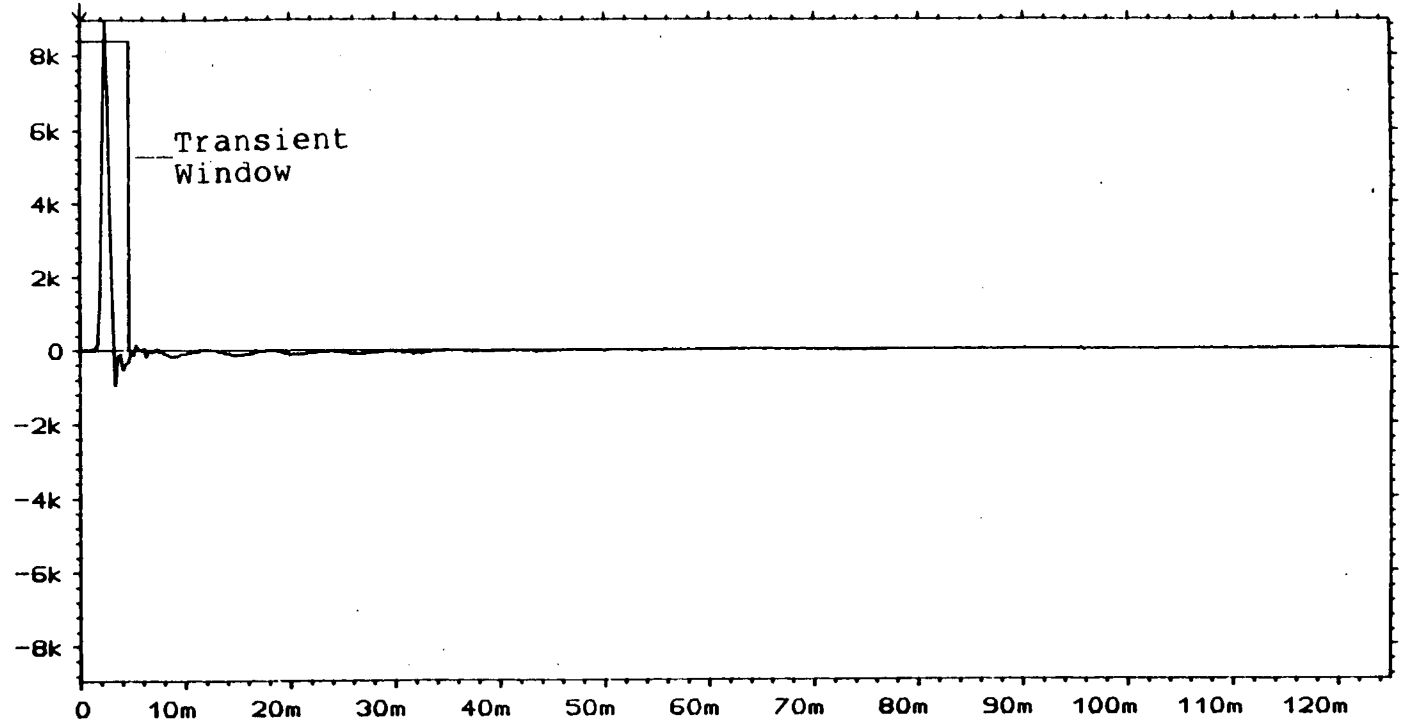

SETUP W9

MEASUREMENT: DUAL SPECTRUM AVERAGING
TRIGGER: CH.A +SLOPE LEVEL: +0.10 MAX INPUT
DELAY: TRIG→A: -0.97ms CH.A→B: 0.00ms
AVERAGING: LIN 5

FREQ SPAN: 1.6kHz ΔF:2Hz T:500ms ΔT:244μs
CENTER FREQ: BASEBAND
WEIGHT CH.A: TRANSIENT SHIFT:0.00ms LENGTH:4.63ms
WEIGHT CH.B: EXPONENTIAL SHIFT:0.00ms LENGTH:50.04ms
CH.A: 6V + 3Hz DIR FILT:BOTH 184μV/N
CH.B: 6V + 3Hz DIR FILT:BOTH 31.6V/m/s
GENERATOR: DISABLED

COLUMNS: FREQUENCY DOMAIN MEASUREMENT SET-UP AND HAMMER INPUT SIGNAL

FIGURE 7.30

W5 TIME CH.B REAL INPUT MAIN Y: -58.0μU
Y: 30.2mU X: 0.00ms
X: 0.00ms + 125ms

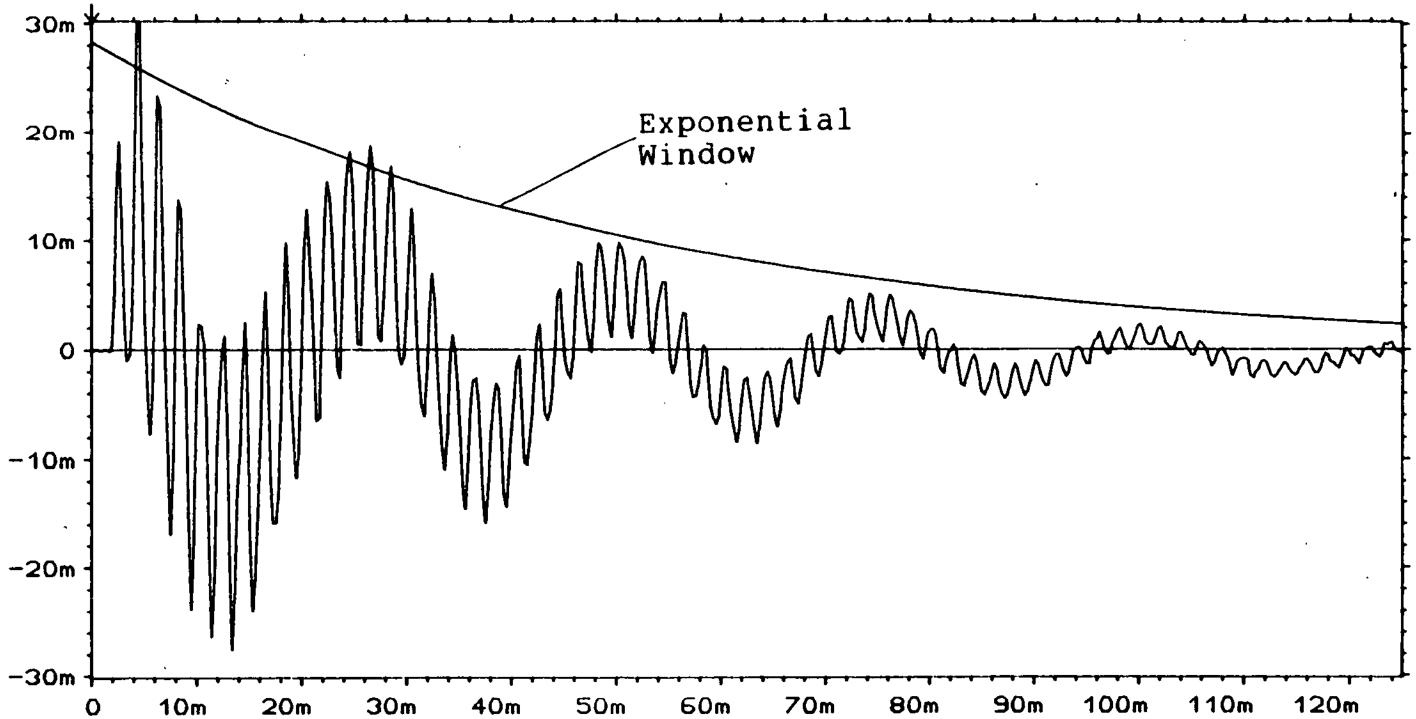

SETUP W9

MEASUREMENT:	DUAL SPECTRUM AVERAGING			
TRIGGER:	CH.A	+SLOPE	LEVEL: +0.10 MAX INPUT	
DELAY:	TRIG→A: -0.97ms		CH.A→B: 0.00ms	
AVERAGING:	LIN 5			
FREQ SPAN:	1.6kHz	ΔF:2Hz	T:500ms	ΔT:244μs
CENTER FREQ:	BASEBAND			
WEIGHT CH.A:	TRANSIENT	SHIFT:0.00ms		LENGTH:4.63ms
WEIGHT CH.B:	EXPONENTIAL	SHIFT:0.00ms		LENGTH:50.04ms
CH.A:	6V +	3Hz DIR	FILT:BOTH	184μV/N
CH.B:	6V +	3Hz DIR	FILT:BOTH	31.6V/m/s
GENERATOR:	DISABLED			

FIGURE 7.31

COLUMNS: FREQUENCY DOMAIN MEASUREMENT SET-UP AND VELOCITY TIME RECORD

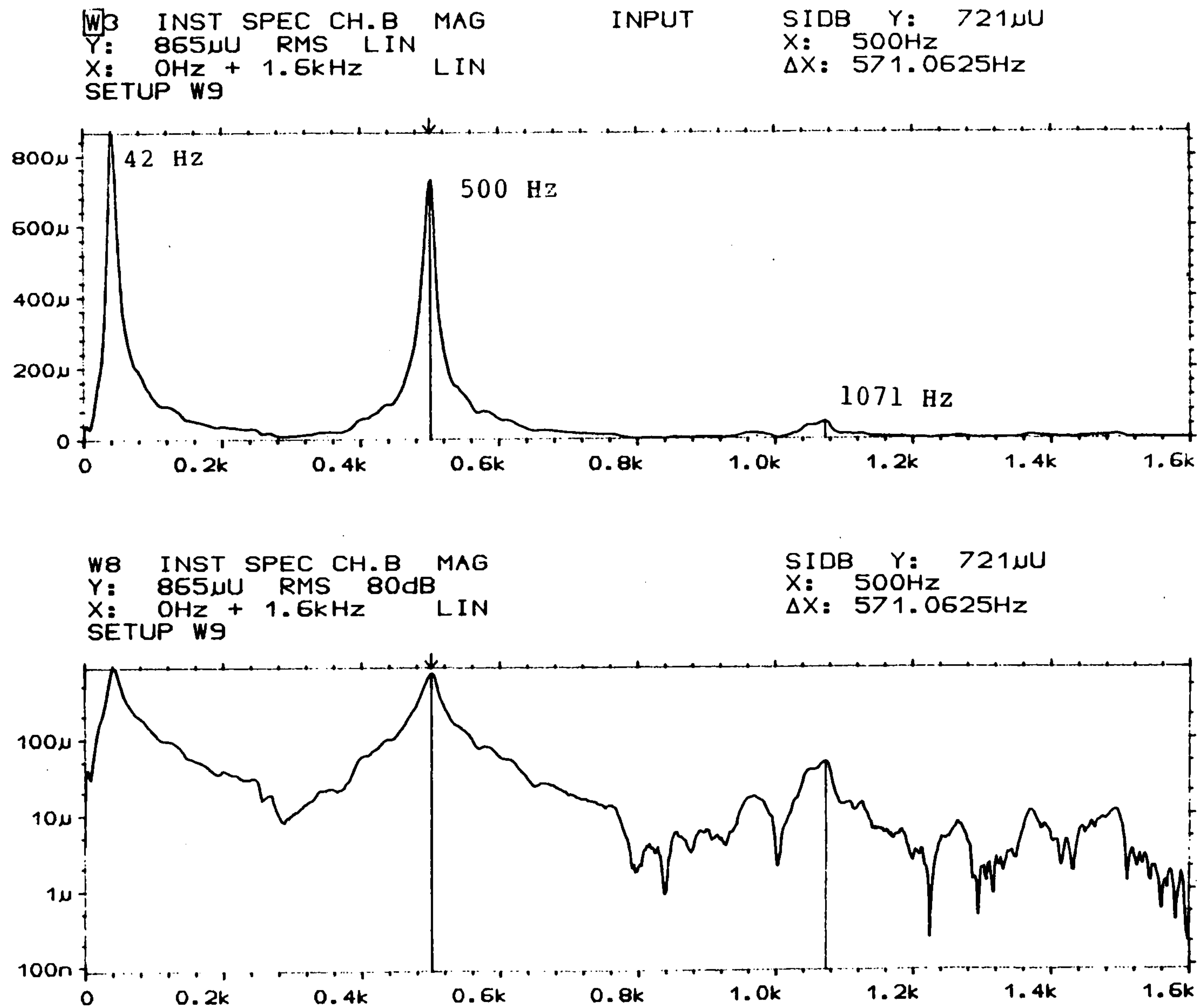

TYPICAL INSTANTANECUS SPECTRUM
COLUMN 2: NO DEFECTS

FIGURE 7.32

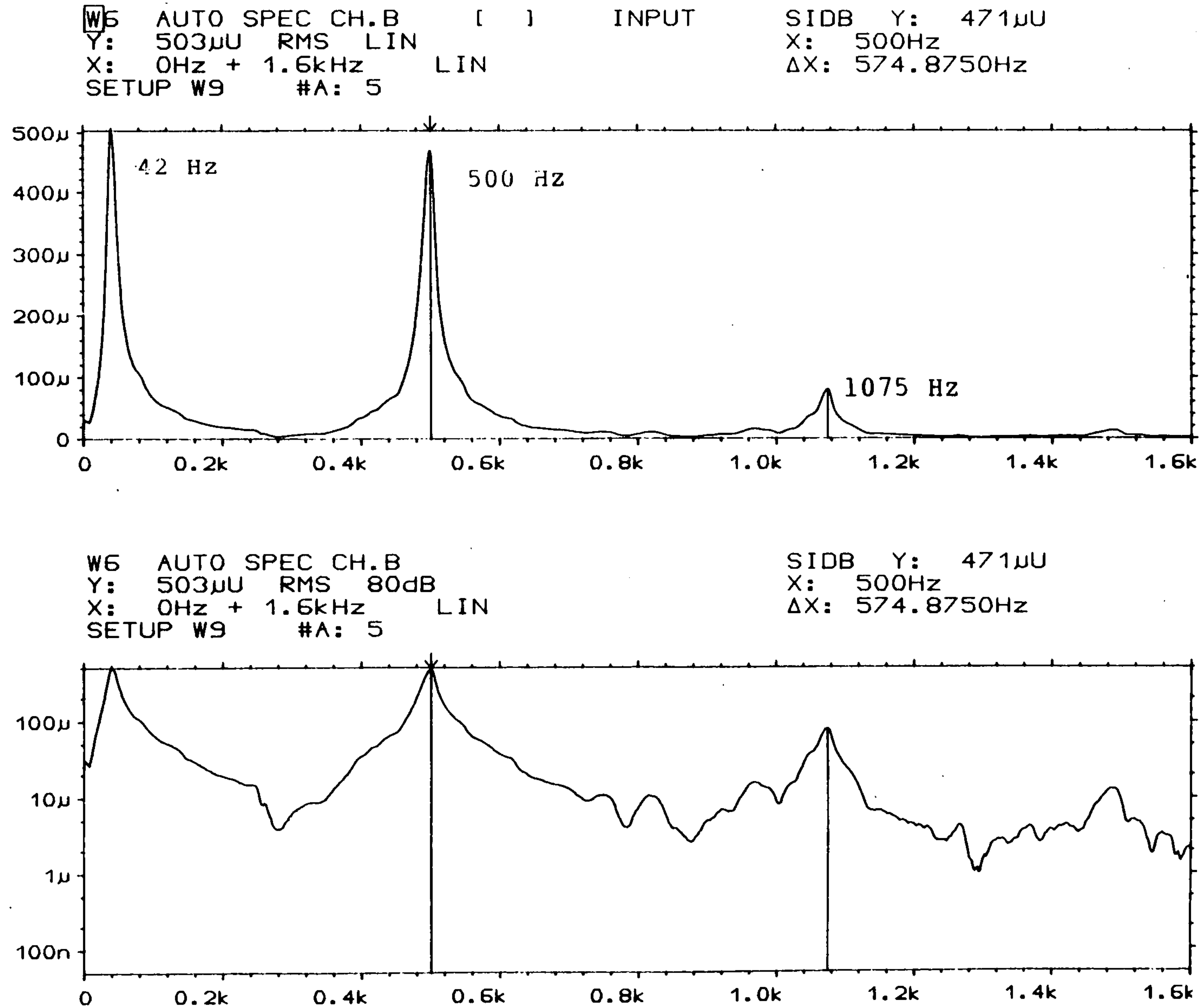

TYPICAL AUTO-SPECTRUM
COLUMN 2: NO DEFECTS

FIGURE 7.33

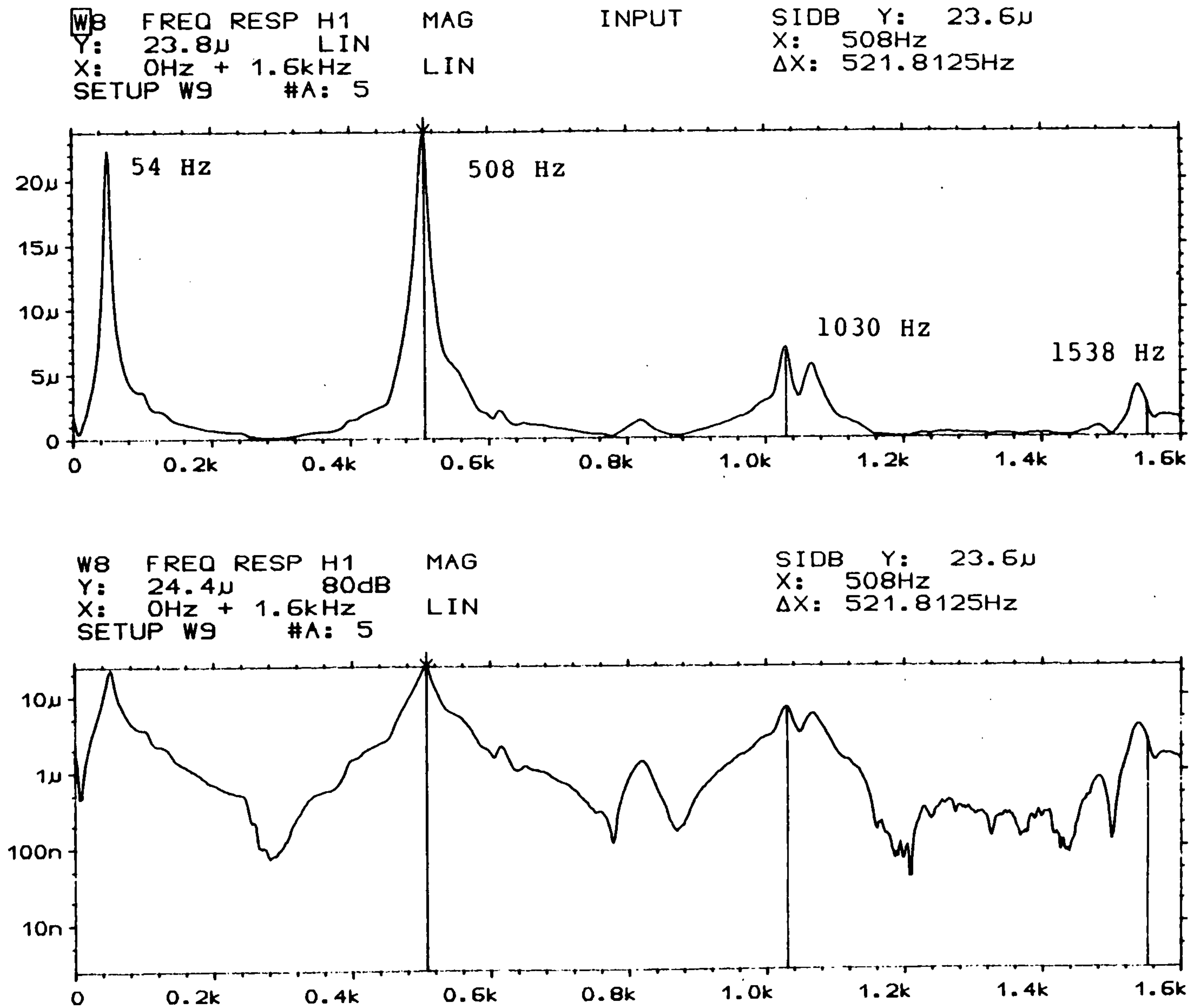

FREQUENCY RESPONSE FUNCTION
COLUMN 1: NO DEFECTS

FIGURE 7.34

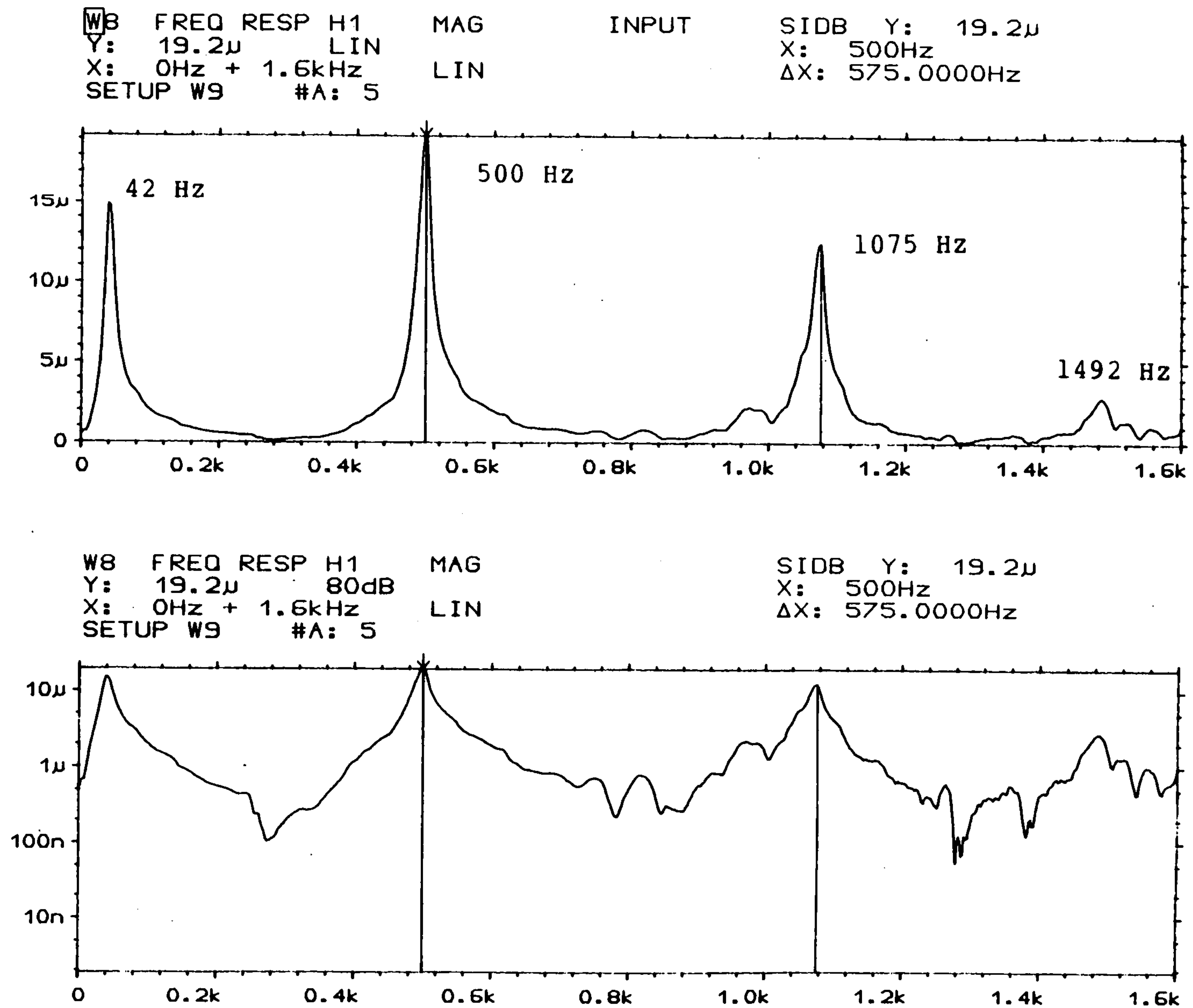

FREQUENCY RESPONSE FUNCTION
COLUMN 2: NO DEFECTS

FIGURE 7.35

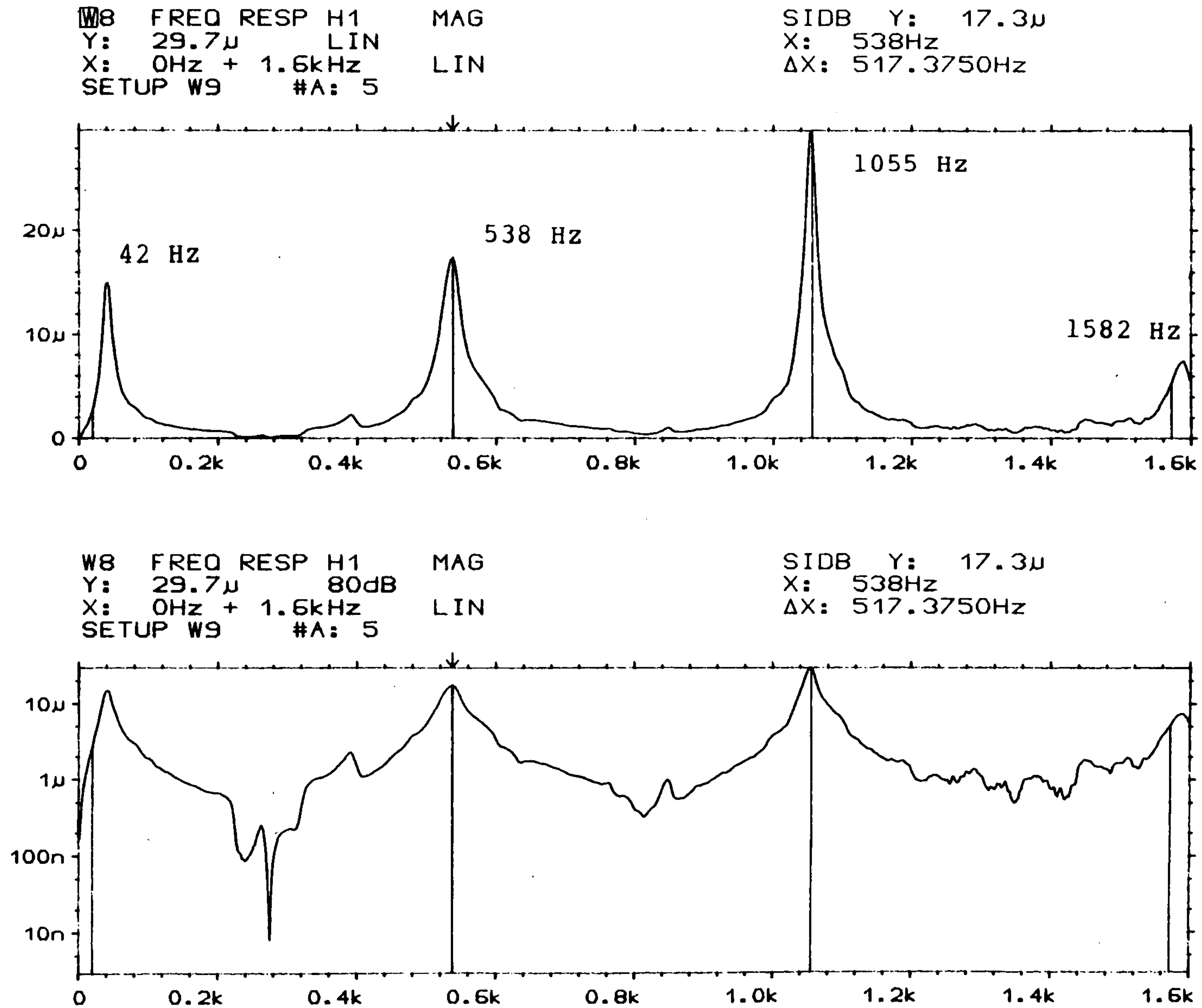

FREQUENCY RESPONSE FUNCTION
COLUMN 3: NO DEFECTS
FIGURE 7.36

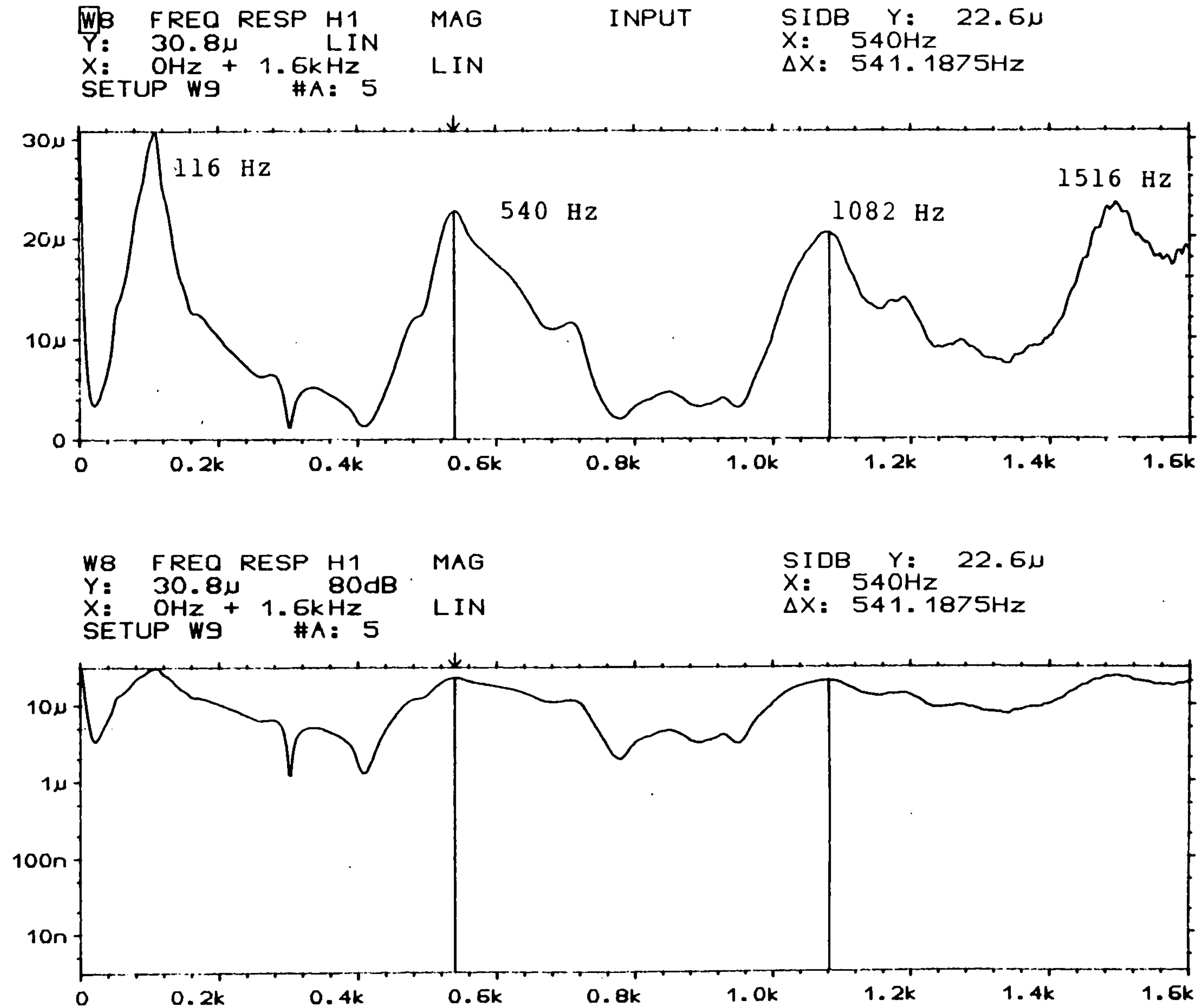

FREQUENCY RESPONSE FUNCTION
COLUMN 4: NO DEFECTS
FIGURE 7.37

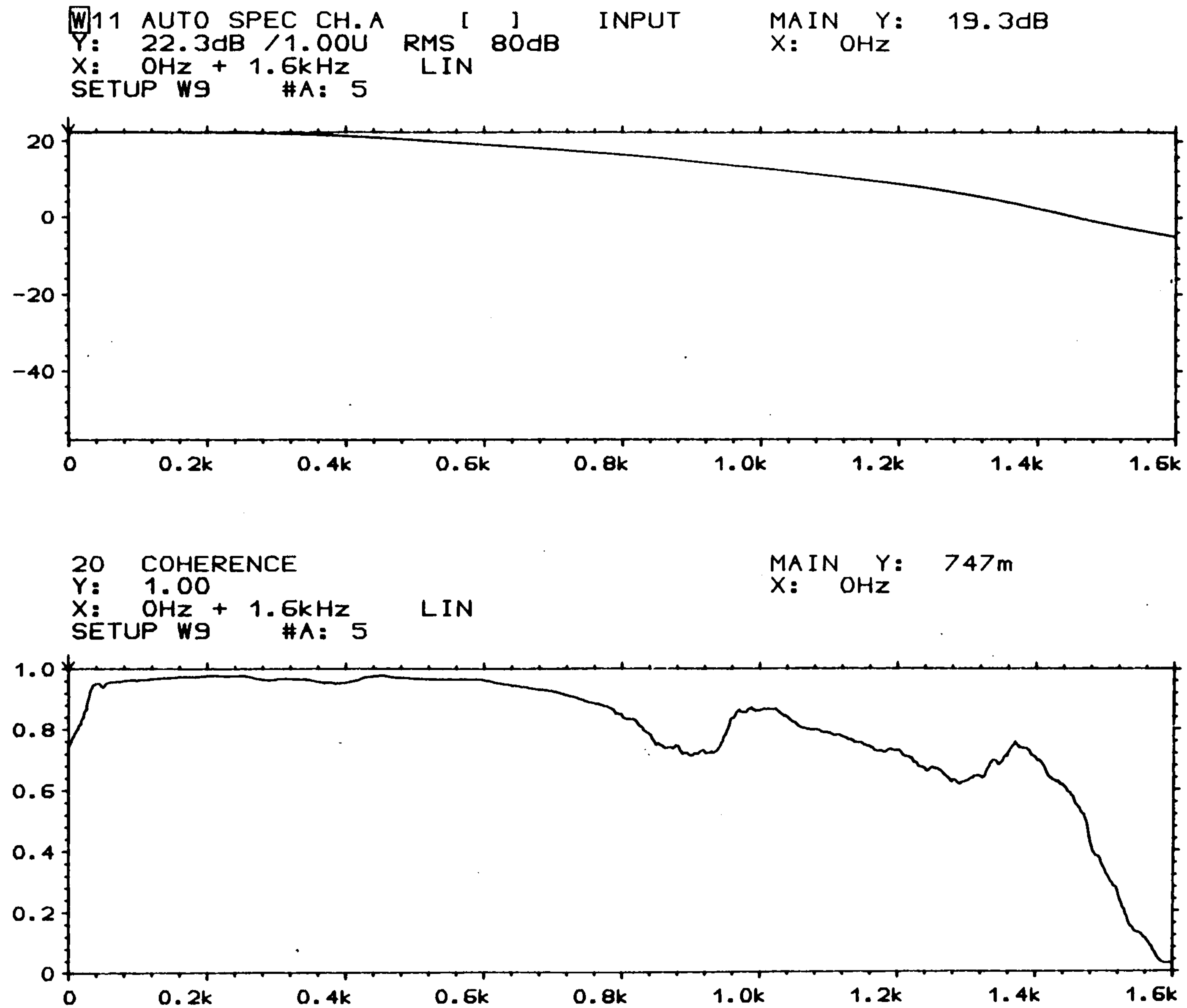

FIGURE 7.38

FORCE AUTO-SPECTRUM AND COHERENCE

TYPICAL COLUMN

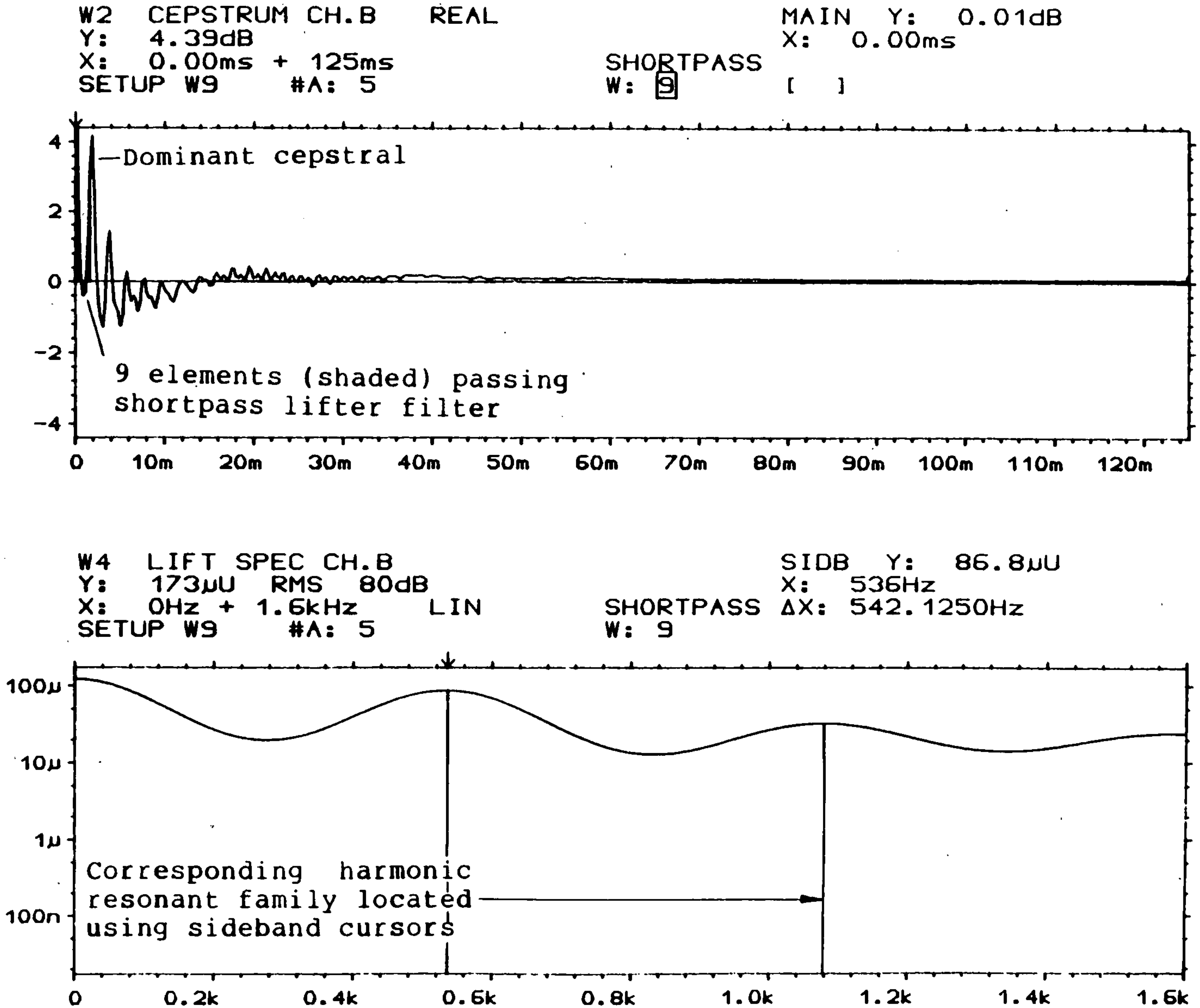

CEPSTRUM AND LIFTERED SPECTRUM
COLUMN 1: NO DEFECTS
FIGURE 7.39

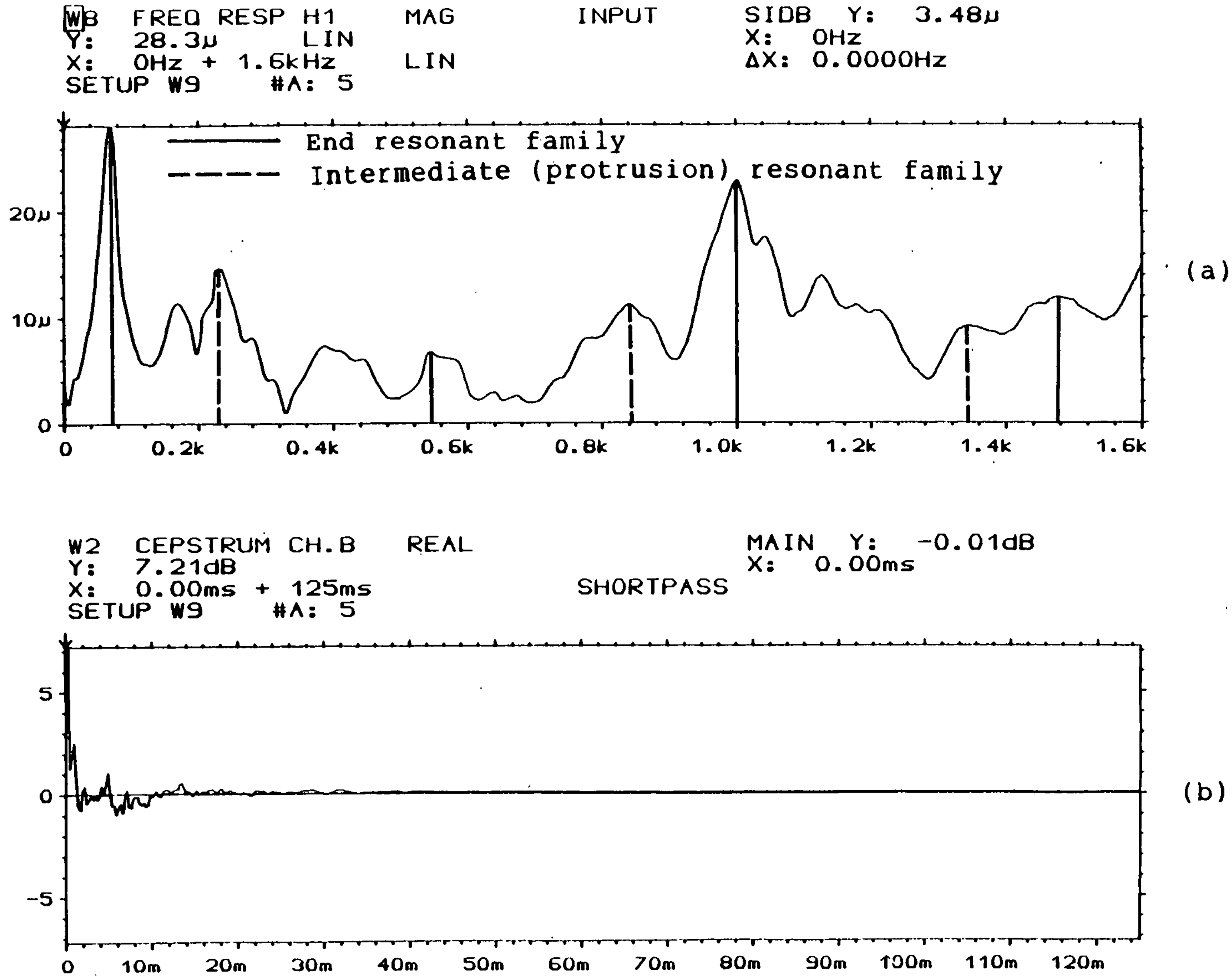

FIGURE 7.40

FREQUENCY RESPONSE FUNCTION AND CEPSTRUM
COLUMN 1: FIXED BASE

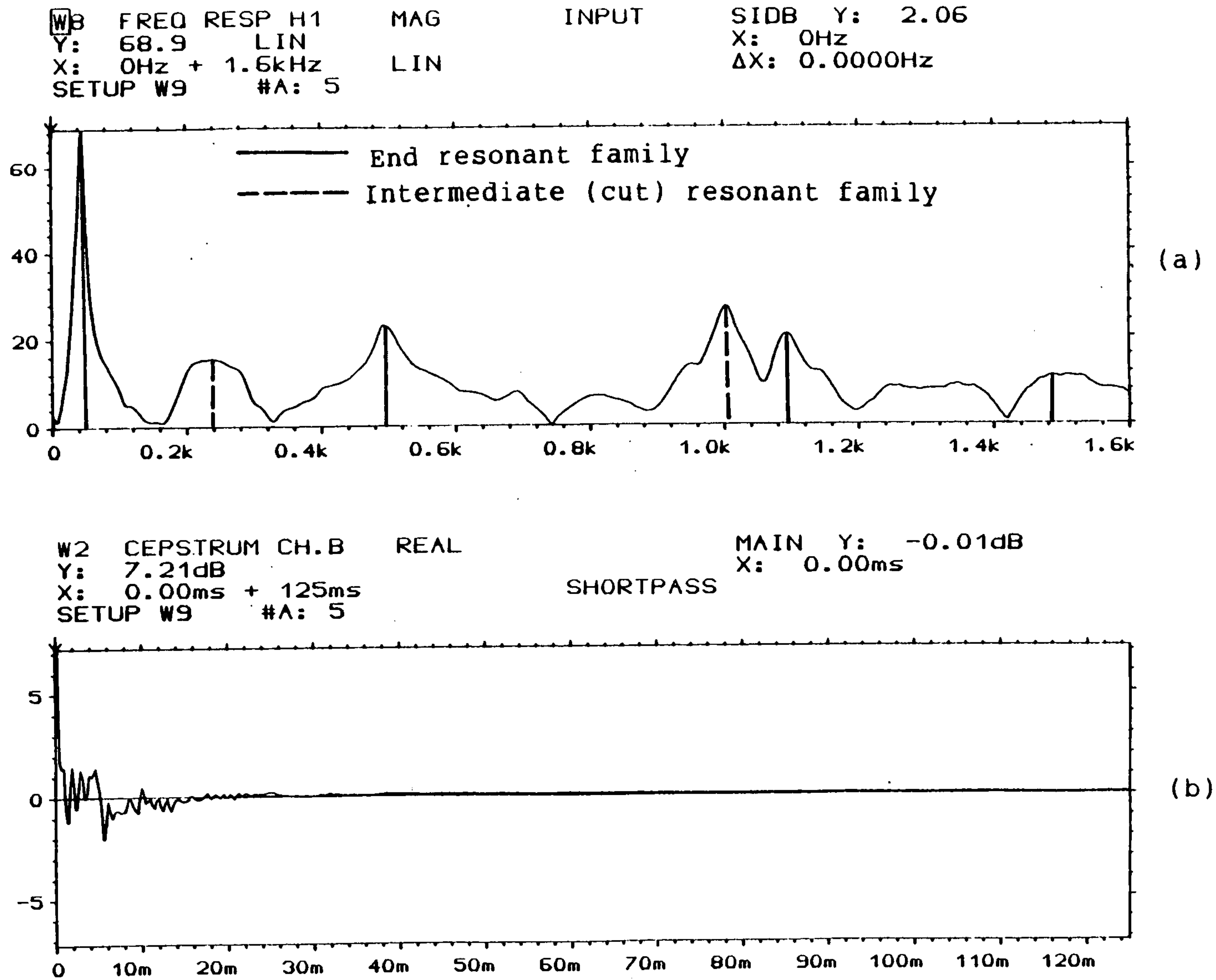

FIGURE 7.41

FREQUENCY RESPONSE FUNCTION AND CEPSTRUM
COLUMN 2: 50 % MORTAR DEFECT

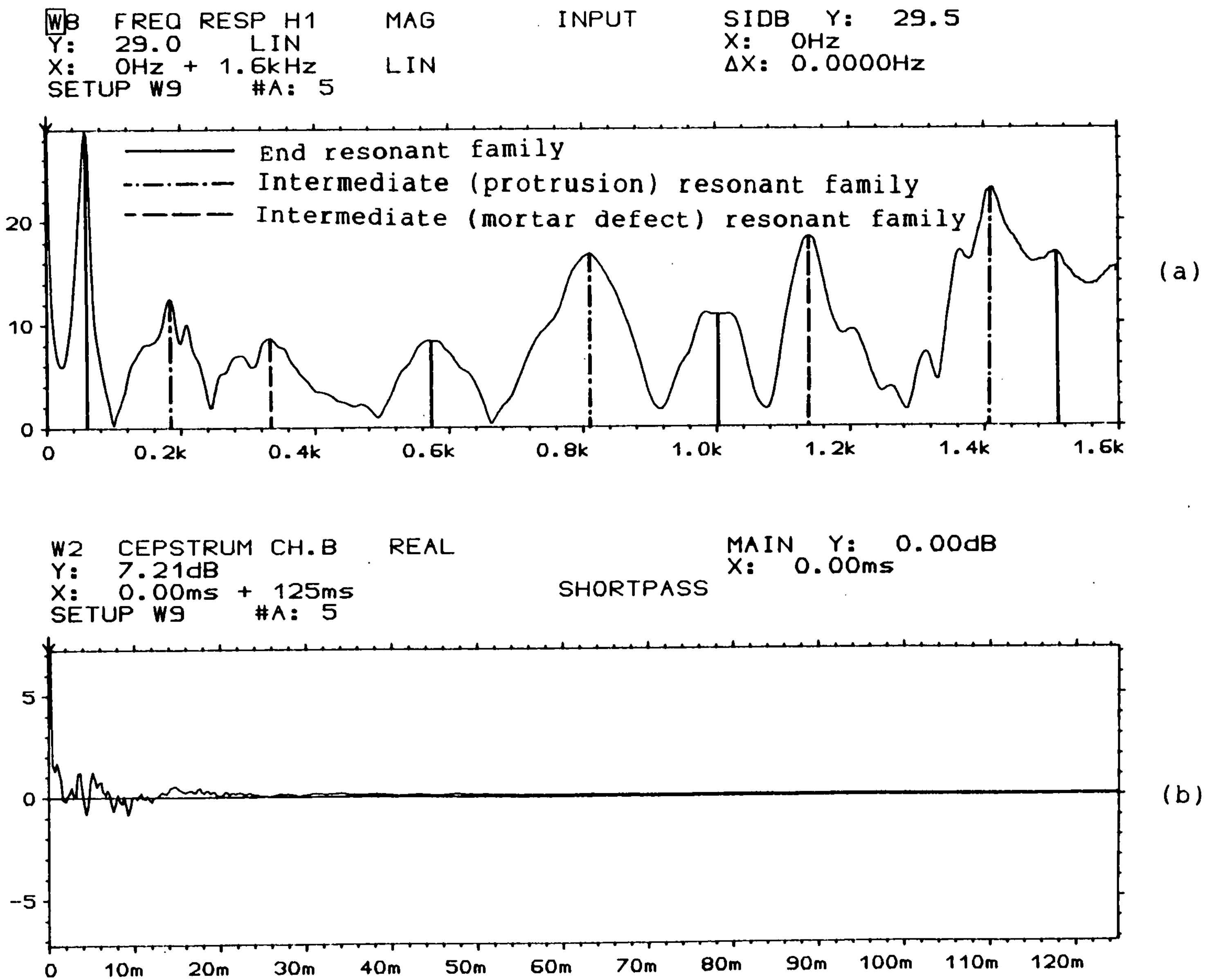

FREQUENCY RESPONSE FUNCTION AND CEPSTRUM
COLUMN 1: FIXED BASE AND 50 % MORTAR CUT

FIGURE 7.42

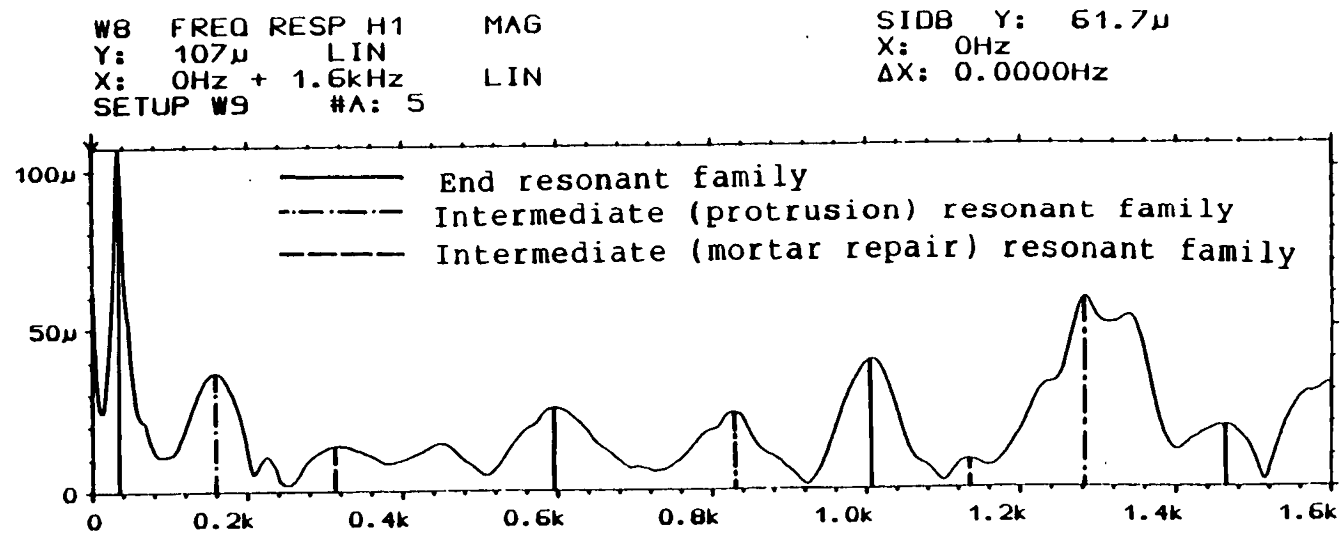

(a)

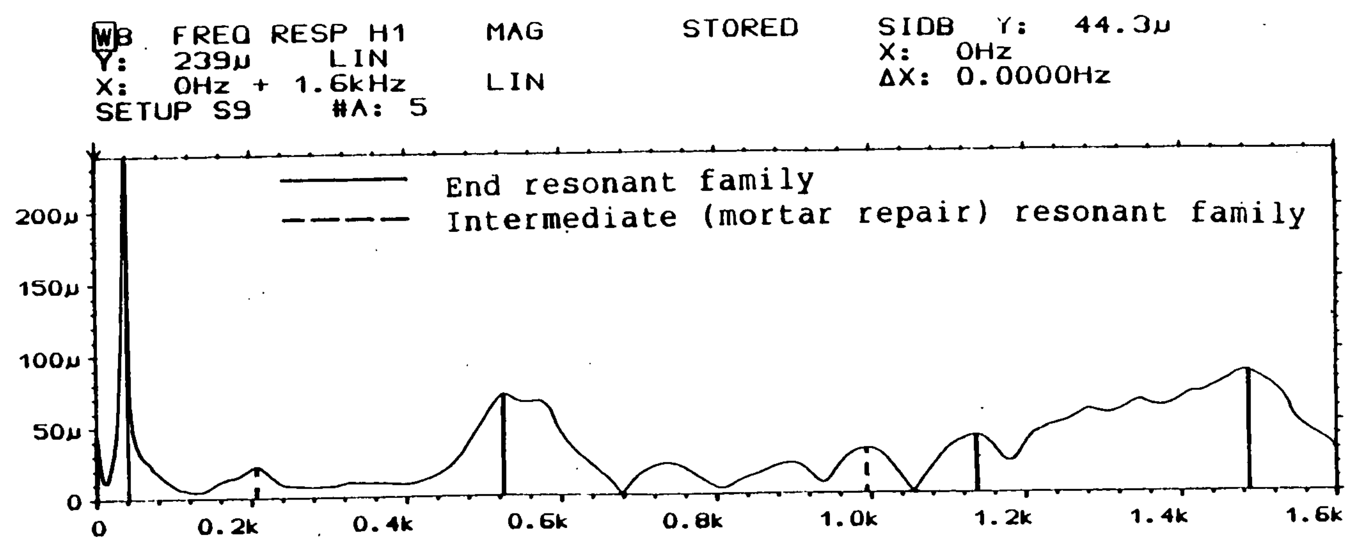

(b)

FREQUENCY RESPONSE FUNCTIONS
COLUMNS 1 AND 2: REPAIRS

FIGURE 7.43

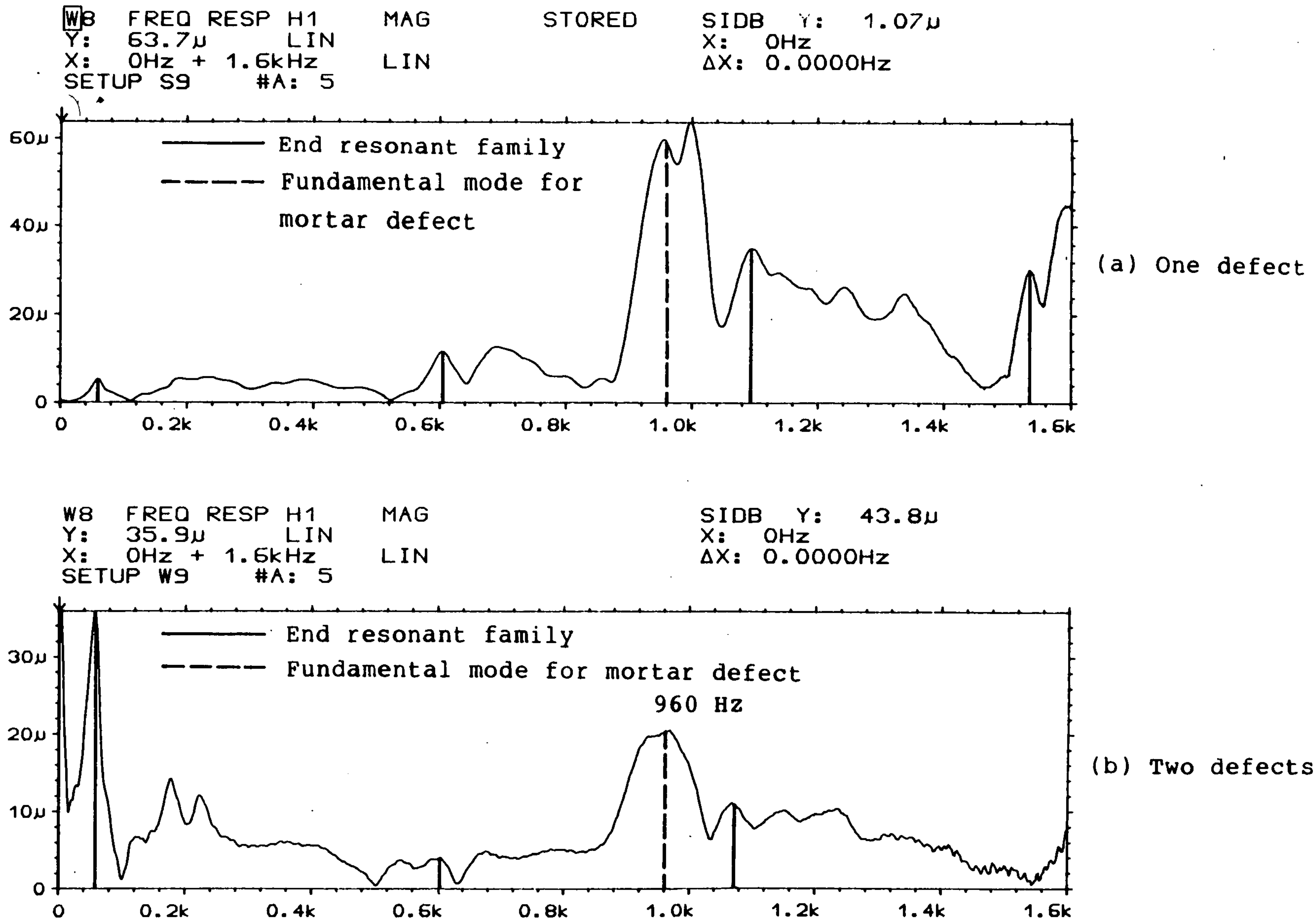

FIGURE 7.44

COLUMN 3: ONE AND TWO DEFECTS

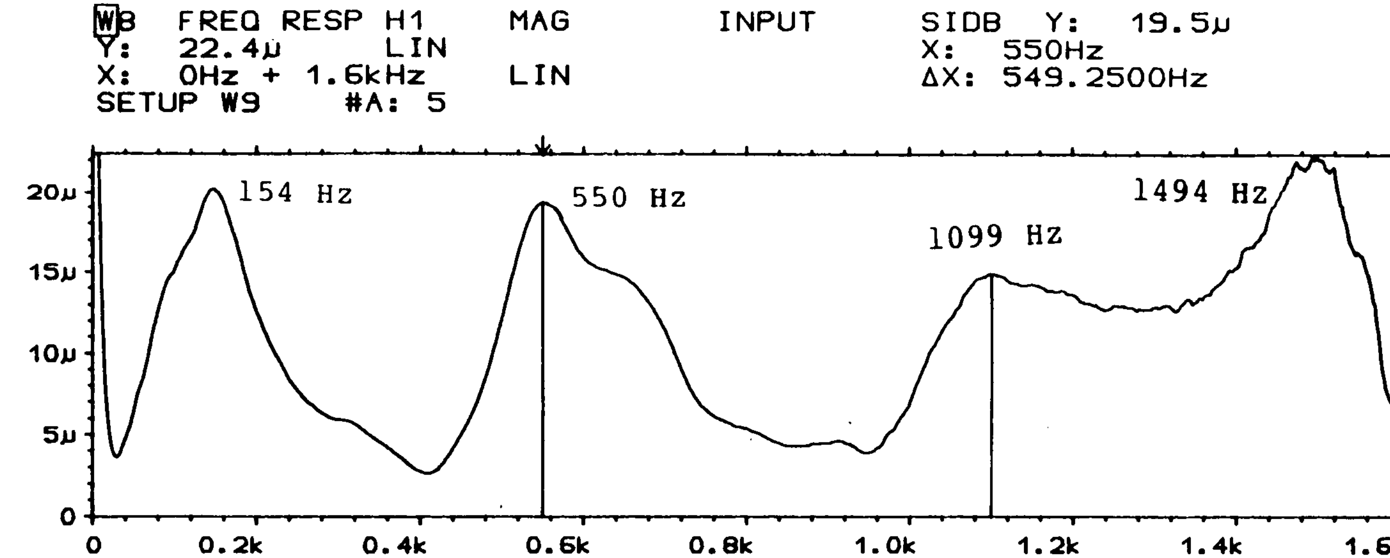

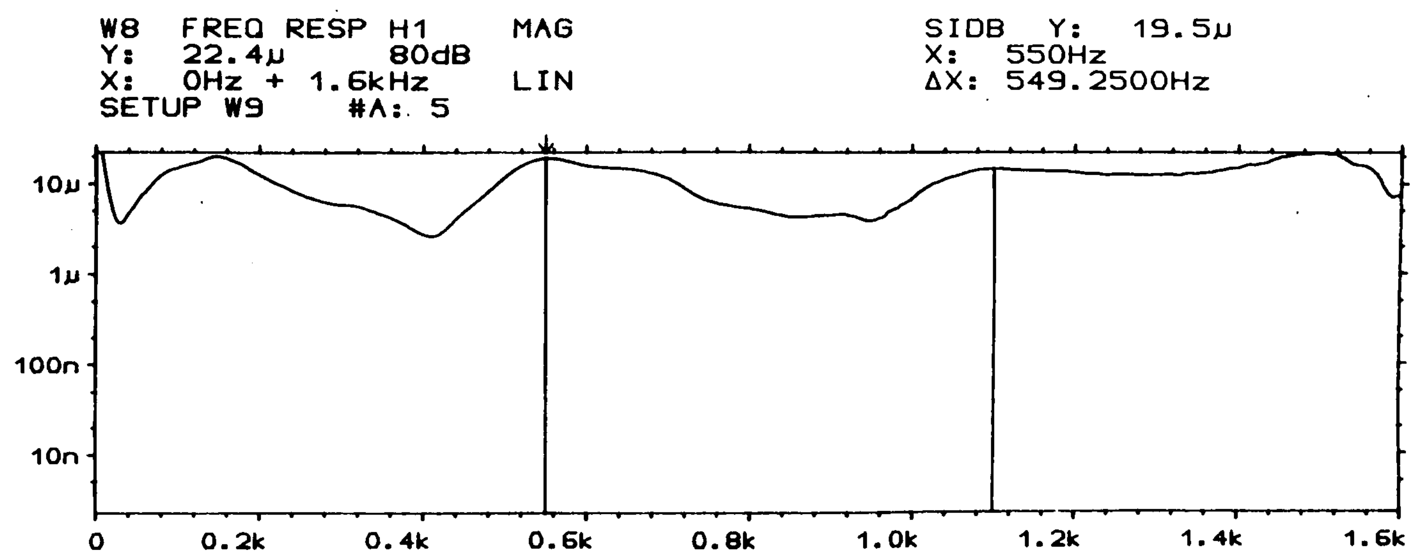

FREQUENCY RESPONSE FUNCTION
COLUMN 4: DAMPED
FIGURE 7.45

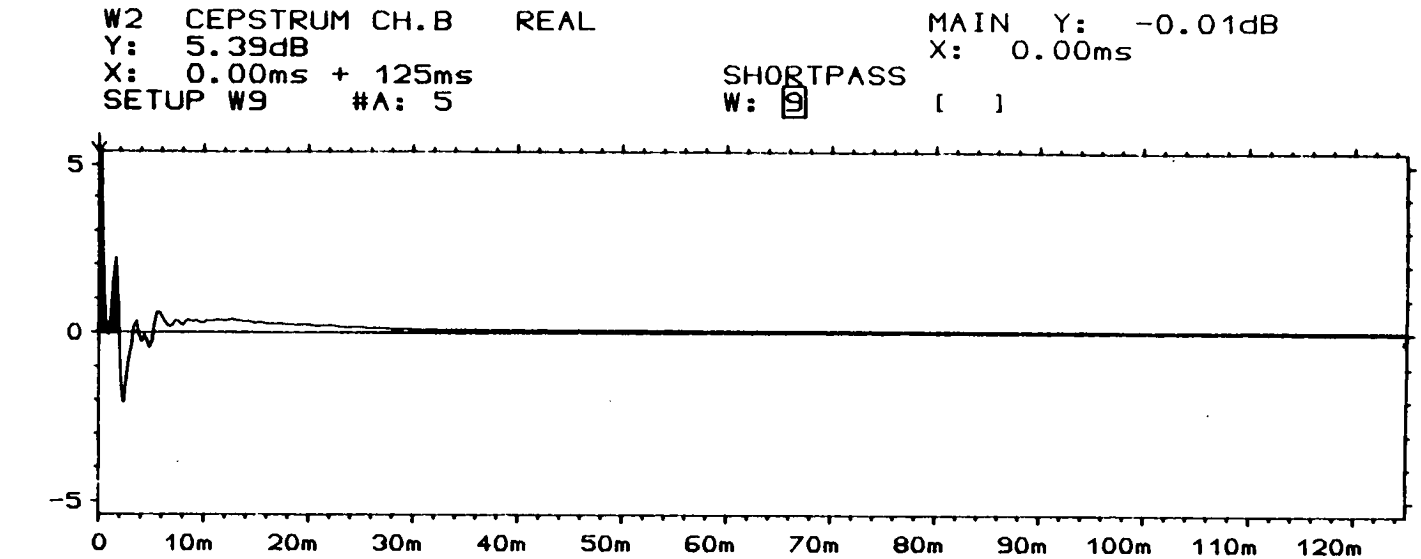

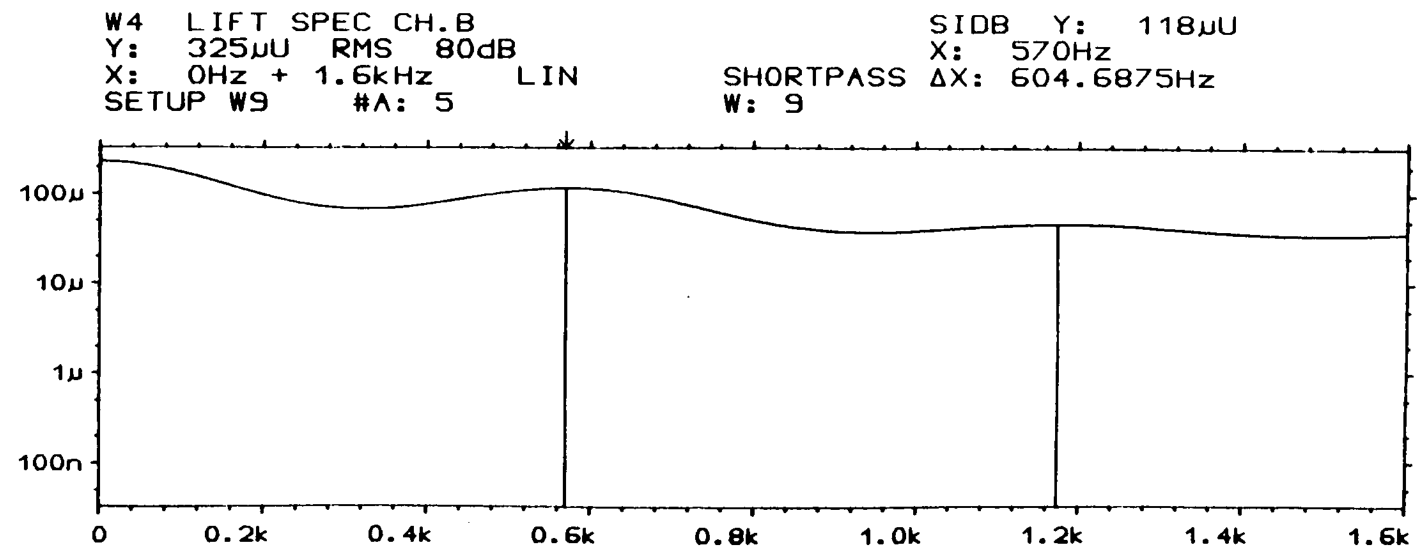

FIGURE 7.46

CEPSTRUM AND LIFTERED SPECTRUM
COLUMN 4: DAMPED

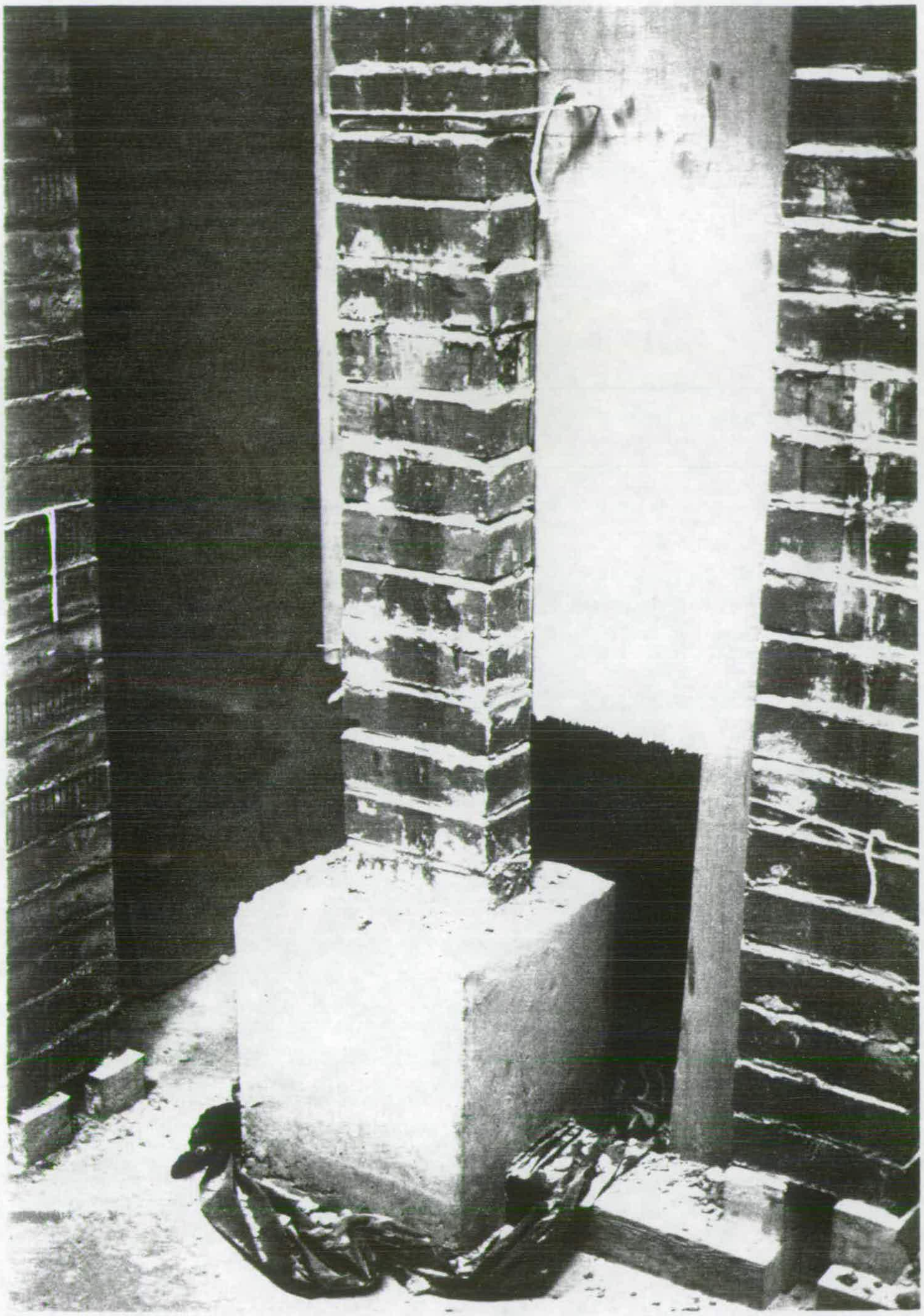

COLUMN 1: FIXED BASE

PLATE 7.1

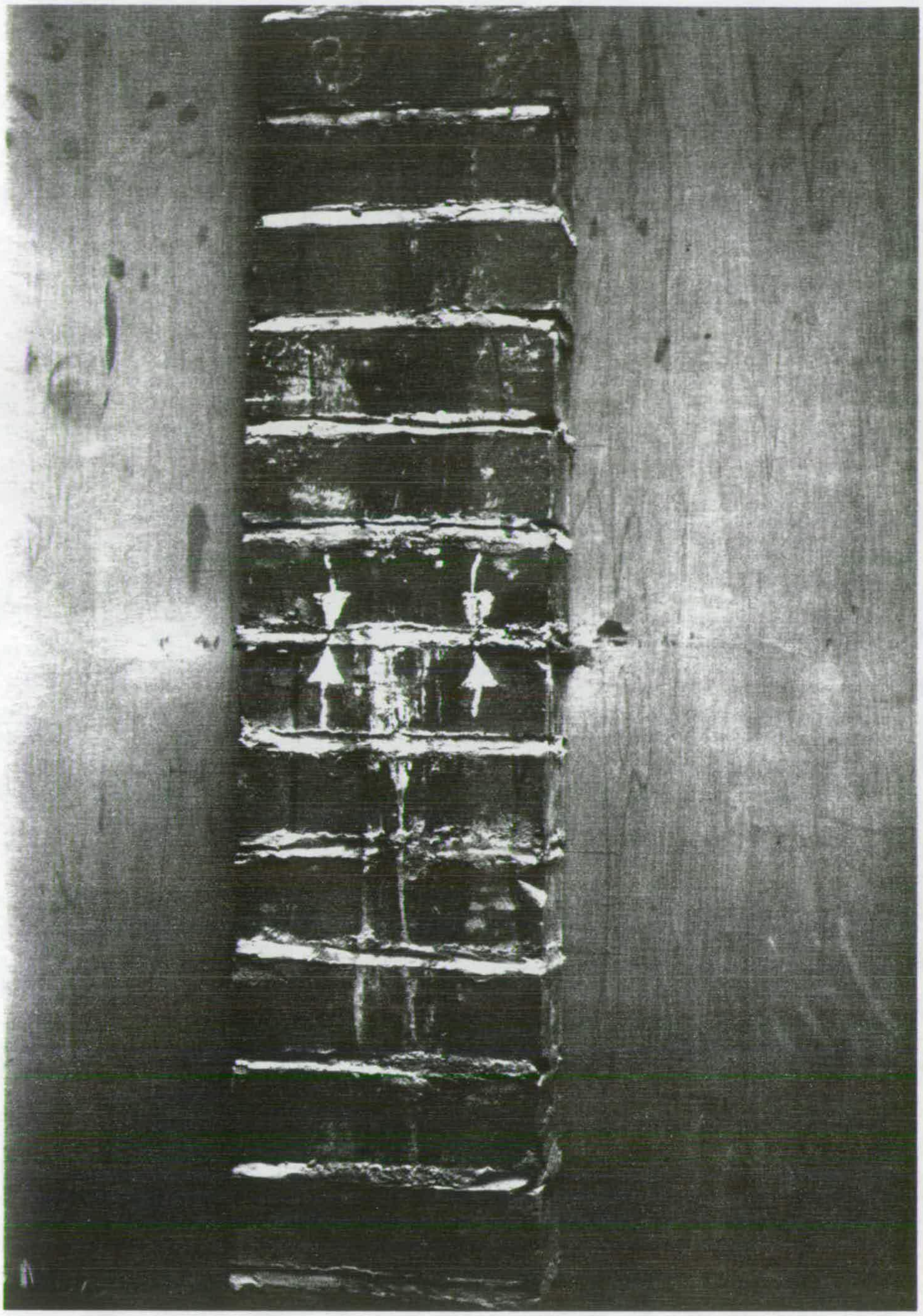

COLUMN 2: DEFECT IN MORTAR

PLATE 7.2

CHAPTER 8

LABORATORY SEWER TESTS

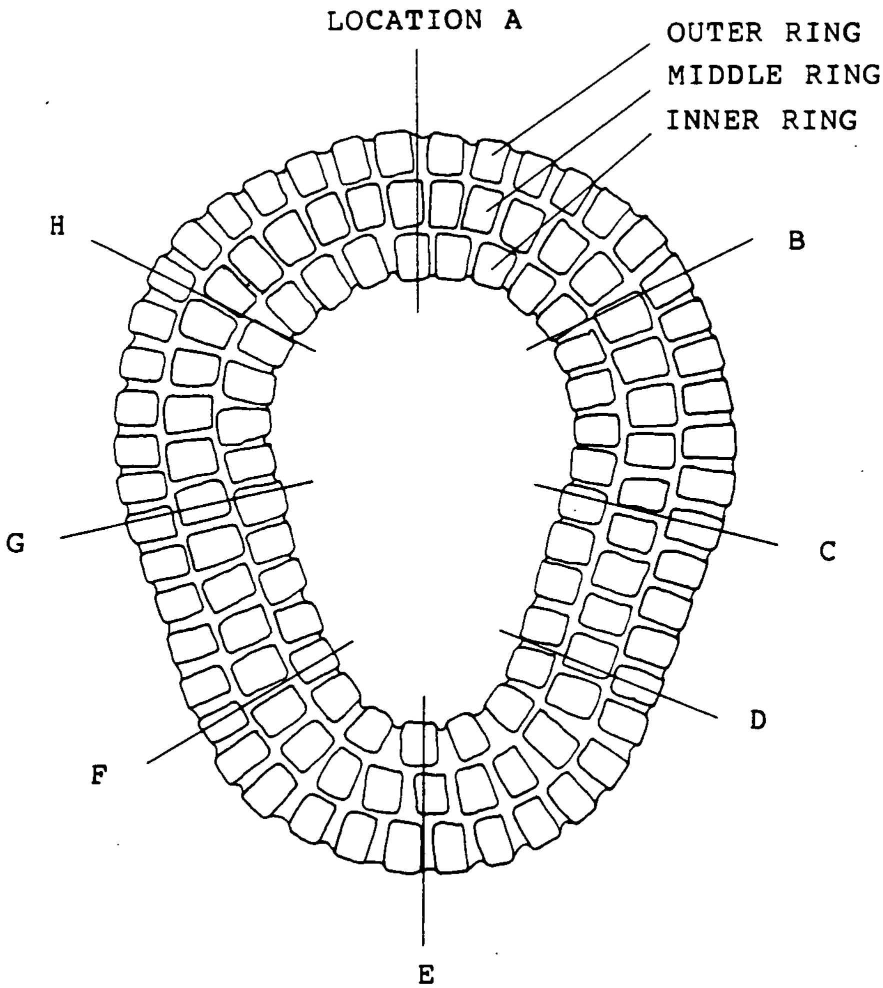

REFERENCE KEY
SEWER CROSS-SECTION

FIGURE 8.1

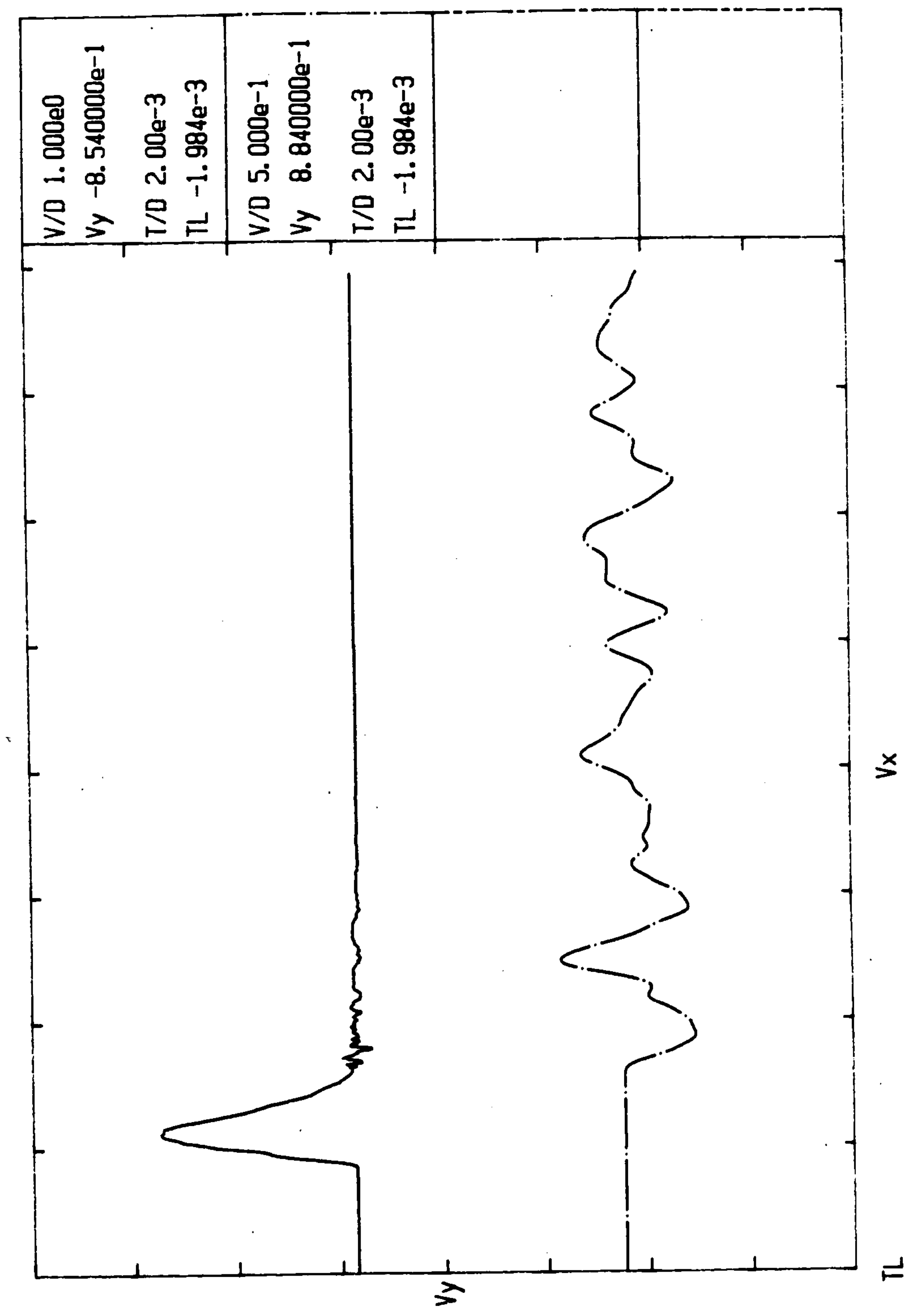

TYPICAL "DELAY" VELOCITY RECORD (DIGITAL OSCILLOSCOPE)
LABORATORY SEWER: 3 BRICK END TO 1 BRICK END

FIGURE 8.2

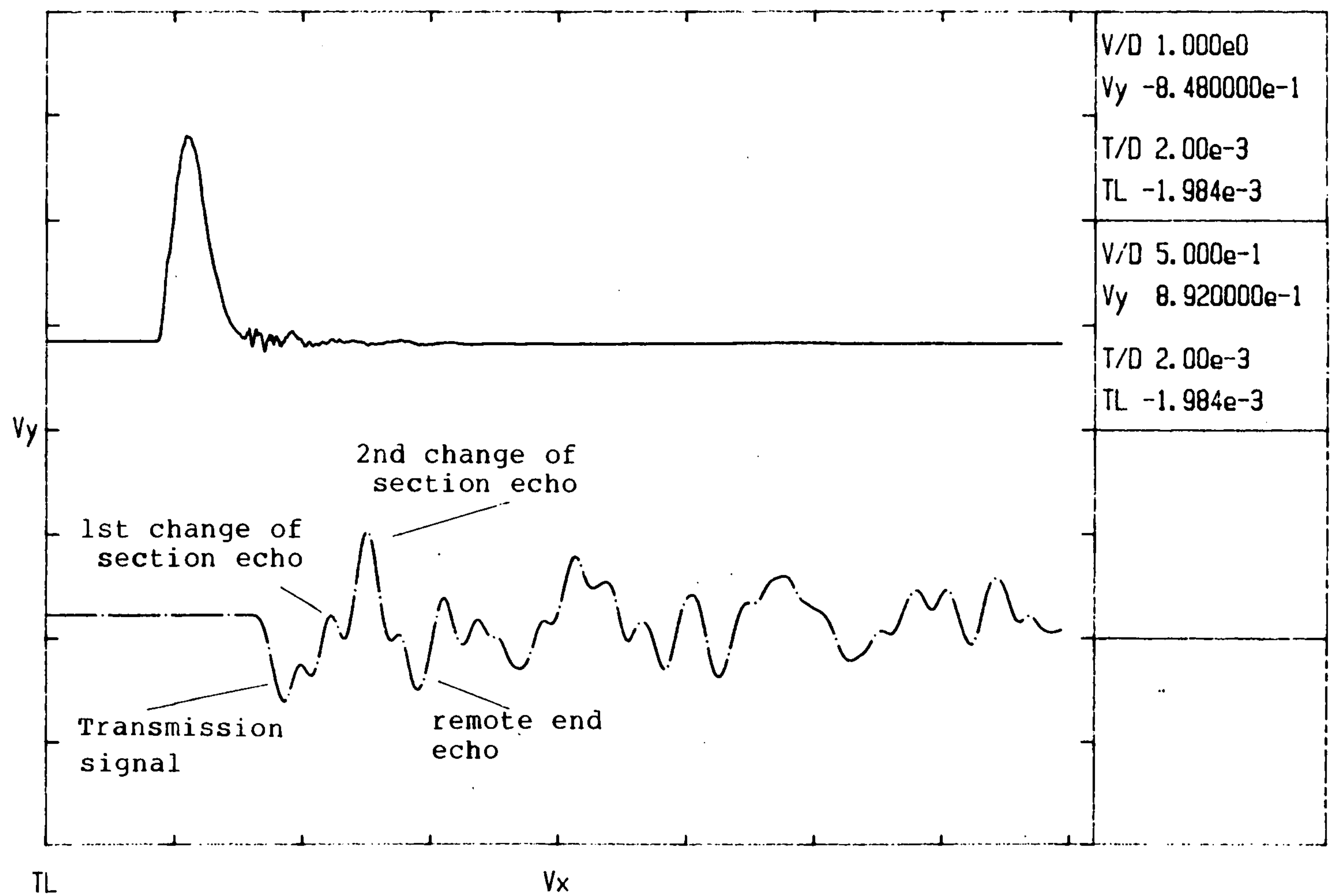

TYPICAL "DELAY" VELOCITY RECORD (DIGITAL OSCILLOSCOPE)
LABORATORY SEWER: 1 BRICK END TO 3 BRICK END

FIGURE 8.3

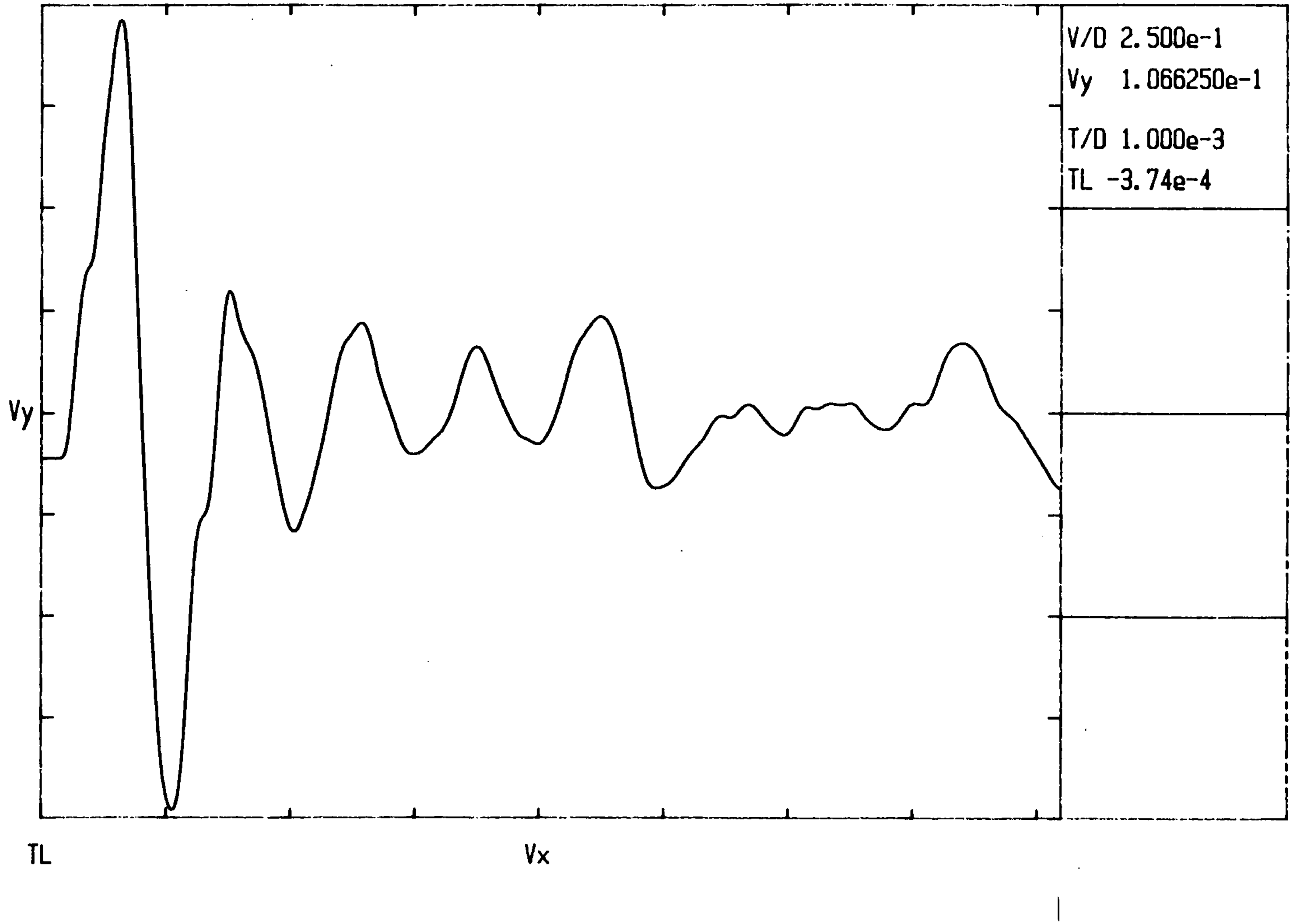

TYPICAL "ECHO" VELOCITY RECORD (DIGITAL OSCILLOSCOPE)
LABORATORY SEWER: 3 BRICK END (INNER) TO 1 BRICK END

FIGURE 8.4

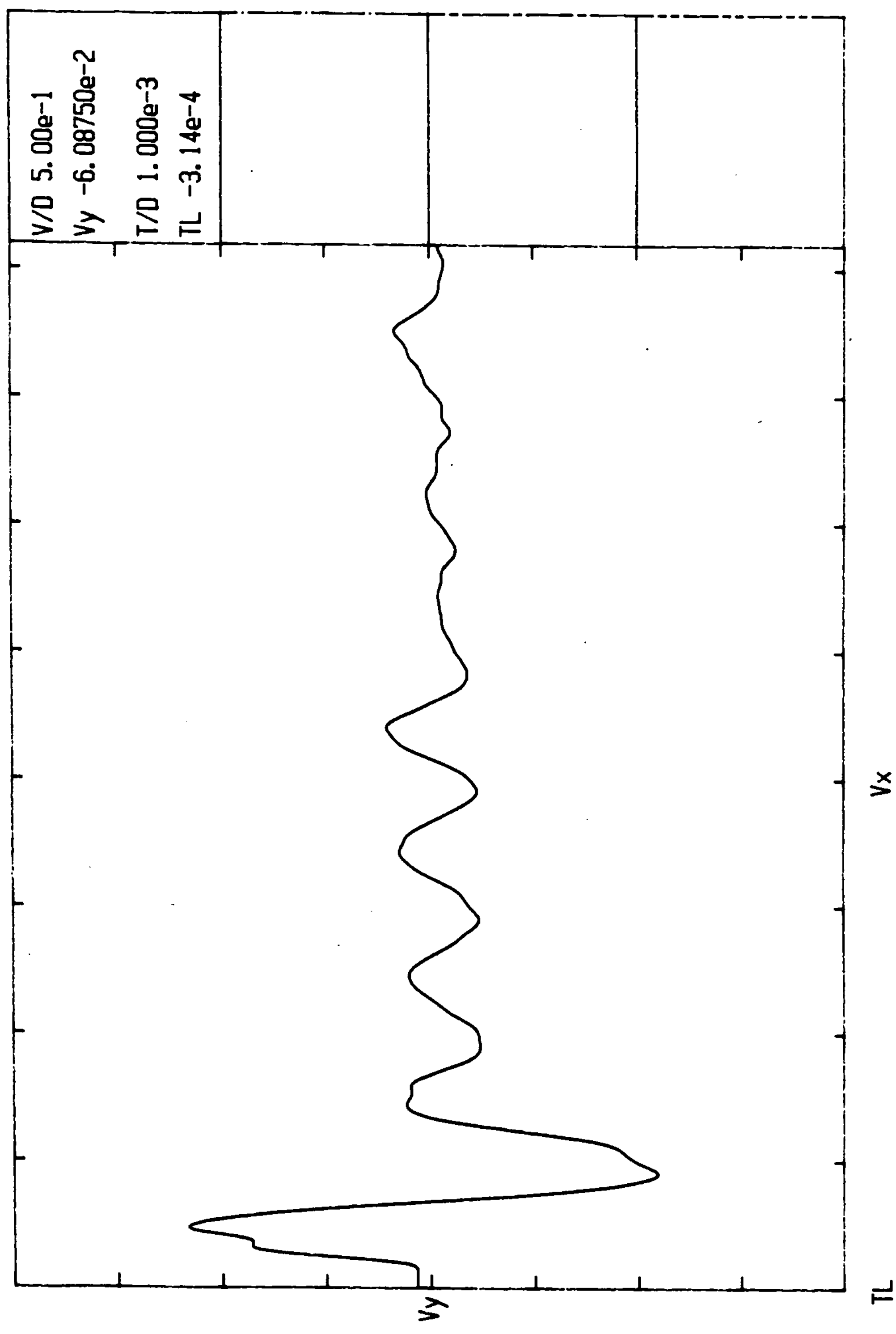

TYPICAL "ECHO" VELOCITY RECORD (DIGITAL OSCILLOSCOPE)
LABORATORY SEWER: 3 BRICK END (MIDDLE) TO 1 BRICK END

FIGURE 8.5

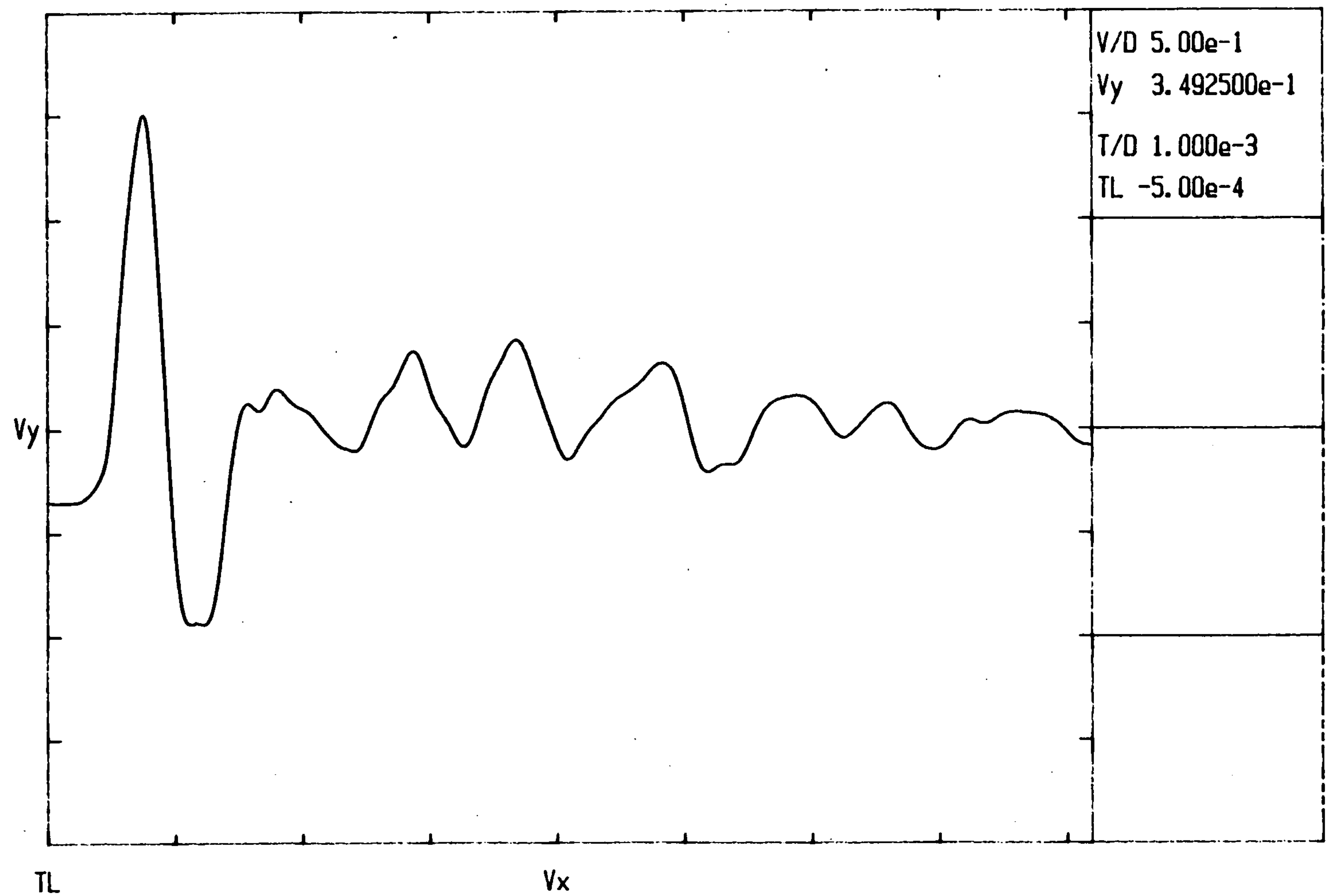

TYPICAL "ECHO" VELOCITY RECORD (DIGITAL OSCILLOSCOPE)
LABORATORY SEWER: 3 BRICK END (OUTER) TO 1 BRICK END

FIGURE 8.6

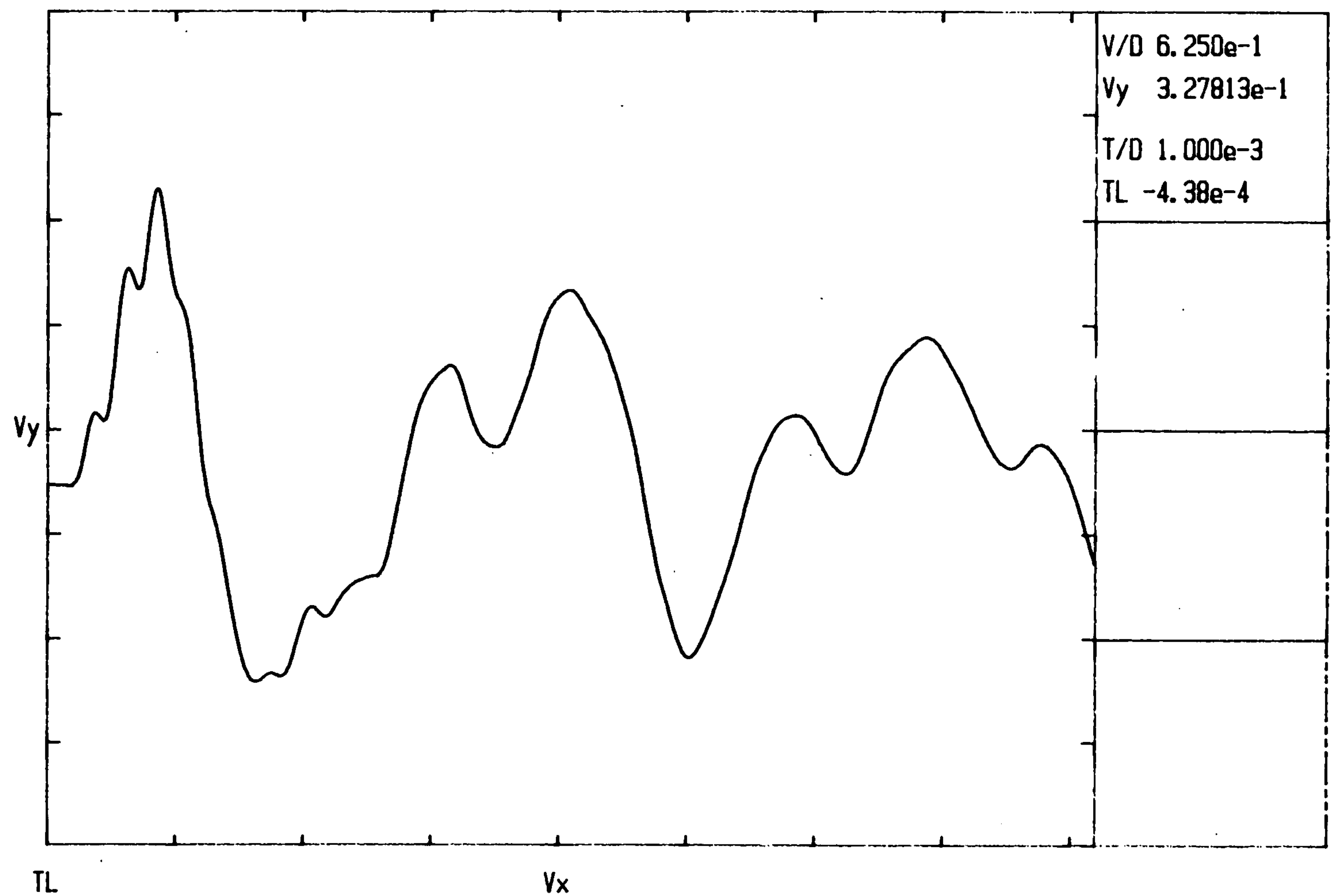

TYPICAL "ECHO" VELOCITY RECORD (DIGITAL OSCILLOSCOPE)
LABORATORY SEWER: 1 BRICK END TO 3 BRICK END

FIGURE 8.7

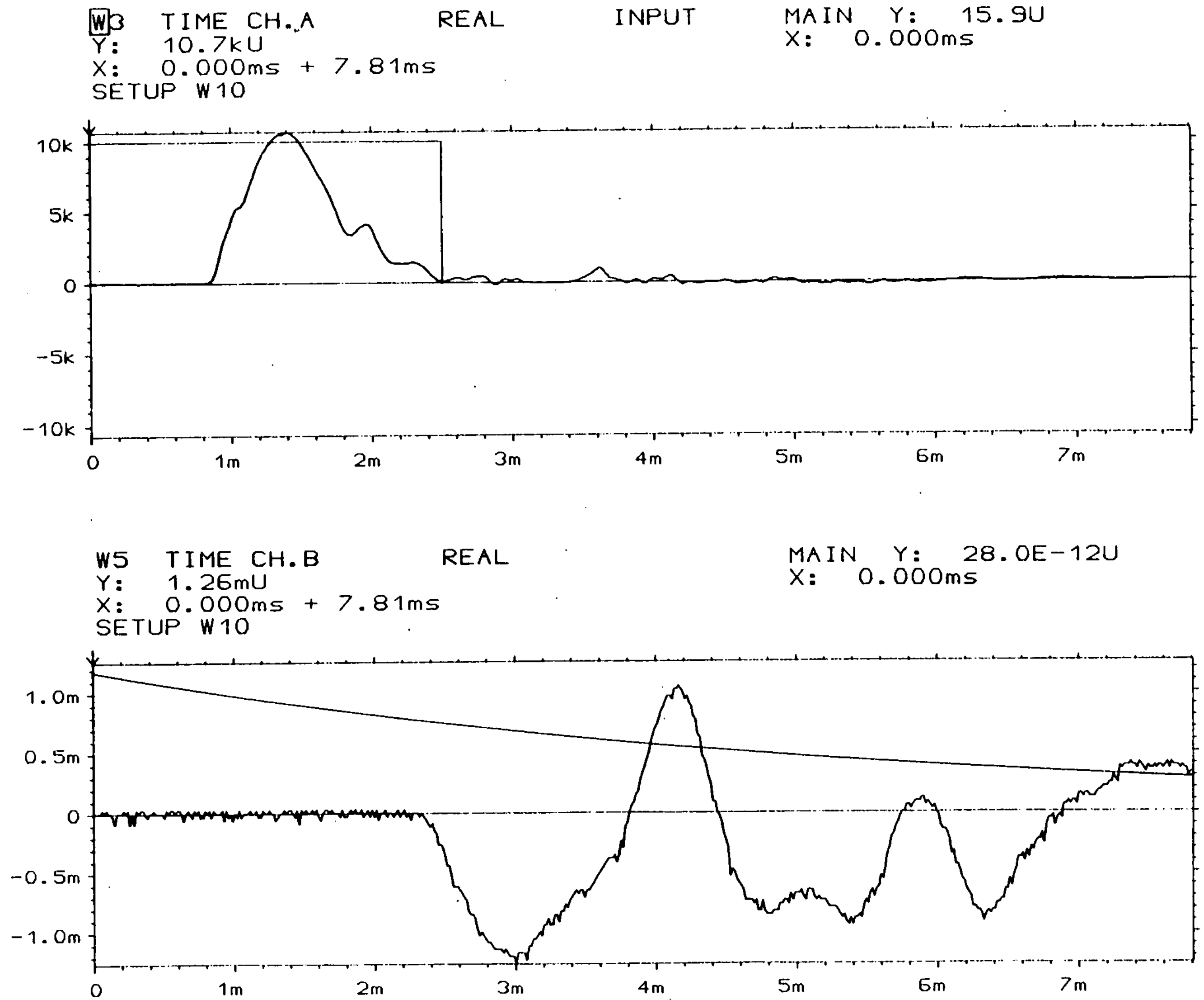

TYPICAL "DELAY" VELOCITY RECORD (SIGNAL ANALYSER)
LABORATORY SEWER: 3 BRICK END TO 1 BRICK END

FIGURE 8.8

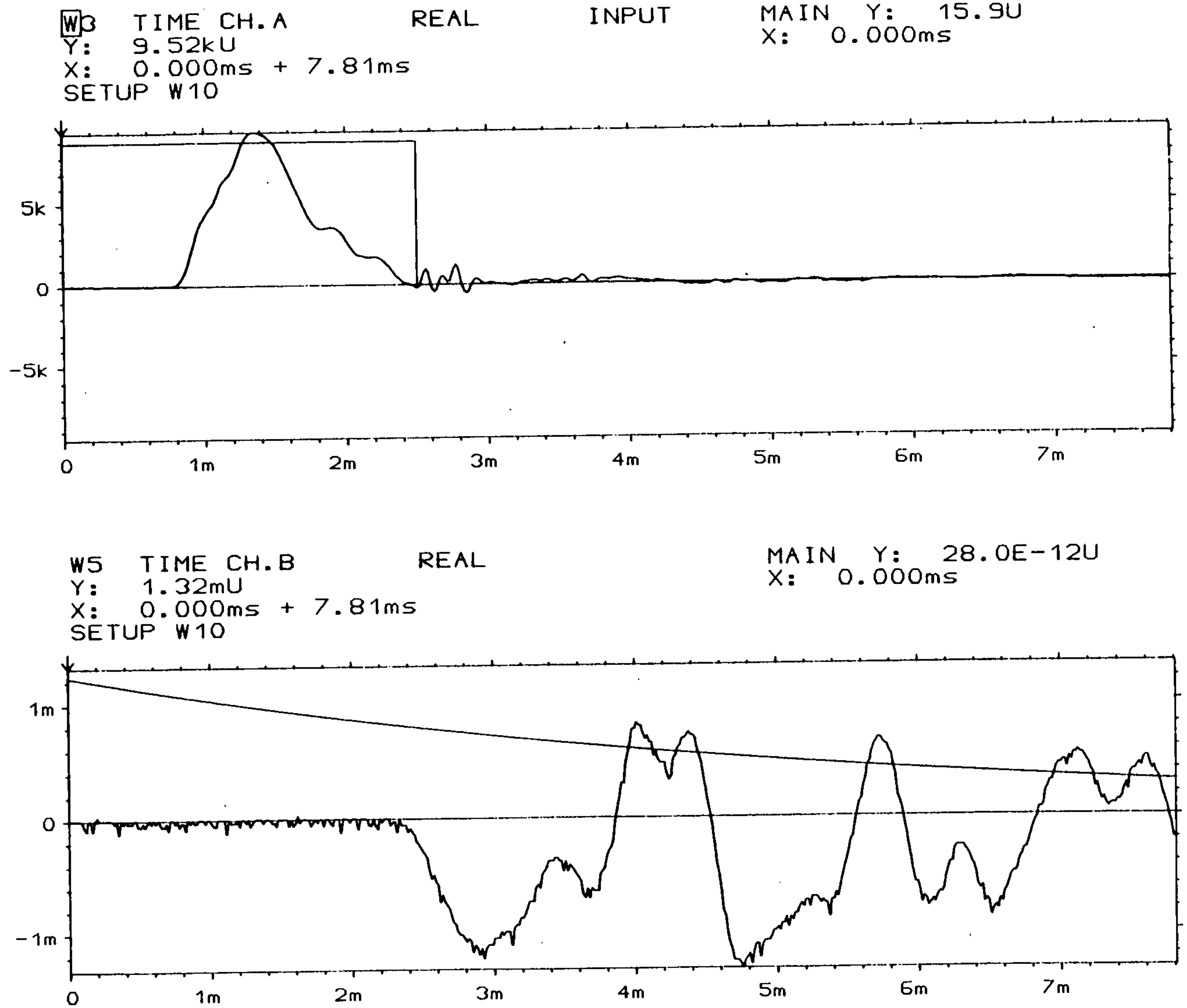

TYPICAL "DELAY" VELOCITY RECORD (SIGNAL ANALYSER)
LABORATORY SEWER: 1 BRICK END TO 3 BRICK END

FIGURE 8.9

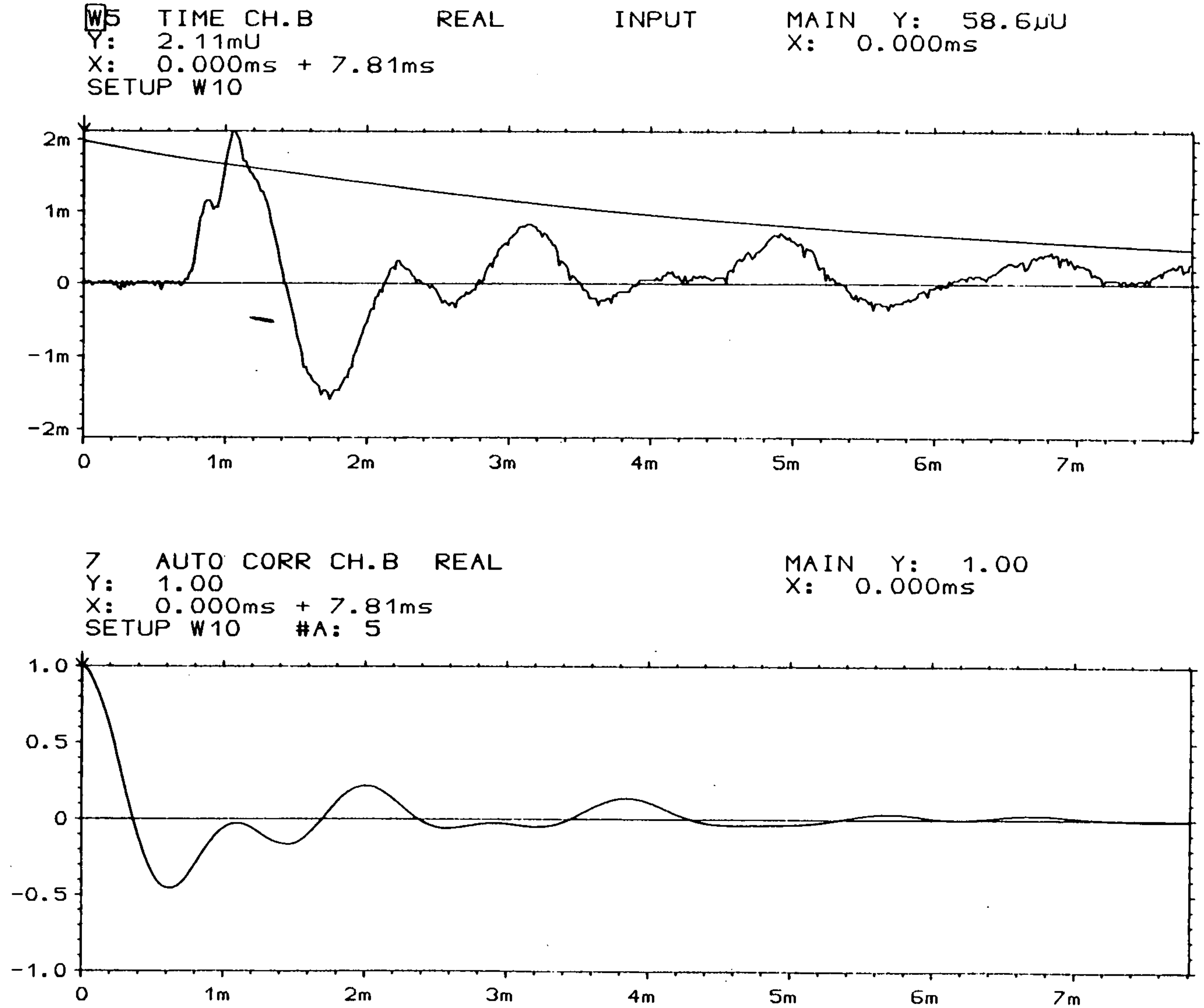

TYPICAL "ECHO" VEL. & AUTO-CORR. RECORD (SIGNAL ANALYSER)
LABORATORY SEWER: 3 BRICK END (INNER) TO 1 BRICK END

FIGURE 8.10

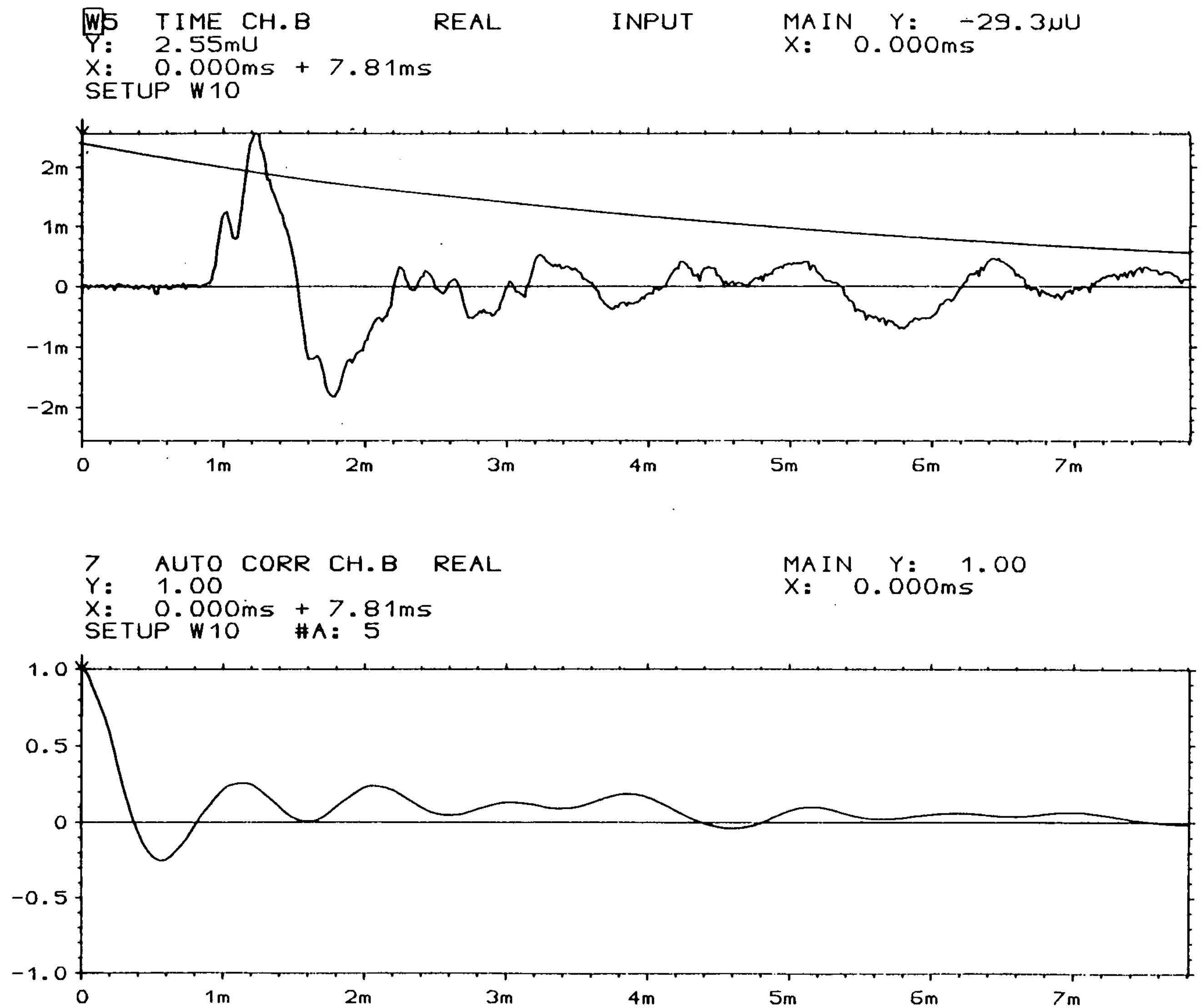

TYPICAL "ECHO" VEL. & AUTO-CORR. RECORD (SIGNAL ANALYSER)
LABORATORY SEWER: 3 BRICK END (MIDDLE) TO 1 BRICK END

FIGURE 8.11

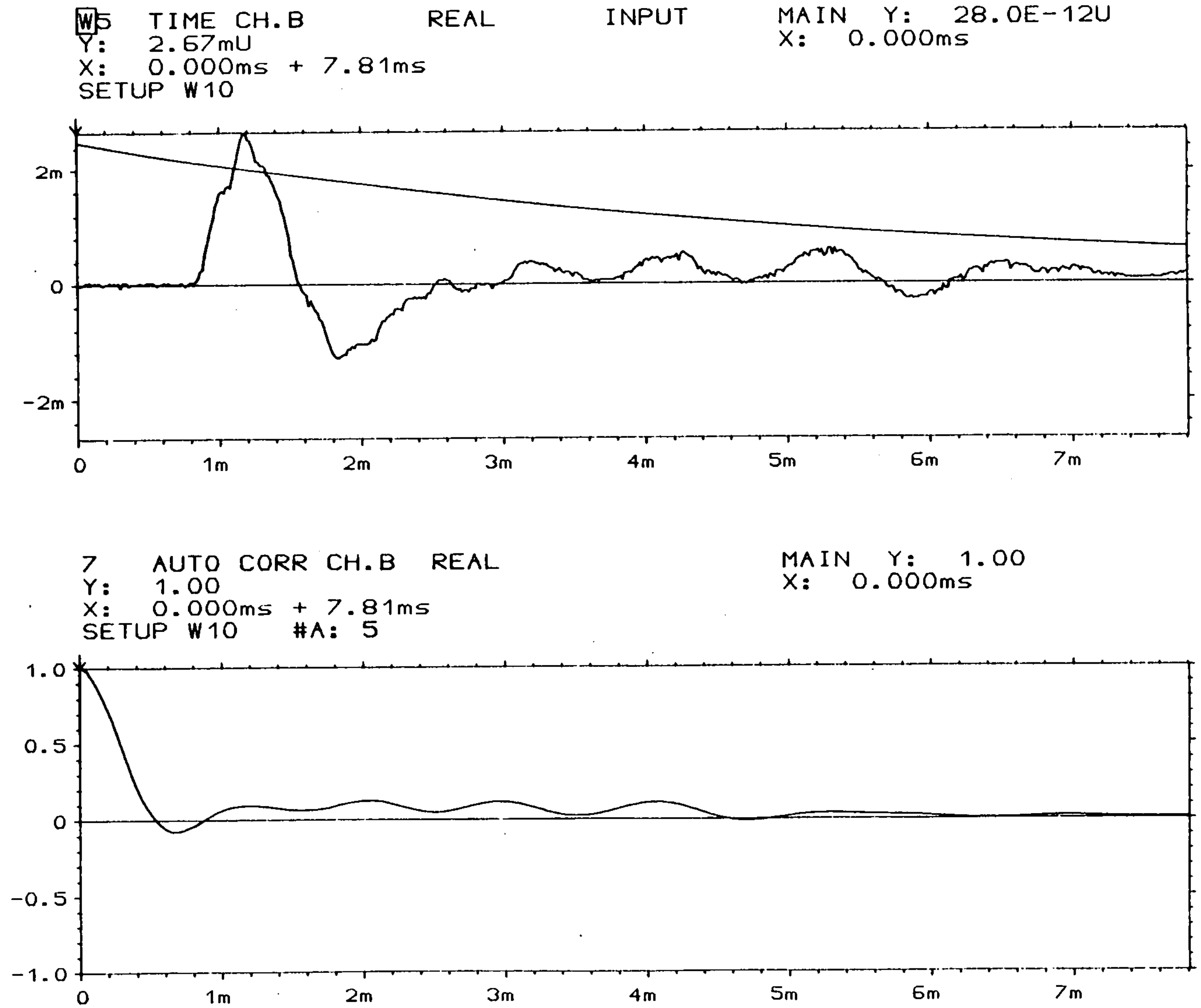

TYPICAL "ECHO" VEL. & AUTO-CORR RECORD (SIGNAL ANALYSER)
LABORATORY SEWER: 3 BRICK END (OUTER) TO 1 BRICK END

FIGURE 8.12

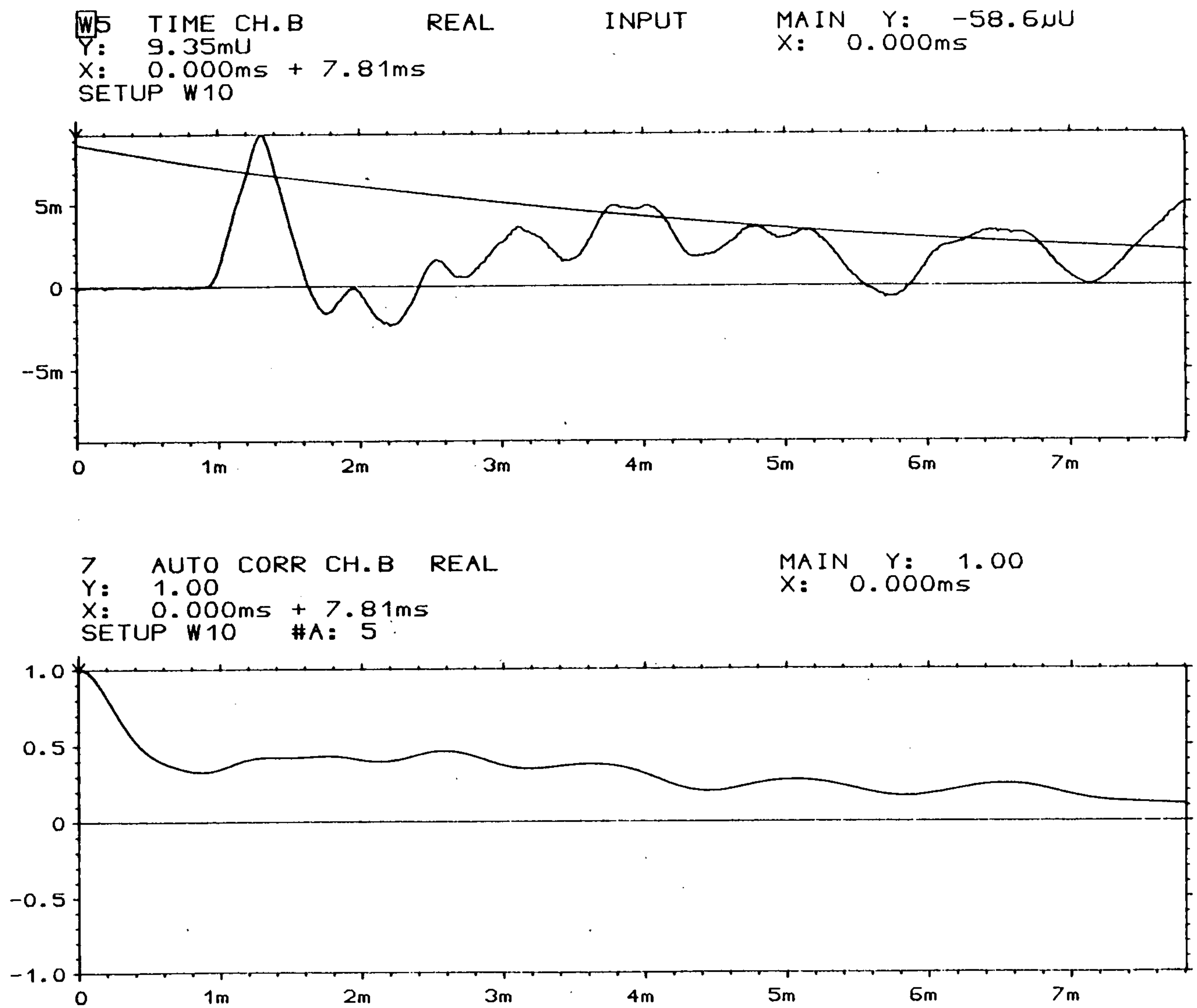

TYPICAL "ECHO" VEL. & AUTO-CORR. RECORD (SIGNAL ANALYSER)
LABORATORY SEWER: 1 BRICK END TO 3 BRICK END

FIGURE 8.13

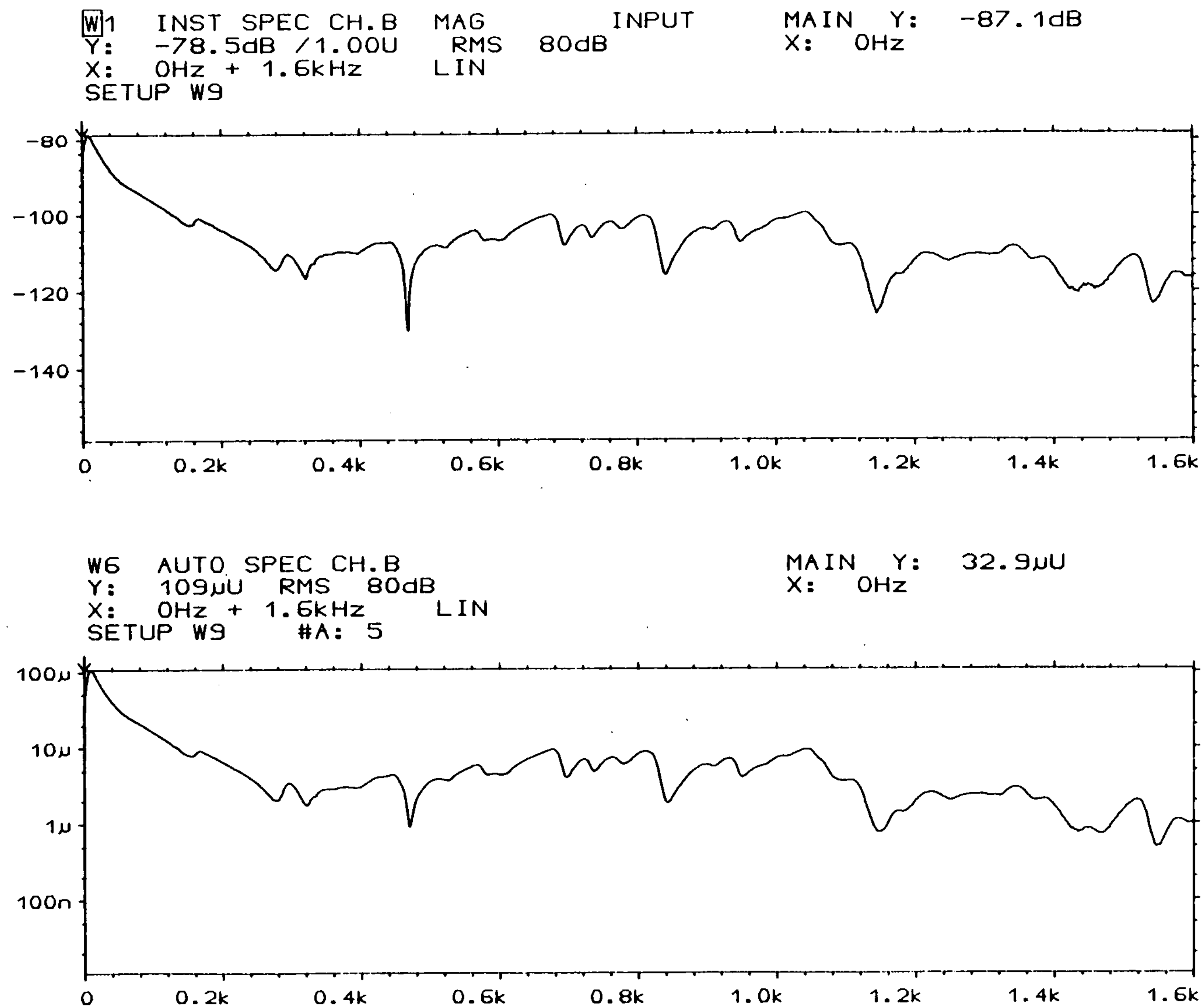

FIGURE 8.14

TYPICAL INSTANTANEOUS AND AUTOSPECTRA
LABORATORY SEWER: 3 BRICK END

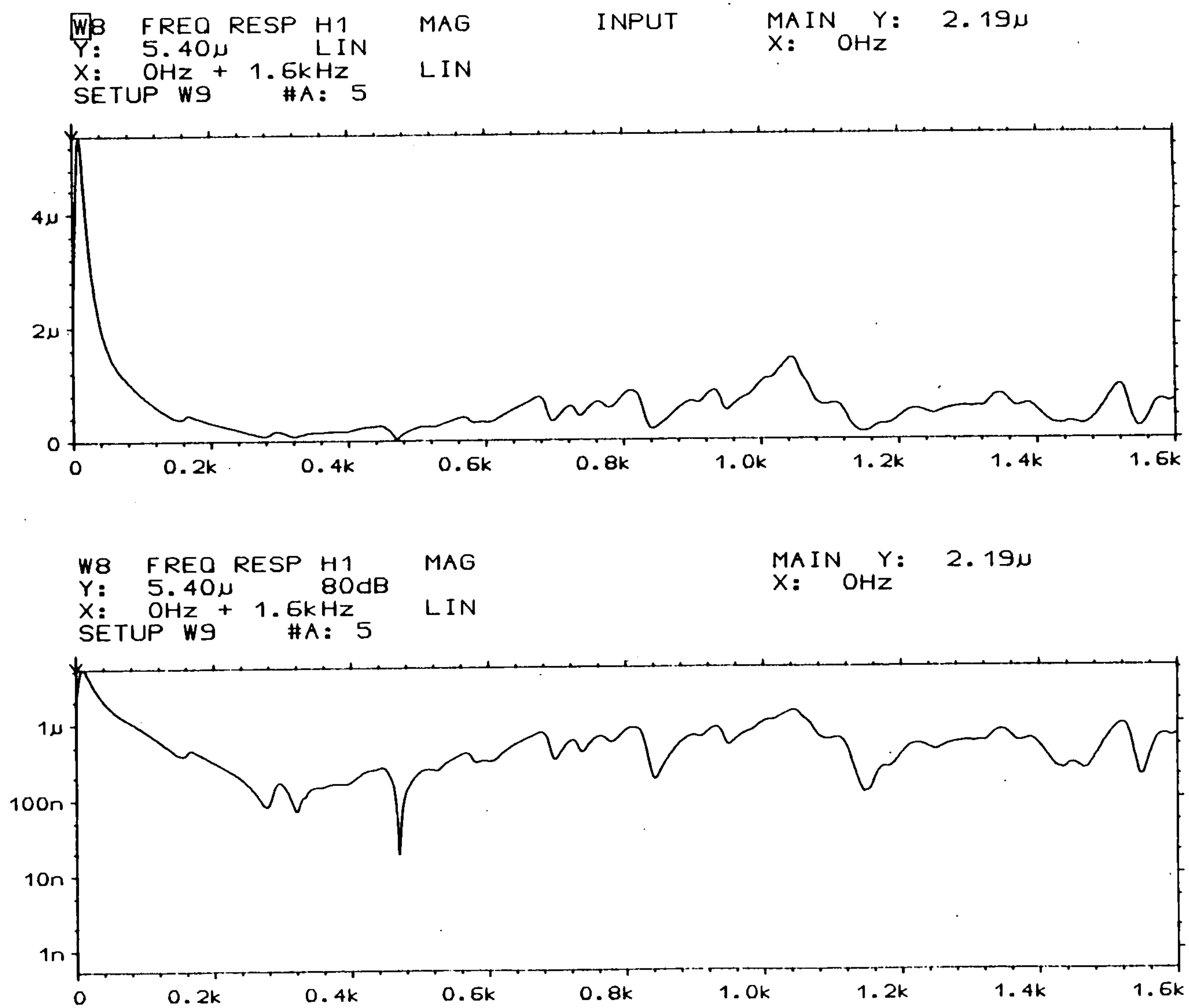

TYPICAL FREQUENCY RESPONSE FUNCTION
LABORATORY SEWER: 3 BRICK END

FIGURE 8.15

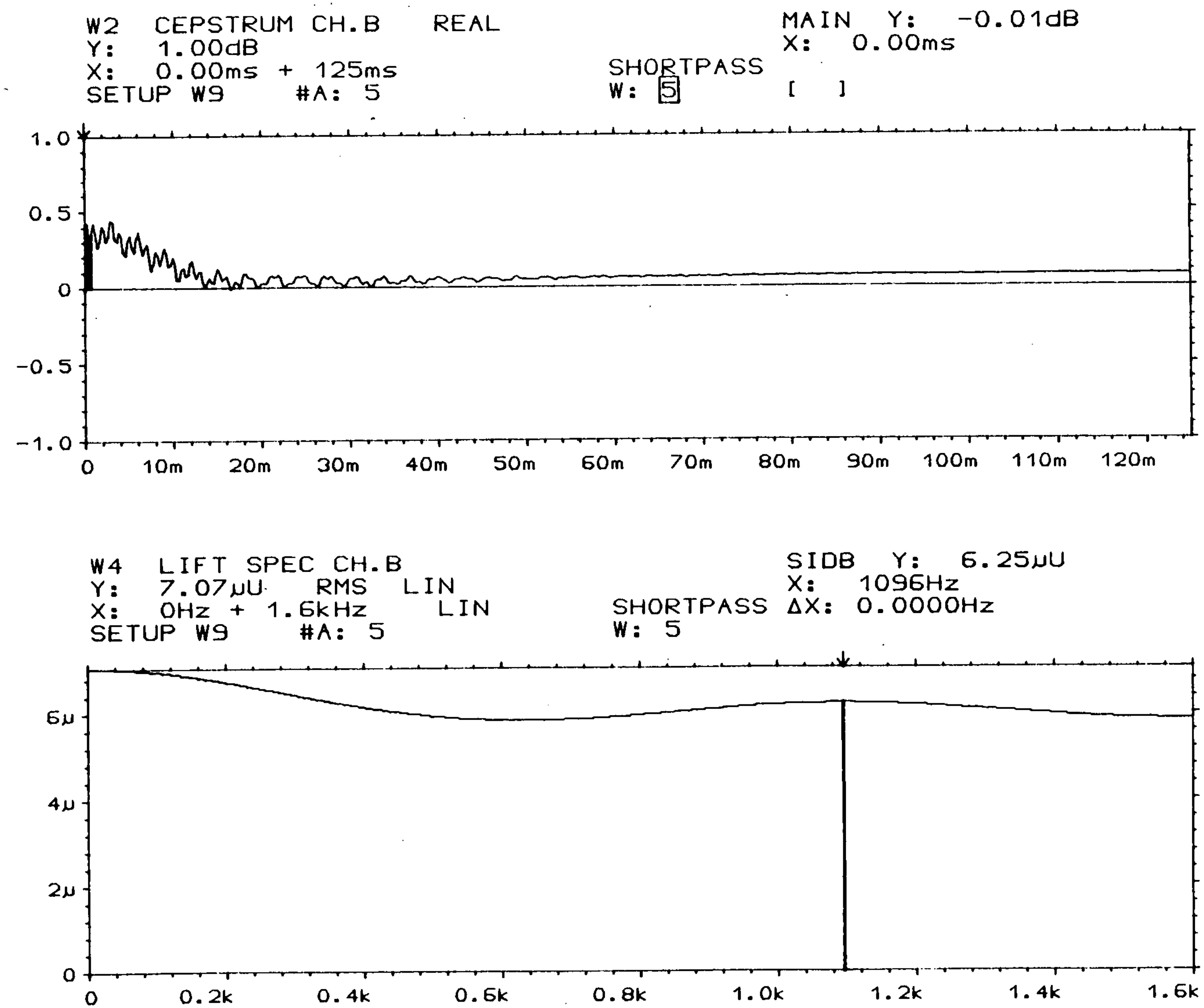

USING CEPSTRUM AND LIFTERED SPECTRUM
TO LOCATE FIRST CHANGE OF CROSS-SECTION
LABORATORY SEWER: 3 BRICK END

FIGURE 8.16

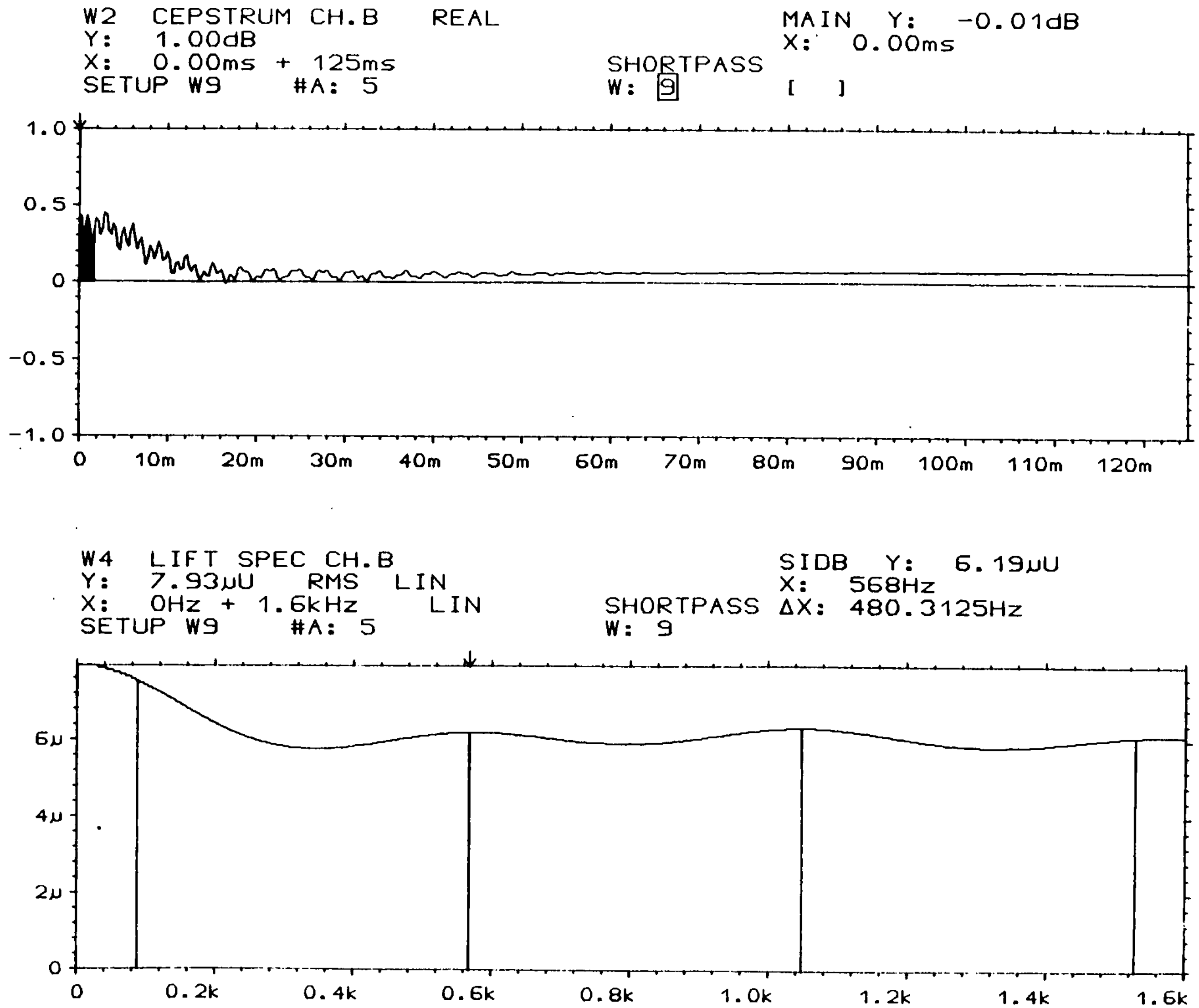

USING CEPSTRUM AND LIFTERED SPECTRUM
TO LOCATE SECOND CHANGE OF CROSS-SECTION
LABORATORY SEWER: 3 BRICK END

FIGURE 8.17

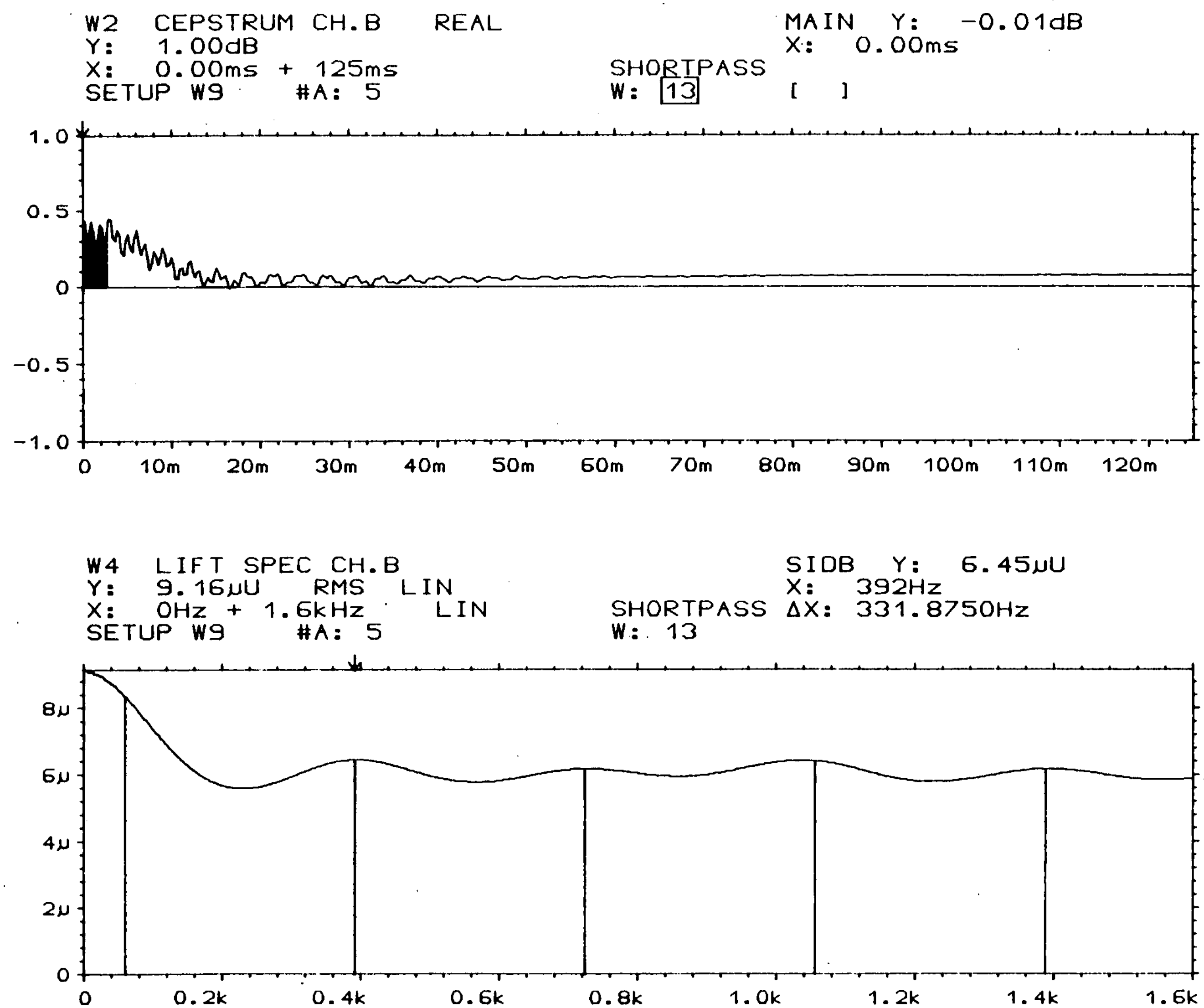

USING CEPSTRUM AND LIFTERED SPECTRUM
TO LOCATE FAR END OF THE SEWER
LABORATORY SEWER: 3 BRICK END

FIGURE 8.18

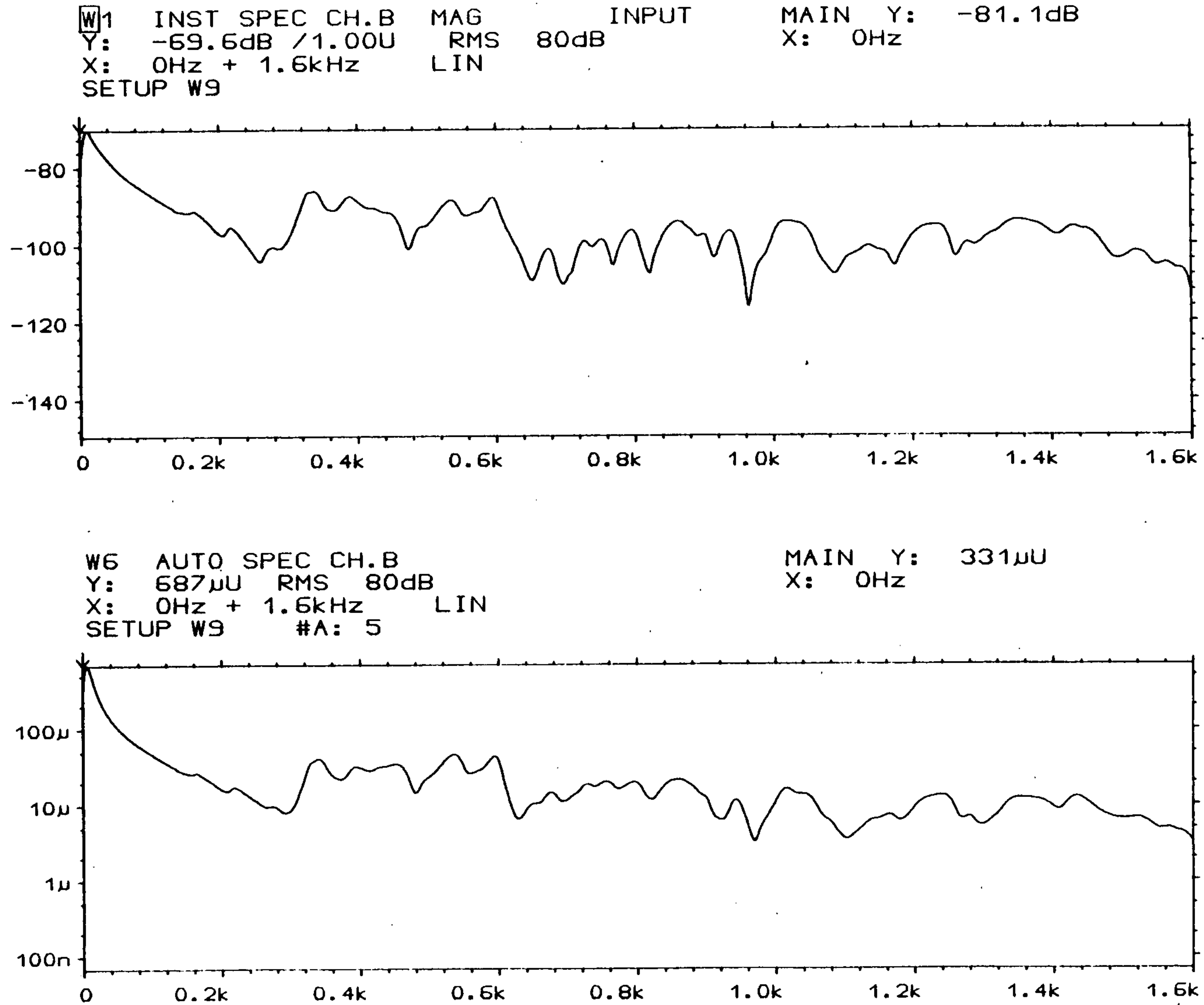

TYPICAL INSTANTANEOUS AND AUTOSPECTRA
LABORATORY SEWER: 1 BRICK END

FIGURE 8.19

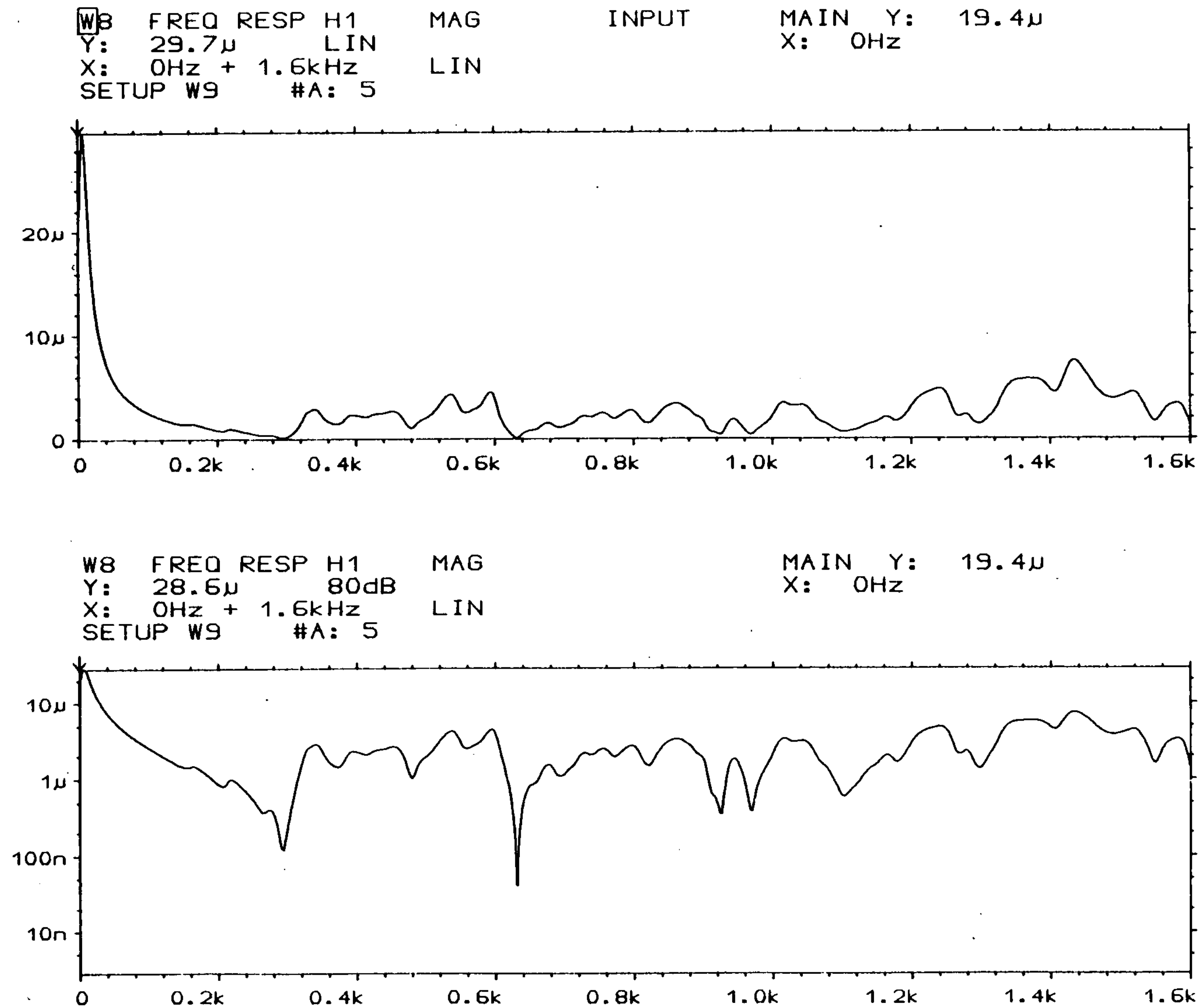

TYPICAL FREQUENCY RESPONSE FUNCTION
LABORATORY SEWER: 1 BRICK END

FIGURE 8.20

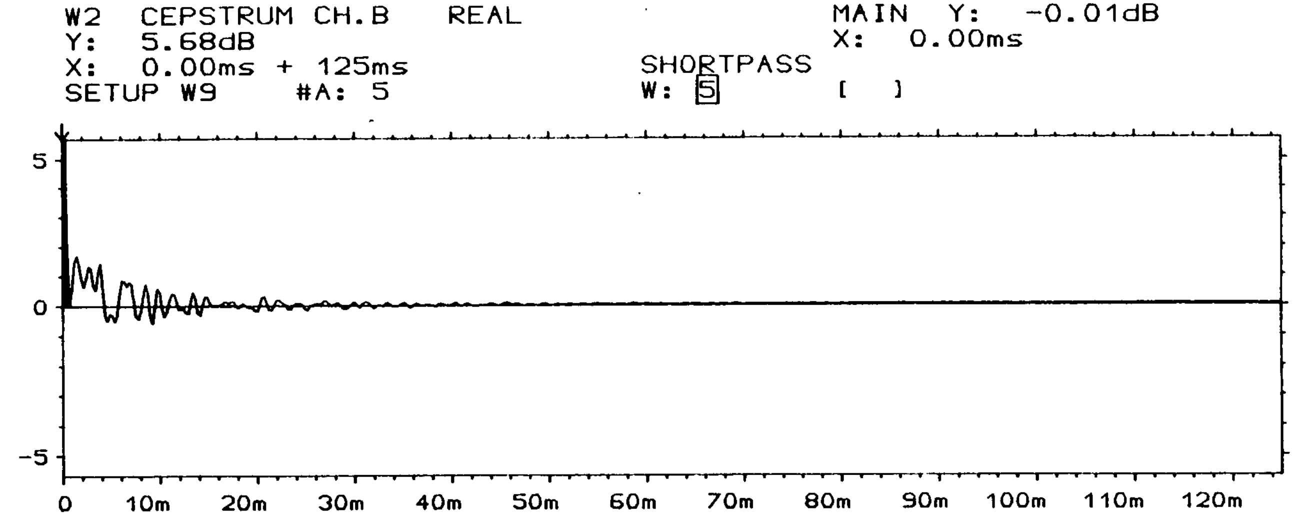

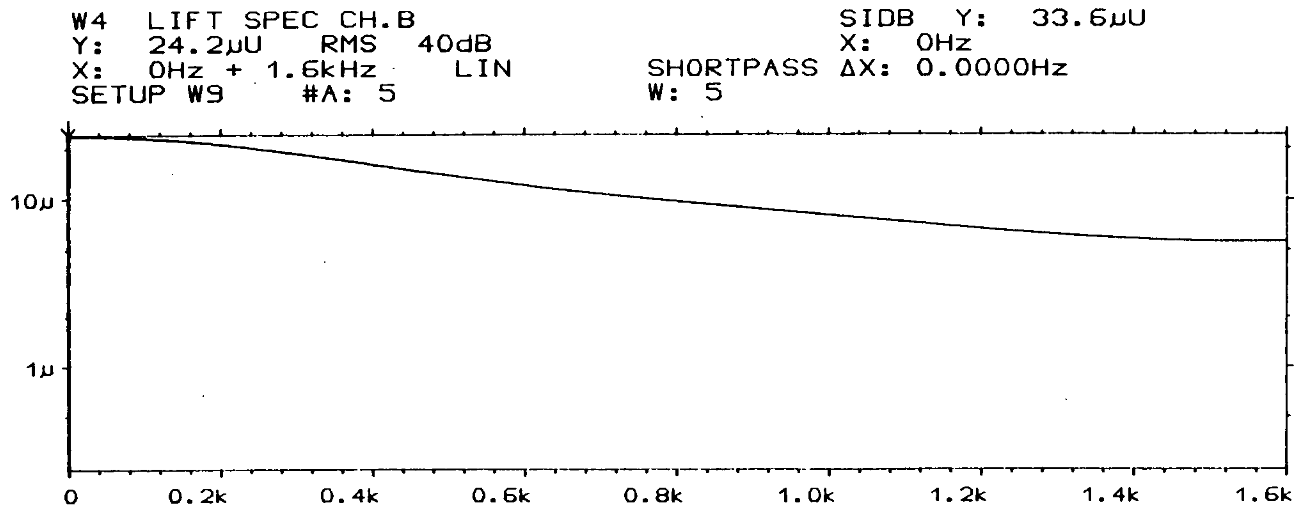

USING CEPSTRUM AND LIFTERED SPECTRUM
TO LOCATE FIRST CHANGE OF CROSS-SECTION
LABORATORY SEWER: 1 BRICK END

FIGURE 8.21

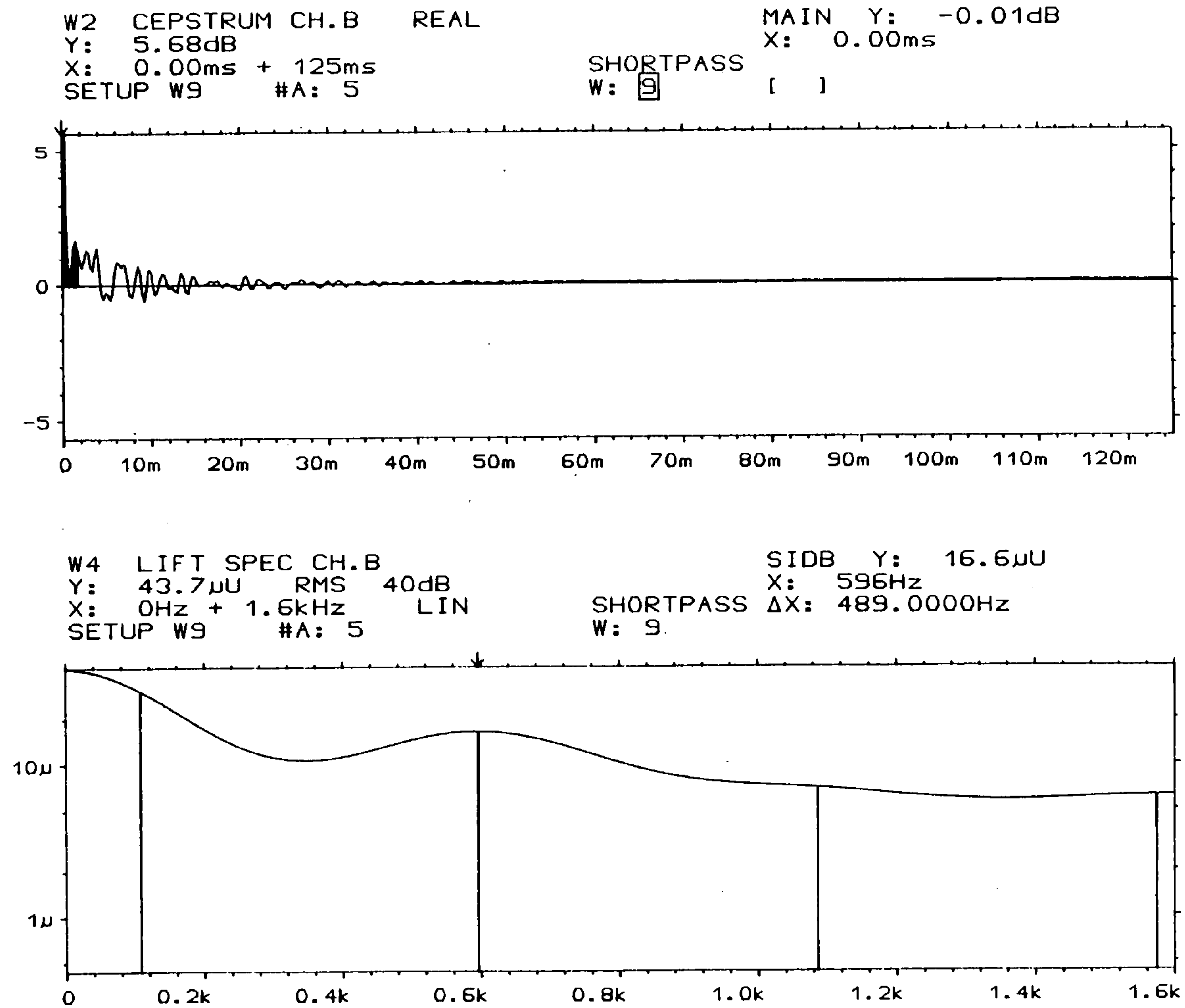

USING CEPSTRUM AND LIFTERED SPECTRUM TO LOCATE SECOND CHANGE OF CROSS-SECTION LABORATORY SEWER: 1 BRICK END

FIGURE 8.22

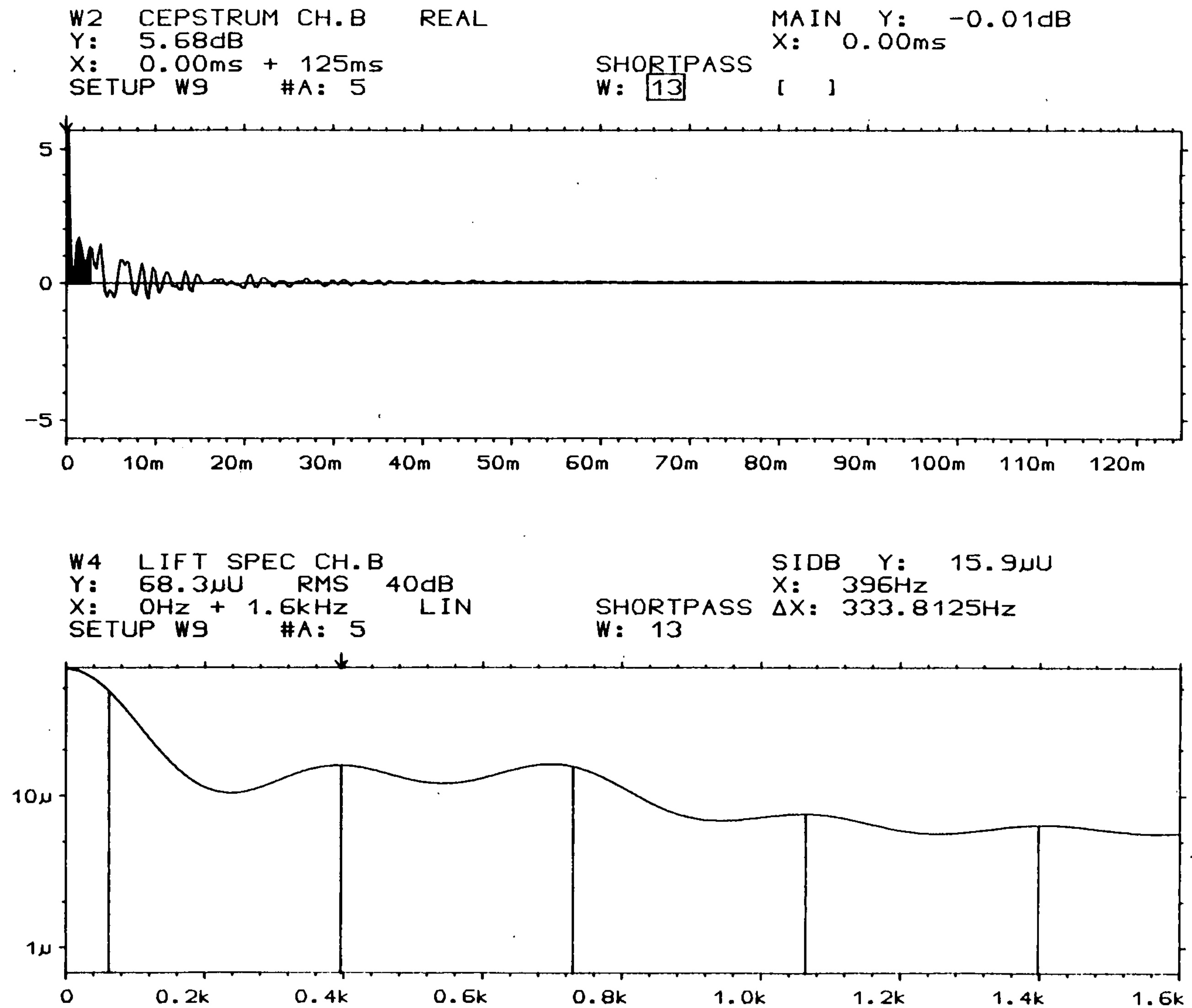

USING CEPSTRUM AND LIFTERED SPECTRUM
TO LOCATE FAR END OF THE SEWER
LABORATORY SEWER: 1 BRICK END

FIGURE 8.23

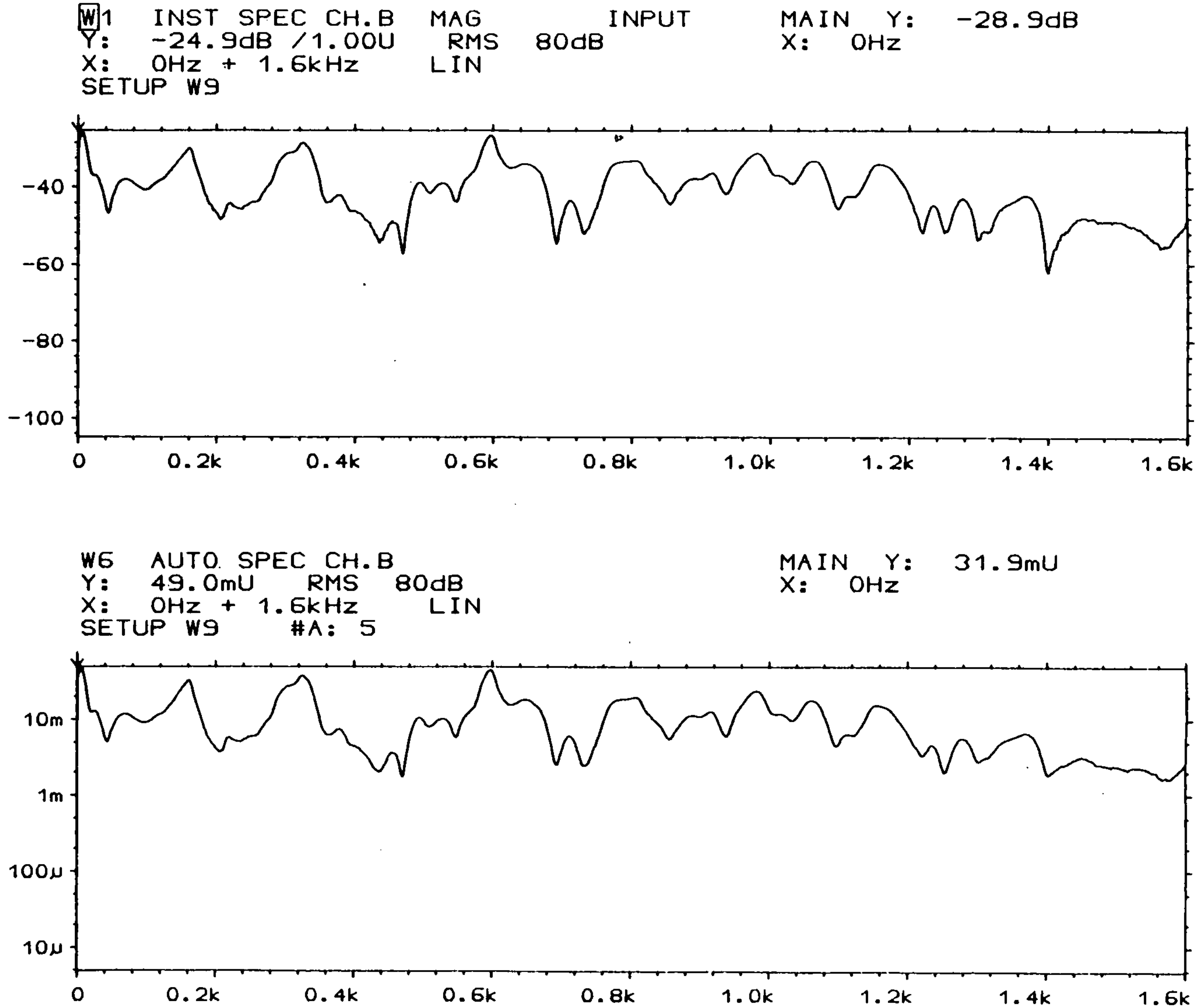

TYPICAL INSTANTANEOUS AND AUTOSPECTRA

LABORATORY SEWER: HAMMER 3 BRICK END, ACCEL 1 BRICK END

FIGURE 8.24

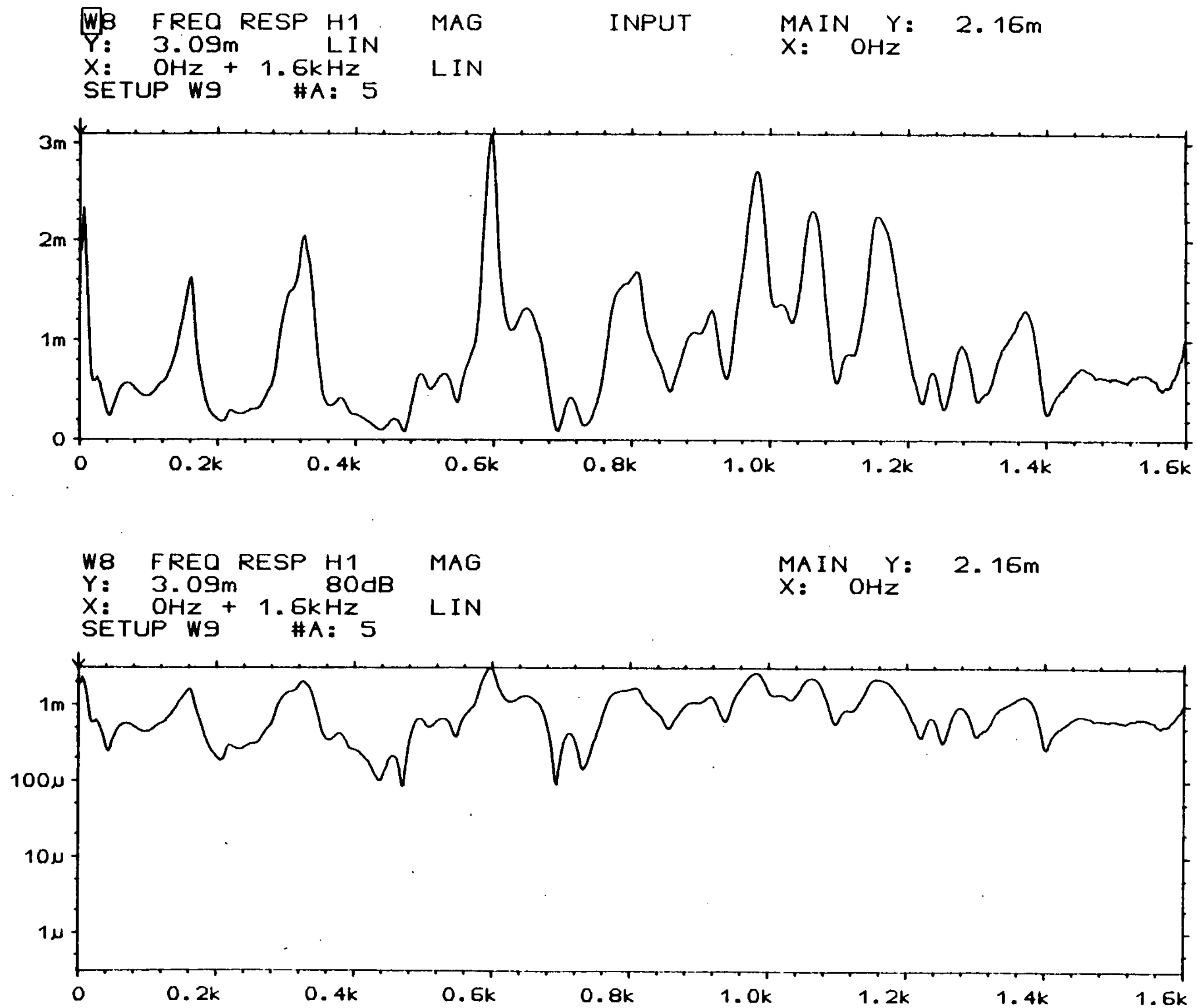

TYPICAL FREQUENCY RESPONSE FUNCTION
LABORATORY SEWER: HAMMER 3 BRICK END, ACCEL 1 BRICK END

FIGURE 8.25

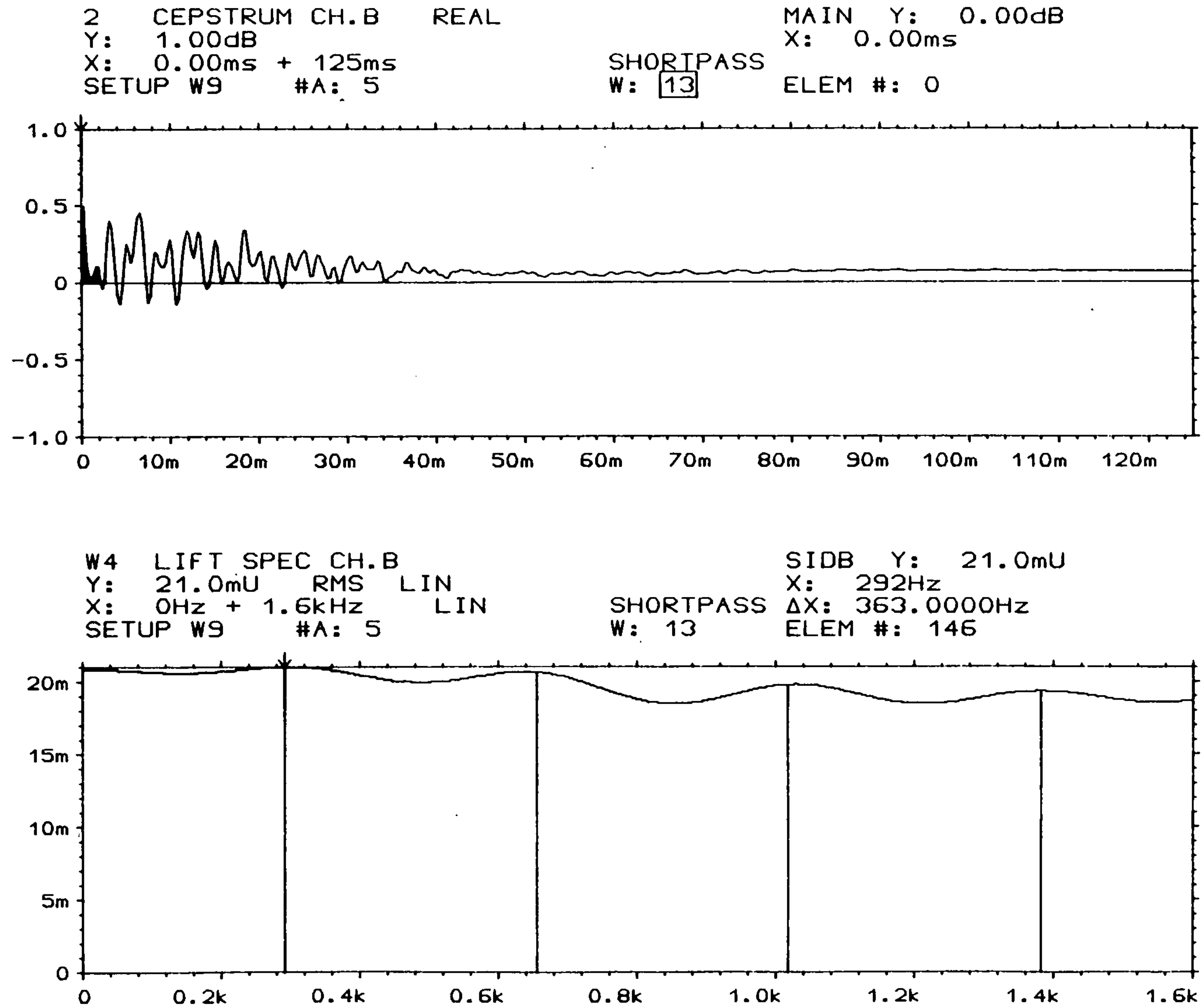

USING CEPSTRUM AND LIFTERED SPECTRUM
TO LOCATE FAR END OF THE SEWER
LABORATORY SEWER: HAMMER 3 BRICK END, ACCEL 1 BRICK END

FIGURE 8.26

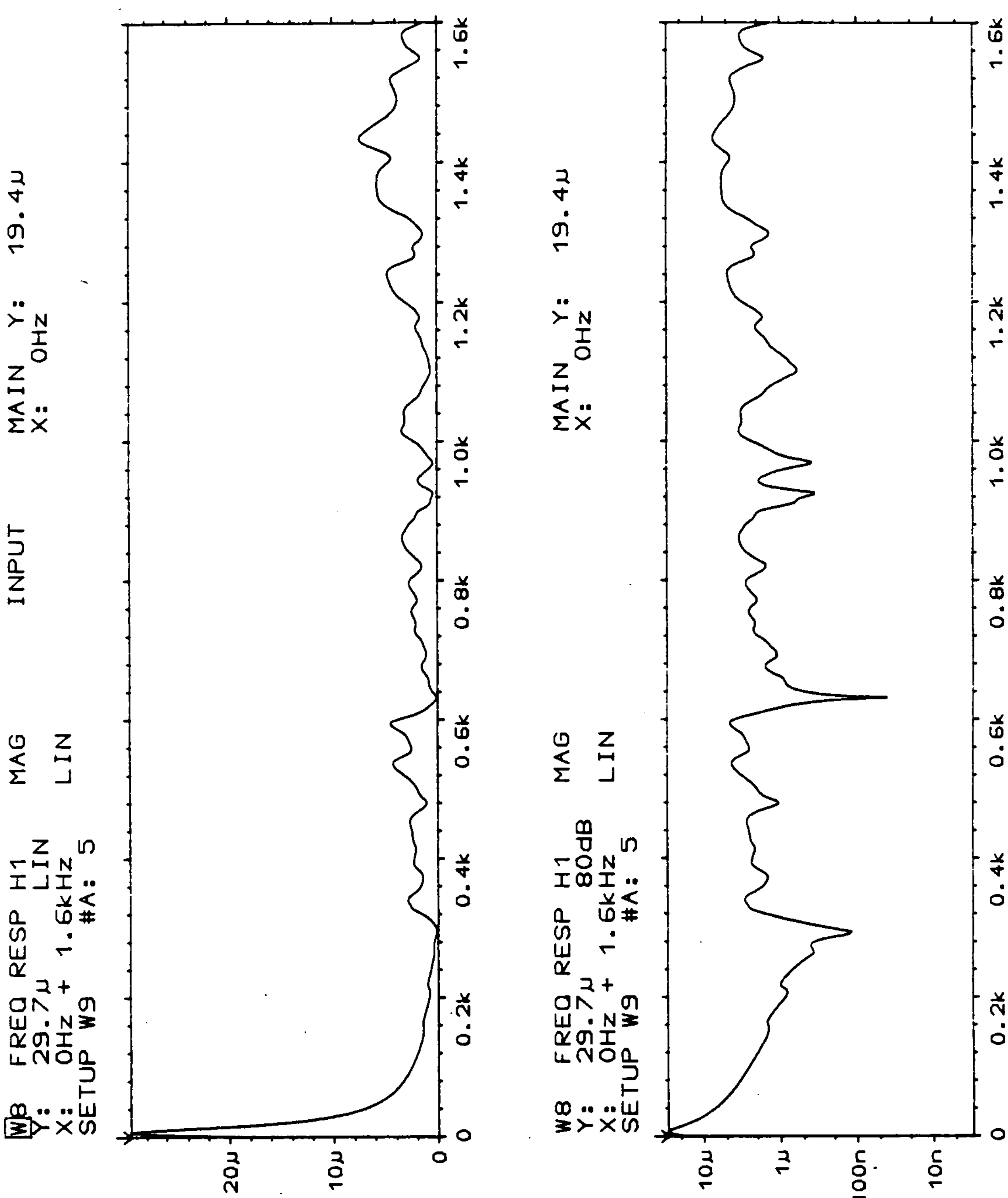

TYPICAL INSTANTANEOUS AND AUTOSPECTRA
LABORATORY SEWER: HAMMER 1 BRICK END, ACCEL´ 3 BRICK END

FIGURE 8.27

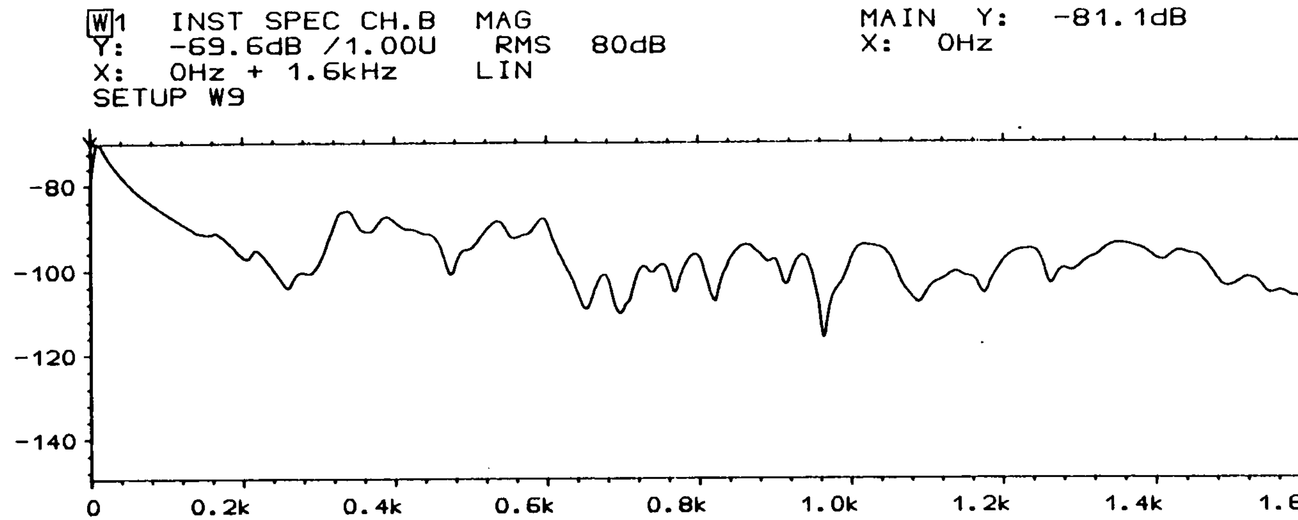

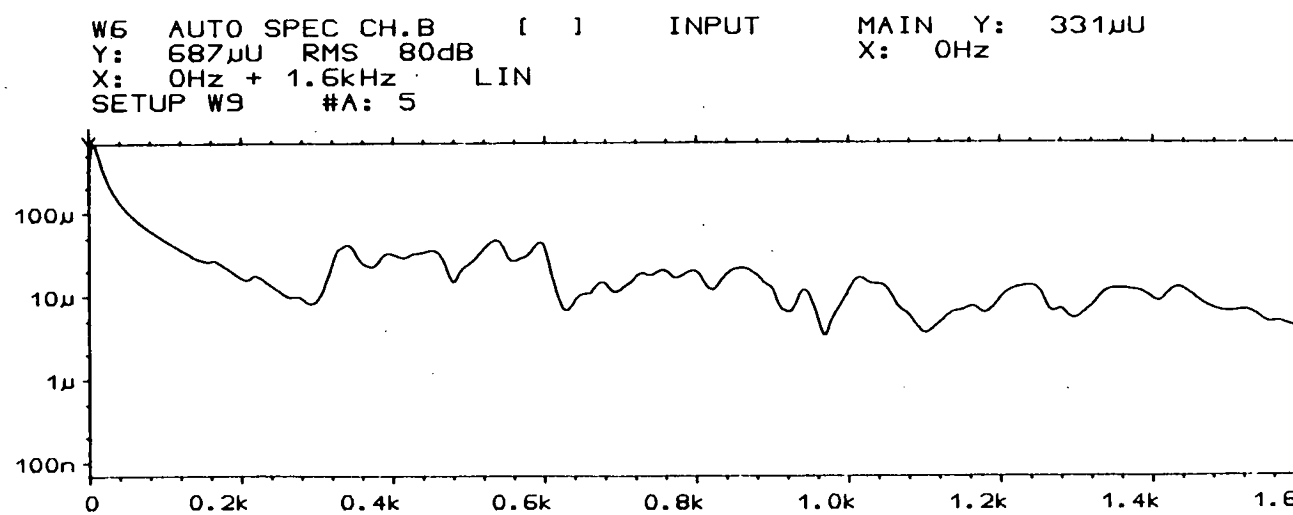

TYPICAL FREQUENCY RESPONSE FUNCTION
LABORATORY SEWER: HAMMER 1 BRICK END, ACCEL 3 BRICK END

FIGURE 8.28

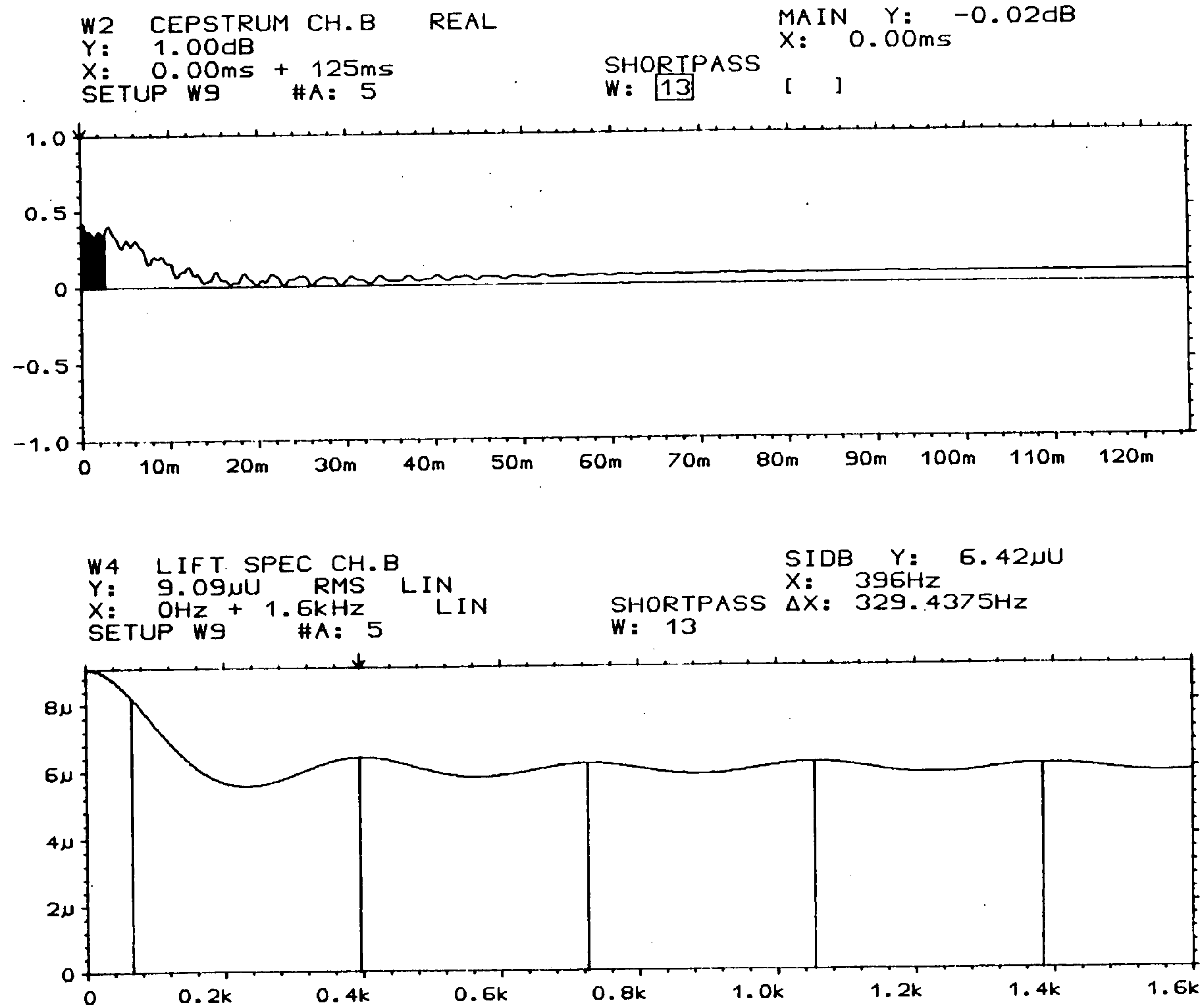

USING CEPSTRUM AND LIFTERED SPECTRUM
TO LOCATE FAR END OF THE SEWER
LABORATORY SEWER: HAMMER 1 BRICK END, ACCEL 3 BRICK END

FIGURE 8.29

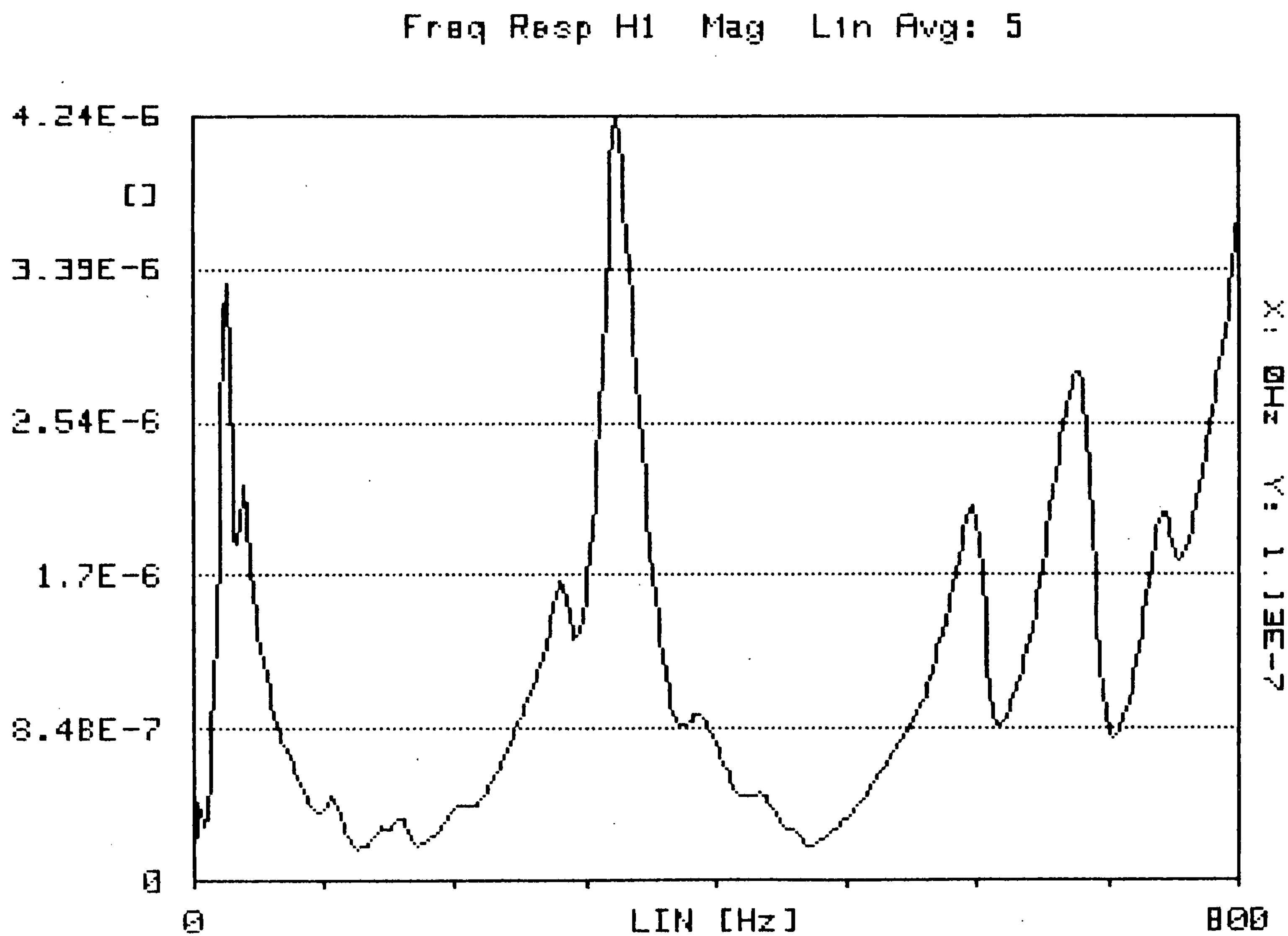

TYPICAL "NORMAL" FREQUENCY RESPONSE FUNCTION
LABORATORY SEWER: SINGLE BRICK RING

FIGURE 8.30

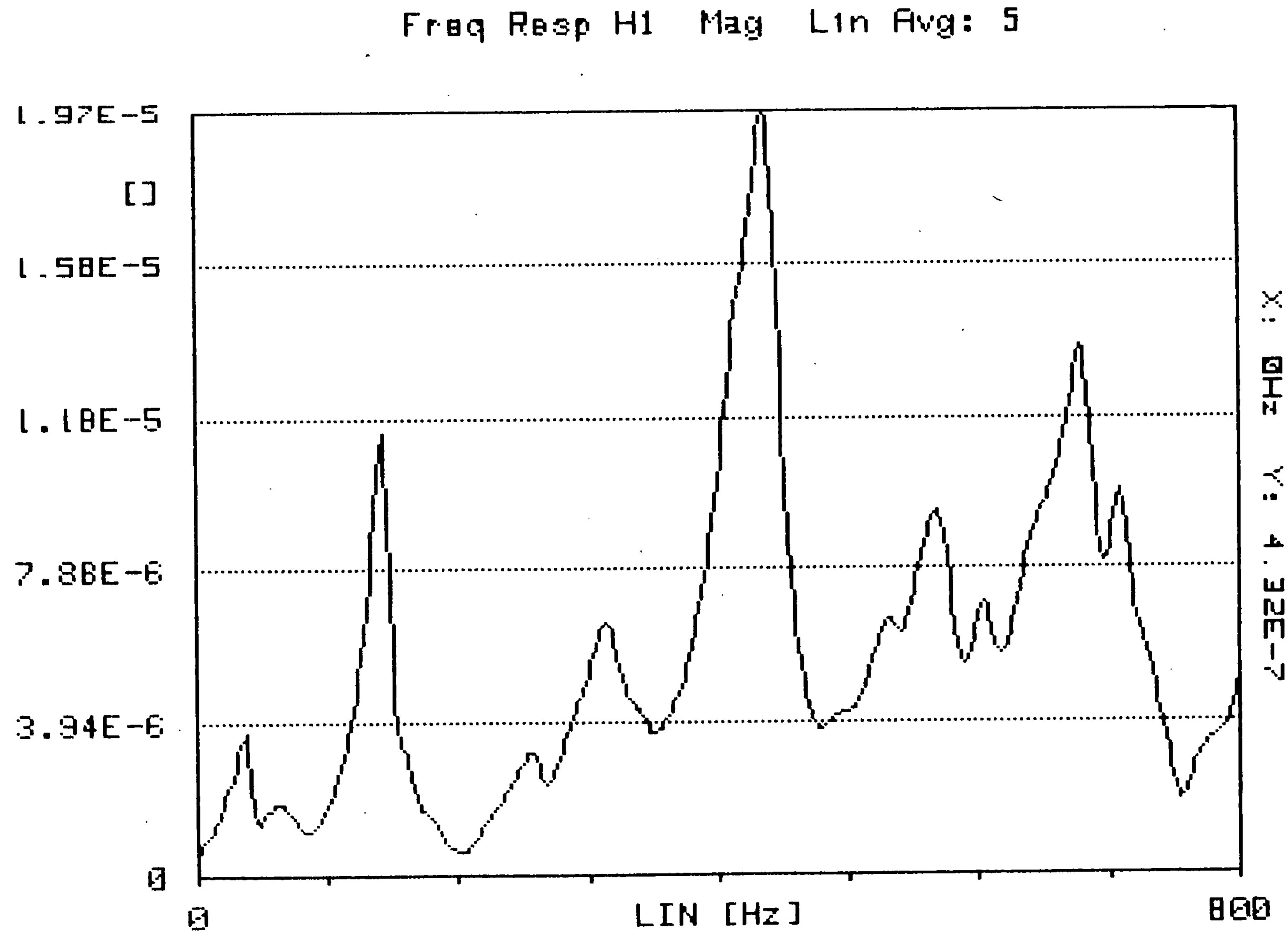

TYPICAL "NORMAL" FREQUENCY RESPONSE FUNCTION
LABORATORY SEWER: DOUBLE BRICK RING

FIGURE 8.31

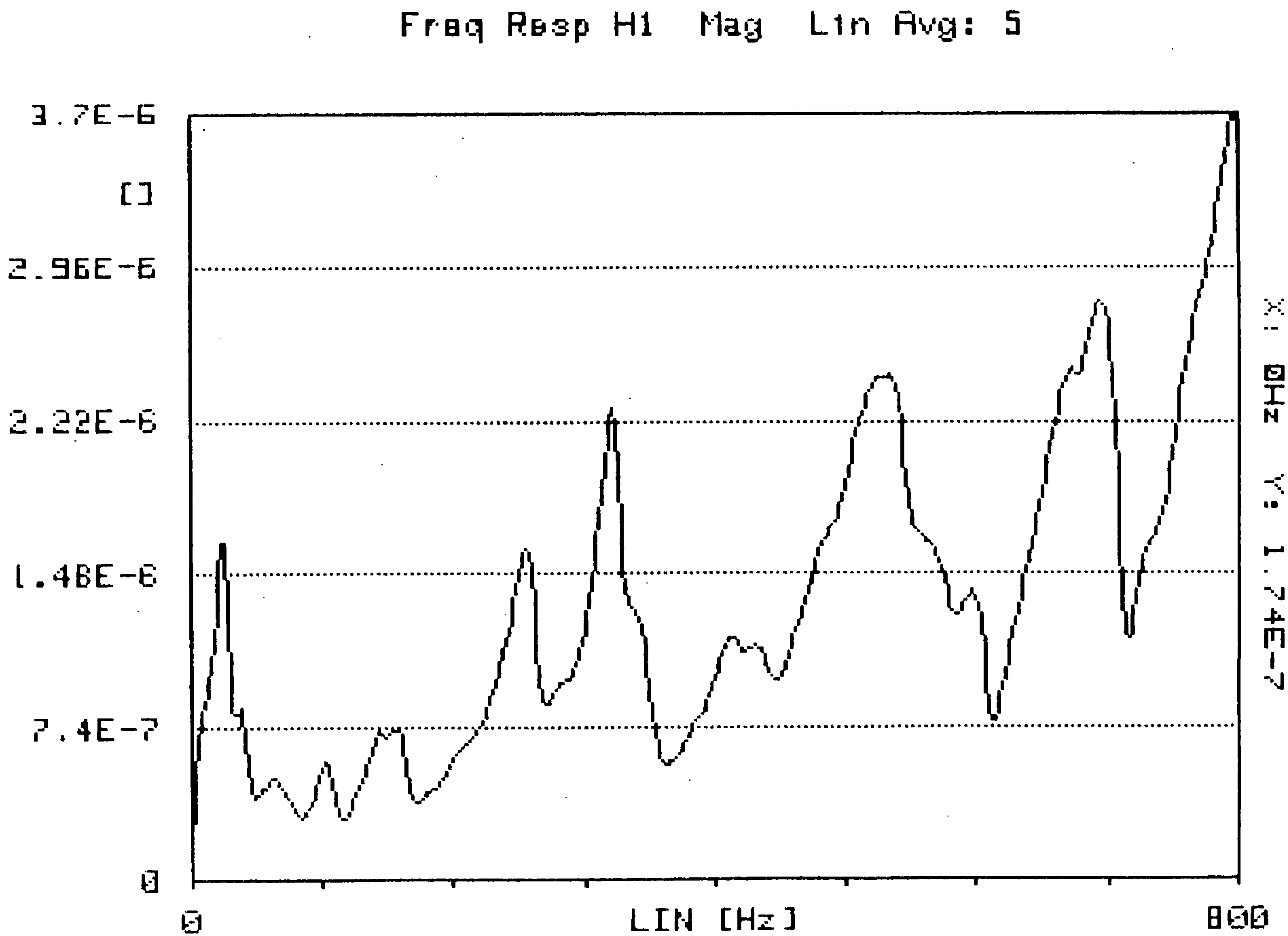

TYPICAL "NORMAL" FREQUENCY RESPONSE FUNCTION
LABORATORY SEWER: TRIPLE BRICK RING

FIGURE 8.32

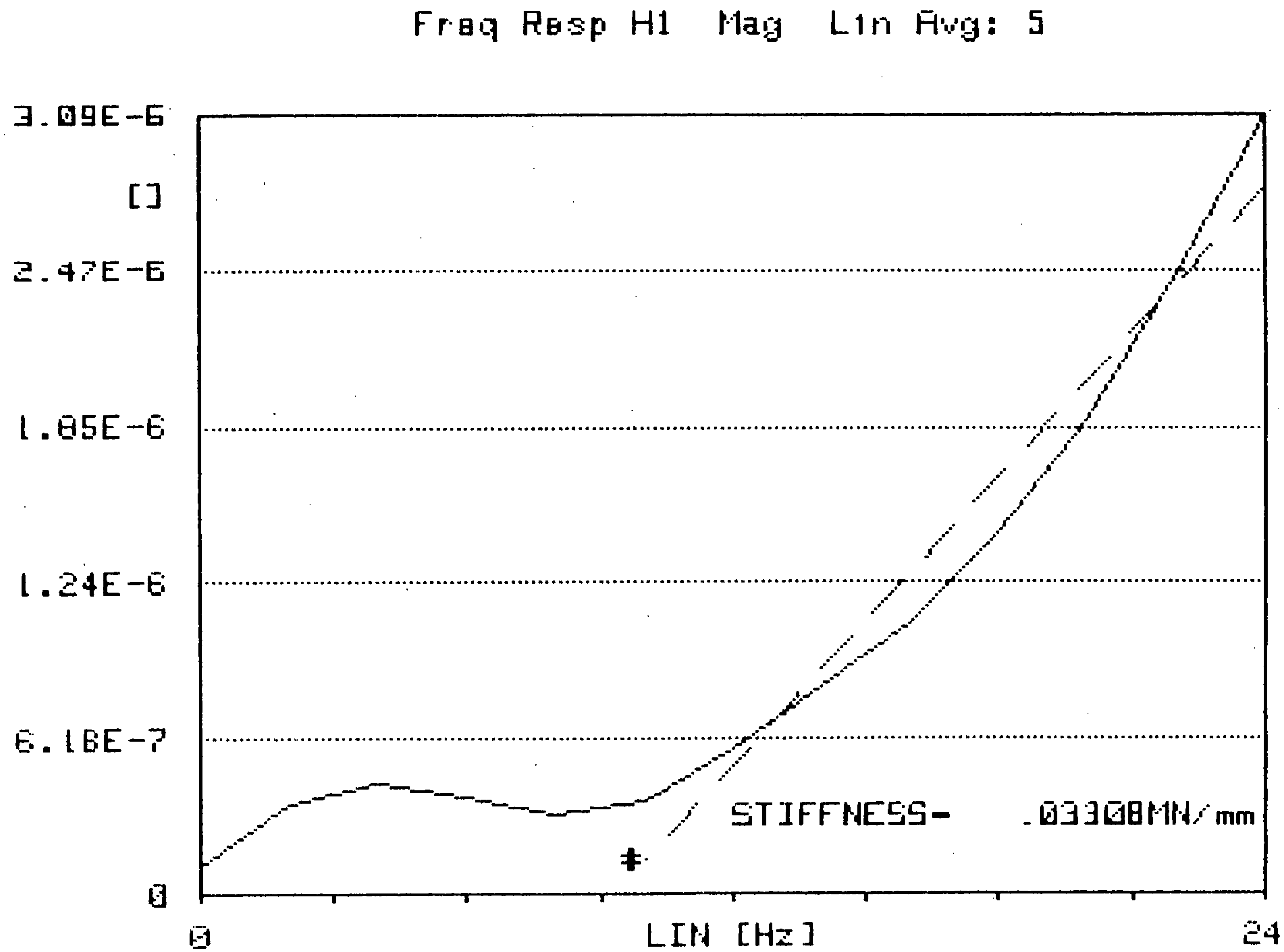

TYPICAL SEWER RING STIFFNESS
LABORATORY SEWER: SINGLE BRICK RING

FIGURE 8.33

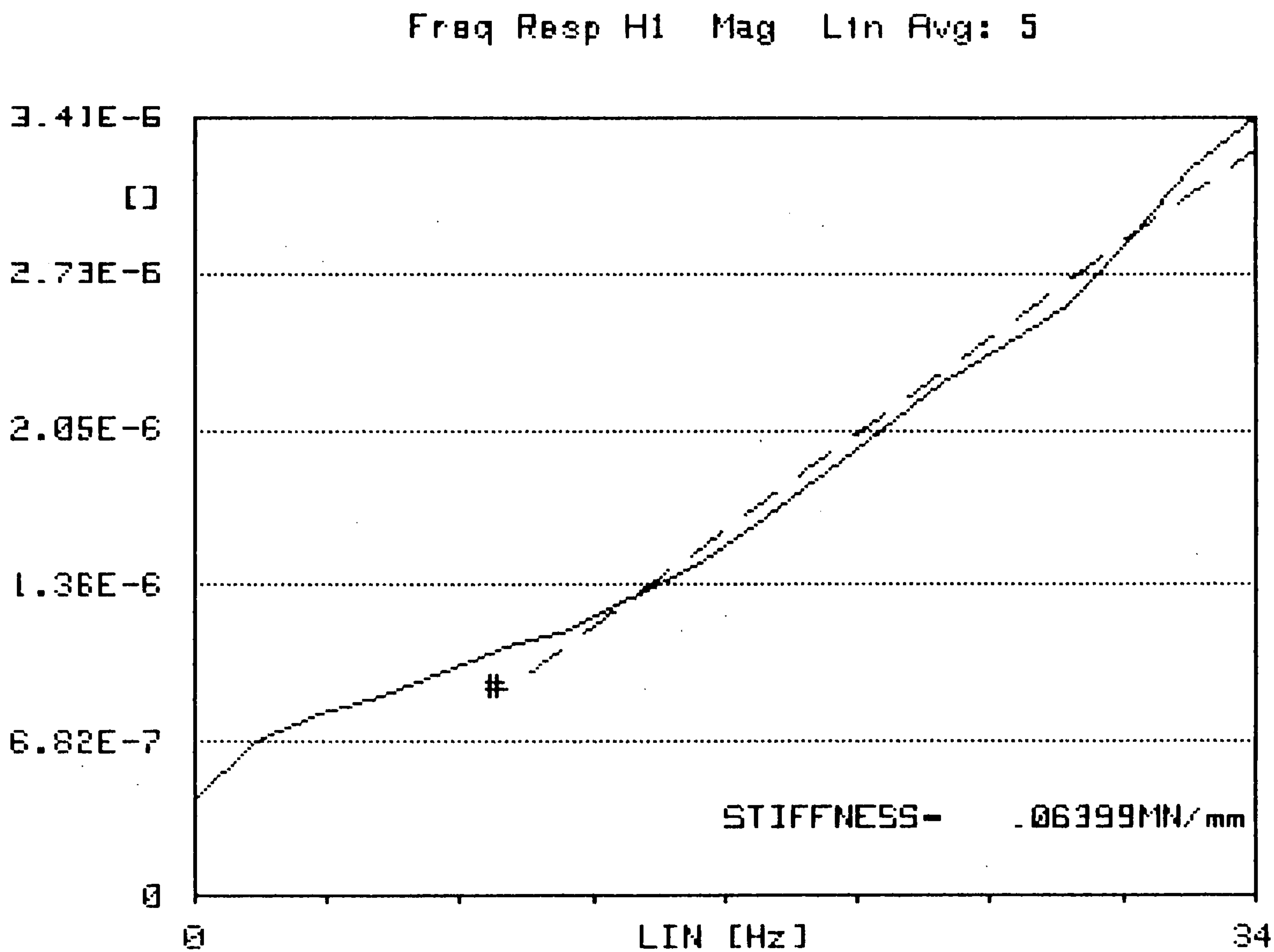

TYPICAL SEWER RING STIFFNESS
LABORATORY SEWER: DOUBLE BRICK RING

FIGURE 8.34

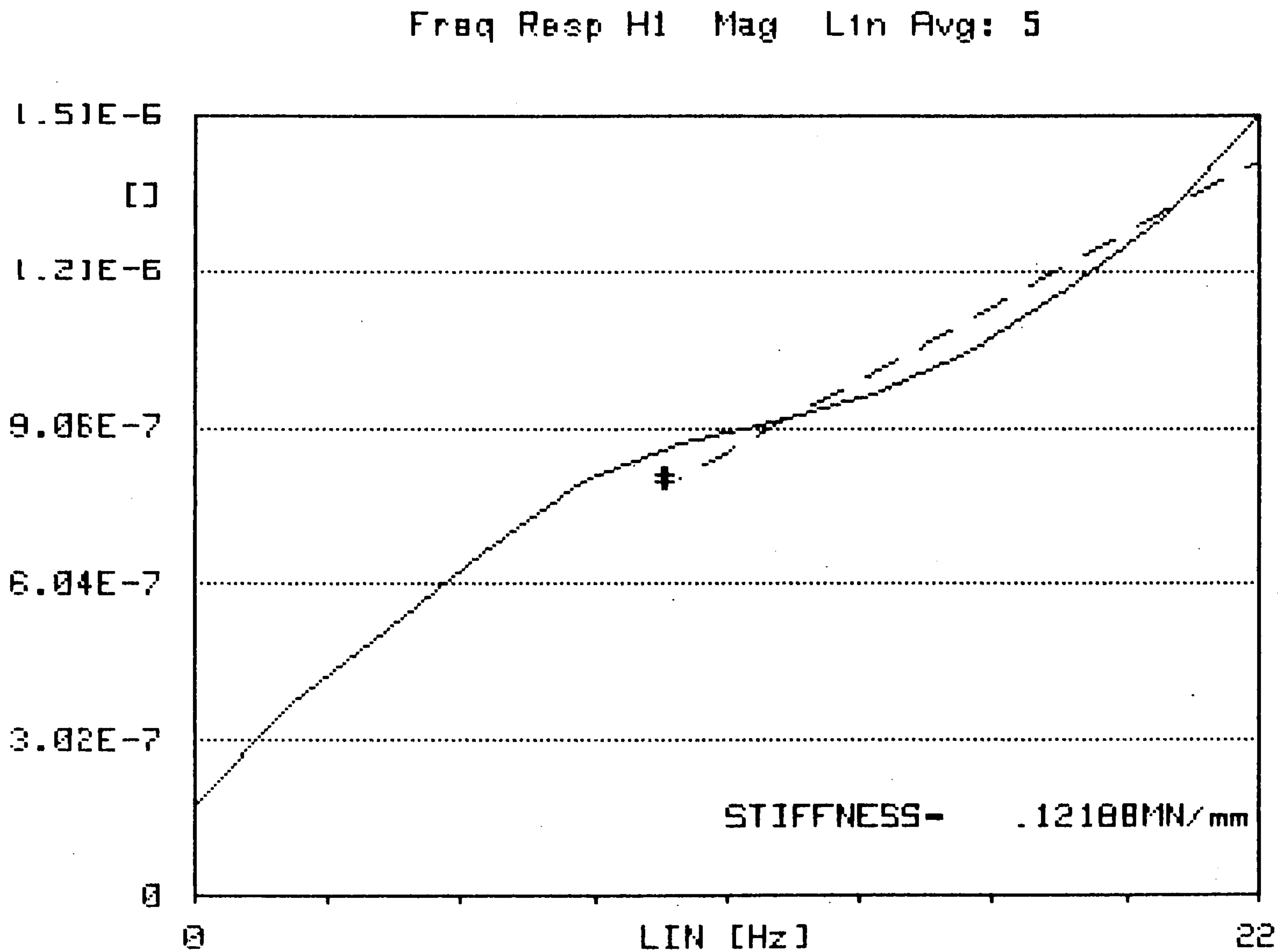

TYPICAL SEWER RING STIFFNESS
LABORATORY SEWER: TRIPLE BRICK RING

FIGURE 8.35

CHAPTER 9

FIELD SEWER TESTS

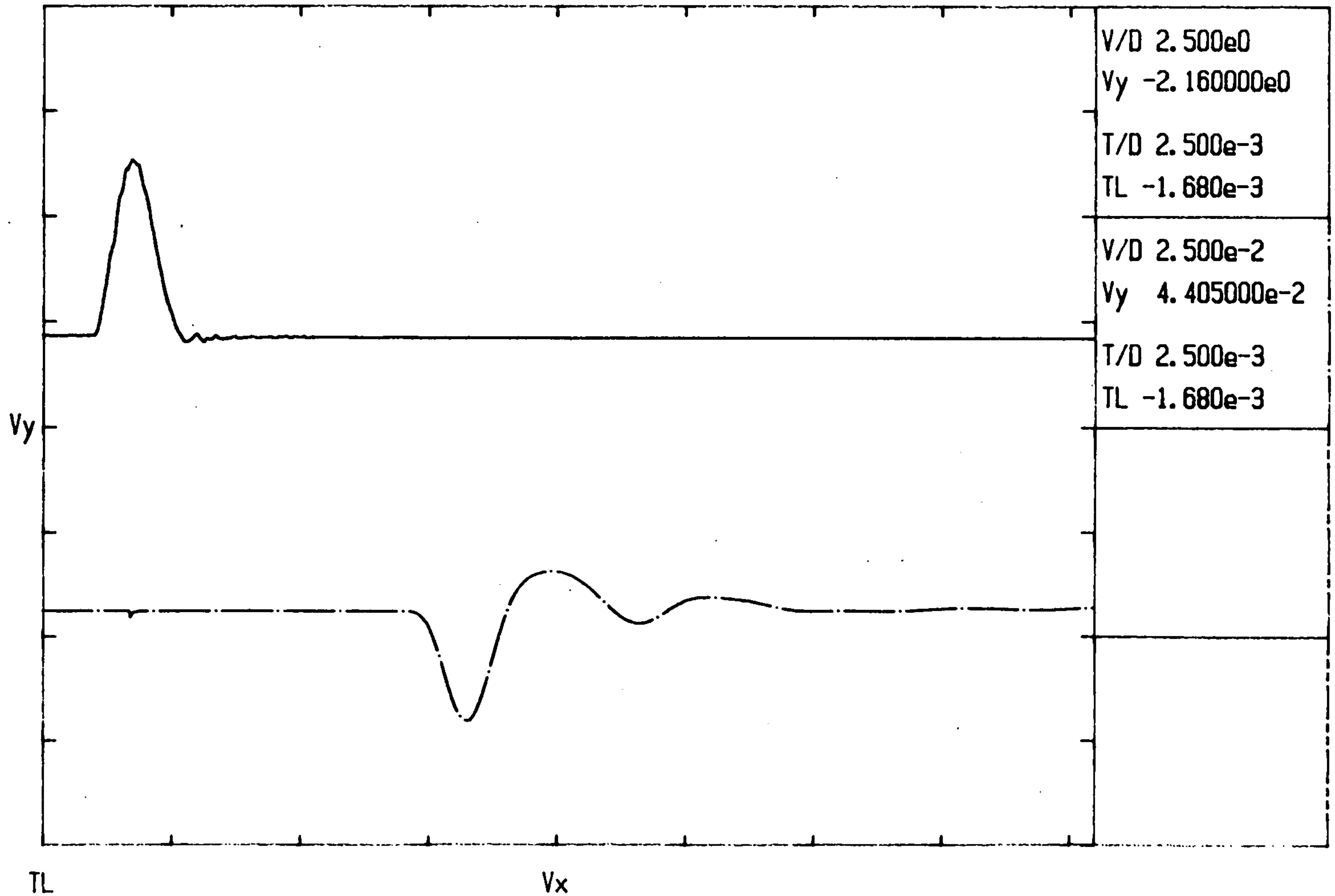

TYPICAL "DELAY" VELOCITY RECORD (DIGITAL OSCILLOSCOPE)
FIELD SEWER: 1 BRICK END TO 3 BRICK END

FIGURE 9.1

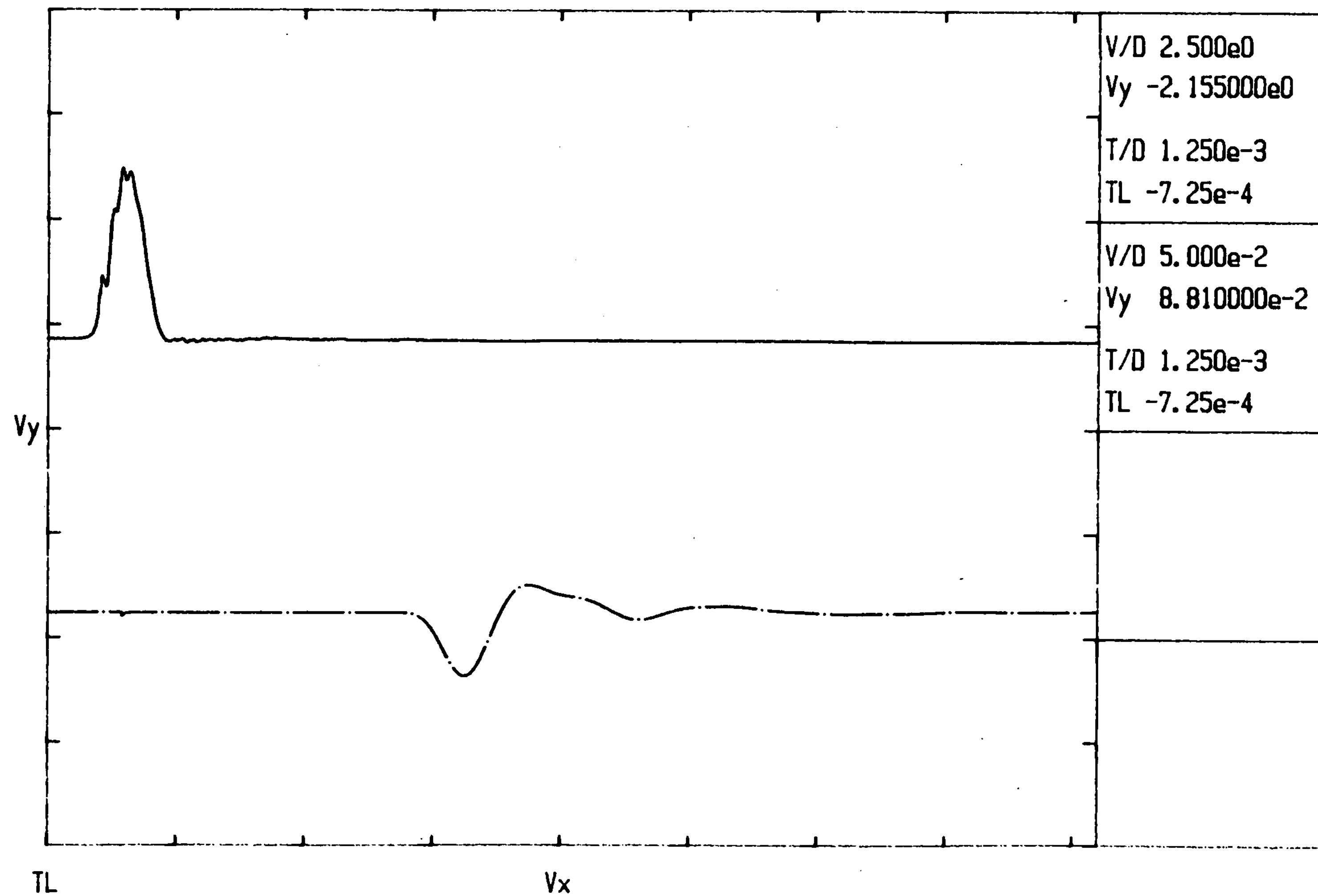

TYPICAL "DELAY" VELOCITY RECORD (DIGITAL OSCILLOSCOPE)
FIELD SEWER: 3 BRICK END TO 1 BRICK END

FIGURE 9.2

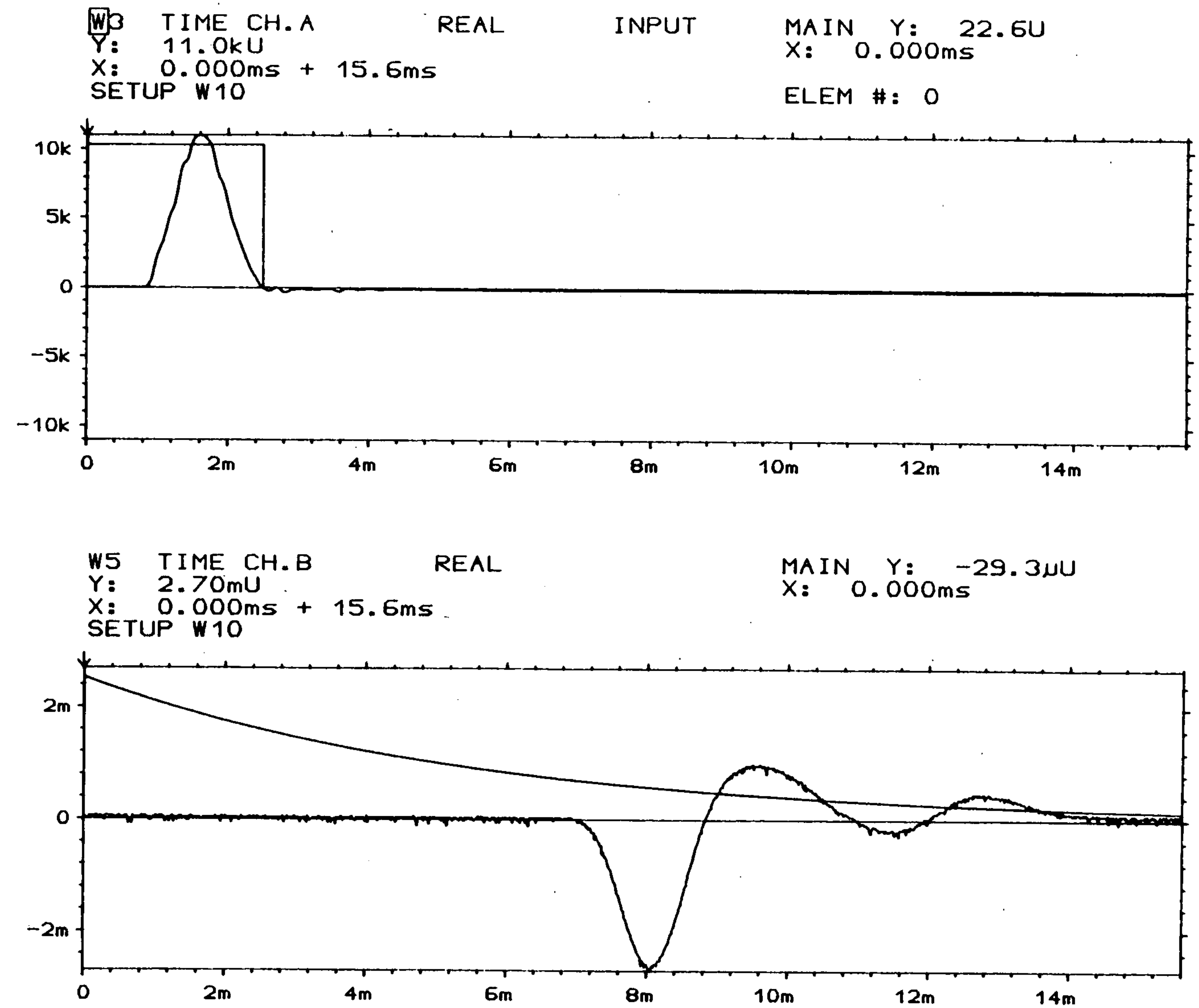

TYPICAL "DELAY" VELOCITY RECORD (SIGNAL ANALYSER)
FIELD SEWER: 1 BRICK END TO 3 BRICK END

FIGURE 9.3

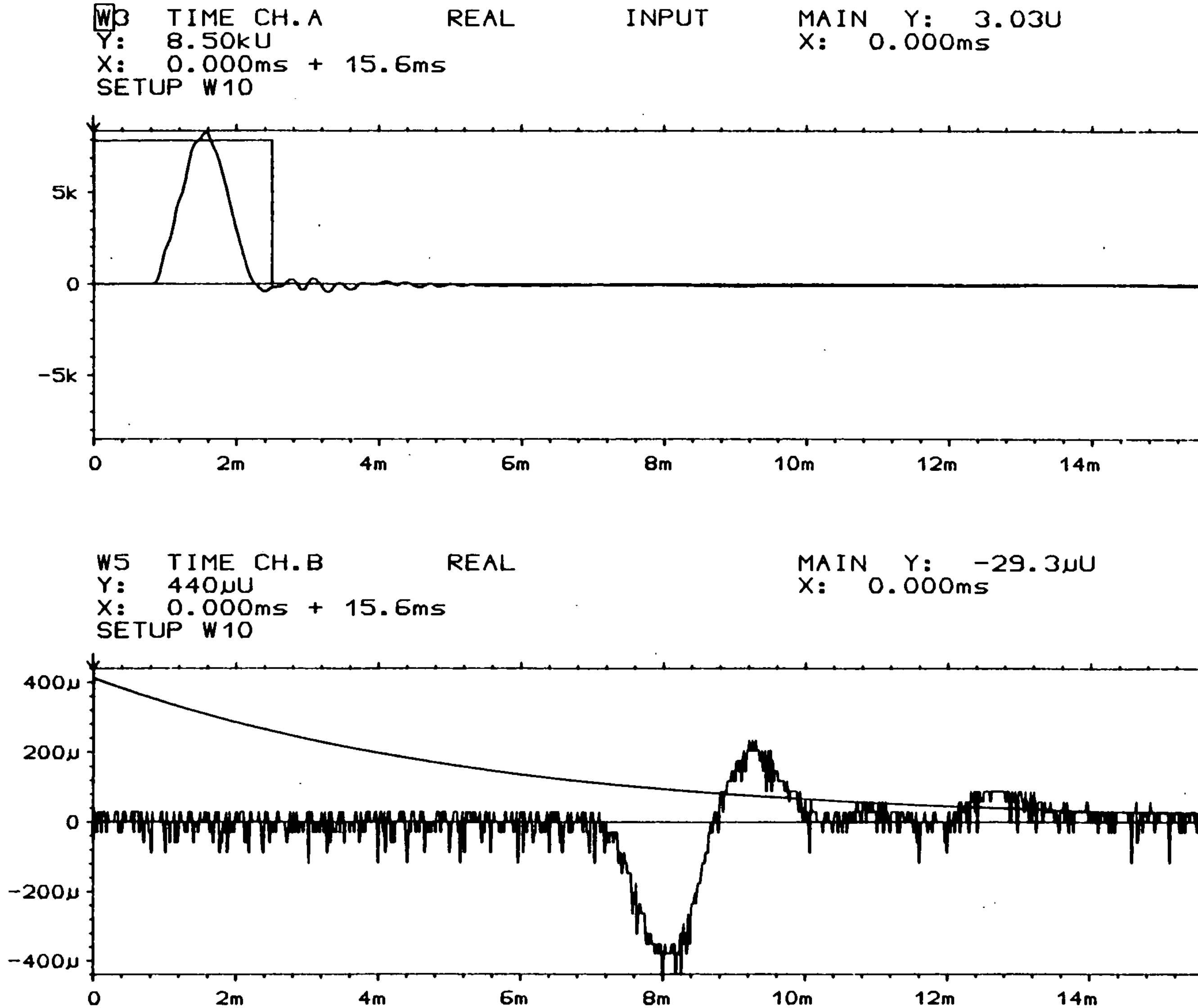

TYPICAL "DELAY" VELOCITY RECORD (SIGNAL ANALYSER)
FIELD SEWER: 3 BRICK END TO 1 BRICK END

FIGURE 9.4

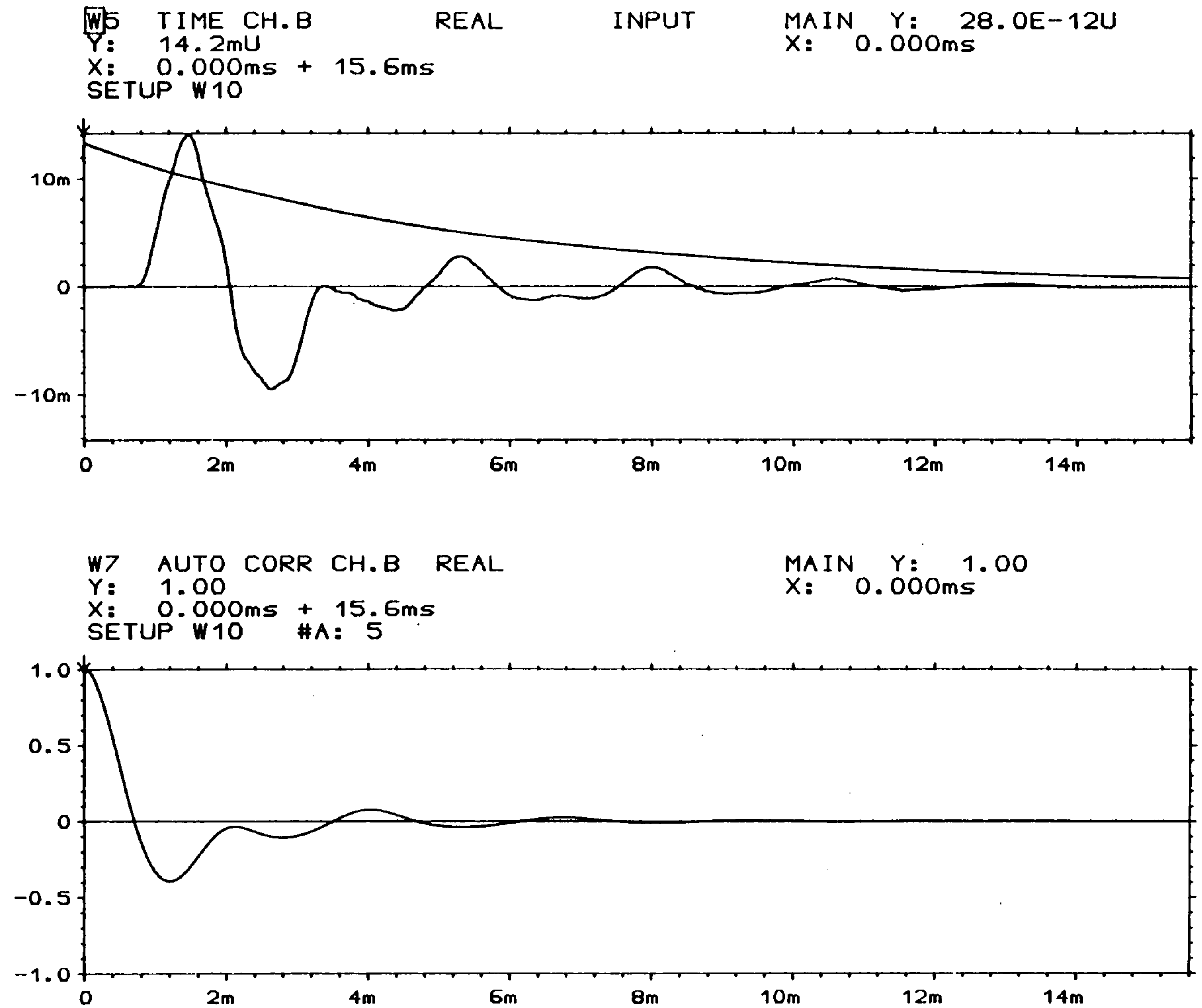

TYPICAL "ECHO" VEL. & AUTO-CORR. RECORD (SIGNAL ANALYSER)
FIELD SEWER: 1 BRICK END TO 3 BRICK END

FIGURE 9.5

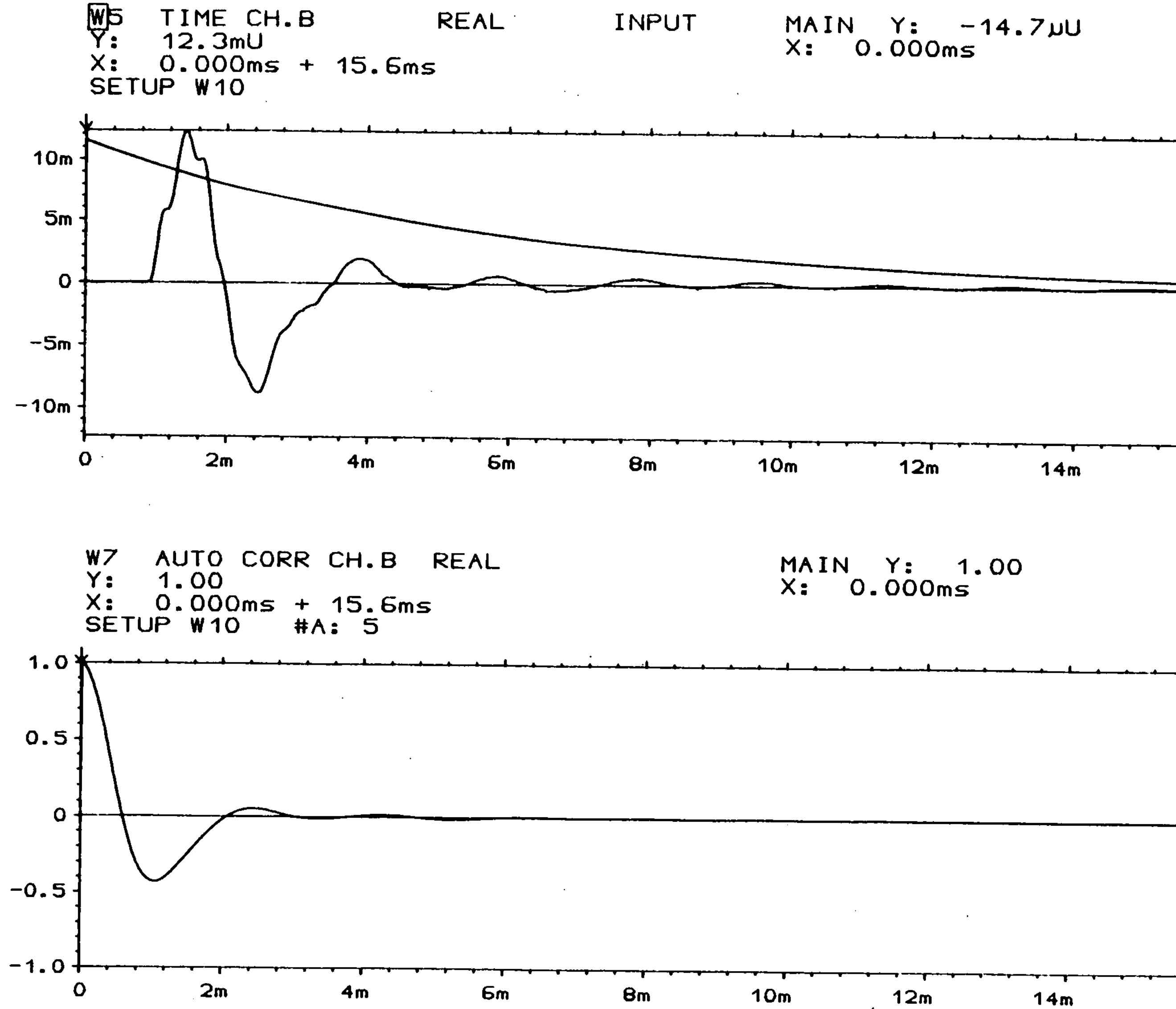

TYPICAL "ECHO" VEL. & AUTO-CORR. RECORD (SIGNAL ANALYSER)
FIELD SEWER: 3 BRICK END (INNER) TO 1 BRICK END

FIGURE 9.6

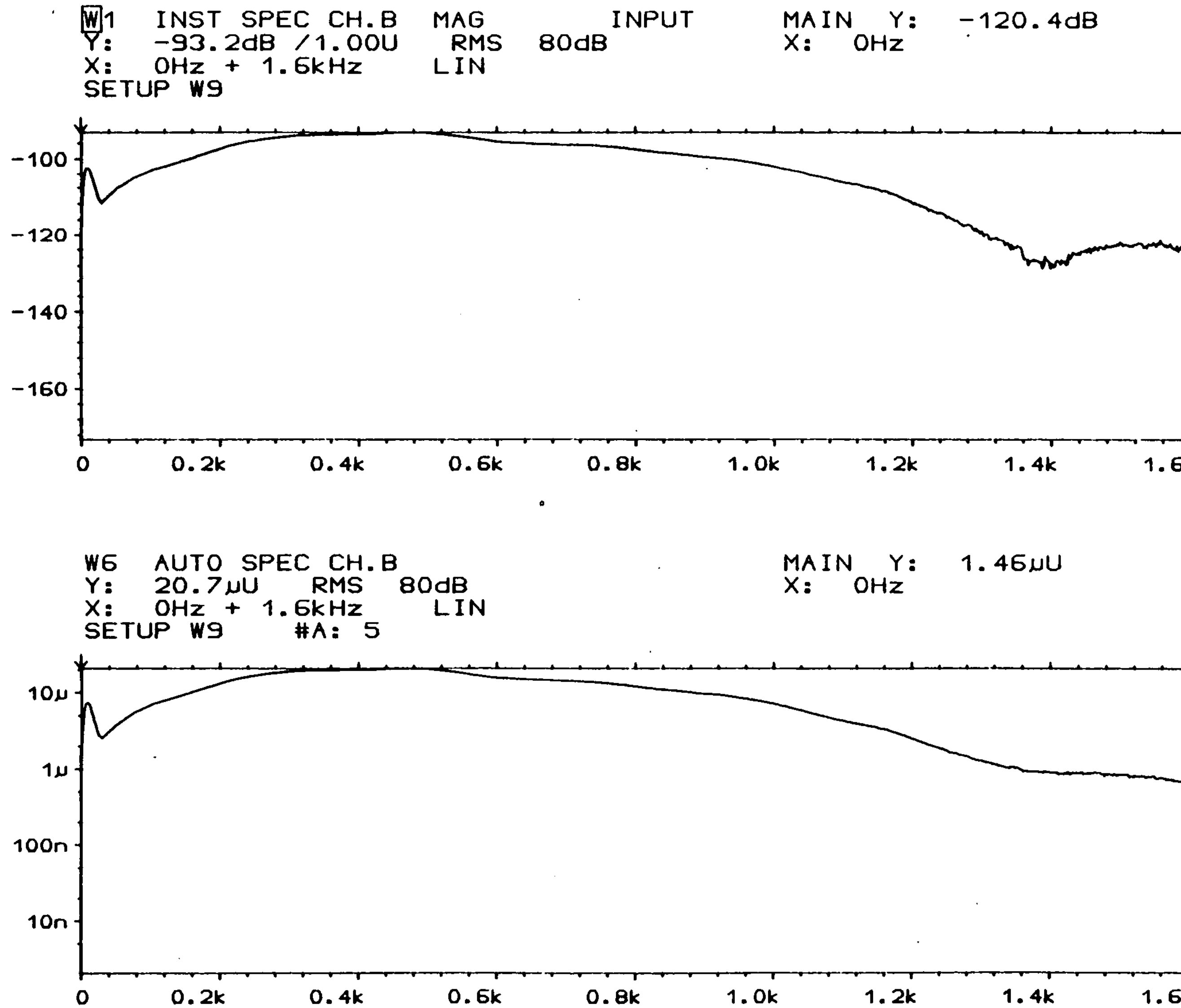

TYPICAL INSTANTANEOUS AND AUTOSPECTRA
FIELD SEWER: 3 BRICK END

FIGURE 9.7

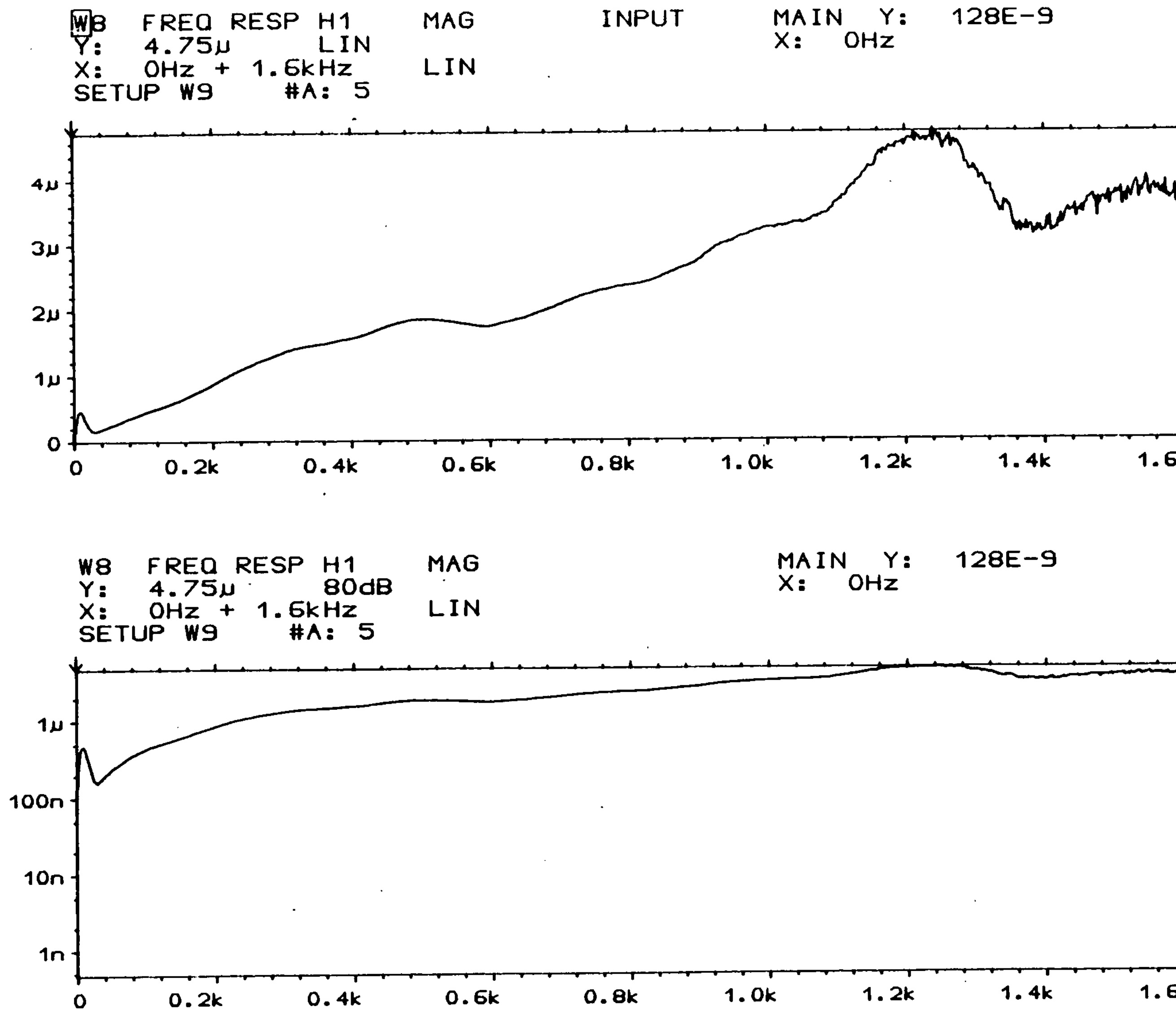

TYPICAL FREQUENCY RESPONSE FUNCTION
FIELD SEWER: 3 BRICK END

FIGURE 9.8

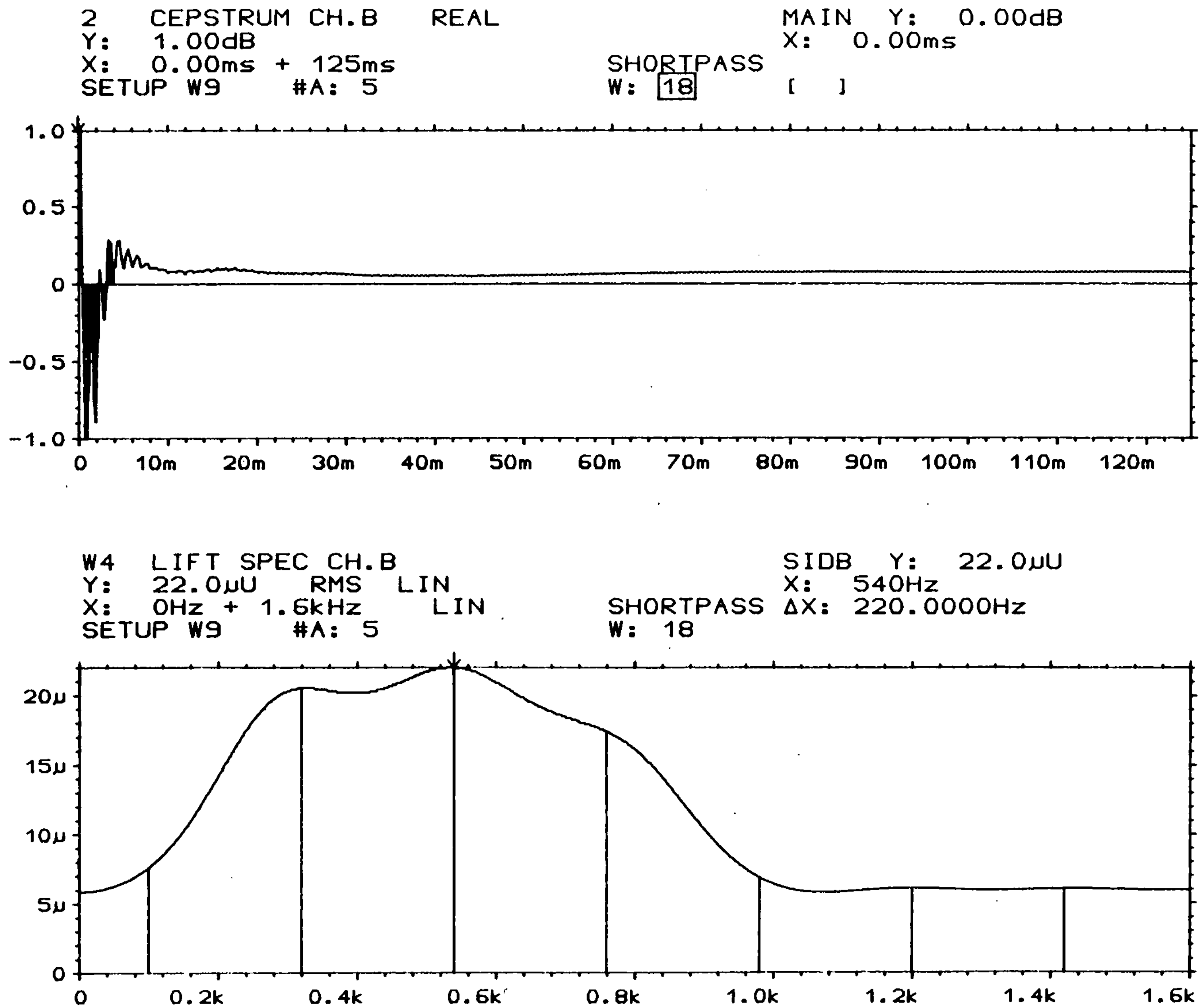

FIGURE 9.9

USING CEPSTRUM AND LIFTERED SPECTRUM
TO LOCATE FIRST CHANGE OF CROSS-SECTION
FIELD SEWER: 3 BRICK END

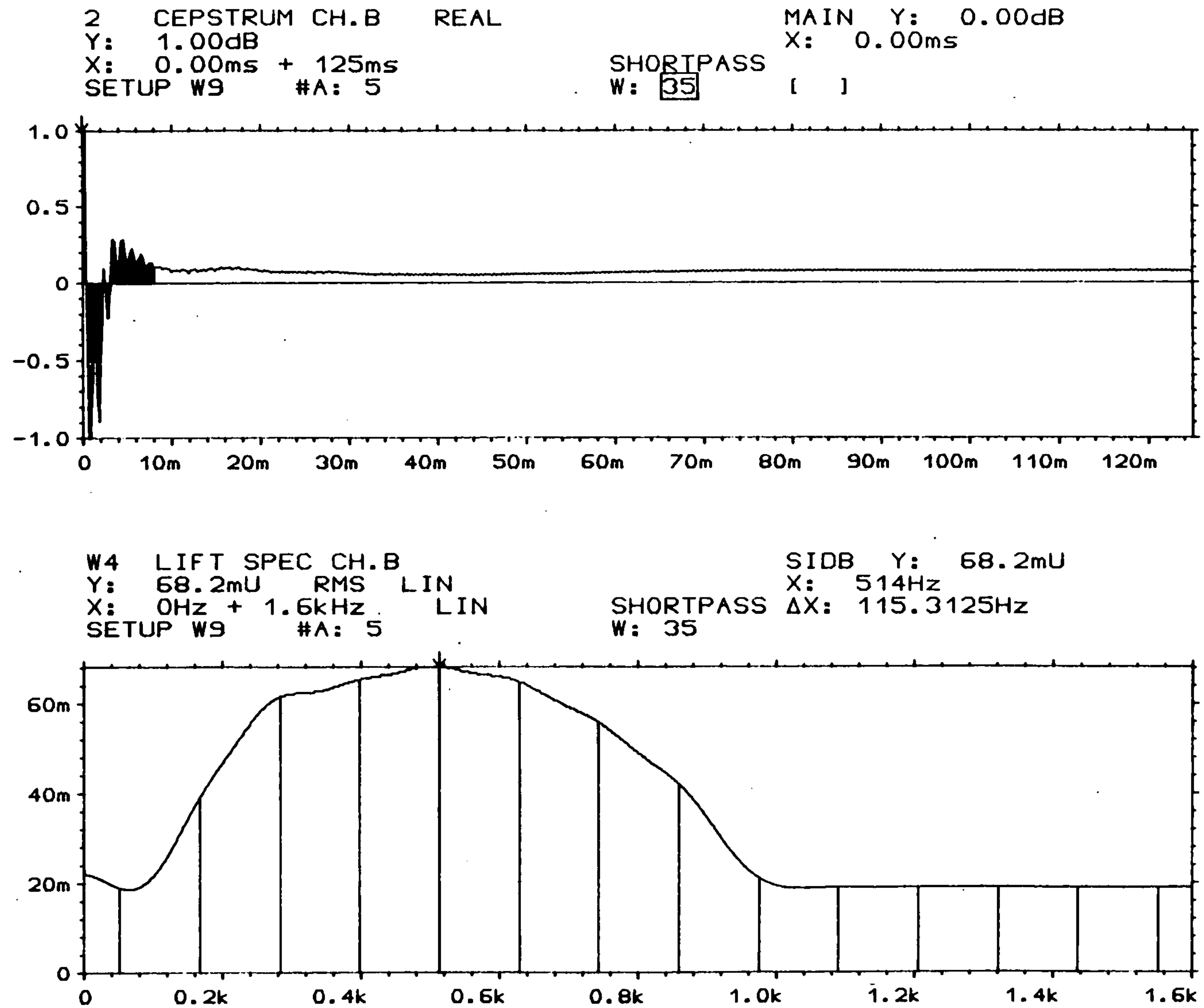

USING CEPSTRUM AND LIFTERED SPECTRUM
TO LOCATE SECOND CHANGE OF CROSS-SECTION
FIELD SEWER: 3 BRICK END

FIGURE 9.10

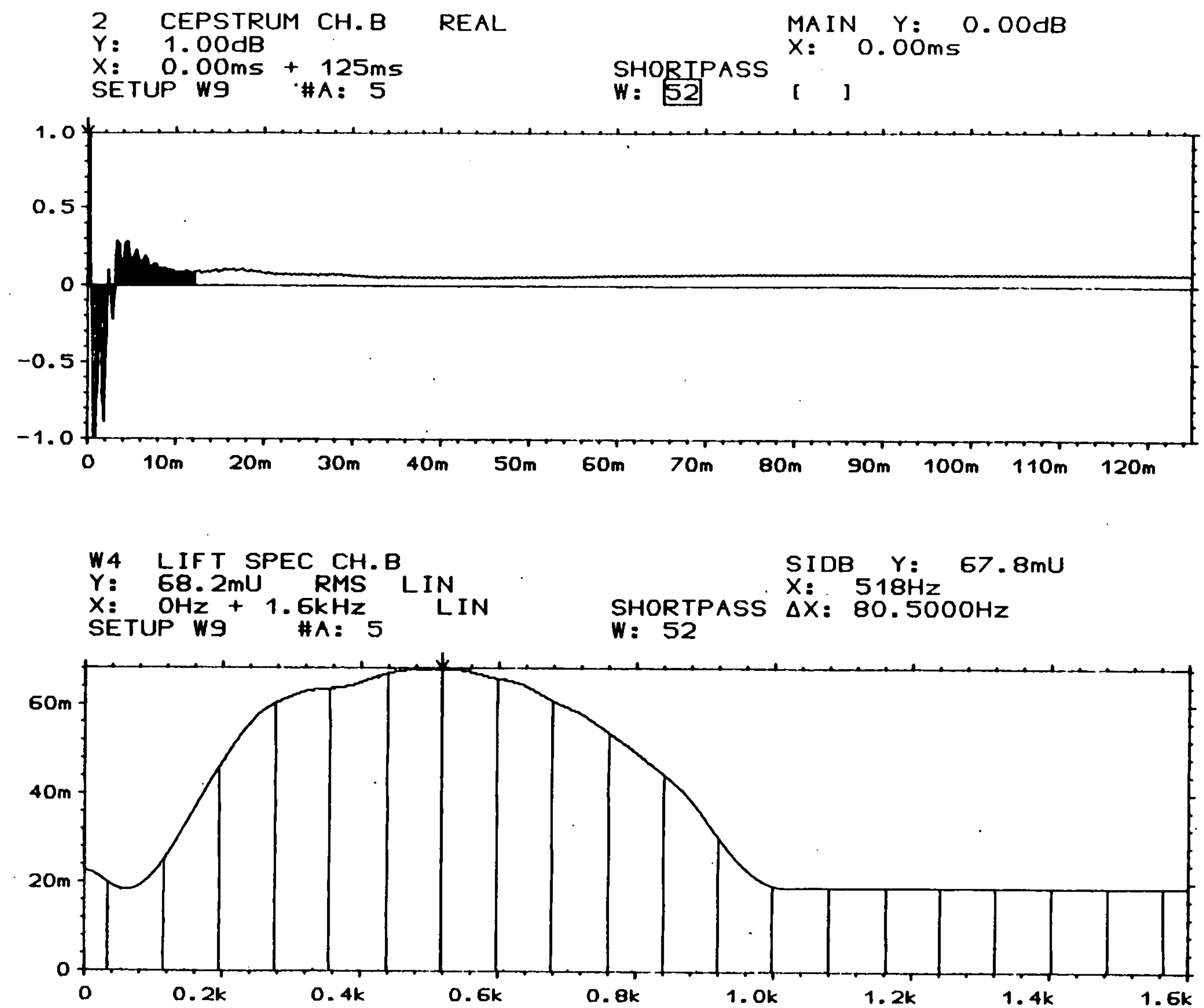

USING CEPSTRUM AND LIFTERED SPECTRUM
TO LOCATE FAR END OF THE SEWER
FIELD SEWER: 3 BRICK END

FIGURE 9.11

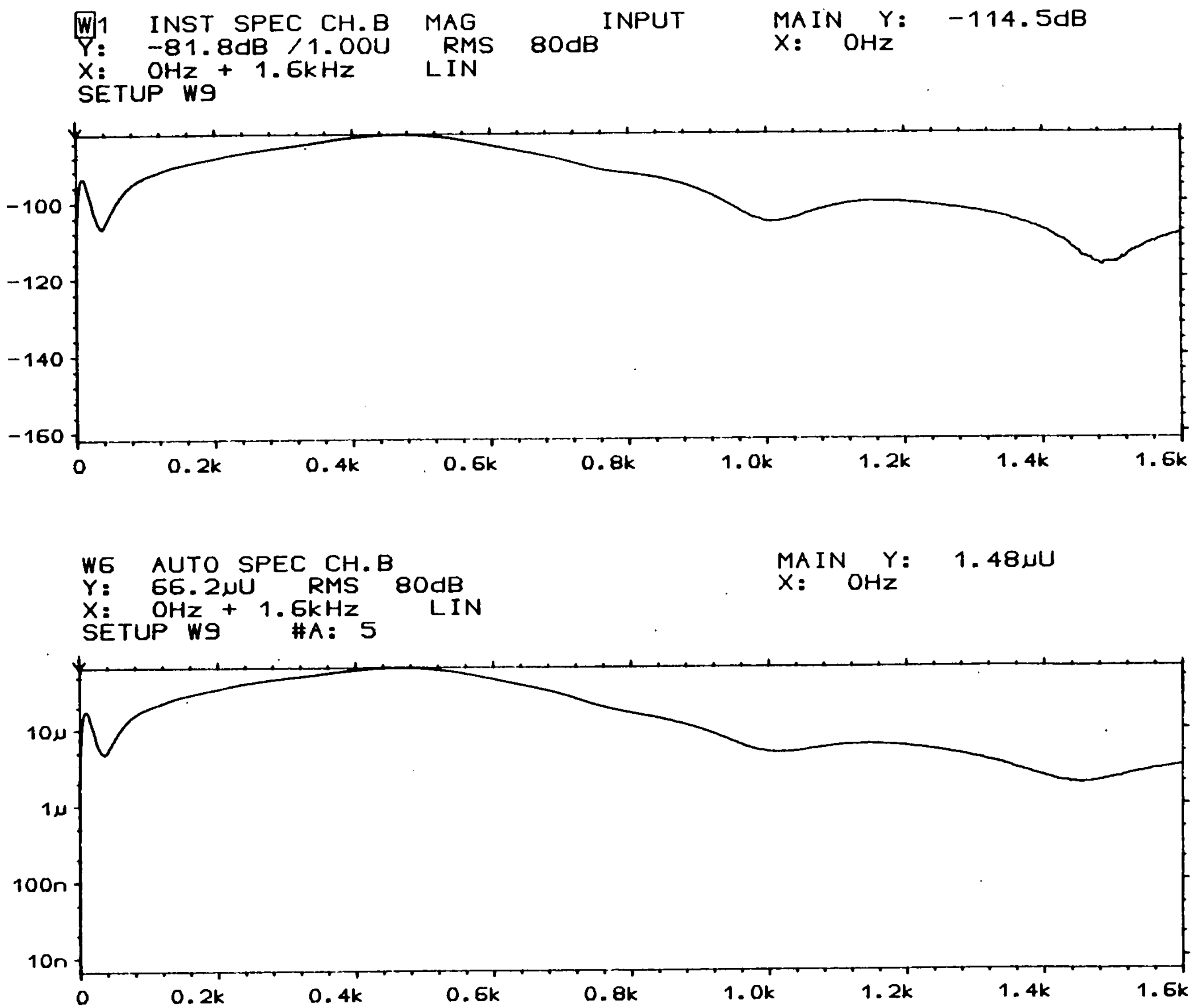

TYPICAL INSTANTANEOUS AND AUTOSPECTRA
FIELD SEWER: 1 BRICK END

FIGURE 9.12

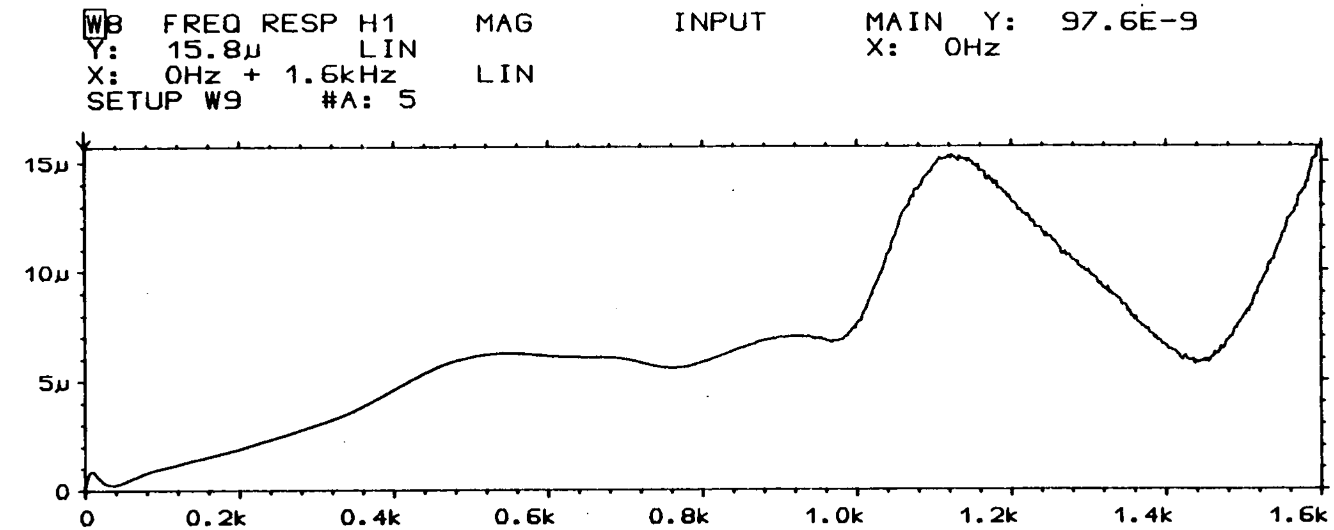

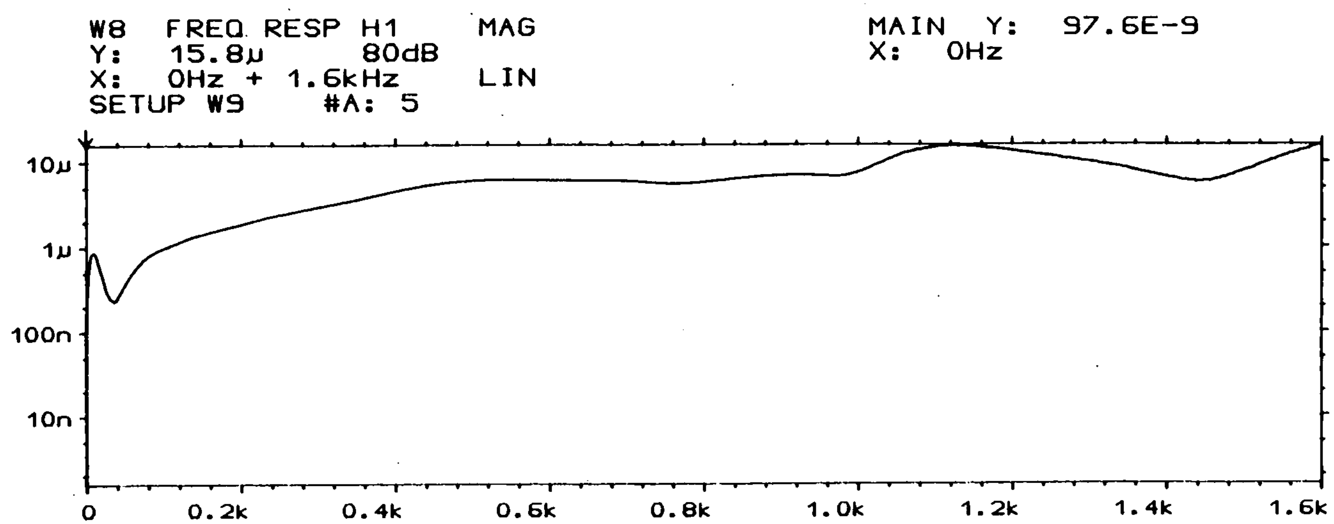

TYPICAL FREQUENCY RESPONSE FUNCTION
FIELD SEWER: 1 BRICK END

FIGURE 9.13

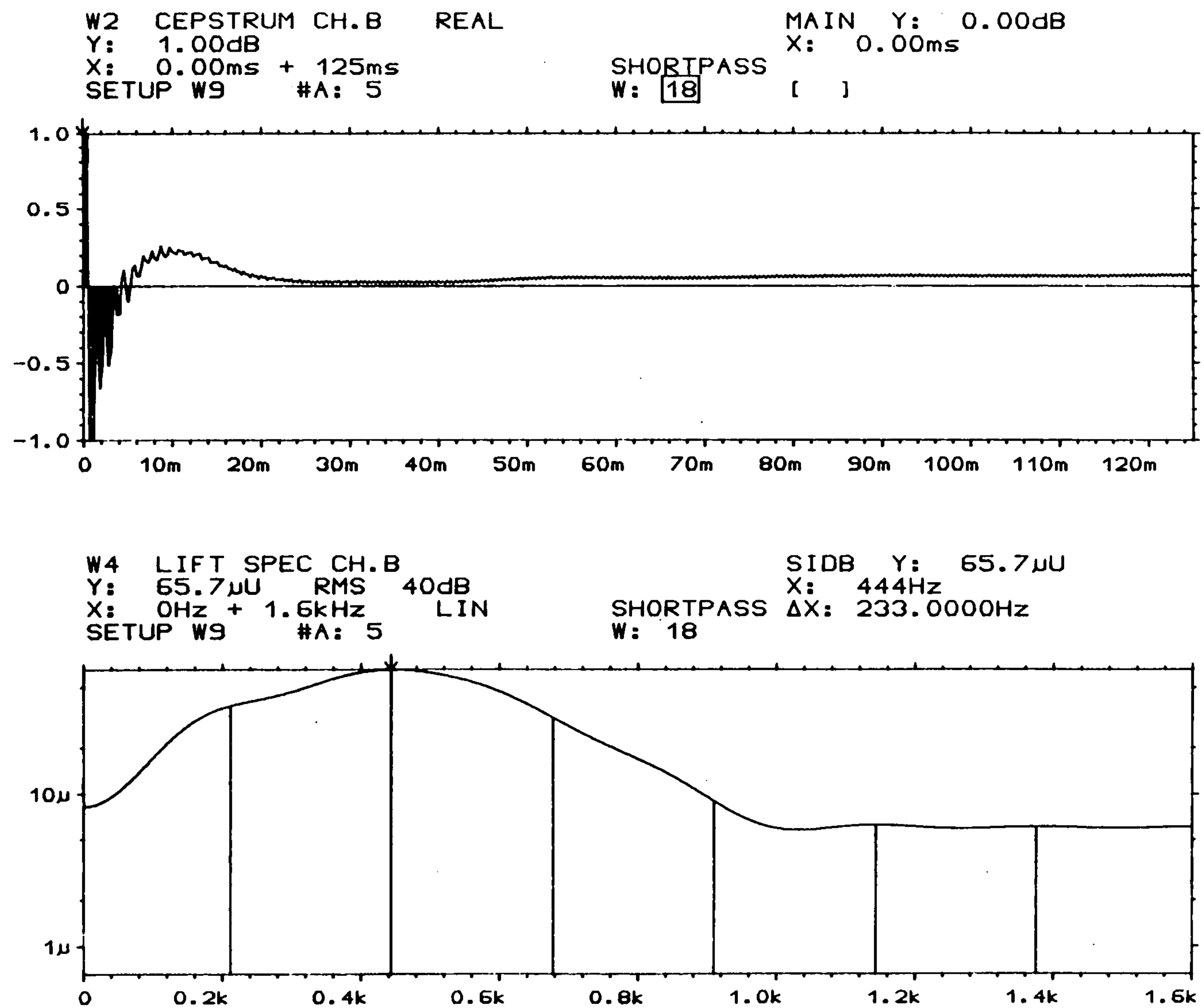

USING CEPSTRUM AND LIFTERED SPECTRUM
TO LOCATE FIRST CHANGE OF CROSS-SECTION
FIELD SEWER: 1 BRICK END

FIGURE 9.14

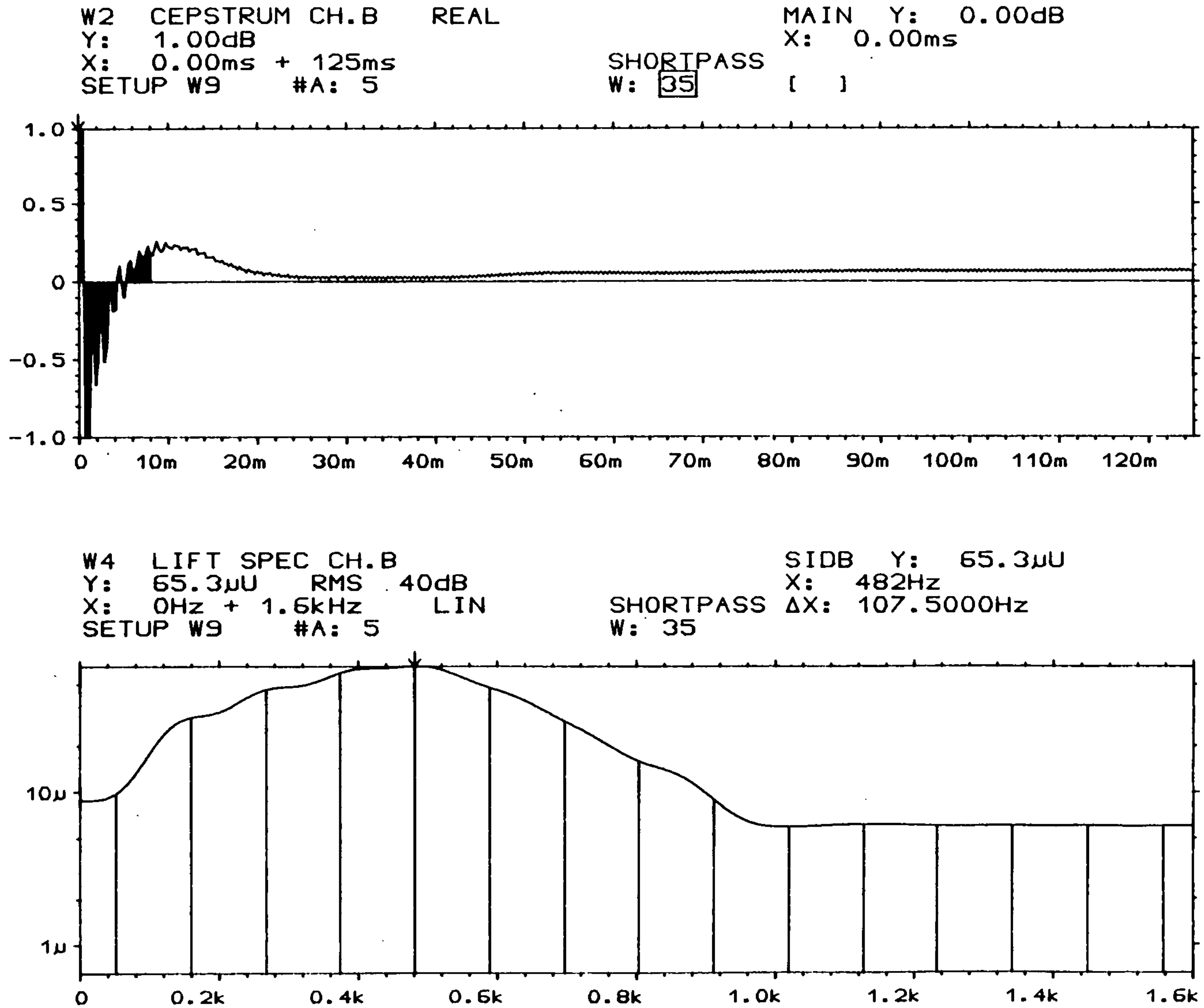

FIGURE 9.15

USING CEPSTRUM AND LIFTERED SPECTRUM
TO LOCATE SECOND CHANGE OF CROSS-SECTION
FIELD SEWER: 1 BRICK END

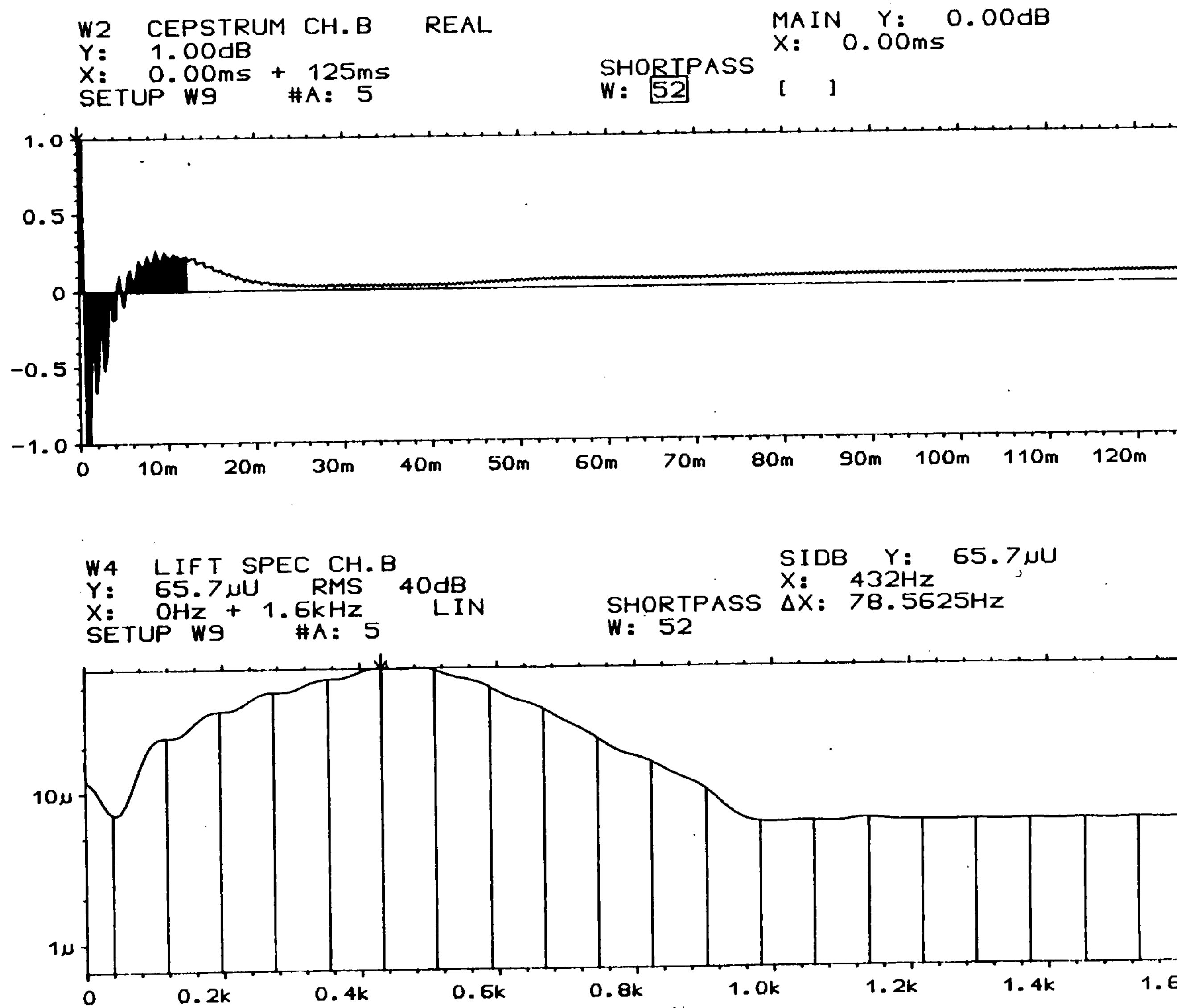

USING CEPSTRUM AND LIFTERED SPECTRUM
TO LOCATE FAR END OF THE SEWER
FIELD SEWER: 1 BRICK END

FIGURE 9.16